Joana Oliveira Gama Soares

Targeting p53 in cancer: from innovative yeast screening strategies to new drugs

Tese do 3º ciclo de estudos conducentes ao grau de doutoramento em Ciências Farmacêuticas, especialidade Microbiologia

Orientadora: Professora Doutora Lucília Helena Ataíde Saraiva

Co-orientadores: Doutora Clara Isabel Ferreira Pereira
Professor Doutor Alberto Inga

Janeiro 2016

ACKNOWLEDGEMENTS

"The more complex the world became, the more difficult it is to complete something without the cooperation with others."

Alexander Fleming

First of all I would like to thank to my supervisor Prof Doutora Lucília Saraiva for believing in my desire to do scientific research and in my abilities, giving me the opportunity to perform my PhD thesis in her research group. Thank you for all the time invested in me, teaching me, listening my doubts, for your patient, dedication and hardworking and for sharing your scientific knowledge. Thanks also for all hopefulness and confidence given in my work. Thank you for inspire, encourage and support me to continue my career in scientific research area. Finally, thank you for your friendship.

I would also like to thank to my co-supervisor Doutora Clara Pereira to teach me the first steps in the "real science", giving me the guide stars of research. For clarifying all my doubts and support me in the lab, and for your friendship.

I am deeply grateful to my co-supervisor Prof Doutor Alberto Inga who gave me the possibility to work in his lab. For all dedication, availability to teach me, and for sharing your knowledge. I also thank to his collaborators Yari Ciribilli and Alessandra Bisio for all techniques that I learned and for making me feel so welcome in your lab.

I would like to thank to my "lab family" constituted for all people who share "our place", namely Cláudia Bessa, Sara Gomes, Liliana Raimundo, Ana Sara Gomes, Helena Ramos and Brian Fernandes for the unconditional help, scientific discussions and mainly for the friendship. And to all that passed by our lab, namely Mariana Leão, Cláudia Maciel and Isabel Coutinho for the support and friendship too.

All Master students that gave me the opportunity to pass my knowledge and that at same time, help me in my lab work, namely Samara Salomão, Sofia Mendonça, Raquel Pereira, Helena Ramos and Joana Loureiro. And especially thanks to Liliana Raimundo for all the support both at work and personal and for feel so proud of your evolution as a scientist. I wish I could one day return all dedication and hardworking that you have given me.

Many thanks to Professor Doutor Flávio Reis and Professora Doutora Célia Gomes for all the patience, support and warmth that greeted me in their laboratories.

I would also like to thank the chemical groups that synthesized the compounds to test during my PhD, namely the Santo's group from iMedUL (Prof Doutora Maria MM Santos, Nuno AL Pereira, Ângelo Monteiro and Margarida Espadinha) and Prof Doutora Honorina

Cidade and Prof Doutora Madalena Pinto from CEQUIMED-UP, Faculty of Pharmacy, University of Porto.

I also acknowledge to the Cancer Drug Resistance group from IPATIMUP, particularly to Prof Doutora Helena Vasconcelos who gave me the possibility to work in her research group.

Many thanks to the Department of Pharmacology, particularly to Prof Doutora Glória Queiroz for all the support in the human cell lines field. Thanks also to the lab technicians Céu and Mónica.

I would also like to acknowledge to the lab technicians, Nuno and Cristina, from the Department of Microbiology for all the support, patient and friendship along the years.

Aos meus pais e irmã gostaria de agradecer por tudo o que me proporcionaram, por sempre acreditarem em mim, pelo apoio incondicional e por todo o amor e paciência ao longo destes anos.

Aos meus amigos muito obrigada por toda a compreensão, apoio e verdadeira amizade. Em especial gostaria de agradecer à Catarina por estar sempre disponível tanto nos melhores momentos como nos menos bons, pelo carinho e lealdade ao longo deste tempo.

Ao meu melhor amigo, namorado e companheiro de vida, Carlos, por todo o extremo apoio, carinho, atenção, paciência, compreensão… Obrigada pela motivação, inspiração e por acreditares em mim e fazeres com que eu própria acredite.

I also thank to FCT (Fundação para a Ciência e Tecnologia) for the financial support of my doctoral fellowship (SFRH/BD/78971/2011) and to the Faculty of Pharmacy of University of Porto for provided the logistical support. This work was funded by FEDER funds through the Operational Programme for Competitiveness Factors – COMPETE, national funds provided by FCT under the Strategic Funding UID/Multi/04378/2013 (UCIBIO/REQUIMTE) and the project PTDC/DTP-FTO/1981/2014, in the framework of the programme PT2020. I also thank to Research Institute for Medicines (iMed.ULisboa), to IBILI-Faculty of Medicine of University of Coimbra and to the Italian Association for Cancer Research, AIRC (IG#12869 to AI).

ABSTRACT

Oncological diseases remain one of the major worldwide Public Health concerns. Despite this, the therapeutic options for many cancer patients are still limited and disappointing, mainly due to chemoresistance and severe side effects. On the other hand, the development of new anticancer therapies has shown to be a slow and highly unreliable process.

Compelling evidence has demonstrated that inactivation of the p53 pathway underlies tumor development and maintenance. In fact, in the majority of human cancers, the p53 function is compromised, either by mutation or by inhibition through interaction with negative regulators, such as murine double minute (MDM)2 and MDMX. Based on this, the inhibition of the p53 interaction with MDMs and the restoration of wild-type (wt)-like function to mutant p53 have been recognized as hopeful strategies in anticancer treatment. However, despite all the efforts made to find new small molecule activators of p53, to date, few entered into clinical trials and none has reached the clinic.

Hence, with the present thesis, we intended to find new pharmacological options against cancer by targeting p53, focusing on inhibitors of the p53 interaction with MDM2/MDMX (MDMs) and reactivators of mutant p53. For that, a drug screening strategy, based on yeast, tumor cell lines and animal models, was used to test several chemical libraries, comprising compounds with scaffolds previously reported to be promising in the search for modulators of p53 activity, namely containing indole and/or isoindolinone moieties. With this approach, an enantiopure phenylalaninol-derived oxazolopyrrolidone lactam (oxazoloisoindolinone 3a) was identified as new inhibitor of the p53-MDM2 interaction with potent *in vitro* p53-dependent tumor growth-inhibitory effect through stimulation of apoptosis and cell cycle arrest. However, a dual inhibition of the p53 interaction with MDM2 and MDMX is the most effective strategy for a full activation of wt p53, particularly against MDMX-overexpressing tumor cells that are highly resistant to MDM2-only inhibitors. Therefore, this thesis was also focused on the identification of dual inhibitors of p53-MDMs interactions. In fact, a dual inhibitor of p53-MDMs interactions, the compound OXAZ-1, was identified from the chemical family of tryptophanol-derived oxazolopiperidone lactams. This compound activated a p53-dependent mitochondrial apoptotic pathway, and presented promising p53-dependent synergistic effects with conventional chemotherapeutic drugs, in human tumor cells. However, the modest *in vitro* tumor growth-inhibitory activity of OXAZ-1 led us to pursue our search for more potent dual inhibitors. This conducted to the second inhibitor of p53-MDMs interactions found in this thesis, the tryptophanol-derived oxazoloisoindolinone DIMP53-1. Besides its higher *in vitro*

growth-inhibitory effect, DIMP53-1 exhibited potent p53-dependent *in vivo* antitumor activity with no apparent toxic side effects. With these results, DIMP53-1 became the first small molecule dual inhibitor with *in vivo* anticancer properties described to date.

In order to streamline the identification of reactivators of mutant p53, a new yeast-based screening assay was developed encompassing human mutant p53 R280K and Y220C. Using the developed cell system, the first reactivator of mutant p53 R280K, the compound SLMP53-1, an enantiopure tryptophanol-derived oxazoloisoindolinone, was discovered. This compound also activated wt p53, and exhibited a potent p53-dependent *in vivo* antitumor activity with no apparent toxic side effects. Furthermore, SLMP53-1 inhibited tumor cell migration and presented synergistic effects with conventional chemotherapeutics.

In conclusion, an efficient and reliable screening approach to search for new reactivators of mutant p53 emerged from this thesis. Most importantly, four new activators of p53 were discovered, two of them (DIMP53-1 and SLMP53-1) revealing to be promising anticancer drug candidates. Besides the incontestable impact of this thesis to the advance of p53 pharmacology and targeted drug discovery strategy, it gave rise to new hopes and therapeutic opportunities in anticancer treatment.

Key words: Anticancer agents; Cancer; p53; MDM2/MDMX; Yeast targeted screening assays.

RESUMO

As doenças oncológicas continuam a ser uma das maiores preocupações de Saúde Pública. Apesar disso, as opções terapêuticas existentes para muitos doentes oncológicos permanecem limitadas e com resultados insatisfatórios devido, nomeadamente, à quimioresistência e aos seus graves efeitos secundários. Por outro lado, o desenvolvimento de novas terapias anticancerígenas tem-se demonstrado um processo lento e muito falível.

Vários estudos têm indicado que a inativação da via da p53 está na base do desenvolvimento e subsistência tumoral. De facto, na maioria dos cancros humanos, a função da p53 está comprometida, tanto por mutações como por inibição através da interação com reguladores negativos, como as proteínas *Murine Double Minute* (MDM)2 e MDMX. Desta forma, a inibição da interação da p53 com as proteínas MDMs e o restabelecimento da função nativa às mutantes da p53 têm sido consideradas estratégias promissoras no tratamento do cancro. Contudo, até à data, apesar de todos os esforços realizados no sentido de encontrar novas pequenas moléculas ativadoras da p53, apenas um número reduzido de moléculas seguiu para ensaios clínicos e nenhuma se encontra aprovada para tratamento oncológico.

Deste modo, a presente tese teve como objetivo encontrar novas opções farmacológicas no tratamento cancro tendo como alvo a proteína p53, nomeadamente através da descoberta de inibidores da interação da p53 com MDM2/MDMX (MDMs) e de reativadores das mutantes da p53. Com este objetivo, usou-se uma estratégia de pesquisa farmacológica baseada em modelos de levedura, células tumorais humanas e animais para testar várias bibliotecas químicas, que compreendem compostos com estruturas químicas previamente descritas como promissoras na alteração da atividade da p53, nomeadamente moléculas contendo os grupos indole e/ou isoindolinona.

Com esta abordagem foi identificado um novo inibidor da interação p53-MDM2, uma oxazolopirrolidona lactama derivada do fenilalaninol (oxazoloisoindolinona 3a), com efeito inibidor do crescimento tumoral, dependente da p53 e associado à indução de apoptose e retenção do ciclo celular. Contudo, a dupla inibição da interação da p53 com MDM2/MDMX é uma estratégia mais eficaz para uma completa ativação da p53 nativa, nomeadamente em células tumorais que sobreexpressam MDMX, resistentes aos inibidores seletivos do MDM2. Assim, esta tese teve também como objetivo, a identificação de novos inibidores duais das interações p53-MDMs. De facto, a partir da família química de oxazolopiperidona lactamas derivadas do triptofanol foi identificado um inibidor dual das interações p53-MDMs, o composto OXAZ-1. Este composto ativou uma via apoptótica mitocondrial

dependente da p53 e apresentou efeitos sinérgicos promissores, também dependentes da p53, com quimioterápicos convencionais em células tumorais humanas. Porém, a modesta inibição do crescimento tumoral do OXAZ-1 levou à pesquisa de inibidores duais mais potentes. Tal facto, conduziu à identificação do segundo inibidor das interações p53-MDMs, a oxazoloisoindolinona derivada do triptofanol DIMP53-1. Este composto, para além do marcado efeito inibidor do crescimento tumoral *in vitro*, apresentou uma potente atividade anti-tumoral *in vivo* dependente da p53, sem efeitos secundários aparentes. Com estes resultados, DIMP53-1 torna-se a primeira pequena molécula inibidora dual, com propriedades anticancerígenas *in vivo,* descrita até à presente data.

De forma a agilizar a identificação de reactivadores das mutantes da p53, foi desenvolvido um novo ensaio de pesquisa farmacológica baseado em células de levedura expressando as mutantes humanas da p53 R280K ou Y220C. Com a utilização deste sistema de pesquisa farmacológica foi descoberto o primeiro reactivador da mutante p53R280K, o composto SLMP53-1, uma oxazoloisoindolinona derivada do triptofanol. Este composto foi também capaz de ativar a p53 nativa tendo demonstrado atividade antitumoral dependente da p53 *in vivo,* sem sinais aparentes de efeitos adversos. Além disso, o composto SLMP53-1 inibiu a migração das células tumorais humanas e apresentou efeitos sinérgicos com quimioterápicos convencionais.

Em conclusão, com esta tese, foi desenvolvida uma nova abordagem eficaz de pesquisa farmacológica de reactivadores de mutantes da p53. Adicionalmente, no âmbito da mesma, foram descobertos quatro novos ativadores da p53, dois dos quais (DIMP53-1 e SLMP53-1) representam promissores candidatos a fármacos anticancerígenos. De uma forma geral, para além do impacto incontestável no avanço farmacológico da p53 e na estratégia de descoberta de fármacos dirigidos a um alvo específico, com esta tese surgiram novas esperanças e oportunidades na terapia oncológica.

Palavras-chave: Agentes anticancerígenos; Cancro; Ensaios alvo-dirigidos utilizando células de levedura; p53; MDM2/MDMX.

INDEX

INDEX OF FIGURES

INDEX OF SCHEMES

TABLE INDEX

ABBREVIATIONS

a.a.	Amino acids
Apaf-1	Apoptosis protease-activating factor 1
BAX	Bcl-2 associated X protein
BAK	Bcl-2-antagonist/killer
Bid	BH3 interacting-domain death agonist
Cdc25c	Cell division cycle 25 homolog c
CDK	Cyclin-dependent kinase
CFU	Colony-forming unit
Co-IP	Co-immunoprecipitation
Cyt *c*	Cytochrome *c*
DBD	DNA binding domain
DMSO	Dimethyl sulfoxide
DNE	Dominant negative effect
FASAY	Functional analysis of separated alleles
GADD45	Growth arrest and DNA-damage inducible protein
G1	GAP1
G2	GAP2
GI_{50}	Growth inhibition of 50%
GOF	Gain-of-function
HTS	High throughput screening
LOF	Loss-of-function
MDM2	Murine double minute 2
MDMX	Murine double minute X
M	Mitosis
MN	Micronucleus
MOMP	Mitochondrial outer membrane permeabilization
NES	Nuclear export signal
NLS	Nuclear localization signal
NMR	Nuclear magnetic resonance
OD	Oligomerization domain
OD_{600}	Optical density at 600 nm
p53AIP1	p53-regulated apoptosis inducing protein 1
PARP	poly (ADP-ribose) polymerase
PBS	Phosphate-buffered saline
PCR	Polymerase chain reaction

PI	Propidium iodide
PTF-α	Pifthrin-α
PUMA	p53 upregulated modulator of apoptosis
Rb	Retinoblastoma protein
RE	Response element
RLU	Relative light units
ROS	Reactive oxygen species
SRB	Sulforhodamine B
TAD	Transactivation domain
TNF	Tumor necrosis factor
TRADD	TNF receptor-associated death domain
TRAIL	Tumor necrosis factor-related apoptosis-inducing ligand
TUNEL	Terminal deoxynucleotidyl transferase dUTP nick end lab
wt	Wild-type
Y2H	Yeast two-hybrid
$\Delta\psi_m$	Mitochondrial membrane potential

CHAPTER 1

Introduction

1.1. Cancer: General concepts

1.1.1. Epidemiology of cancer

Cancer is a worldwide public health concern, particularly in developed countries (Ferlay et al., 2015). In fact, in 2012, it was reported 14.1 million new cancer cases, 8.2 million cancer deaths and 32.6 million people living with cancer (within 5 years of diagnosis) worldwide (Ferlay et al., 2015). In Portugal, cancer is the second cause of death (https://www.ine.pt) and, following the worldwide trend, it is predicted an increase in the new cancer cases, mainly due to an ageing population, human lifestyle, and infections (mostly in developing countries). Accordingly, it is predicted 20 million new cancer cases for 2025 worldwide, and in Portugal it is expected 53 thousand new cases (Ferlay et al., 2013; Bray et al., 2013; Ferlay et al., 2015).

Lung cancer is one of the most common cancers in the world, associated with high incidence (due to tobacco consumption and pollution) and mortality (1.8 million cases, 1.6 million deaths; Figure 1.1), mostly because of its aggressiveness, invasion capacity and treatment resistance (Ferlay et al., 2015). The breast cancer is the second most common overall, but ranks fifth as cause of death (1.7 million cases, 522,000 deaths; Figure 1.1) because of the relatively favorable prognosis. Colorectal (1.4 million cases, 694,000 deaths), prostate (1.1 million cases, 307,000 deaths), stomach (951,000 cases, 723,000 deaths) and liver (782,000 cases, 745,000 deaths) cancers are the following more common in worldwide (Figure 1.1). These six cancers represent more than 50% of the global incidence burden in 2012 (Ferlay et al., 2015; Figure 1.1). In Portugal, although lung cancer is the most lethal, it ranks fourth in terms of incidence. The large bowel, prostate and breast cancers are more incident, following this order (Ferlay et al., 2013; https://www.ine.pt).

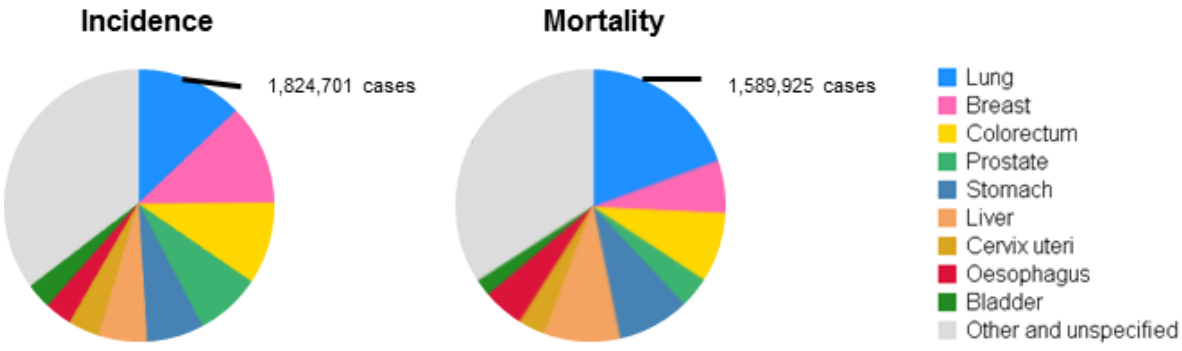

Figure 1.1. Estimated incidence and mortality of different types of cancer worldwide in 2012 [Graphs from GLOBOCAN 2012: Estimated cancer Incidence Mortality and Prevalence Worldwide in 2012 (http://globocan.iarc.fr/Pages/fact_sheets_population.aspx)].

Early diagnosis, universal access to health care and new therapies has resulted in a significant improvement of cancer survival. Despite this, the high incidence and mortality can justify the intense research conducted around cancer, especially towards finding more efficient therapeutic strategies.

1.1.2. Hallmarks of cancer

Nowadays, cancer is considered more than masses of proliferating cells, characterized by complex tissues composed by distinct cell types involved in heterotypic interactions between them (Hanahan and Weinberg, 2011). Furthermore, beyond tumor biology with all cross-talking pathways inside and between cells, the "tumor microenvironment" is also a fundamental part, contributing to tumor progression and maintenance (Figure 1.2).

The tumor microenvironment reinforces the recognition of tumors as complex organs that are constructed during the course of multistep tumorigenesis. There are many cells, molecules and blood vessels that surround and feed the tumor (Figure 1.2). Due to the hyperproliferation and genetic instability, tumors are heterogeneous, containing different types of subclonal populations (Hanahan and Weinberg, 2011). Cancer stem cells are very common in tumors and are responsible for its poor prognosis. They are classified as stem cells due to their ability to efficiently seed new tumors upon inoculation in mice, and because they share transcriptional profiles with normal tissue stem cell populations (Cho and Clarke, 2008; Lobo et al., 2007). These cells initiate tumors and are essential for its progression (Hanahan and Weinberg, 2011), contributing to tumor heterogeneity due to their different stages of differentiation. On the other hand, their heterogenic profiles contribute to the chemotherapeutic resistance and tumor recurrence (Singh and Settleman, 2010; Creighton et al., 2009).

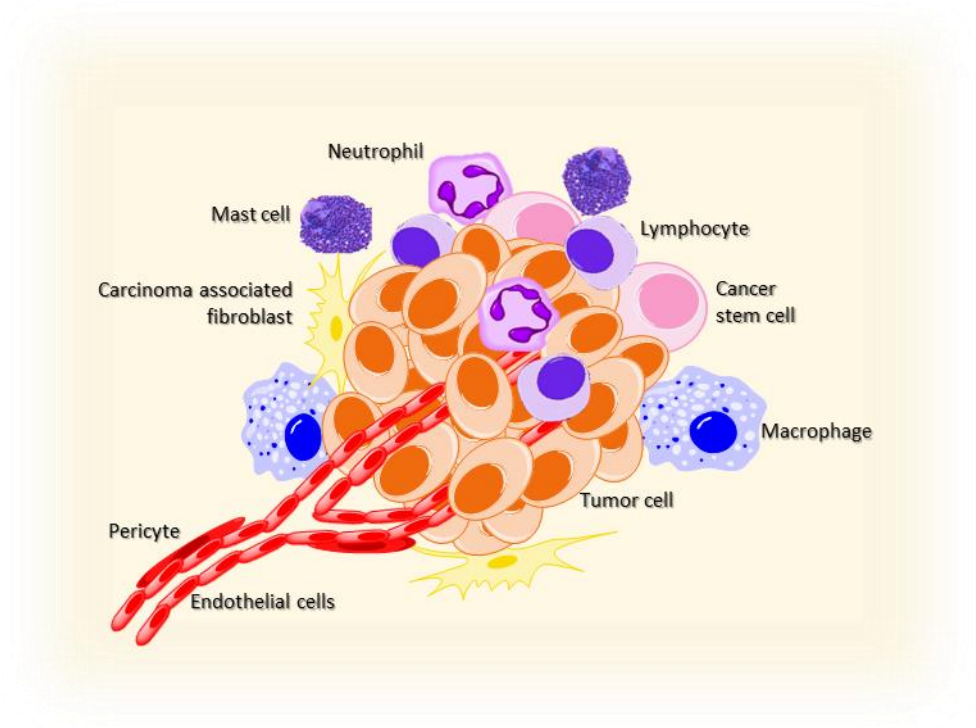

Figure 1.2. Tumor microenvironment: representation of the different cell types constituints of solid tumors.

In some tumors, fibroblasts are the preponderant cells. They can be found in both forms, as a similar form to the normal fibroblasts supporting epithelial cells, and as myofibroblasts with different functions compared to the normal ones (Figure 1.2). In chronic inflammation, myofibroblasts may lead to the pathological fibrosis in tissues such as lung, kidney and liver (Hanahan and Weinberg, 2011).

The angiogenic process is crucial to feed, oxygenate and maintain tumor cells. In "angiogenic switch", quiescent endothelial cells are activated, inducing them to enter into a cell biological program that allows the construction of new blood vessels (Baeriswyl and Christofori, 2009). This process is coordinated by signaling proteins that bind to endothelial cell surface receptors that either stimulate (such as vascular endothelial growth factor-A, VEGF-A, and fibroblast growth factor, FGF), or inhibit (such as thrombospondin-1, TSP-1) angiogenesis (Baeriswyl and Christofori, 2009). Moreover, although pericyte cells (Figure 1.2) are known for supporting mechanically and physiologically the endothelial cells, in tumor context, they are fundamental pieces in the maintenance of the tumor structure and in the construction of new blood vessels (Raza et al., 2010; Hanahan and Weinberg, 2011).

The presence of inflammatory cells is well-established in tumor microenvironment (Figure 1.2), in which they can have different functions. They can either antagonize the tumor progression, such as natural killer (NK) cells and cytotoxic T lymphocytes (CTLs), or

to promote its progression, such as macrophages, mast cells, neutrophils, and T and B lymphocytes (DeNardo et al., 2010; Hanahan and Weinberg, 2011; Murdoch et al., 2008). The tumor promoting inflammatory state is also characterized by the presence of some signaling molecules released by inflammatory cells, such as tumor epidermal growth factor (EGF), VEGF, FGF2, chemokines, and cytokines (Qian and Pollard, 2010; Murdoch et al., 2008). Additionally, other pro-invasive enzymes are released, and all together contribute to tumor angiogenesis, proliferation, invasion and metastasis (Mantovani, 2010; Hanahan and Weinberg, 2011; Murdoch et al., 2008).

In 2000, the complexity of tumor biology and their surrounding microenvironment led to the identification of six hallmarks of cancer (Hanahan and Weinberg, 2000). For the development and metastatic dissemination of a tumor, the following requirements were determined: 1) sustaining proliferative signaling to support a chronic proliferation; 2) evading growth suppressors, such as the known retinoblastoma-associated (*RB1*) and the *TP53* tumor suppressor genes; 3) resisting cell death by down-regulation of pro-apoptotic signaling, autophagic and necrotic death; 4) enabling replicative immortality by abolishment of senescence and crisis events, and telomerase overexpression; 5) inducing angiogenesis; and 6) activating invasion and metastasis through a complex cascade initiated by some cellular modifications, such as the loss of cell-to-cell adhesion molecule E-cadherin (Figure 1.3; Hanahan and Weinberg, 2000). In 2011, two other emerging hallmarks were included: 7) the deregulation of cellular energetics, through modification of cellular metabolism to most effectively support neoplastic proliferation; and 8) avoiding immune destruction particularly by NK cells and CTLs (Figure 1.3; Hanahan and Weinberg, 2011). Moreover, considering the tumor microenvironment, two more enabling characteristics, that promote the achievement of both core and emerging hallmarks, the genome instability and mutation and the tumor-promoting inflammation, were established (Figure 1.3; Hanahan and Weinberg, 2011).

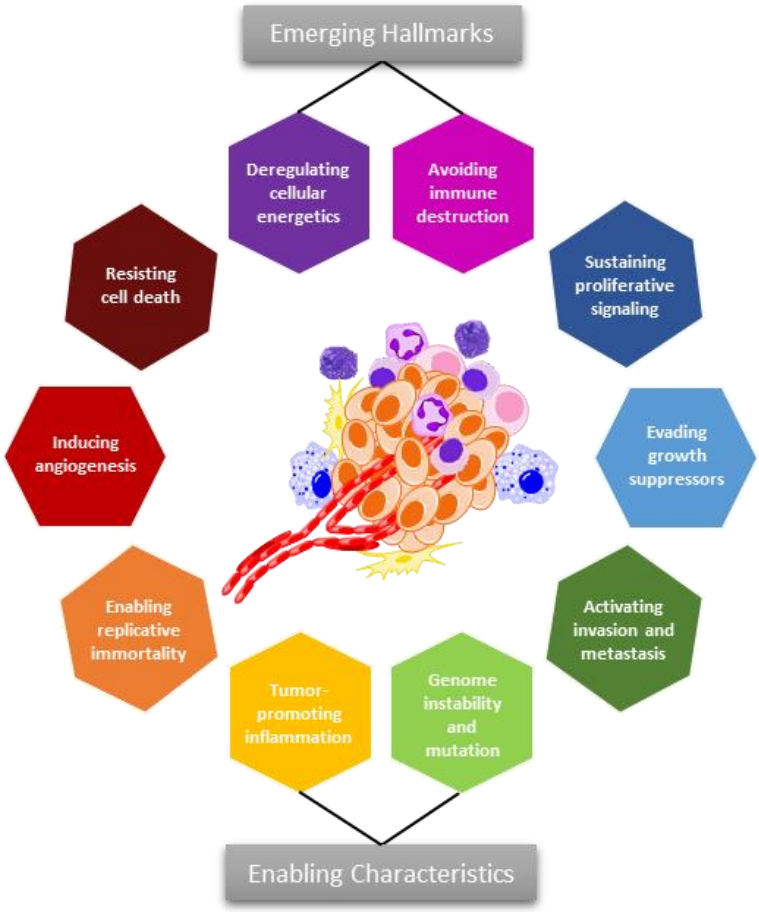

Figure 1.3. The hallmarks of cancer. Schematic representation of the eight core and emerging hallmark capabilities currently proposed, and two more enabling characteristics. [Adapted from (Hanahan and Weinberg, 2011)].

1.1.3. Anticancer therapeutic strategies

At the beginning of the 20th century, the only treatment recognized for cancer was surgery. To date, surgery is the most effective treatment for localized primary tumors. However, for advanced cancers, the ineffectiveness of this approach led, in the 1920s, to the use of radiation therapy (Urruticoechea et al., 2010). In the 1940s, the first anticancer drug was discovered, through serendipity, based on bone marrow depletion effects of sulfur mustard gas on victims of World Wars I and II (Cheung-Ong et al., 2013; DeVita and Chu, 2008). Nevertheless, nitrogen mustard compounds revealed to be not enough to a complete remission of tumor, with the development of drug resistance. However, this discovery motivated the search for new anticancer chemotherapeutic alternatives (Cheung-Ong et al.,

2013; DeVita and Chu, 2008). Actually, after that, the scenario of cancer treatment has been dramatically changed over the last decades.

In spite of the great advances in biomedical research, which have contributed to our deeper understanding of cancer hallmarks, the success of anticancer drug development remains low. In fact, even though anticancer drugs represent a substantial proportion of total new drug approvals, their success in clinical trials remains unsatisfactory (7% from phase I and <50% from phase III) (Hay et al., 2014).

In anticancer drug development, the major challenge is to kill tumor cells without affecting the healthy ones. Based on this, due to the underlying toxicity of the traditional DNA-damaging drugs on non-tumor cells, the attempt to replace these compounds by targeted anticancer drugs has been carried out. Despite this, although the targeted therapy has gained strength, the traditional cytotoxic drugs remain the most widely used in cancer therapy.

In this thesis, the two types of anticancer chemotherapy, the conventional chemotherapeutic drugs and the targeted anticancer drugs, will be briefly described and some examples of each class will be presented.

1.1.3.1. *Conventional chemotherapeutic drugs*

The conventional chemotherapy, mostly including DNA-damaging agents, usually affects cell division/DNA integrity, not directly interfering with the invasion capacity, the loss of differentiation or the tendency to metastization. When cell cycle checkpoint proteins detect high levels of damaged DNA, cell cycle arrest is induced to prevent the transmission of damaged DNA during mitosis. If the damaged DNA is irreparable, cell death may occur (Rang et al., 2015). Cancer cells are known for their ability to ignore cell cycle checkpoints and to have an undemanding DNA repair system, allowing high cell proliferation rates. Therefore, a weaker DNA repair makes cancer cells more susceptible to cell death induced by DNA damaging agents (Rang et al., 2015). These cytotoxic drugs affect rapidly dividing cells, targeting both tumor and all normal cells that are in accelerate division. Therefore, they are commonly associated with a high toxicity, being responsible for depress bone marrow, impair wound healing, depress growth in children, alopecia, damage to gastrointestinal epithelium (including oral mucous membranes), sterility, teratogenicity and carcinogenicity (www.cancer.org; Rang et al., 2015). Consequently, these drugs are often administrated in single doses, or short courses of therapy, at the highest concentrations possible without no life-threatening levels of toxicity (Maximum Tolerated Dose – MTD). Besides, these high doses require subsequent treatment-free periods for recovery of patient normal cells (Venkatakrishnan et al., 2014).

The conventional chemotherapeutic anticancer drugs are divided into several groups taking into account their mechanism of action: alkylating agents, antimetabolites, topoisomerase inhibitors, mitotic inhibitors and glucocorticoids (Table 1.1).

Table 1.1. Conventional chemotherapeutic anticancer drugs grouped according to their mechanism of action.

Group (mechanism of action)	Classes (examples)	Therapeutic applications	Observations	References
Alkylating agents (directly damage DNA - intercalation between bases, DNA crosslinking)	Nitrogen mustards (cyclophosphamide) Nitrosoureas (carmustine, lomustine) Alkyl sulfonates (busulfan) Triazines (temozolomide) Ethylenimines (altretamine) Platinum drugs (cisplatin, carboplatin)	Leukemia, lymphoma, multiple myeloma, sarcoma and lung, breast, ovary and testicular cancers	Long-term damage to the bone marrow (except platinum drugs)	Cheung-Ong et al., 2013; Rang et al., 2015; Kelland, 2007.
Antimetabolites (block the synthesis of DNA and/or RNA)	Folate antagonists (methotrexate, pemetrexed) Pyrimdine pathway (cytarabine, decitabine, 5-fluorouracil, gemcitabine) Purine pathway (fludarabine, 6-mercaptopurine, pentostatin, tioguanine)	Leukemia, breast, ovary, gastrointestinal and other cancers	Potent myelosuppression	Rang et al., 2015; Cheung-Ong et al., 2013.
Topoisomerase inhibitors (dysregulation of DNA topology with induction of DNA cleavage)	Topoisomerase I inhibitors (topotecan, irinotecan) Topoisomerase II inhibitors (etoposide, teniposide)	Leukemia, lung, ovarian, gastrointestinal, and other cancers	Topotecan and irinotecan have low toxicity	Rang et al., 2015; Cheung-Ong et al., 2013.
Mitotic inhibitors (bind tubulin, stabilize microtubules)	Vinca alkaloids (vinblastine, vincristine, vinorelbine) Taxanes (paclitaxel, docetaxel) Others (ixabepilone, estramustine)	Breast and lung cancers, myelomas, lymphomas, and leukemias	Cumulative neurotoxicity, and in some cases hypersensitivity	Rang et al., 2015; www.cancer.org
Glucocorticoids (inhibit lymphocyte proliferation)	Prednisolone, dexamethasone	Leukemia and lymphoma	Also used to prevent side effects (nausea, vomiting and hypersensitivity) of chemotherapeutics	Rang et al., 2015.
Antibiotics (inhibit topoisomerase II, interfere with helicase activity, intercalate DNA, crosslink DNA, and other mechanisms)	Anthracyclines (doxorubicin, daunorubicin) Others (dactinomycin, bleomycin, mitomycin)	Breast cancer, small-cell lung tumors, soft tissue sarcomas, lymphomas, and acute lymphoblastic or myeloblastic leukemias	High cardiotoxicity	Minotti et al., 2004; Rang et al., 2015

1.1.3.2. *Targeted anticancer drugs*

These less toxic anticancer drugs inhibit the growth, progression and dissemination of cancer by interfering with specific molecules involved in its pathobiology (Urruticoechea et al., 2010; Chessum et al., 2015). The recognition of the hallmarks of cancer has opened the way to the identification of promising molecular targets in anticancer therapy. These targets include growth factors, signaling molecules, modulators of cell cycle and apoptosis, as well as molecules involved in angiogenesis (Hanahan and Weinberg, 2011). Currently, there are already several targeted therapies in the clinic for the treatment of many cancer types, and many others are in clinical trials waiting for approval (Hay et al., 2014).

Considering the molecular target and the type of agent, anticancer targeted therapies can be divided into several groups: hormone therapies, monoclonal antibody therapies, protein kinase inhibitors, proteasome inhibitors, histone deacetylase inhibitors, and poly (ADP-ribose) polymerase (PARP) inhibitors (Table 1.2).

Hormone therapies are usually used in hormone-sensitive tumors. They can reduce or completely abolish the tumor cell growth by acting as physiological agonists, antagonists or hormone synthesis inhibitors (Table 1.2). The antioestrogen tamoxifen is widely used in the treatment of breast cancer. However, tamoxifen is not devoid of side effects, causing menopause-like symptoms. More severe effects are hyperplastic events in the endometrium, which may progress to cancer and the risk of thromboembolism (Kreipe and von Wasielewski, 2007). Aromatase inhibitors are other class of hormone therapy used in the treatment of breast cancer, which act by suppressing the synthesis of oestrogen from androgens in the adrenal cortex (Rang et al., 2015).

As mentioned above, the overexpression of growth factors is widely frequent in tumors to support tumor growth. The therapeutic monoclonal antibodies can prevent the survival pathways and promote apoptosis by interaction with growth factors (e.g. VEGF), or with the extracellular domain of the growth factors receptors (Table 1.2; Figure 1.4; Rang et al., 2015; Urruticoechea et al., 2010). Furthermore, they can act directly on lymphocyte cell surface proteins as CD20 or CD52, to cause lysis and elimination of lymphocytes in lymphoma and leukemia cases (Rang et al., 2015; Kreipe and von Wasielewski, 2007). Although monoclonal antibodies have less severe side effects, their high cost is still a limitation (Rang et al., 2015; www.cancer.org). Alternatively, the protein kinase inhibitors may inhibit protein kinases preventing the downstream signaling cascade triggered by growth factors (Table 1.2; Figure 1.4). The side effects of this group of drugs differ depending on the drug and the target, but are less aggressive compared to the ones described for the conventional therapy.

Table 1.2. Anticancer targeted therapies grouped according to the molecular target and type of agent.

Group	Classes/targets (examples)	Therapeutic applications	References
Hormone therapies	Gonadotrophin-releasing hormone antagonist (degaralix)	Prostate cancer	Rang et al., 2015
	Oestrogen receptor antagonists (tamoxifen, toremifene and fulvestrant)	Hormone-dependent breast cancer	
	Androgen antagonists (flutamide, cyproterone and bicalutamide)	Prostate cancer	
	Aromatase inhibitors (anastrozole, letrozole and exemestane)	Breast cancer in postmenopausal women	
Monoclonal antibodies	VEGF (bevacizumab)	Colorectal cancer	Rang et al., 2015; Urruticoechea et al., 2010
	EGF receptor (panitumumab, cetuximab)		
	HER-2 receptor (trastuzumab)	Breast cancer	
	CD20 (rituximab) CD52 (alemtuzumab)	Leukemia and lymphoma	Rang et al., 2015; Kreipe and von Wasielewski, 2007
Protein kinase inhibitors	Bcr/Abl, c-kit and PDGF kinases (imatinib, nilotinib)	Chronic myeloid leukaemia	Chessum et al., 2015; Kreipe and von Wasielewski, 2007; Rang et al., 2015; Urruticoechea et al., 2010
	EGF receptor (erlotinib, gefitinib)	Non-small-cell lung carcinoma	
	HER-2 and EGF receptors (lapatinib)	Breast cancer	
	VEGF receptor (axitinib)	Renal cell carcinoma	
	JAK1 and JAK2 kinases (ruxolitinib)	Myelofibrosis	
	Pan-kinase inhibitors (sorafenib, dasatinib, sunitinib)	Different types of cancer	
	mTOR kinase, also classified as pan-kinase inhibitors (everolimus, temsirolimus)		
Proteasome inhibitor	Bortezomib	Myeloma	Rang et al., 2015
Histone deacetylase inhibitors	Vorinostat and romidepsin	Refractory cutaneous T-cell lymphoma	West and Johnstone, 2014
	Panobinostat	Multiple myeloma	www.ema.europa.eu/ema/index
PARP inhibitor	Olaparib	BRCA mutated advanced ovarian cancers	www.fda.gov

The proteasome inhibitor bortezomib selectivelly affect rapidly dividing cells, with small impact on normal cells, making it a useful anticancer agent. The bortezomib inhibits the proteasome by destroying proteins such as growth regulatory proteins, promoting tumor cell death (Rang et al., 2015). The histone deacetylases are critical regulators of gene expression (West and Johnstone, 2014). Thus histone deacetylases inhibitors exert their antitumor effect by changing the expression profile of oncogenes and tumor suppressor genes, through modulation of the histones acetylation state. PARP is involved in DNA repair and its inhibitors cause multiple double strand breaks. In tumors with mutations on DNA reparatory proteins (like BRCAs), these double strand breaks induced by PARP inhibitors cannot be efficiently repaired, what conducts to tumor cell death (Liu et al., 2014b).

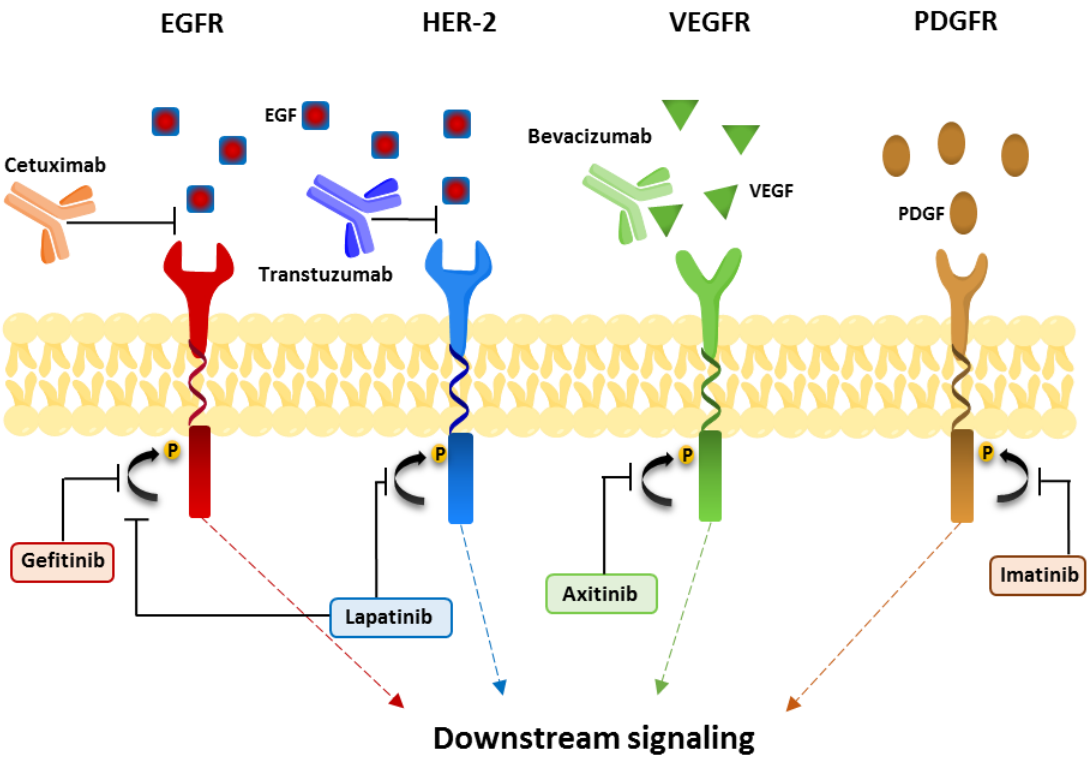

Figure 1.4. Mechanism of action of anticancer monoclonal antibodies and protein kinase inhibitors. Therapeutic monoclonal antibodies can prevent the overexpression of growth factors as EGFR, HER-2 and VEGFR by interacting directly with the receptor itself (e.g. cetuximab, trastuzumab) or with the ligand (e.g. bevacizumab). Protein kinase inhibitors prevent downstream signaling triggered by growth factors by inhibiting protein kinases (e.g. gefitinib, lapatinib, axitinib and imatinib). EGFR, epidermal growth factor receptor; HER, human epidermal growth factor; P, phosphate group; PDGFR, platelet-derived growth factor receptor; VEGFR, vascular endothelial growth factor receptor [adapted from (Rang et al., 2015)].

However, although targeted therapies are a promising way to personalize cancer treatment, leading to less severe side effects and to more effective treatments than the standard chemotherapy, they are currently associated with increased tumor resistance. This resistance can be attributed to the occurrence of mutations on the molecular target and/or to the adoption by cancer cells of alternative growth pathways that are independent of the molecular target. Combination therapy may overcome this limitation, as demonstrated by some clinical studies (Chessum et al., 2015). Actually, targeted therapies have gained strength in combination either with other therapies that target different parts of the cell signaling pathway, or with conventional chemotherapeutic drugs.

The development of targeted therapies requires the identification of targets with a key role in cancer development and mantainance. Proteins expressed by cancer cells, but not by normal cells, would be potential targets, especially if they are involved in cell growth and survival. Another approach to identify potential targets is to determine whether cancer cells express mutant proteins that drive cancer progression. One of such promising target is the p53 tumor suppressor protein.

1.2. The p53 tumor suppressor proteins

In 1979, the p53 protein was discovered in a complex with the simian virus 40 (SV40) large T-antigen (Linzer and Levine, 1979; Lane and Crawford, 1979). At that time the importance of this protein was far from being imagined. Initially, p53 was classified as an oncogene due to the association between the high levels of this protein and the occurrence of tumors (DeLeo et al., 1979; Rotter, 1983). This incorrect idea was supported by other publications during almost ten years (Freed-Pastor and Prives, 2012). Currently, accumulated data clearly demonstrate the tumor-suppressing properties of p53. A very plausible explanation for the first contradictory findings is attributed to the fact that the p53 highly expressed in those tumors was actually a mutant form (Levine and Oren 2009; Freed-Pastor and Prives, 2012).

As a transcription factor, the p53 tumor suppressor protein is able to induce the transcription of many genes controlling crucial stress responses with a major role in preventing malignant transformation. p53 has been recognized as the most frequently inactivated protein in cancer (in about 80% of cancers) (Olivier et al., 2004). In fact, the *TP53* gene is mutated or deleted in approximately half of tumors, and in tumors that retain a wild-type (wt) form, p53 is inactivated due to diverse mechanisms, including the overexpression of endogenous inhibitors, such as the murine double minute (MDM)2 and MDMX proteins (Shadfan et al., 2012; Selivanova, 2014). These findings, together with other evidences from innumerous studies, strongly support the idea that p53 inactivation is a required condition for tumor development and maintenance (Zawacka-Pankau and Selivanova, 2015). Based on this, the p53 protein has been subject of intensive research over the last 30 years. Despite this, many aspects concerning the p53 biology and pharmacology remain unclear.

With the discovery of the p53 family, composed by p53, p63 and p73, with high structural homology, many functions initially attributed to p53 only are now shared by the other family members (Kaghad et al., 1997; Schmale and Bamberger, 1997; Yang et al., 1998; Trink et al., 1998). Still, p53 remains the family member with the highest impact on

tumorigenesis, as demonstrated by knockout mouse models. In fact, while the knockout of p53 leads to increased tumor susceptibility (Donehower et al., 1992), the knockout of p63 or p73 leads to severe developmental abnormalities, but not to increased spontaneous tumors (Yang et al., 1999; Yang et al., 2000). Actually, in the absence of stress, the most important role of p63 and p73 seems to be the regulation of cell differentiation and tissue development (Moll and Slade, 2004). Despite this, it is well-established that p63 and p73 cooperate with p53 in the regulation of tumorigenesis, either in a p53-synergistic or in a p53-antagonistic nature (Moll and Slade, 2004).

1.2.1. Structure of p53

The *TP53* gene is located at the short arm of the chromosome 17p13.1 region. It encodes the p53 protein composed by 393 amino acids (a.a.) with different functional domains encompassing well-defined and natively unfolded regions that form tetramers in a reversible equilibrium (Bell et al., 2002; Veprintsev et al., 2006). The structure of p53 comprises two *N*-terminal transcriptional activating domains (TAD)1 (1-42 a.a.) and TAD2 (43-63 a.a.), a proline-rich domain (64-97 a.a.), a DNA binding domain (DBD, 102-292 a.a.), an oligomerization domain (OD, 323-356 a.a.), and a basic or regulatory domain (363-393 a.a.) (Figure 1.5; Millau et al., 2009).

The TADs are critical for the regulation of p53 activity, because they interact with regulatory proteins such as MDM2 (Momand et al., 1992), components of the transcription initiation complex as human TATA-binding-protein-associated factor TAFII31 (Lu and Levine, 1995), and with acetyltransferases, such as p300 and CBP, which act as co-activators and regulate the p53 function via acetylation (Grossman, 2001). The proline-rich domain contains five PXXP motifs and seems to also have an important role in the regulation of p53 activity, as evidenced by a mice model expressing a truncated p53 (without proline-rich domain) (Toledo et al. 2006). This truncated p53 showed increased sensitivity to MDM2-dependent degradation and decreased transactivation capacity, associated with deficient cell cycle arrest and reduced apoptotic response (Toledo et al. 2006). The DBD is highly conserved and specifically binds to a double-stranded target DNA, allowing the transcription of several target proteins. This region presents a high homology (~60%) to that of p63 and p73 (Wei et al., 2012), what justifies the resemblance of the transcription targets and functions between p53 family proteins. Additionally, the majority of p53 missense mutations occur in this region (Muller and Vousden, 2014). Contrary to the unfolded *N*-terminal, the DBD and OD adopt a well-defined conformation. The OD at the *C*-terminal is essential for the formation of tetramers, which are organized as dimers of p53 (Jeffrey et

al., 1995). The structure of the tetramerization domain has been solved by X-ray crystallography and by nuclear magnetic resonance (NMR) (Jeffrey et al., 1995; Mittl et al., 1998; Clore et al., 1995). These tetramers are known to be the most active transcriptional form of p53. Additionally, the regulatory domain (consisting of a lysine-rich region) is involved both in the positive (by post-translational modifications involving acetylation, methylation, phosphorylation and sumoylation) and negative (by ubiquitination or neddylation) regulation of p53 (Wahl, 2006).

The p53 protein also contains three nuclear localization signals (NLS) at *C*-terminal that specifically bind to nuclear receptors (Shaulsky et al., 1990; Liang and Clarke, 1999), and two nuclear export signal (NES) regions, one localized at TAD and other at *C*-terminal (Stommel et al., 1999; Zhang and Xiong et al., 2001). Both NLS and NES are involved in the regulation of the p53 transcriptional activity through the p53 nuclear/cytosolic shuttling.

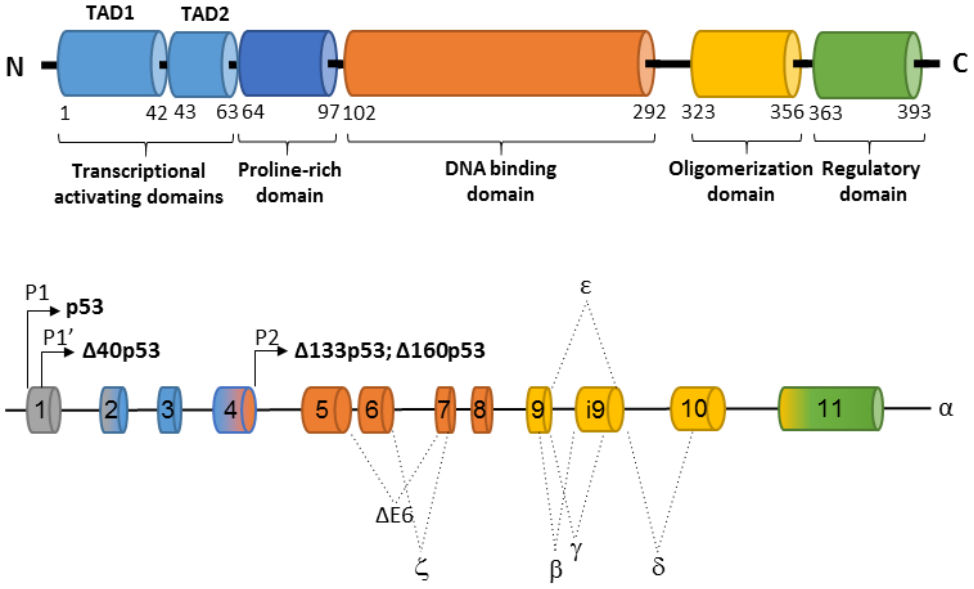

Figure 1.5. Structure of p53 protein and respective isoforms. The structure of p53 comprises two transcriptional activating domains (TAD)1 and TAD2, a proline-rich domain, a DNA binding domain (DBD), an oligomerization domain (OD) and a regulatory domain. Three different *N*-terminal isoforms Δ40p53, Δ133p53 and Δ160p53 can be combined with *C*-terminal isoforms α, β, γ, δ, ε, ζ, ΔE6.

A large variety of p53 transcripts can be found as result of alternative splicing and of the action of different promoters (P1, P1' or P2). Some examples of Δp53 isoforms (without part of the *N*-terminal) are Δ40p53, Δ133p53 and Δ160p53, lacking the first 40, 133 and 160 a.a., respectively (Figure 1.5). Δ40p53, produced by alternative splicing of intron 2 or

internal initiation of translation from codon 40, does not complex with MDM2, but it is able to oligomerize with full-length p53, inhibiting its transcriptional activity (Yin et al, 2002; Courtois et al., 2002). Δ133p53 and Δ160p53 are both regulated by P2, located in intron 4 of the *TP53* gene (Marcel et al., 2011). Moreover, it was described that Δ133p53 expression induces tumor growth progression and angiogenesis in full-length p53-expressing tumors (Bernard et al., 2013*).* Instead, its knockdown increases apoptosis, cell cycle arrest and senescence, what demonstrated the oncogenic properties of Δ133p53 (Fujita et al., 2009; Aoubala et al., 2011). However, in clinic, high Δ133p53 expression levels resulted in a risk reduction of 43% for recurrence and of 64% for death, when compared with low Δ133p53 expression levels in mutant p53-expressing serous ovarian cancers (Hofstetter et al., 2011). Additionally, the clinical relevance of Δ40p53 has been investigated, and its presence has been associated with a favorable prognostic in the mucinous histological subtype of ovarian cancer (Hofstetter et al., 2012). This may be explained by the fact that the *in vivo* effects of these isoforms depend on the p53 status (wt/mutant). In fact, this may indicate that the heteroligomer formation with the isoforms inactivates the p53 function (the p53 wt anti-tumoral or the p53 mutant pro-tumoral effects).

Moreover, the alternative splicing at *C*-terminal originates a diversity of transcripts referred by Greek alphabet letters, leading to seven variants for p53 (α, β, γ, δ, ε, ζ, ΔE6) (Figure 1.5; Wei et al., 2012). Some of these truncated proteins, which lack the oligomerization domain, fail to bind DNA and for this reason are transcriptionally deficient (Murray-Zmijewski et al., 2006). As for TAD truncated isoforms, it was reported that patients whose tumors expressed both mutant p53 and p53γ had a prognosis as good as the wt p53-expressing tumors, while tumors only expressing mutant p53 demonstrated poor prognosis (Bourdon et al., 2011). This suggested that the expression of p53γ may abrogate the poor prognosis commonly associated with *TP53* mutations. However, exception made for α, β and γ, very few studies addressed the other transcripts (Wei et al., 2012).

Despite this, more studies about the biology and tumorigenesis of these isoforms, particularly taking into consideration different cellular contexts, isoforms expression levels and p53 status, are required.

1.2.2. Functional aspects of p53

Under no stress conditions, p53 is maintained at low levels not interfering with the cell fate. Nevertheless, as transcription factor, p53 regulates the cell homeostasis, acting on biological processes such as metabolism, cell differentiation, immune response, among others (Aylon and Oren, 2011; Suzuki and Matsubara, 2011).

In response to stress signals, such as DNA damage and oxidative stress, the activation of p53 leads to the transcription of several genes involved in apoptosis, DNA repair, cell cycle arrest or senescence (Figure 1.6), in order to suppress genetic mutations and to prevent the accumulation of abnormal cells that can lead to tumors (Vousden and Prives, 2009; Aylon and Oren, 2011; Martinez et al., 2010). However, beyond triggering classical responses, p53 can modulate several additional cellular processes that are relevant to suppress tumor development. This includes opposing oncogenic metabolic reprogramming and stem cell self-renewal, and limiting the invasion, metastasis and angiogenesis, promoting communication within the tumor microenvironment and immunosurveillance (Figure 1.6; Vousden and Prives, 2009).

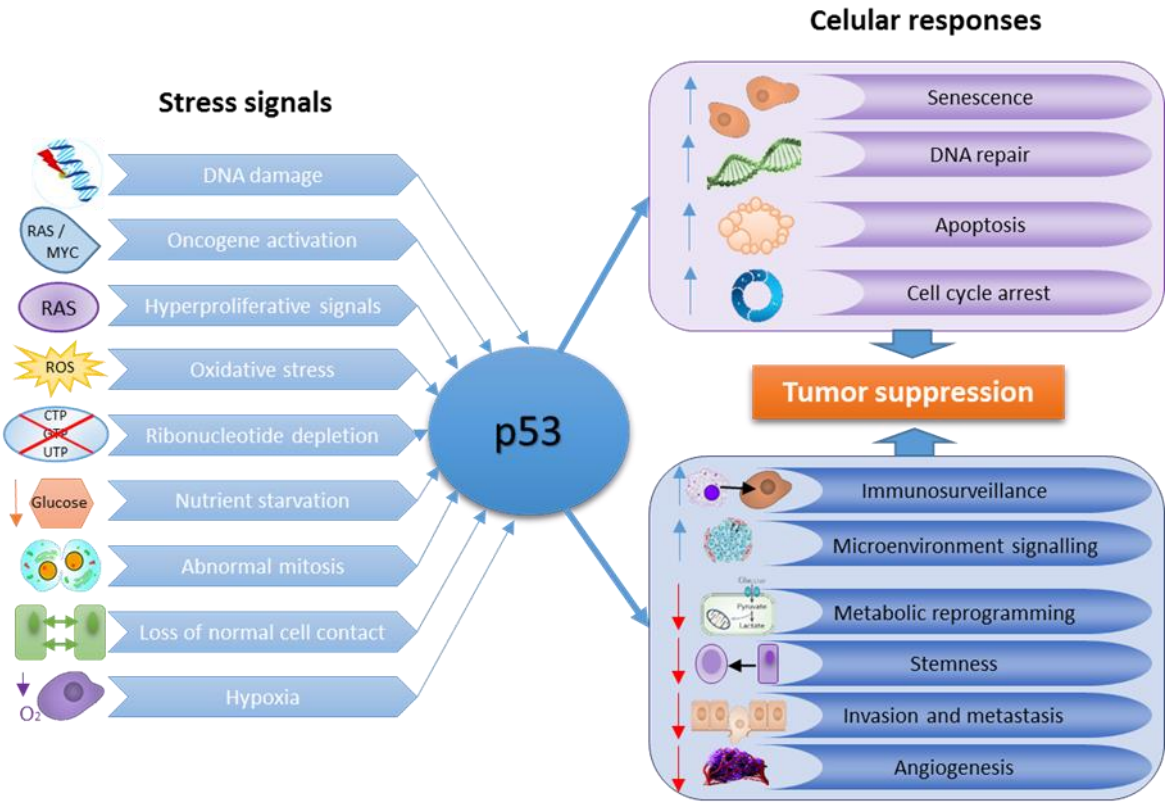

Figure 1.6. Overview of p53-activating stress signals and key cellular responses promoted by p53 for tumor suppression [adapted from (Bieging et al., 2014)].

The p53 response depends on the type, severity and persistence of the stress (Maddocks and Vousden, 2011). Indeed, under low stress levels that cause reparable damage, p53 induces cell cycle arrest and activates the DNA repair machinery to promote cell survival. However, in case of irreparable damage caused by high stress levels, p53

drives cellular senescence or irreversible apoptosis (Maddocks and Vousden, 2011). This justifies that in tumors with inactivated p53, cells are resistant to apoptosis and able to survive (Amaral et al., 2010). It should be noted that for certain types of cellular stresses, such as starvation and metabolic stress, the p53 activation triggers different cellular pathways such as the antioxidant response and autophagy (Mollereau and Ma, 2014). One of the first mechanisms proposed to determine cell fate was the amount of p53 after stress induction. Actually, it was demonstrated that low p53 levels correlate with cell cycle arrest, while high p53 levels with apoptosis (Chen et al., 1996; Kracikova et al., 2013). Thereafter, it was revealed different p53 DNA binding affinities for the different target genes (Resnick-Silverman et al., 1998). Taken together, it was proposed that under low levels of p53, this protein preferentially binds to high-affinity target genes (involved in cell cycle arrest). Conversely, under high p53 levels, more p53 is available to bind to low-affinity target genes (involved in apoptosis) (Resnick-Silverman et al., 1998; Inga et al., 2002; Weinberg et al., 2005). Additionally, it seems that the binding to apoptosis-inducing genes requires the cooperative p53 DNA binding to multiple binding sites (Schlereth et al., 2010; Timofeev et al., 2013). This justifies that some mutant p53 only induce cell cycle arrest and senescence and not apoptosis (Schlereth et al., 2010; Timofeev et al., 2013). Another mechanism of regulation is mediated by p53 recruited cofactors through the differential transcription of downstream genes. For example, p53 recruits the cofactor ASPP1 (apoptosis-stimulating of p53 protein 1), which can promote the p53 binding to the promoters of the pro-apoptotic Bcl-2 associated X *(BAX)* or p53-inducible protein 3 (*PIG3*), but not to the Cyclin-Dependent Kinase Inhibitor 1A (*CDKN1A*; responsible for cell cycle arrest) promoter (Samuels-Lev et al., 2001). By contrast, the p53 binding to the protein inhibitor of ASPP (iASPP) activates genes that mediate cell cycle arrest (Bergamaschi et al., 2006).

The regulation of cell fate by p53 post-translational modifications, such as phosphorylation, acetylation and ubiquitination, has been also shown to be determinant. For example, in response to DNA damage, the phosphorylation of p53 at Ser46 seems to promote the transcription of pro-apoptotic genes, such as p53-regulated apoptosis-inducing protein (p53AIP) (Oda et al., 2000).

Additionally, p53 has an important role in the regulation of the expression of several microRNAs that contribute to cell fate decision, either promoting cell cycle arrest (e.g. miR107; Böhlig et al., 2011) or apoptosis (e.g. miR-200c; Schickel et al., 2010). In turn, some microRNAs may control the expression levels and activity of p53, both directly, such as miR-125b that suppresses apoptosis by blocking the expression of p53 (Le et al., 2009), or indirectly, such as miR-143/145 that regulates the MDM2 expression (Zhang et al., 2013; Otsuka and Ochiya, 2014).

Despite all these data, the molecular mechanism responsible for the switch between survival (cell growth arrest) and death (apoptosis) is still not well understood. Therefore, more studies, particularly around the regulatory transcriptional pathways of p53 target genes, are still required.

1.2.2.1. *The p53 function under reparable stress*

As described above, under low stress conditions, the cell tends to follow cell cycle arrest with activation of the DNA repair machinery to preserve its viability. The inhibition of cell cycle progression is one of the most important functions of p53.

The cell cycle is a highly controlled process composed by four phases: Mitosis (M), Gap1 (G1), Synthesis (S), and Gap2 (G2). This process allows cell division, with DNA replication (S phase), and the duplication of cell population (Nurse, 2000). To prevent the transmission of DNA errors to the daughter cells, cell cycle is regulated by three principal checkpoints: one between G1 and S phases, other in the S phase, and the last one between G2 and M phases. Cyclin-dependent kinase (CDK) complexes are responsible for the regulation of G1/S and G2/M checkpoints, and their activity is regulated by the respective cyclins (Nurse, 2000). One important regulator of the cell cycle is the family of E2F transcription factors, which control the expression of many key proteins required for proliferation. In G1 phase, the E2F protein is linked to the hypophosphorylated retinoblastoma protein (Rb). After G1 restriction point, cyclin E/CDK2 and cyclin D/CDK4/6 complexes start the Rb phosphorylation and, when hyperphosphorylated, E2F is dissociated from Rb in order to promote the progress of cell cycle to the next phase (S) by activation of the E2F transcriptional program (Amundson et al., 1998; Chellappan et al., 1991).

Depending on the type of cellular stress, p53 can induce either G1 arrest or G2/M transition arrest. p53 promotes the transcription of the *CDKN1A* gene, which encodes p21, a CDK inhibitor. The overexpressed p21 binds to cyclin E/CDK2 complex, inhibiting the Rb phosphorylation and the subsequent cell cycle progression at G1 phase (Figure 1.7; Adams et al., 1996; Chen et al., 1996). Additionally, p21 is involved in the inhibition of cyclin D/CDK4/6 complexes, which also prevents the Rb phosphorylation (Figure 1.7; el-Deiry, 1998). On the other hand, p53 is able to inhibit the cyclin E by induction of hCDC4b, an F box protein component of the Skp1–Cul1–F-box-protein (SCF) ubiquitin ligase complex that promotes the ubiquitin-mediated degradation of phosphorylated cyclin E (Kimura et al., 2003). The p21 protein has also an important role in p53-mediated G2/M arrest. This protein

also interacts with cyclin B/CDK1 complex, blocking the phosphorylation and subsequent activation of CDK1 (Smits et al., 2000).

Additionally, p53 induces the overexpression of Growth Arrest and DNA Damage inducible 45 (GADD45) and 14-3-3σ proteins (Figure 1.7). GADD45 binds to CDK1, inhibiting the cyclin B/CDK1 complex formation and its subsequent kinase activity (Zhan et al., 1999). Moreover, high levels of 14-3-3σ remove the cyclin B/CDK1 from the nucleus, physically separating cyclin B/CDK1 from its target proteins (Hermeking et al., 1997). As such, these two proteins promote the inhibition of cyclin B/CDK1 function, inducing G2/M cell cycle arrest.

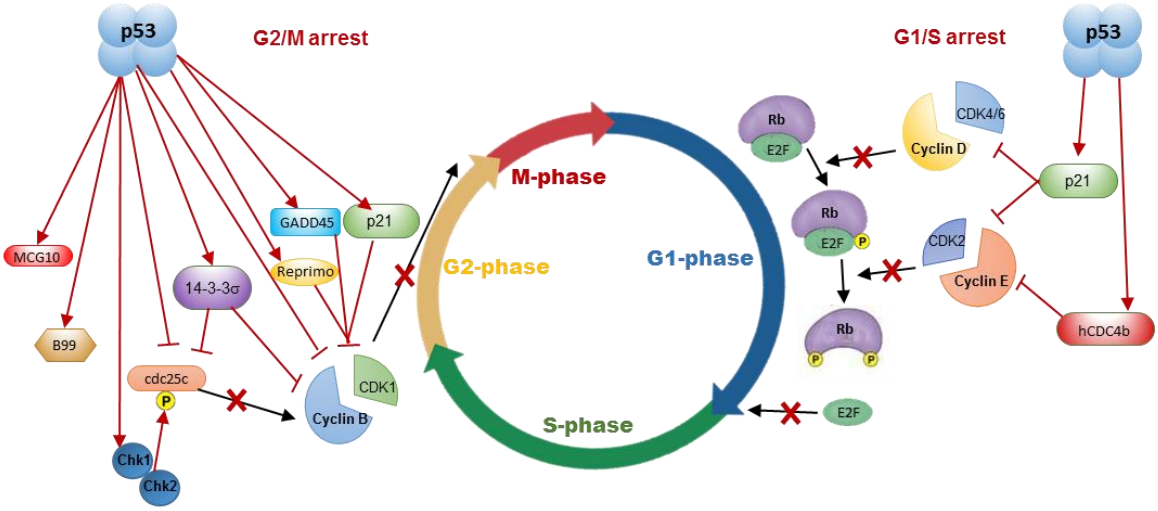

Figure 1.7. Regulation of cell cycle by p53. Under normal conditions, the cyclin/CDK complexes are functional and Rb is hyperphosphorylated, leading to the release and activation of the E2F transcriptional factor, and to G1 and G2 progression. When activated, p53 induces (red lines) the transcription of p21 and hCDC4b, which inhibit cyclin/CDK complexes, resulting in the accumulation of hypophosphorylated Rb and in the subsequent inhibition of E2F activity, resulting in G1-phase arrest. In G2/M arrest, p53 directly downregulates the expression of cyclin B and promotes the expression of p21, GADD45, Reprimo and 14-3-3s, which inhibit the cyclin B/CDK1 complex formation. p53 also controls the G2 arrest by inhibition of Cell division cycle 25 homolog C (Cdc25C) and by induction of B99 and MCG10; P: phosphorylation.

There are other genes regulated by p53, whose induction promotes G2/M arrest, like *MCG10* (encodes a RNA-binding protein), *Reprimo* (encodes a glycosylated protein that promotes the cytoplasmic localization of cyclin B/CDK1) and *B99* (encodes a protein that

may cause G2/M arrest independently of CDK1) (Figure 1.7; Zhu and Chen, 2000; Ohki et al., 2000; Utrera et al., 1998). Moreover, it was reported that p53 represses the expression of important proteins involved in the progression of cell cycle from G2 to M phase, like CDK1, cyclin B and Cdc25c (Taylor et al., 2001; Krause et al., 2000; Yun et al., 1999). In addition to the repression of the expression of Cdc25C (a mitosis promoting phosphatase that activates the cyclin B1/CDK1 complex) by p53, the Cdc25C activity can be inhibited via phosphorylation by checkpoint kinases, Chk1 and Chk2, both activated by p53. This, in turn, generates a consensus binding site for 14-3-3σ protein, allowing this protein to exert its negative effect (Figure 1.7; Taylor and Stark, 2001).

After entered in a cell cycle arrest stage, p53 is able to promote the DNA repair through transcriptional activation of *GADD45* and *p53R2* genes (Smith et al., 1996; Yamaguchi et al., 2001). Together, GADD45 and p53R2 proteins, assist the DNA repair response contributing to the p53-mediated genetic stability.

1.2.2.2. *The p53 function under irreparable stress*

Under severe DNA damage, cells may be eradicated via activation of programmed cell death pathways, particularly apoptosis. However, high stress conditions can also lead to senescence (permanent cell cycle arrest that can culminate in phagocytosis) (Xue et al., 2007).

Apoptosis is considered a “clean” death that does not stimulate an inflammatory response. It is typically characterized by chromatin condensation and fragmentation, membrane blebbing and mitochondrial swelling. The dying cell or cell body is finally recognized and engulfed by phagocytosis (Edinger and Thompson, 2004). There are two primary apoptotic pathways, the extrinsic and the intrinsic, although both converge into the same terminal or execution pathway. The extrinsic pathway starts with the binding of external ligands to death receptors, such as type 1 of tumor necrosis factor receptor (TNFR1), Fas (also called CD95/Apo-1), and TNF-related apoptosis-inducing (TRAIL) (Jin and El-Deiry, 2005; Guicciardi and Gores, 2009). These receptors send signals that activate caspase 8, with the induction of apoptotic events (Figure 1.8; Ryan, 2011). Inflammatory states, and others extracellular events, are responsible for the stimulation of this pathway. In contrast, the intrinsic mitochondrial pathway is dependent on intracellular stimulus, like genotoxic stress and the unfolded protein response (Ryan, 2011). In this pathway, members of the Bcl-2 family, with an important role in mitochondria membrane permeability, are responsible for the regulation of cytochrome *c* (cyt *c*) release from mitochondria. The released cyt *c* interacts with apoptosis protease-activating factor 1 (Apaf-1), forming a

complex recognized as apoptosome that leads to caspase-9 activation, followed by the subsequent activation of caspases 3, 6 and 7 (Figure 1.8; Yip and Reed, 2008).

The crucial role of p53 in apoptosis regulation was first demonstrated *in vivo,* in a choroid plexus epithelial tumor model (Symonds et al., 1994). In this model, they showed that the inactivation of p53 abolished apoptosis and promoted tumor growth. Some genes that are regulated by p53 transcriptional activity are essential for triggering extrinsic and intrinsic apoptotic pathways (Figure 1.8). Regarding to extrinsic pathway, p53 increases the expression levels of Fas, death receptor 5 (DR5/Killer, a TRAIL receptor), and of p53-induced protein with a death receptor domain (PIDD) (Amaral et al., 2010). p53 can also trigger this pathway enhancing the cell surface levels of Fas, by promoting its traffic from Golgi complex (Bennett et al., 1998).

In the intrinsic mitochondrial apoptotic pathway, p53 is responsible for the increase of the expression levels of several proteins of the Bcl-2 family, as BAX and Bcl-2-antagonist/killer (BAK; Figure 1.8). Other p53 transcription target proteins are p53 upregulated modulator of apoptosis (PUMA) and NOXA, which are involved in apoptosis incitation. PUMA binds to mitochondrial anti-apoptotic proteins, such as Bcl-2, Bcl-XL, Bcl-W, Mcl1 and Bcl-2-related protein A1 (Bcl-2A1), inhibiting their activities. Instead, NOXA only binds to Mcl1 and Bcl-2A1 (Khoo et al., 2014). p53 can also stimulate the intrinsic apoptotic pathway via activation of factors, like Scotin, that causes cellular perturbations such as endoplasmic reticulum stress, which ultimately leads to an intrinsic cell death response (Figure 1.8; Bourdon et al., 2002). Additionally, p53 can activate the apoptosome via induction of Apaf-1 expression (Moroni et al., 2001).

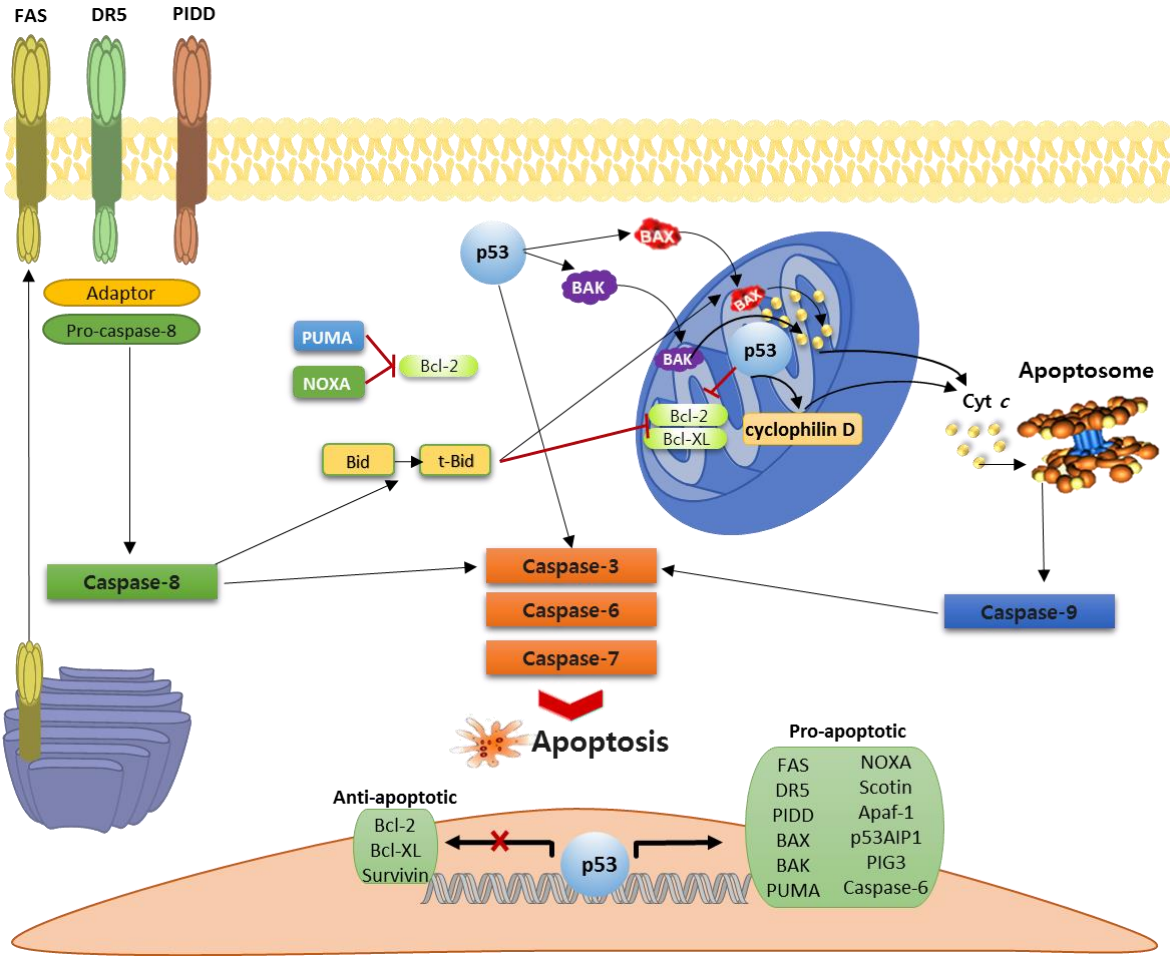

Figure 1.8. Regulation of intrinsic and extrinsic apoptotic pathways by p53. The p53 protein regulates the apoptotic process by inducing and repressing the transcription of pro-apoptotic and anti-apoptotic proteins, respectively. Additionally, p53 has a transcriptional-independent function in both apoptotic pathways. In the extrinsic pathway, p53 induces the expression of FAS, DR5 and PIDD, promoting the recruitment of the adaptor molecule, which binds to procaspase-8 leading to caspase-8 activation. Activated caspase-8 directly activates the executioner caspases 3, 6, and 7, with subsequent BH3 interacting-domain death agonist (Bid) cleavage. Additionally, p53 promotes the translocation of FAS from Golgi complex to cell surface. In the intrinsic pathway the stress-induced mitochondrial translocation of p53 results in interactions between several anti- and pro-apoptotic members of the Bcl-2 family to induce mitochondrial outer membrane permeabilization (MOMP) and cyt *c* release. Indeed, p53 interacts with Bcl-XL/Bcl-2 blocking their inhibitory effect on BAX. Besides, p53 upregulates the transcription of proteins, such as PUMA and NOXA that bind to and inhibit the activity of Bcl-2. The release of cyt *c* from mitochondria results in the formation of the apoptosome that activates caspase-9. The activation of the executioner caspases 3, 6 and 7 by caspase 9 leads to cell death.

Many other proteins involved in apoptosis are transcriptionally regulated by p53, the majority of them are pro-apoptotic being overexpressed, such as PIG3 and tumor p53 regulated apoptosis inducing protein 1 (p53AIP1; Figure 1.8). Some examples of anti-apoptotic proteins downregulated by p53 are Bcl-2, Bcl-XL and survivin (Figure 1.8; Harms et al., 2004; Riley et al., 2008; Hoffman et al., 2002). Another relevant p53 transcriptional target is Bid, which is responsible for the link between the extrinsic and intrinsic apoptotic pathways. In fact, the cleavage of Bid by caspase 8 promotes its translocation to mitochondria, where it triggers the intrinsic apoptosis by activation of BAX and BAK, and by inhibition of Bcl-2 and Bcl-XL (Figure 1.8; Sax et al., 2002).

Despite the relevance of its transcriptional activity, p53 has also crucial transcriptional-independent pro-apoptotic functions. In fact, besides its nuclear localization, p53 can be also found in cytoplasm and mitochondria. Several factors can influence the localization of p53, namely its tetramerization, which prevents the nuclear exportation of p53 by masking its *C*-terminal NES (Stommel et al., 1999). Furthermore, post-translational modifications and protein-protein interactions have been demonstrated to be crucial to p53 mitochondrial translocation, such as the MDM2-mediated p53 multi-mono-ubiquitylation and the p53 phosphorylation at Ser46 (Marchenko et al., 2007; Sorrentino et al., 2013). After activation, p53 translocates to mitochondria, where it induces BAX and BAK oligomerization, physically interacts with Bcl-XL and Bcl-2 inhibiting their anti-apoptotic effects, and forms a complex with cyclophilin D, leading to mitochondrial outer membrane permeabilization (MOMP) (Wolff et al., 2008). Moreover, in cytoplasm, p53 can induce homo-oligomerization of BAX, followed by BAX mitochondrial translocation (Chipuk et al., 2004).

Moreover, p53 can directly affect the executioner caspases 3 and 6 (Figure 1.8). In fact, it was shown that p53 induces caspase-6 expression, and it interacts with pro-caspase-3 enhancing caspase 3 activation (MacLachlan and El-Deiry, 2002; Frank et al., 2011). Although numerous studies about the role of p53 in apoptosis have been published in the last years, the contribution of p53 transcription-dependent and -independent activities to the cell fate needs further elucidation.

Despite the reported antioxidant properties of p53 (Sablina et al., 2005), when p53 is overexpressed in a stress-induced apoptotic pathway, an increase of reactive oxygen species (ROS) can also be found. In fact, high levels of ROS have been detected before MOMP and cyt *c* release (Fleury et al., 2002). Additionally, besides its role in apoptosis induction, the p53 transcriptional target PIG3 has been implicated in the accumulation of ROS (Polyak et al., 1997).

Multiple factors, such as the type and intensity of the cellular stress, tissue type, and cellular microenvironment, may determine if a cell stays in cell cycle arrest as a permanent form, or if it follows apoptotic death. Cellular senescence is another mechanism of tumor suppression, characterized by an irreversible cell cycle arrest by blocking malignant transformation (at the initial step of tumorigenesis) and by clearance of cancer cells (at the late stage of tumor progression) (Rufini et al., 2013). The p53 activity in senescence is mainly mediated by its transcription targets p21, plasminogen activator inhibitor 1 (PAI-1), promyelocytic leukemia protein (PML) and embryo chondrocyte expressed 1(DEC1) (Rufini et al., 2013; Kortlever et al., 2006; Barboza et al., 2006). However, other proteins were described to be involved in this process. For instance, due to the accumulation of p53 and p16, the expression of the oncogene ras results in cellular senescence (Serrano et al., 1997). Despite the involvement of senescence in tumor suppression, targeting this effect is opposed by the cost of accelerated aging. Actually, the challenge to develop senescence-based cancer therapy is to disclose the targets and pathways that control the balance between cancer and longevity (Qian and Chen, 2013).

1.2.3. Regulation of p53 by MDM2 and MDMX

The p53 inactivation can lead to tumor development, or the own tumor can provide the perfect conditions to the inactivation of p53. In tumors that retain wt p53, this protein can be inactivated by overexpression of its negative regulators MDM2 and MDMX (also called MDM4) (Zawacka-Pankau and Selivanova, 2015). In fact, transgenic mice overexpressing MDM2/MDMX (MDMs), either globally or in a specific tissue, develop spontaneous tumors, what established a connection between the overexpression of these two proteins and tumor onset (Jones et al., 1998; Ganguli et al., 2000; Xiong et al., 2010). The overexpression of MDMs occurs in at least 10% of total human tumors (Toledo and Wahl, 2006). The degree of overexpression of these two proteins differs among the different types of tumors, and their expression is not related, what suggests specific roles for MDM2 and MDMX in tumorigenesis (Toledo and Wahl, 2006). For example, MDM2 is overexpressed in 24% to 56% of osteosarcomas, 45% to 75% of brain glioblastomas, 33% to 41% of prostate cancers, while MDMX is overexpressed in 65% of cutaneous melanomas, 60% of retinoblastomas, 50% of hepatocellular carcinomas, 5% of breast cancers, and 4% of glioblastomas (Rayburn et al., 2005; Riemenschneider et al., 1999; Danovi et al., 2004; Laurie et al., 2006; Gembarska et al., 2012). Importantly, the deletion of MDM2 and MDMX results in embryonic lethality, which is completely rescued, in both

cases, by concomitant *p53* loss (Jones et al., 1995; Parant et al., 2001). These data confirm the MDMs function and show the significance of these two negative regulators of p53.

The *MDM2* gene encodes a 491 a.a. protein with several domains (Figure 1.9). The MDM2 protein contains an *N*-terminal domain that comprises the p53 binding site, an acidic domain capable of interacting with the tumor suppressor p14/ARF (that inhibits the MDM2-mediated degradation of p53), a zinc finger domain that mediates MDM2's interaction with ribosomal proteins and its ability to degrade p53, and a RING finger domain with the E3-ligase activity responsible for p53 ubiquitination (Lee and Gu, 2010). MDM2 also contains the NLS and NES regions, responsible for shuttling MDM2 between the nucleus and cytoplasm (Iwakuma and Lozano, 2003).

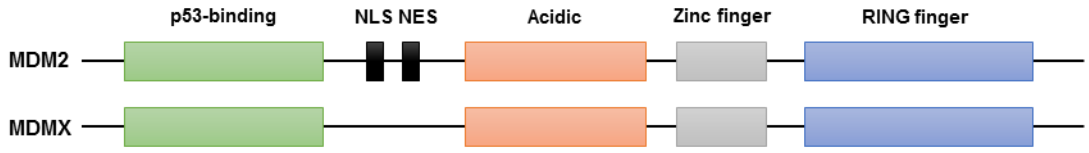

Figure 1.9. Structure of MDM2 and MDMX proteins. Domains: p53 binding, acidic, zinc finger, and RING finger. NLS, nuclear localization signal; NES, nuclear export sequence.

Under normal conditions, there is an auto-regulatory feedback loop between p53 and MDM2 (Figure 1.10). Actually, p53 promotes MDM2 expression by binding to the P2 promoter of the *MDM2* gene. In turns, MDM2 binds to the *N*-terminal transactivation domain of p53 inhibiting its transcriptional activity and promoting its monoubiquitination. The p53 monoubiquitination enhances the nuclear export of p53 and can also endorse the polyubiquitination and subsequent degradation by proteasome (Figure 1.10; Michael and Oren, 2003; Zawacka-Pankau and Selivanova, 2014). In addition, MDM2 may negatively affect the p53 mRNA translation (Ofir-Rosenfeld et al., 2008).

Under stress conditions, the p53 stabilization can result from an inefficient p53-MDM2 binding, or from the inhibition of the MDM2 E3-ligase activity by stress-induced interactions of MDM2 with other proteins. For example, p14/ARF, whose expression increases in response to oncogenic stress, can bind to MDM2 inhibiting its ubiquitin ligase activity on p53 (Honda and Yasuda, 1999). Similarly, ribosomal proteins L5, L11 and L23 can also interact with MDM2 inhibiting its E3 function (Lohrum et al., 2003; Dai and Lu, 2004; Dai et al., 2004).

MDMX is an MDM2-related protein with high homology to MDM2, particularly in the *N*-terminal (Shvarts et al., 1996). However, MDMX has no NLS and NES domains (Figure 1.9). Like MDM2, MDMX binds with high affinity to the *N*-terminal transactivation domain of p53, inhibiting its transcriptional activity (Figure 1.10). However, contrary to MDM2, MDMX does not target p53 for degradation, because the RING domain lacks the E3-ligase activity (Stad et al., 2001). Despite this, the hetero-oligomerization of MDMX with MDM2, through RING finger domains, increases the efficiency of MDM2 E3-ligase activity towards p53 (Figure 1.10; Wade et al., 2013). Interestingly, in mice with MDMX RING domain alterations, it was shown that the MDM2 interaction with MDMX through this RING domain is required for modulating the p53 activities, in embryonic stages. However, it has shown to be dispensable for MDM2 and p53 stabilization in adult mouse (Pant et al., 2000; Huang et al., 2011). Upon DNA damage stimuli, MDM2 degrades itself and can also directly ubiquitinate and degrade MDMX (Nag et al., 2013).

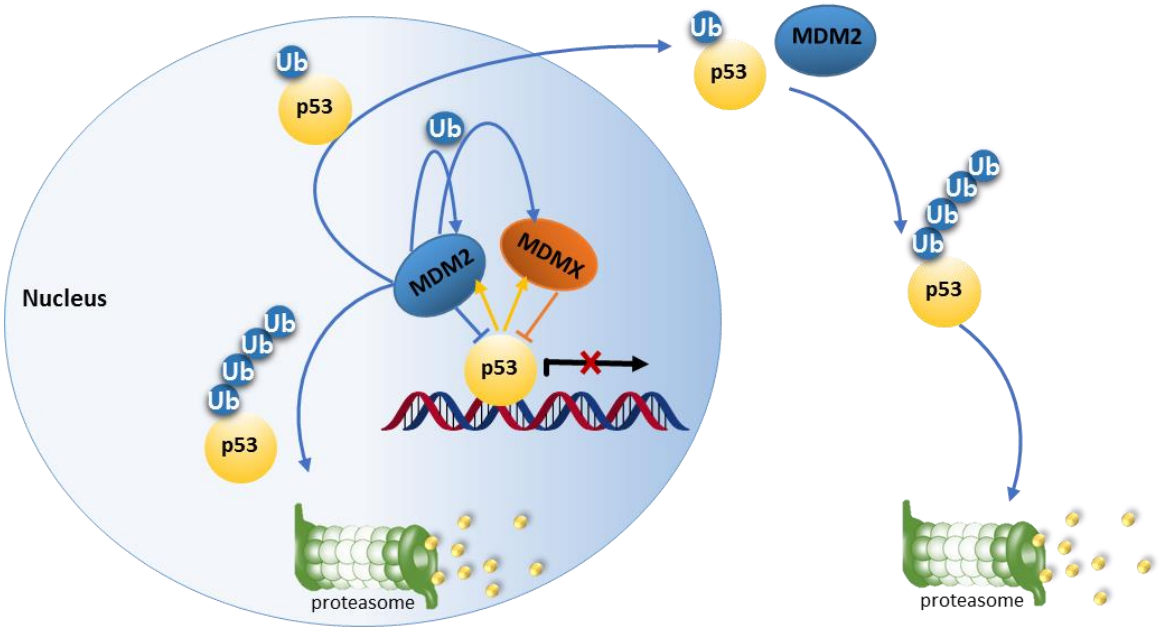

Figure 1.10. Regulation of p53 by MDM2 and MDMX. p53 is responsible for the regulation of MDM2 and MDMX transcription levels (yellow arrows). In turn, MDM2 and MDMX cooperate to inhibit the p53 transcriptional function. MDM2 also promotes p53 nuclear export to the cytoplasm for ubiquitin-mediated degradation by proteasome. Additionally, MDM2 can promote the nuclear degradation of p53 (polyubiquitination), MDMX ubiquitination and its own ubiquitination and degradation. Ub: ubiquitin.

Recently, it was discovered that, similarly to MDM2, also MDMX can establish an auto-regulatory feedback loop with p53 (Figure 1.10). The p53 protein can bind to a functional p53-binding site in MDMX intron 1, increasing the MDMX expression (Li et al., 2010a). Furthermore, it was discovered that, like MDM2, also MDMX contains a P2 promoter that is regulated by p53. Activated p53 induces the expression of a MDMX transcript from the P2 promoter that encodes a novel "long-form" of the protein. Curiously, this long-form of MDMX appears to function with MDM2 promoting p53 ubiquitination during recovery from stress (Phillips et al., 2010).

The overexpression of MDM2 in tumor cells can result from gene amplification, increased mRNA stability, enhanced translation, altered post-translational modification, or from the presence of a single nucleotide polymorphism at position 309 (SNP309) in the P2 promoter of MDM2 (creating an additional binding site for the transcriptional activator Sp1 enhancing MDM2 expression) (Li and Lozano, 2013; Bond et al., 2004).

Similar mechanisms of overexpression to those described for MDM2 have been found for MDMX. However, no corresponding of SNP has been observed in MDMX (Schlaeger et al., 2008; Valentin-Vega et al., 2007; Laurie et al., 2006).

In addition to the overexpression of MDMs, the expression of more stable isoforms can be also observed. For example, the *MDM4-S* transcript produces a MDMX isoform containing the p53-binding domain, but lacking the negative regulatory sites, which are more stable and oncogenic than the full-length MDMX. Thus, the overexpression of MDMX-S has been associated with decreased survival and poor prognosis in cancer patients (Li and Lozano, 2013).

Although the major functions of MDM2 and MDMX are associated with p53, emerging data have suggested that these two proteins may also have p53-independent roles, namely in the regulation of genomic instability, apoptosis and metastasis, contributing to tumor formation and progression (Li and Lozano, 2013).

Taking into consideration that MDMs overexpression correlates with poor clinical prognosis and with poor response to current cancer therapies (Zhao et al., 2015), it is important to develop new therapeutic alternatives targeting both MDM2 and MDMX, for a full reactivation of p53 tumor cells.

1.2.4. Mutant p53

The *TP53* gene is the most commonly mutated gene in human cancers (Kandoth et al., 2013). Although p53 mutations can be found in all regions of the protein, only the most frequent mutations has been deeply studied (Leroy et al., 2013). In fact, more than 80% of

somatic and germline *TP53* mutations are missense that lead to stable mutant proteins (Soussi and Wiman, 2015). The missense mutations, characterized by the substitution of a single amino acid in the p53 protein, commonly occur within the DBD region, particularly in six hotspot residues (175, 245, 248, 249, 273, 282) (Figure 1.11). The frameshift or nonsense mutations occur with less frequency, and in some cases, they result in the loss of p53 protein expression (Muller and Vousden, 2014). It is important to note that more than 90% of p53 mutations are located in the core domain of the protein, affecting all p53 protein isoforms (Leroy et al., 2014). Due to the high fragility of the core domain, which can be easily destabilized by amino acid substitutions, at least five occurrences of each mutation and up to 2,000 for hotspot mutations can be observed in independent tumors (Figure 1.11; Leroy et al., 2014; Soussi, 2011).

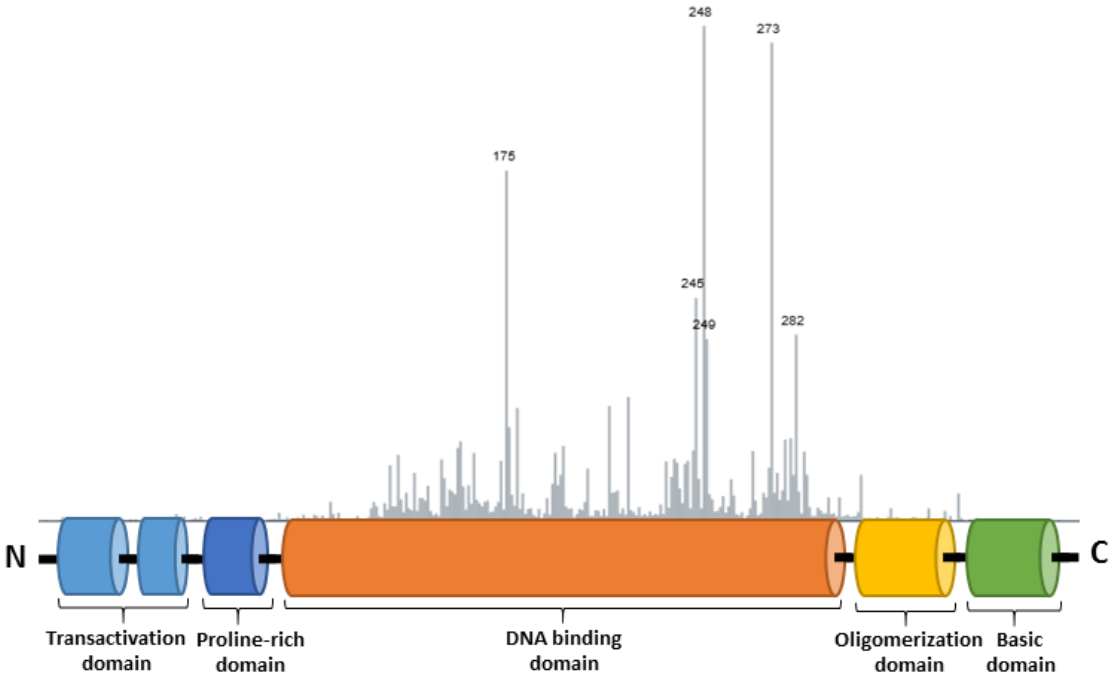

Figure 1.11. Distribution of somatic mutations by codon in p53. The peaks indicate the relative frequency of cancer-associated mutations for each residue according to IARC *TP53* Database. Missense mutations, at hotspot codons located in the DNA binding domain of p53, are the most frequent alterations in human cancers [adapted from (version R17 2013; Petitjean et al., 2007b)].

The missense p53 mutations can be classified as structural (e.g., R175H, Y220C) or DNA contact (e.g., R273H, R280K), based on whether they lead to a protein conformational change, or simply affect its DNA binding ability with no profound structural alterations, respectively (Khoo et al., 2014). Nuclear magnetic resonance, circular dichroism and X-ray diffraction analyses have confirmed and expanded this description, suggesting that multiple

thermodynamic stages may be associated with the various mutations depending on their position (Wong et al., 1999; Bullock et al., 1997; Cho et al., 1994). Interestingly, these studies also confirmed that even some contact mutants are unfolded to some degree (Bullock et al., 1997). Despite the differences, both types of mutations modify the ability of p53 to interact with DNA, leading to the loss of wt p53 transcriptional activity (Khoo et al., 2014; Zawacka-Pankau and Selivanova, 2015).

Different tumor types show different spectra of *TP53* mutations. For example, in high-grade serous ovarian cancer, the frequency of *TP53* mutation is higher than 90%, in colorectal, head and neck cancers it ranges from 50% to 70%, while in haematopoietic malignancies it is lower than 10% (Leroy et al., 2014; Soussi and Wiman, 2015; Olivier et al., 2010). The different mutation rates can be related with the mutagenic event that leads to tumor development or with geographic factors. The frequency of missense mutations also differs in different subclasses of tumors of the same organ. For example, almost all basal breast tumors carry p53 truncations, while luminal breast cancers frequently carry point mutations in *TP53* (Dumay et al., 2013).

Whereas somatic *TP53* mutations contribute to sporadic cancer, germline mutations cause a rare type of cancer predisposition, known as Li–Fraumeni Syndrome. In this syndrome, the residues 248 and 273 are the most commonly mutated, and it is characterized by the early onset of tumors as sarcomas, osteosarcomas, breast carcinomas and leukaemias (Malkin et al., 1993). Patients with this disease and heterozygous for mutant *TP53* allele have a 50% risk for developing tumors by the age of 30, and a 90% risk after 70 years old (Malkin et al., 1993). Importantly, both somatic and germline *TP53* mutations are usually followed by loss of heterozygosity during tumor progression, which suggests that a selective force inactivates the remaining wt allele (Brosh and Rotter, 2009).

Under unstressed conditions, the wt p53 is a very short-lived protein, while p53 mutations provide a prolonged half-life. For this reason, wt p53 appears at lower levels in heterozygous cells. The hyperstability of mutant p53 can be attributed to its inability to act as a transcription factor and to induce sufficient levels of MDM2 for p53 ubiquitination and degradation (Li et al., 2011b). In fact, a complete lack of ubiquitination of mutant proteins was demonstrated in a large survey of tumor cells expressing wt and mutant p53, leading to mutant protein stabilization (Li et al., 2011b).

However, beyond this loss-of-function (LOF), that is based on the loss of normal transcriptional activity, accumulating evidence supports that some of these mutant p53 have additional oncogenic activities, collectively referred as mutant p53 dominant-negative effect (DNE) and gain-of-function (GOF) (Figure 1.12). Despite the complexity to study each of these valences, it is important to considerer that different mutants show a distinct profile

towards them (Halevy et al., 1990; Petitjean et al., 2007b). Moreover, DNE and GOF events are usually associated with more aggressive tumor profiles, characterized by increased metastasis and resistance to anticancer treatments, and, consequently, with poor prognosis (Muller and Vousden, 2014).

1.2.4.1. *Functional activities of mutant p53: LOF, DNE and GOF*

In 1997, tumor suppressor genes were defined as genes that sustain LOF mutations in the development of cancer (Haber and Harlow, 1997). Today, although LOF is still being the main characteristic of tumor suppressor genes, we know that this definition is not complete. The Haber and Harlow definition does not take into account the heterogeneity of the different protein variants, or other activities such as DNE on wt protein or GOF.

Numerous studies about LOF of mutant p53 have been carried out. The majority of them are based on the analysis of p53 transcriptional activity. In fact, the transcriptional analysis of 2500 mutant p53 on 8 different target genes, representative of different *TP*53 functions, demonstrated heterogeneous prevalence of the various mutant p53 with more than 50% presenting only partial loss of activity (Kawaguchi et al., 2005; Kakudo et al., 2005; Shiraishi et al., 2004; Kato et al., 2003). However, the most prevalent mutant p53 demonstrated a completely loss of their transcriptional function.

Besides LOF, in a p53 heterozygous environment, many stable mutant p53 are able to exert a DNE on the remaining wt p53, preventing its normal activity. The DNE can be observed through formation of mutant/wt p53 cotetramers (Chan et al. 2004), by the incorporation of wt p53 into mutant p53 supratetrameric aggregates (Xu et al. 2011), or by preventing wt p53 from binding to the promoter of its target genes (Willis et al., 2004; Figure 1.12). The DNE has been experimentally studied in yeast, human cells and mouse models. To date, there is information about DNE for over 200 mutants. These studies supported the notion that DNE property is correlated with cancer occurrence, being DNE promoter- and cell-type dependent (Dearth et al., 2007).

The first systematic study to evaluate the DNE of mutant p53 was performed in yeast, and measured the ability of 35 mutants to inhibit the transcriptional activity of wt p53 on its consensus response element (RE) (Brachmann et al., 1996). Latter, it was found that 80% of the most common mutant p53 have the capacity to exert DNE over wt p53, compared to only 45% of the less frequent mutants studied. This suggests that DNE plays a role in the selection of mutant p53 in sporadic cancers (Petitjean et al. 2007a). Interestingly, it was observed a correlation between LOF and DNE (Dearth et al., 2007), which was in

accordance with the finding that mutant p53 alleles with partial-function have not a DNE over wt p53 (Shi et al., 2002).

Importantly, it was demonstrated that the inactivation of wt p53 by DN mutants depends on several factors: the wt to mutant subunit ratio within the heterotetramers, the conformation of the mutant protein, the DNA affinity of mutant subunits present in the heterotetramers, and the DNA binding site (Chène, 1998).

The DNE is correlated with some types of cancer and with some aggressive tumor profiles. For example, DN mutation of the *TP*53 gene was related to serous adenocarcinoma (Sakuragi et al., 2001), to early recurrence of oral cancer (Hassan et al., 2008), and to accelerated development and/or growth of glioblastomas (Marutani et al., 1999). Despite the relevance of the DN classification of mutant p53 to the clinical outcome of some types of cancer, in carriers of germline p53 mutations, the transactivation-based classification of p53 alleles seems to be more important for genotype/phenotype correlations than the DN classification (Monti et al., 2011). The GOF was firstly suggested in 1993 with the observation of a new phenotype with the induction of mutant p53 expression in p53-null cells (Dittmer et al., 1993). Since then, many GOF have been described for different mutant p53. *In vivo* evidences, namely from mutant p53-expressing mice, have shown a tumor profile that is more aggressive and metastatic than p53-null or wt p53 mice (Doyle et al., 2010; Lang et al., 2004; Morton et al., 2010; Olive et al., 2004).

Contrary to what happens for DNE, no systematic studies have been performed to distinguish mutant p53 with GOF properties. In fact, current studies about GOF have only considered one or a small group of mutant p53 proteins and a GOF property. Although some mechanisms of GOF may be shared by a group of mutant p53 proteins, it has become clear that each individual mutant p53 may act on its own specific way, while they may converge to affect the same pathway (Muller and Vousden, 2014). According to different works published to date, some examples of mechanisms by which mutant p53 may exert their GOF are: genomic instability, the activation of genes normally unaffected or repressed by wt p53, the interference with other transcription factors, the interaction with other proteins, and the modification of miRNAs expression (Figure 1.12; Oren and Rotter 2010). These GOF activities contribute to tumor development by enhancing cell proliferation, migration, invasion, angiogenesis, metabolic changes and chemoresistance (Figure 1.12; Muller and Vousden, 2014).

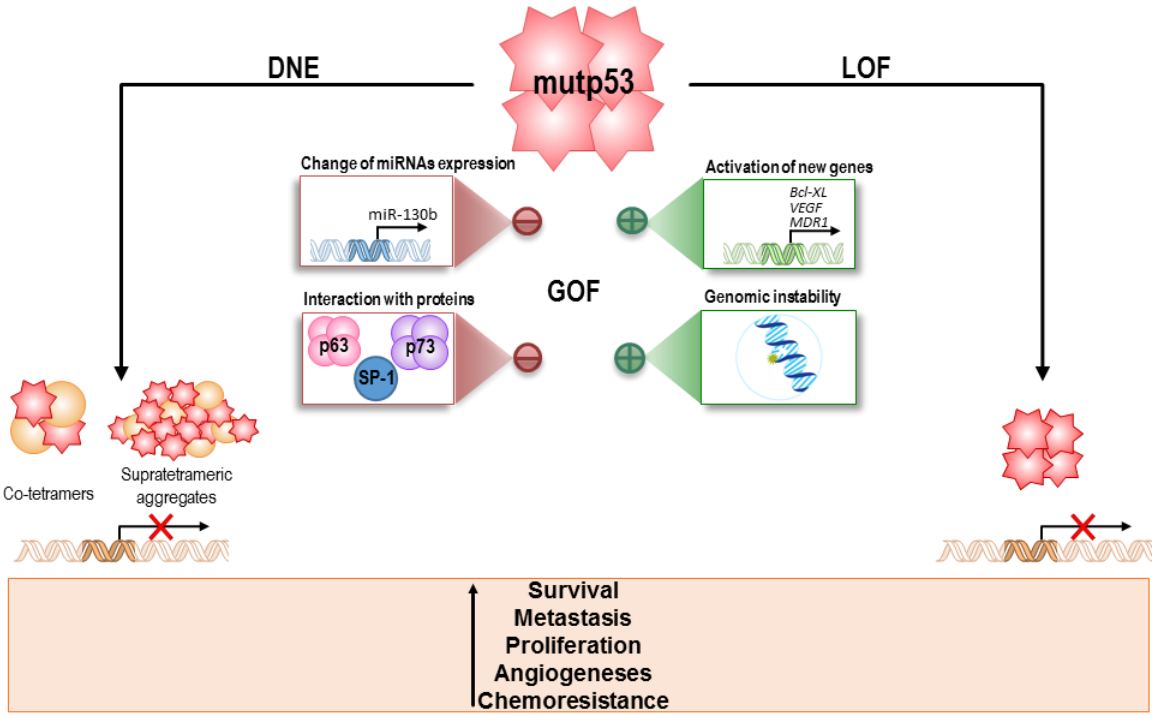

Figure 1.12. Functional activities of mutant p53: dominant-negative effect (DNE), loss-of-function (LOF) and gain-of-function (GOF).

Although mutant p53 proteins are generally characterized by LOF due to their incapacity to bind to consensus p53 DNA binding regions in target gene promoters, it seems that they have the ability to regulate the gene expression by binding to DNA with some degree of selectivity (Weisz et al., 2007; Brázdová et al., 2013; Göhler et al., 2005; Quante et al., 2012). One example is the transcription activation of the multidrug resistance 1 (MDR1) gene, responsible for drug resistance in mutant p53-expressing cancers (Lin et al., 1995). Additionally, mutant p53 has been involved in the regulation of genes, such as FAS, Bcl-XL and VEGF, which are key proteins in apoptosis and angiogenesis (Zalcenstein et al., 2003; Bossi et al., 2008; Khromova et al., 2009). Besides the direct regulation of gene expression, mutant p53 is able to interact with transcription factors as p63 and p73 (Liu et al., 2014a). These interactions deplete the p63 and p73 transcriptional activity and, consequently, their ability to prompt growth suppression and apoptosis. Additionally, these interactions seem to be highly involved in migration, invasion, metastasis and chemoresistance (Di Como et al., 1999; Strano et al., 2002; Gaiddon et al., 2001; Bergamaschi et al., 2003; Liu et al., 2014a). In fact, the p63 inhibition by mutant p53 triggers a pro-invasive transcription program involving the expression of Dicer, DEPDC1, Cyclin G2 (through interaction with Smad), and Sharp1 (through interaction with Pin1) (Adorno et al.,

2009; Girardini et al., 2011). However, it was shown that the loss of *TAp63* alone is less potent in inducing metastases compared to the effect of mutant p53 expression in the presence of *TAp63* in a mouse model of pancreatic ductal adenocarcinoma. This suggests additional functions of mutant p53 besides inhibiting p63 (Tan et al., 2014). Moreover, mutant p53 may interact with other proteins, such as the MRE11-Rad51-NSB complex (recruit ATM kinase to double-strand breaks) and SP-1, impairing their activities to induce proliferation, genomic instability, or chemoresistance (Chicas et al., 2000; Song et al., 2007). The genomic instability was further supported in a recent analysis of 3000 tumors showing that *TP*53 mutations were strongly associated with a high frequency of copy number changes (Ciriello et al., 2013). Additionally, numerous studies using xenograft mouse models demonstrated that mutant p53 enhances invasion and motility, through modification of the signaling of receptors such as transforming growth factor β (TGF-β), EGF, and MET (Adorno et al., 2009; Grugan et al., 2013; Muller et al., 2009; Muller et al., 2013; Wang et al., 2013). Moreover, a recent report highlights an important function of mutant p53 in promoting the inflammatory environment of colorectal tumors, by protracting NF-kB activation and cell survival (Cooks et al., 2013). Other important GOF property of mutant p53 is the contribution to tumor initiation via enhanced generation and expansion of cell populations with stem cell/cancer stem cell properties (Yallowitz et al., 2015; Hanel et al., 2013; Sarig et al., 2010). In the last years, a new mechanism of GOF has been described, which consists in the ability of mutant p53 to regulate the expression of certain miRNAs to gain new oncogenic activities. For example, mutant p53 binds to the promoter of miR-130b and inhibits its transcription. As negative regulator of ZEB1, miR-130b promotes epithelial-mesenchymal transition and cancer cell invasion in endometrial cancer (Dong et al., 2013).

In conclusion, accumulated data have demonstrated the relevant contribution of mutant p53 to tumor proliferation, survival, limitless replication, cell death resistance, evading growth suppression, sustained proliferative signaling, genomic instability, inflammation, migration, invasion, angiogenesis, and metastasis. This provides to mutant p53 a central role in tumorigenesis, with impact on all cancer hallmarks (Solomon et al., 2011; Freed-Pastor and Prives, 2012; Girardini et al., 2014). Moreover, the high frequency of *TP53* mutation, the poor prognostic of patients with mutant p53-expressing cancers, and the high amount of mutant p53 in tumors, make mutant p53 a promising target for the development of new anticancer therapies. Besides this, the *TP53* status can give relevant clinical information about patient's prognosis. In fact, in clinical studies, p53 mutation is found to be associated with resistance to radiotherapy and chemotherapy and with poor survival rates (Robles and Harris, 2010).

1.3. Targeting the p53 pathway

Several mouse models have demonstrated that the reactivation of p53 results in tumor regression with no evidence of toxicity in normal tissues (Xue et al., 2007; Martins et al., 2006; Ventura et al., 2007; Zawacka-Pankau and Selivanova, 2015). This together with the correlation between inactive p53 pathways and aggressive tumor phenotypes and poor prognosis, as well as the key role of p53 in central processes related to tumor development and progression has become p53 one of the most appealing therapeutic targets in cancer, Actually, in contrast with the majority of anticancer therapies, acting on p53 will allow to attack all cancer hallmarks (Luo et al., 2009; Solomon et al., 2011; Hanahan and Weinberg, 2011). Additionally, the high protein levels of mutated p53 in tumors and the high frequency of the inactive p53 pathway in cancer, makes this protein a selective target in cancer treatment (Zawacka-Pankau and Selivanova, 2015).

Moreover, the functional integrity of the p53 pathway showed to be essential for the action of several conventional chemotherapies, particularly for the chemotherapeutics that act on DNA, such as doxorubicin, etoposide, and cisplatin. In fact, several reports have demonstrated the increased resistance of tumors with deleted or mutated p53 to this type of conventional anticancer therapies (Do et al., 2012; Dunkern et al., 2003; Chee et al., 2013). Considering that the therapeutic outcome of many tumors is highly dependent on these chemotherapeutics (the only therapeutic option for many types of tumors) the reestablishment of the normal status of p53 is therefore an effective strategy to overcome this chemoresistance.

After p53 has been recognized as an ideal anticancer therapeutic target, several strategies to reactivate the p53 pathway have emerged, including: wt p53 delivery or oncolytic gene therapy, elimination of p53 mutant-expressing cells by p53-based vaccines, therapies based on elimination of mutant p53, activation of p53 by inhibiting histone deacetylases, synthetic lethality, inhibition of p53-MDMs interactions, and restoration of wt function to mutant p53 (Figure 1.13; Hong et al., 2014). Actually, in last years, an impressive number of p53-based therapies have emerged, with several drugs in clinical trials and new lead compounds under development.

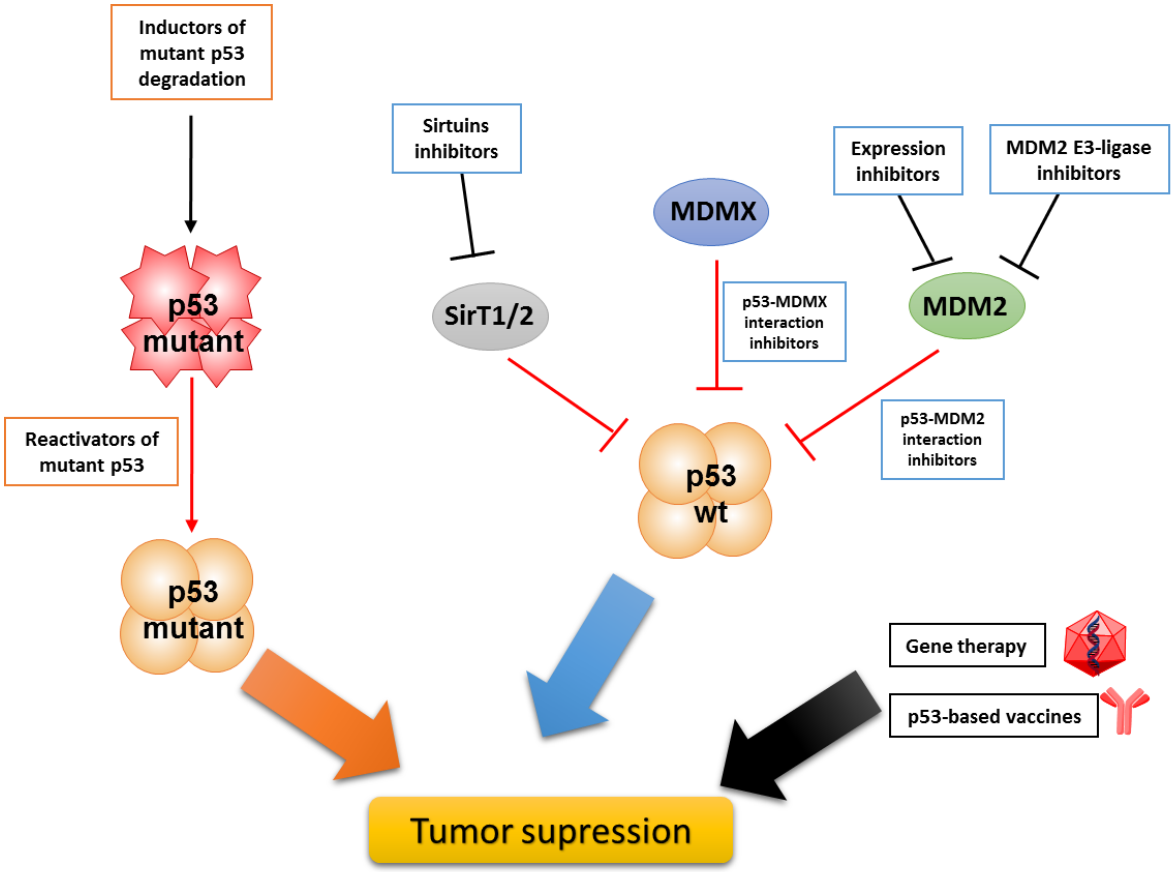

Figure 1.13. Different strategies for activation of the p53 pathway.

Gene therapy is a recent approach that has been explored for the treatment of many diseases. The delivery of wt p53 by adenovirus into cancer cells has been shown to be a promising strategy to rescue the p53 activity in cancer (Hong et al., 2014). This approach uses virus as vector, which maintain the capacity to allow the input of new genetic material into the cell but lacking, at the same time, certain early proteins for replication (preventing the infection). In China (Gendicine) and in USA (ADVEXIN), this therapy was tested in clinical trials for the treatment of several cancers, demonstrating to be advantageous when combined with radiotherapy in the treatment of hepatocellular carcinoma and nasopharyngeal carcinoma (Yang et al., 2010; Pan et al., 2009). However, this approach has some limitations, namely the incapacity to infect all cancer cells due to the limitation of virus delivery, and the reduction of adenovirus infectivity by host antibodies (Hong et al., 2014). Currently, just China approved the Gendicine for clinical use in combination with radiotherapy. FDA did not approve the ADVEXIN due to some cases of tumor resistance (Golubovskaya and Cance, 2013). Other gene therapy approach was developed to eliminate tumor cells with deleted or mutated p53, the oncolytic therapy. One example is

the E1B-deleted adenovirus, designated as ONYX-015, which selectively replicates in p53-deficient cancer cells and subsequently lyses the cells (Bischoff et al., 1996). Despite the efficiency of this treatment, particularly in combination with other chemotherapies, FDA did not approve ONYX-015 due to its hepatotoxicity and to difficulties to assess p53-dependent responses versus non-specific effects of virus on tumor (Khuri et al., 2000; Golubovskaya and Cance, 2013).

Taking advantage from tumor specificity and high expression levels in cancer cells, a vaccine was developed against mutant p53. In fact, antibodies against p53 have been found in patients with different types of cancer, which indicates that the human immune system can recognize and respond to tumor-associated p53 (Chada et al., 2003). Two different types of vaccines entered in phase I/II of clinical trials, the p53-SLP (a p53 synthetic long peptide vaccine) for colorectal cancer and the INGN-225 (a p53-modified adenovirus-transduced dendritic cell vaccine) for small cell lung cancer (Speetjens et al., 2009; Chiappori et al., 2010). Both vaccines demonstrated specific anti-p53 immune response without toxicity, and INGN-225 also showed synergistic effects when conjugated with chemotherapy (Speetjens et al., 2009; Chiappori et al., 2010).

The DNE and GOF properties of mutant p53, together with the high expression levels of mutant p53 in tumor cells, led to the development of strategies to eliminate mutant p53. For example, arsenic trioxide, a drug for the treatment of acute promyelocytic leukemia, was found to degrade mutant p53 (Yan et al., 2011). Other strategy to eliminate mutant p53 is based on the inhibition of their conformational stabilizing chaperones. For example, the 17AAG is an inhibitor of HSP90 (a chaperone that interacts with mutant p53), which can decrease mutant p53 levels by destroying the complex of mutant p53 and HSP90 to release mutant p53 for its degradation (Li et al., 2011a). In addition, the SAHA is an inhibitor of histone deacetylase, HDAC6 (a positive regulator of HSP90 chaperone activity), with preferential cytotoxicity for mutant p53-expressing cancer cells due to its ability to degrade mutant p53 by inhibition of the HDAC6-HSP90 chaperone axis (Li et al., 2011b).

Using a yeast genetic screen, tenovins 1/6 were identified as activators of p53 through inhibition of SirT (sirtuin 1 and 2; histone deacetylases) (Lain et al., 2008). The inhibition of SirT1 and 2 by tenovins results in increased acetylation of p53, at lysine-382, and in p53 subsequent activation. Despite the potent *in vivo* antitumor activity of tenovins, the mechanism of action may be independent of p53 (Lain et al., 2008).

An alternative strategy is the exploration of cell-specific vulnerabilities imposed by alterations in p53 status. In fact, several studies have reported that cells that have lost functional p53 exhibit specific functional dependencies on several secondary pathways that could be targeted in therapy. In this way, in cells with deleted or mutated p53, it is possible

to inhibit crucial proteins regulators of vital pathways, in order to cause cell death (synthetic lethality). A well-studied example of synthetic lethal interactions involves p53 and the ATR/Chk1 pathway. Cancer cells deficient on p53 become dependent on G2/M cell cycle arrest for DNA repair and survival. Therefore, targeting the ATR/Chk1 pathway that regulates G2/M progression with small-molecule inhibitors, the synthetic lethality can be conducted in p53 null or mutant p53-expressing cancer cells (Nghiem et al., 2001; Gurpinar and Vousden, 2015). Actually, the combination of the selective Chk1 inhibitor AZD7762 with irinotecan (a topoisomerase I inhibitor), in early-passage human-in-mouse (HIM) models of triple-negative breast cancer, significantly enhanced the therapy response and prolong survival in mice bearing p53-deficient tumors (Ma et al., 2012). Although the synthetic lethality has been already applied in clinic for other proteins, as PARP inhibitors in the treatment of breast cancer with mutated BRCAs, concerning to p53, clinical studies with this principle has not been performed yet.

The other two approaches, inhibition of p53-MDMs interactions and restoration of wt function to mutant p53, since they are the basis of this thesis, will be discussed in the following subsections.

1.3.1. Inhibition of MDMs and of their interactions with p53

Until now, several approaches to inhibit MDM2 and MDMX have been described. Using anti-sense oligonucleotides to decrease MDM2 expression, it was possible to reduce xenograft tumors in mouse models (Sato et al., 2000; Zhang et al., 2005). Despite these promising results, the high promiscuity of siRNAs, as well as problems related with delivery and cellular uptake, made this approach not feasible to apply in clinical studies. However, the recent identified benzofuroxan derivative XI-066 (NSC207895) and the pseudourea derivative XI-011 (NSC146109), which inhibit the MDMX expression by MDMX promoter inhibition, increased the expectations around this strategy (Wang et al., 2011b, Wang and Yan, 2011).

Other group of agents that inhibit the MDM2-dependent ubiquitination of p53, preventing the p53 degradation, was also developed. The first compound identified was the HDM2 ligase inhibitor 98 class (HLI98), a 7-nitro-5-deazaflavin, that inhibits the E3-ligase activity of MDM2, leading to p53 stabilization and apoptosis in tumor cells. Later, an optimized derivative, HLI373, was identified, showing improved solubility and potency. Additionally, the natural compounds Lissoclinidine B (Clement et al., 2008) and Sempervirine (Sasiela et al., 2008) were also identified as inhibitors of the MDM2 E3 ubiquitin ligase activity. The JNJ-26854165 (Serdemetan), a p53 activating tryptamine

derivative, was initially described as an E3 ubiquitin ligase inhibitor (Arts et al., 2008). Due to its potent antitumor activity, JNJ-26854165 entered into phase I clinical trials, but it is no longer in clinical development (Yu et al., 2014).

However, the most explored approach, due to its high efficacy and safety, has been the development of chemical agents that inhibit the p53-MDMs interactions. Particularly, the inhibition of the p53 interaction with MDM2 has been the most extensively studied strategy. The characterization of the crystal structure of the p53-MDM2 interaction was fundamental to the structure-based design of small molecule inhibitors of this interaction. Moreover, with the characterization of the crystal structure, three critical a.a. in the p53-MDM2 interaction (*LEU26*, *TRP23* and *PHE19*) were identified, which were the focus of chemical library screens from which emerged Nutlin-3a (Vassilev et al., 2004).

Nutlin-3a, a cis-imidazoline, is a potent and selective p53-MDM2 interaction inhibitor, which binds to the deep hydrophobic p53-binding pocket of MDM2 (Vassilev et al., 2004). The disruption of the p53-MDM2 interaction by Nutlin-3a increases the p53 expression and functional activity, leading to cell cycle arrest and apoptosis in both human tumor cells and xenograft mouse models (Vassilev et al., 2004). Nutlin-3a does not bind to MDMX; therefore it fails to activate p53 in MDMX-overexpressing tumor cells (Hu et al., 2006; Patton et al., 2006). Later, the optimized compound RG7112, from Nutlin family, was identified as a potent and selective p53-MDM2 interaction inhibitor with oral bioavailability (Tovar et al., 2013). In human xenograft models, RG7112 inhibits the tumor growth in a wt p53-dependent manner (Tovar et al., 2013). RG7112 is currently in phase I of clinical trials (Table 1.3; Yu et al., 2014).

Together with Nutlin-3a, the Sulfonamide I (NSC279287) was the first described p53-MDM2 interaction inhibitor. This compound was a fairly weak inhibitor of the p53-MDM2 interaction, with a low impact on p53 transcriptional function even for high concentrations (Galatin and Abraham, 2004).

The benzodiazepinediones are benzodiazepine derivatives that disrupt the p53-MDM2 interaction in a similar manner to nutlins, by binding to the p53-pocket of MDM2 (Grasberger et al., 2005). The optimized benzodiazepinediones TDP521252 and TDP665759 show to stabilize p53 and to increase the p53 transcriptional activity, leading to the reduction of proliferation of wt p53-expressing tumor cells (Grasberger et al., 2005; Koblish et al., 2006; Parks et al., 2006). Additionally, TDP665759 showed *in vivo* antitumor activity (Koblish et al., 2006).

The spiro-oxindoles (MI compounds) were design to interact with MDM2, mimicking the p53 a.a. side chains to interact with the p53-binding pocket of MDM2 (Ding et al., 2006). One of the most potent MI inhibitors initially described was MI-63, and its optimization

resulted in MI-219, which inhibited the tumor growth *in vivo* by oral administration (Shangary et al., 2008). The followed derivative of MI-219 was MI-319 that shows efficient tumor growth suppression of lymphoma cells (Mohammad et al., 2009). Several optimizations of MI-319 led to SAR405838, currently in phase I of clinical trials for patients with advanced wt p53-expressing cancers (Table 1.3).

The isoindolinones represent other family of p53-MDM2 interaction inhibitors that block the p53-binding pocket of MDM2 (Hardcastle et al., 2006). The compound 74a was the most potent isoindolinone described to date. Despite this, it exhibited a lower binding affinity to MDM2 than Nutlin-3a (Hardcastle et al., 2011). The piperidinone AM-8553 also demonstrated to inhibit the p53-MDM2 interaction (Bernard et al., 2012). A further optimization of this compound led to AMG 232 with improved potency, *in vivo* antitumor activity in mice, and pharmacokinetic profile (Sun et al., 2014). The substitution of the piperidinone core by a morpholinone led to compounds with further improved antitumor activity and better pharmacokinetics, such as AM-8735 (Gonzalez et al., 2014).

In 2013, the compound RG7388, with a pyrrolidine core, was identified as p53-MDM2 interaction inhibitor (Ding et al., 2013). This compound binds to MDM2 and induces cell cycle arrest and cell death in both human tumor cells and mice. Due to its high efficacy, this compound is under clinical trials (Table 1.3; Ding et al., 2013). The optimized molecules RO5353 and RO2468 were identified as more potent, selective and orally active in the treatment of human osteosarcoma xenografts in mice (Zhang et al., 2014b).

RITA (reactivation of p53 and induction of tumor cell apoptosis) was identified as an inhibitor of the p53-MDM2 interaction that binds to p53, causing a consequent conformational change (Issaeva et al., 2004), although crystal structures failed to confirm this (Krajewski et al., 2005). Besides its effect on wt p53, RITA also suppresses the growth of different tumors with mutant p53 (Zhao et al., 2010). In fact, it remains unclear how RITA can activate both wt and mutant p53.

Many other small molecules have been described as inhibitors of the p53-MDM2 interaction, such as terphenyl compounds 2 and 6 (Chen et al., 2005), the quinolinole NSC66881 (Lu et al., 2006), the chromenotriazolopyrimidine 1 (Allen et al., 2009), the isoquinolinones PXN727 and PXN822 with *in vivo* antitumor activity by oral administration (Yuan et al., 2011), the pyranoxanthone 1 (Leão et al., 2013c), the dihydroisoquinolinone derivative NVP-CGM097 that is under clinical trials (Table 1.3; Holzer et al., 2015), the spirooxadiazoline oxindole 1a (Ribeiro et al., 2015), the chalcone 2 (Leão et al., 2015b) and the fluspirilene (Patil et al., 2015). Finally, some peptides have been described that bind to the p53-binding pocket on MDM2 thereby preventing the interaction of p53 with MDM2 with subsequent p53 activation (Bernal et al., 2007; Baek et al., 2012). However, despite the

huge number of small molecule inhibitors of the p53-MDM2 interaction that have been described so far, only few have reached clinical trials (Table 1.3).

Although adressed in much less studies, the inhibition of the p53-MDMX interaction is currently recognized as important as the inhibition of the p53-MDM2 interaction. Additionally, due to differences in their p53-binding pockets, small molecule MDM2 inhibitors have shown very low binding affinity to MDMX (Li and Lozano, 2013). Interestingly, high expression levels of MDMX are known to confer tumor cell resistance to MDM2-inhibitors. Just recently, the first small molecule inhibitor of the p53-MDMX interaction, called SJ-172550, was identified (Reed et al., 2010). This compound establishes a reversible covalent complex with MDMX and induces p53-dependent cytotoxic effects in tumor cell lines (Reed et al., 2010).

However, the simultaneous inhibition of the p53 interaction with MDM2 and MDMX (p53-MDMs) showed to be the most successful strategy for a full reactivation of wt p53 in tumors. Despite this, very few dual inhibitors of p53-MDMs interactions have been reported. The pyrrolopyrimidine-based compound 3a, which increases p53 and p21 expression levels and triggers apoptosis through a p53-dependent pathway in tumor cells (Lee et al., 2011), and the cis-imidazoline derivative H109, which reactivates a p53-dependent pathway in tumor cell lines (Qin et al., 2014), showed to inhibit the p53-MDMs interactions through binding to both MDMX and MDM2. Graves and colleagues (2012) identified the high soluble indolyl hydantoin RO-5963, which binds to the p53-binding pockets of both MDM2 and MDMX, by inducing the formation of dimeric protein complexes, and leads to p53-dependent cell cycle arrest and apoptosis in wt p53-expressing tumor cells overexpressing MDMX (Graves et al., 2012). The imidazoyl-indole WK298 was also identified to share similar binding modes for MDMX and MDM2, but cause only minimal induced-fit changes in the structures of both proteins (Popowicz et al., 2010). Nevertheless, WK298 demonstrated a moderate binding affinity to MDMX (Popowicz et al., 2010), and no data are available about its antitumor activity. Additional studies are still required to clarify whether or not WK298 is a dual p53-MDMs inhibitor. Recently, the 2,3'-bis(1'H-indole) scaffold demonstrated to be active as dual inhibitor of p53–MDMs interactions with high affinities, however there are no available data about its antitumor activity (Neochoritis et al., 2015).

Many peptide derivatives have been described as dual inhibitors. However, for most of them, their efficacies in tumor cell lines remain to be elucidated (Hu et al., 2007; Czarna et al., 2009; Kallen et al., 2009; Pazgier et al., 2009; Li et al., 2010b). However, recently two peptide derivatives dual inhibitors of p53-MDMs interactions, SAH-p53-8 and ATSP-7041,

demonstrated *in vivo* antitumor effects with low toxicity to normal tissues (Bernal et al., 2010; Chang et al., 2013).

1.3.2. Restoration of wt p53 function to mutant p53

Targeting p53 protein has been shown to be a very difficult task, even more challenging when a diversity of mutations can be found in this protein. The first described reactivator of mutant p53 with antiproliferative effects in mutant p53-expressing human tumor cells was the alkaloid ellipticine and its derivative 9-hidroxy ellipticine (Shi et al., 1998; Sugikawa et al., 1999). However, further studies demonstrated the off-target effects of ellipticine, namely on topoisomerases (Froelich-Ammon et al., 1995). The same happened with WR1065, the active metabolite of amifostine, whose cytotoxicity involves other mechanisms besides the restoration of the wt conformation to mutant p53 V272M (North et al., 2002). The styrylquinazoline CP-31398 and its derivative STIMA-1 are two additional unspecific reactivators of mutant p53. CP-31398 was originally reported to activate wt p53 and mutant p53 V173A and R249S with *in vivo* antitumor effect (Foster et al, 1999). Despite this, more recent studies demonstrated a p53-independent tumor growth-inhibitory effect for CP-31398, likely due to its ability to intercalate with DNA without direct binding to wt or mutant R249S (Rippin et al., 2002; Tanner and Barberis, 2004). Additionally, unfavorable pharmacokinetics and toxicity profiles were reported in rats and dogs for CP-31398 (Johnson et al., 2011).

PRIMA-1 (p53 reactivation and induction of massive apoptosis) is one of the most studied reactivators of mutant p53. Besides the first described reactivation of R175H and R273H (Bykov et al., 2002b), its growth-inhibitory effect in cells expressing other mutant p53 forms have been reported (Bykov et al., 2002a). PRIMA-1 and its more active metabolite, PRIMA-1^{MET} (APR-246), have shown high *in vivo* antitumor activity with no apparent toxicity (Bykov et al., 2002b; Bykov et al., 2005b). Regarding the molecular mechanism of action, it was shown that the metabolites of PRIMA-1/PRIMA^{MET} have a chemical active double bond that covalently react with thiol groups in mutant p53 (Lambert et al., 2009). Recently, the human phase I clinical trial of APR-246 was completed (Table 1.3; Lehmann et al., 2012). APR-246 was well tolerated with a favorable pharmacokinetic profile. Moreover, the side effects observed were reversible and less severe than the conventional chemotherapy without any apparent bone marrow toxicity (Lehmann et al., 2012).

The maleimide-derived molecule MIRA-1 (mutant p53-dependent induction of rapid apoptosis), and its derivative MIRA-3, seem to restore the apoptotic cell death in tumor cells

through reactivation of mutant p53 R175H and R273H (Bykov et al., 2005a). However, a recent study showed that MIRA-1 was highly toxic in normal cells and exhibited p53-independent cytotoxicity, mediated by activation of caspase-9, in tumor cells (Bou-Hanna et al., 2015).

The SCH529074 is other small molecule described as reactivator of mutant p53 (Demma et al., 2010). However, it also binds to the DNA binding domain of p53, blocking the MDM2-regulated ubiquitination of wt p53 (Demma et al., 2010).

PhiKan083 is a carbazole derivative that binds and stabilizes the conformational mutant p53 Y220C (Boeckler et al., 2008). However, this compound does not have *in vitro* antitumor activity. Later, its derivative PK7088 showed to be a reactivator of mutant p53 Y220C with *in vitro* antitumor activity. Despite this, the potency of PK7088 against tumor cells remains very low (Liu et al., 2013).

The thiosemicarbazone NSC319726 was found to specifically reactivate mutant p53 R175H with potent mutant p53 R175H-dependent *in vivo* antitumor activity (Yu et al., 2012). Nevertheless, its mechanism of action is currently unknown despite some clues related with zinc chelating and ROS inducing properties (Yu et al., 2012).

Recently, it was identified chetomin (CTM) as a mutant p53 R175H reactivator through the p53-Hsp40 regulatory axis, causing a potential conformational change to a wt-like p53 (Hiraki et al., 2015). This compound selectively inhibited the *in vitro* and *in vivo* growth of mutant p53 R175H-expressing cancer cells (Hiraki et al., 2015).

Finally, p53R3, a quinazoline, showed to restore the DNA binding ability to mutant p53 R175H and R273H. Furthermore, p53R3 enhances the mRNA expression of numerous p53 target genes in a p53-dependent manner, in glioma cells bearing mutant or wt p53 (Weinmann et al., 2008).

1.3.3. Combination therapy

The combination therapy, to achieve increased cancer cell death, has been considered one of the most promising strategies to minimize the emergence of drug resistance and to achieve maximal therapeutic outcomes with minimal side effects in cancer therapy (Hoe et al., 2014).

As previously referred, promising opportunities to be explored include the combination of targeted therapies with conventional chemotherapeutic drugs, or alternatively of two targeted therapies that may act on the same or on different cell signaling pathways (Zhang et al., 2014a). Particularly, potent synergistic effects have been observed with the association of reactivators of p53 activity with drugs targeting distinct signaling pathways.

For example, a marked stimulation of cell death has been reported with the combination of Nutlin-3 (MDM2 inhibitor) with inhibitors of ATM or MET, as ku-55933 (for ATM) and crizotinib (for MET) (Sullivan et al., 2012). Additionally, the combination of drugs that act on the same pathway with different target proteins can amplify the activation of this pathway and its final effects. For example, the combination of mutant p53-targeting molecules, such as PK7088, with drugs that act on the p53-MDM2 interaction, as Nutlin-3, has also shown promising outcomes, due to the prevention of p53 rapid degradation by MDM2 after p53 reactivation (Liu et al., 2013). Similarly, the association of MDM2 inhibitors with conventional chemotherapeutic drugs that induce apoptosis through a functional p53-dependent pathway, namely doxorubicin or cytarabine, significantly increased the antitumor activity, in tumors with a compromised p53 pathway by overexpression of MDM2 (Zheng et al., 2010; Koster et al., 2011). The efficacy of this type of associations has been evaluated in clinical trials (Table 1.3). Consistently, the reactivator of mutant p53 APR-246 has also shown synergistic effects in combination with cisplatin and danorubicin, in mutant p53-expressing tumors (Bykov et al., 2005b; Ali et al., 2011). The combination of APR-246 with carboplatin and doxorubicin will be also evaluated in clinical trials (Table 1.3).

Table 1.3. Small molecule activators of p53 currently under clinical trials [Adapted from (Hoe et al., 2014)].

Compound	Mechanism of action	Study phase	ClinicalTrials.gov identifiers
RG7112 (RO5045337)	p53-MDM2 inhibition	Phase I trial in advanced solid tumors, hematological neoplasms, liposarcomas (all completed), AML and myelogenous leukemia (active)	NCT00559533 NCT01164033 NCT00623870 NCT01143740 NCT01677780
RG7112 with cytarabine	p53-MDM2 inhibition	Phase I in AML (completed)	NCT01635296
RG7112 with doxorubicin	p53-MDM2 inhibition	Phase I in soft tissue sarcoma (completed)	NCT01605526
RG7388 (RO5503781)	p53-MDM2 inhibition	Phase I in advanced solid and hematological malignancies (completed)	NCT01462175
RG7388 with cytarabine	p53-MDM2 inhibition	Phase I in AML, leukemia and neoplasms (recruiting)	NCT01773408 NCT02545283
MI-773 (SAR405838)	p53-MDM2 inhibition	Phase I in malignant neoplasms (recruiting)	NCT01636479
DS-3032	p53-MDM2 inhibition	Phase I in advanced solid tumor and lymphoma (recruiting)	NCT01877382
DS-3032b	p53-MDM2 inhibition	Phase I in hematological malignancies (recruiting)	NCT02319369
CGM097	p53-MDM2 inhibition	Phase I in advanced solid tumors	NCT01760525
MK8242	p53-MDM2 inhibition	Phase I in advanced solid tumors	NCT01451437
HDM201	p53-MDM2 inhibition	Phase I in liposarcoma, advanced solid and hematological (recruiting)	NCT02343172 NCT02143635
RG7775 (RO6839921)	p53-MDM2 inhibition	Phase I in AML and malignant neoplasms (recruiting)	NCT02098967
PRIMA-MET (APR-246)	Reactivation of mutant p53	Phase I in hematological and prostatic neoplasms (completed)	NCT00900641
PRIMA-MET with Carboplatin and PLD	Reactivation of mutant p53	Phase Ib/II in platinum sensitive recurrent high-grade serous ovarian cancer with mutated p53 (recruiting)	NCT02098343

AML – Acute myeloid leukaemia PLD - Pegylated liposomal doxorubicin hydrochloride

1.3.4. Cyclotherapy

The cyclotherapy is a very interesting therapeutic strategy, in which drugs are used to selectively protect normal tissues from cytotoxic drugs. Although this concept was first described in 1992 (Lane, 1992), just recently it has been more explored.

In the p53-based cyclotherapy, the selective induction of reversible cell cycle arrest by low doses of a wt p53 activator may protect normal cells from drugs targeting actively proliferating cells, while tumor cells, with a dysfunctional p53 pathway, are not protected and remain susceptible to chemotherapy (Rao et al., 2013). Even in tumors with an intact p53 pathway, the p53 stabilization leads preferentially to apoptosis or senescence, while in normal cells the p53 stabilization usually causes cycle arrest (Rao et al., 2013). With this strategy, the therapeutic window of conventional chemotherapeutic agents may be improved, with the reduction of side effects of chemotherapy, and without loss of efficacy (Rao et al., 2013). Actually, several *in vitro* studies demonstrated the protective effect of low doses of Nutlin in normal cells exposed to chemotherapeutic agents (Carvajal et al., 2005; Kranz and Dobbelstein, 2006; Cheok et al., 2010). Despite this, just one *in vivo* study supports this therapeutic strategy by showing that Nutlin-3 pretreatment protects mice from neutropenia induced by the Polo-Like-Kinase-1 (PLK-1) inhibitor BI2536 (Sur et al., 2009).

1.4. Screening strategies to search for small molecule activators of p53

Even though all the pharmacological efforts developed around the p53-based therapies, new reactivators of the p53 function with improved pharmacological properties are required. However, several aspects related with drug development and screening strategies available have limited such research. Despite this, several screening approaches have been developed to search for p53-MDMs interaction inhibitors, namely based on computational aided drug design, biophysical assays and cell-based assays [reviewed in (Wang and Hu 2012; Wang et al., 2012; Zhao et al., 2013)]. However, few screening assays have been developed to search for mutant p53 reactivators.

The contribution of these assays for the identification of new small molecule reactivators of p53 activity will be addressed. Due to the complexity of drug development targeting p53, the combination of some of these strategies has greatly contributed to the advances observed in this area.

1.4.1. Cell-free assays

1.4.1.1. *Computational aided drug design*

The development of bioinformatics led to the emerging of two major approaches in Medicinal Chemistry, the straightforward *in silico* compound-selection (virtual screening) and the structure-based *de novo* design. These tools have been widely used in the design of MDMs inhibitors, considering the three essential a.a. involved in the interaction between p53 and MDMs (Figure 1.14). Although *PHE19* and *TRP23* interact in a similar way to MDM2 and MDMX, *LEU26* does not (Zhang et al., 2014a). It was also suggested a fourth important residue, *LEU22*, which appears to have an important role in the overall interactions between p53 and MDMs (Fu et al., 2012). Moreover, the contribution of the MDM2 residues *LEU54*, *HIS96* and *ILE99* for the interaction is different from the equivalent MDMX residues *MET53*, *PRO95* and *LEU98*, which may justify the differential binding affinities of p53 to MDM2/MDMX (Zhang et al., 2014).

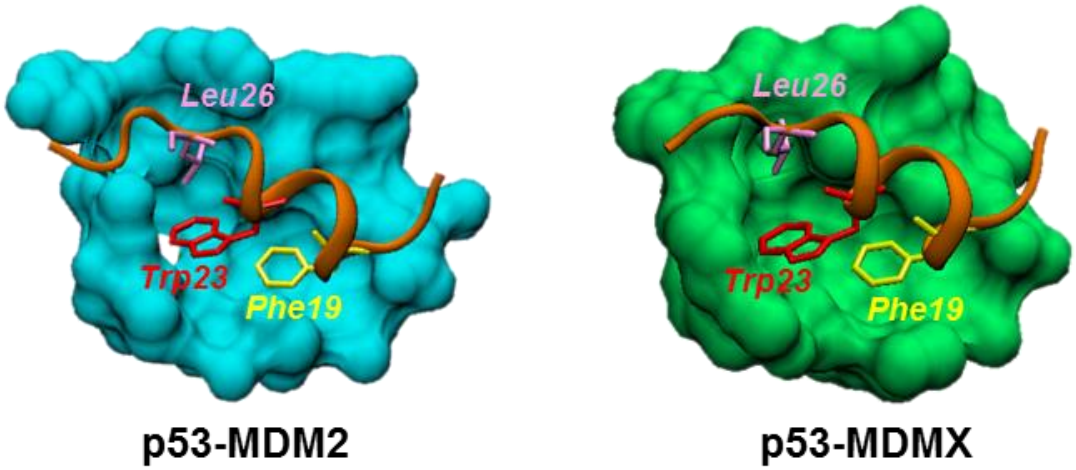

Figure 1.14. Complex of the MDM2 (blue) and MDMX (green) structures with the three residues from p53 (orange) that are involved in p53-MDMs interactions.

The structure-based *de novo* design technique has been used for designing novel small molecule ligands for macromolecular binding pockets. This approach is applied in complementarity with three dimensional (3D) binding site properties of the target protein, such as electrostatics, shape, size, lipophilicity, aromaticity, among others. The spiro-oxindoles MI-63 and MI-219 were discovered using a structure-based *de novo* design (Ding

et al., 2006; Shangary et al., 2008). This design started with the search for chemical moieties that could mimic the interaction of *TRP23* (the most critical amino acid for the interaction). In fact, the oxindole showed to greatly mimic the side chain of *TRP23* for interaction with MDM2. Besides the confirmation of this fact, computational modeling studies revealed that the spiropyrrolidine ring provides a rigid scaffold from which two hydrophobic groups can be projected to mimic the side chain of *PHE19* and *LEU26*. Furthermore, a structure-based optimization that involves the additional interaction of *LEU22* led to MI-63 and thereafter to MI-219 with good oral bioavailability in mice due to improved water solubility (Ding et al., 2006; Shangary et al., 2008). Further modifications were made in this family of compounds, and new small molecules with higher affinity to MDM2 and improved pharmacokinetic profile were obtained, as MI-773, which are waiting to enter in phase I clinical trials (Zak et al., 2013). The structure-based *de novo* design strategy was also used to find a new class of potent p53-MDM2 inhibitors with a piperidinone scaffold (Rew et al., 2012; Lucas et al., 2012). Using computer modeling, SAR (structure–activity relationship) studies and crystal structure, the affinity of known MDM2 inhibitors to MDM2 was improved through conformational control of both the piperidinone ring and the appended *N*-alkyl substituent, emerging the AM-8553 that, besides the high affinity to MDM2, presentes excellent pharmacokinetic properties (Lucas et al., 2012).

Sulfonamide I (NSC279287) was the first example to be identified by virtual screening using the NCBI database and a computational pharmacophore model of MDM2 (Galatin and Abraham, 2004). Using molecular modeling programs to generate predictive QSAR regression equations for p53-MDM2 inhibition, based on the template of the interaction between p53-based peptide inhibitors and MDM2, the development of the pharmacophore model to mimic the portions of p53 necessary to MDM2 binding was possible (Galatin and Abraham, 2004). The mechanism of action of NSC279287 was confirmed using an ELISA-based p53-MDM2 binding assay and a p53 reporter gene assay using MDM2-overexpressing osteosarcoma cells (Galatin and Abraham, 2004). With a library of 150,000 compounds of the NCI (National Cancer Institute) database, and an approach combining pharmacophore and structure-based screening, 354 potential MDM2 inhibitors were identified (Lu et al., 2006). The pharmacophore model consisted of three elements that mimicked the three key hydrophobic binding residues in p53 together with three associated distance constraints. Computational docking was performed to dock each hit to the p53-binding site in MDM2, and their binding affinities were ranked. As result, the quinolinole NSC66811 was identified as MDM2 inhibitor, what was thereafter confirmed using a fluorescence-based binding assay (Lu et al., 2006). Other example was the use of the virtual screening to find the reactivator of mutant p53, the compound PhiKan083 (Boeckler et al.,

2008). After mutant p53 Y220C protein crystallization, 2,066,906 compounds were screened for their binding affinities to mutant p53 Y220C core domain of crystal structure. The 80 selected compounds were then tested for their abilities to induce chemical shift changes using NMR spectroscopy. The results obtained revealed that PhiKan083 was able to bind to mutant p53 Y220C (Boeckler et al., 2008).

1.4.1.2. *Biophysical and biochemical assays*

In general, these assays are simple and reliable, and can be used for the high throughput screening (HTS) of large small molecule libraries. Despite this, a major drawback is the fact that the target proteins are tested in a non-cellular context (Colas, 2008). In order to identify small molecule inhibitors of the p53 interaction with MDM2 and MDMX, a variety of biophysical assays have been established and efficiently used, namely Surface Plasmon Resonance (SPR), Enzyme-Linked Immunosorbant Assay (ELISA), Homogenous Time-Resolved Fluorescence (HTRF) binding assay (also called TR-FRET), ThermoFluor Microcalorimetry, Isothermal Titration Calorimetry (ITC), Fluorescence Polarization (FP) binding assay, among others.

Nutlin-3a was discovered by screening of a library of compounds using the SPR (Vassilev et al., 2004). The SPR assay was performed on a Biacore Series S Sensor chip CM5 derived from immobilization of a PentaHis antibody to capture the His-tagged p53 protein. The assay was conducted with MDM2 fragments that, when in contact with an inhibitor of the p53-MDM2 interaction, do not bind to p53 immobilized in the chip. The resonance signal is dependent on the amount of MDM2 that is able to conjugate with p53 (Vassilev et al., 2004).

The ELISA is a well-known methodology to study protein-protein interactions, as well as to analyze the effect of compounds on such interactions. For instance, to measure the p53-MDM2 protein interaction, one of the proteins is attached to a plate surface, and the amount of the second protein that is able to bind to the attached protein is measured through addition of a specific antibody linked to an enzyme that will bind to the second protein. When a specific substrate is added, the enzyme produces a measurable readout that is proportional to the amount of bound protein (Arkin et al., 2012). The ELISA assay allowed the discovery of Sulfonamide 1 (NSC279287; Galatin and Abraham, 2004), terphenyl compounds 2 and 6 (Chen et al., 2005), and chalcones B and B-1 (Stoll et al., 2001) as inhibitors of the p53-MDM2 interaction.

The HTRF binding assay was also performed to search for inhibitors of the p53 interaction with MDM2 and MDMX. This technique is based on the transference of energy

between two fluorophores, a donor and an acceptor, when in close proximity. Thus, molecular interactions between p53 and MDMs can be assessed by coupling each partner with a fluorescent label and by detecting the level of energy transfer (Arkin et al., 2012). With this screening strategy, chromenotriazolopyrimidine 1 (Allen et al., 2009) and RG7388 (Ding et al., 2013) were identified as p53-MDM2 interaction inhibitors.

The ITC assay is a well-established method to characterize protein-protein interactions, as well as the binding of a small molecule to a target protein. This is a label-free technique, where all the components are in solution. ITC measures the binding energy and provides information concerning thermodynamic parameters (affinity, enthalpy/entropy and stoichiometry) of a binding interaction. The signal measured is the heat generated or absorbed by a binding interaction (Arkin et al., 2012). Using the ITC assay, combined with HTRF, the small molecule RO5963 was identified as dual inhibitor of the p53-MDMs interactions (Graves et al., 2012).

Also based in calorimetry, the ThermoFluor Microcalorimetry technology is an affinity HTS assay that uses fluorescent dyes to monitor protein unfolding as a function of temperature for the identification of compounds that bind to MDM2. The amount of compound bound to MDM2 is measured by the increase in thermal stability. The thermal stability is quantified as a change in midpoint transition temperature in the presence of the compound at a single concentration (Shangary and Wang, 2009). Using this approach, the benzodiazepinediones TDP521252 and TDP665759 were identified as inhibitors of the p53-MDM2 interaction (Koblish et al., 2006).

The FP binding assay is another method through which protein-protein interactions and the binding of a small molecule to a protein can be monitored (Figure 1.15). This is a sensitive nonradioactive screening assay based on the use of a consensus peptide labeled to a fluorophore. In the absence of a small molecule interaction inhibitor, the formation of a peptide-protein complex increases the FP value. On the other hand, in the presence of an inhibitor, the fluorescently labeled peptide is displaced, leading to a decrease of the FP value due to its increased rotational mobility (Lea and Simeonov, 2011). Using this assay, bisarylsulfonamide compounds (Wang et al., 2004) and the therphenyl derivative 14 (Yin et al., 2005) were identified as p53-MDM2 interaction inhibitors. Additionally, WK298 (Popowicz et al., 2010) and SJ-172550 (Reed et al., 2010) were identified as inhibitors of the p53-MDMX interaction using the same assay.

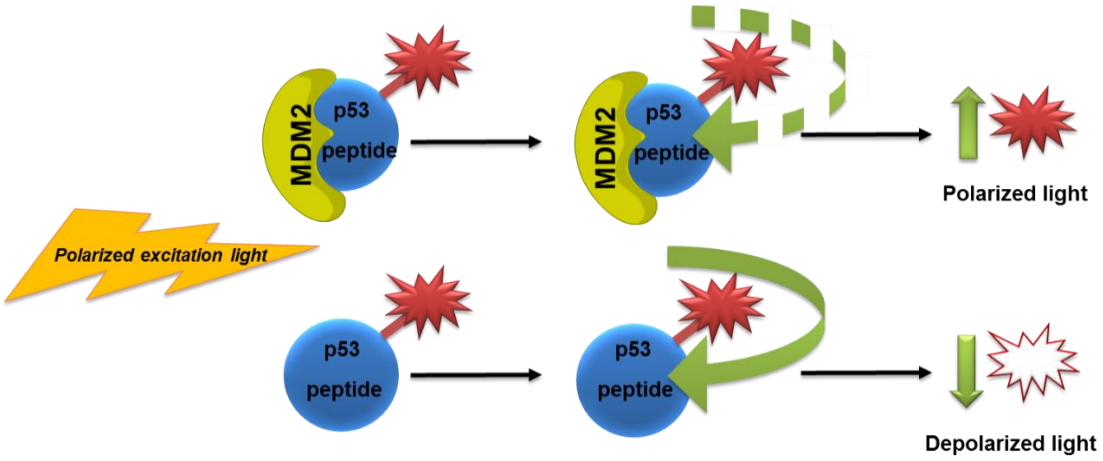

Figure 1.15. Fluorescence polarization assay. After exposure to a polarized excitation light, a rapidly rotating p53 peptide fluorophore gives low FP signal (depolarized light). The association of a relatively large molecule, such as MDM2, with the p53 peptide fluorophore slows down the motion of the fluorophore, leading to increased FP signal (polarized light).

Many other biophysical and biochemical assays have been developed and adapted, in the last years, to search for new p53-MDMs interaction inhibitors. However, those referred above have conducted to the discovery of the most relevant protein-protein interaction inhibitors described to date.

1.4.2. Cell-based assays

Cellular assays are characterized by a higher complexity and variability. However, in contrast to biophysical assays, the cell-based assays provide relevant data about the activity of compounds in a more physiological cellular environment, particularly of their cell permeability and cytotoxicity (Korn and Krausz, 2007). Based on that, human and yeast cells have been used by several research groups to develop screening assays for the search of new small molecule inhibitors of the p53-MDMs interactions and reactivators of mutant p53.

1.4.2.1. *Human cell-based assays*

In cancer research, these assays are usually carried out with tumor cells for the study of the cytotoxic effect of small molecules, as well as of their impact on p53 activity. The

resonance energy transfer (RET) assays, including fluorescence (FRET) and bioluminescence (BRET), have been highly used to study protein-protein interactions in a cellular environment (Mazars and Fahraeus, 2010; Couturier and Deprez, 2012). For FRET, a robust and affordable system for HTS is not available yet, whereas BRET has been widely applied in HTS, namely in the search for p53-MDM2 interaction inhibitors (Yurlova et al., 2014). This assay, known for its reproducibility, is based on the fusing of Renilla Luciferase donor (Rluc) and Yellow Fluorescent acceptor Protein (YFP) to p53 or MDM2. Rluc oxidizes its substrate Coelenterazine h, resulting in the emission of energy (Mazars and Fahraeus, 2010). If a suitable energy acceptor is under the proximity, and is favorably oriented, this energy can be transferred, with the subsequent emission of energy at a longer wavelength by the excited acceptor molecule (Mazars and Fahraeus, 2010). The BRET assay was validated using Nutlin-3a as control, and showed to be an efficient method for the fast analysis of inhibitors of the p53-MDM2 interaction (Mazars and Fahraeus, 2010). However, small changes in the positioning of the donor and acceptor can result in signal decline, which does not necessarily reflect a splitting of the p53-MDM2 interaction (Yurlova et al., 2014). Contrary to this approach, one elegant way to detect protein-protein interactions in mammalian cells is based on protein complementation, which reconstitutes a functional enzymatic or fluorescent reporter from the interaction of two proteins. One example is the cellular model to evaluate the capacity of small molecules to disrupt the p53-MDM2 interaction, based on a bimolecular fluorescence complementation assay (Figure 1.16; Amaral et al., 2013). This assay involves the fusion of two non-fluorescent fragments of a reporter protein to p53 and MDM2 proteins. In the case of interaction, the reporter fragments come together, fold into an almost-native conformation, and thereby reconstitute the functional fluorophore (Amaral et al., 2013). After validation with the positive control Nutlin-3, this efficient assay was used to test a commercially available chemical library of 33 protein phosphatase inhibitors, with the subsequent identification of potential small molecule inhibitors of the p53-MDM2 interaction (Amaral et al., 2013).

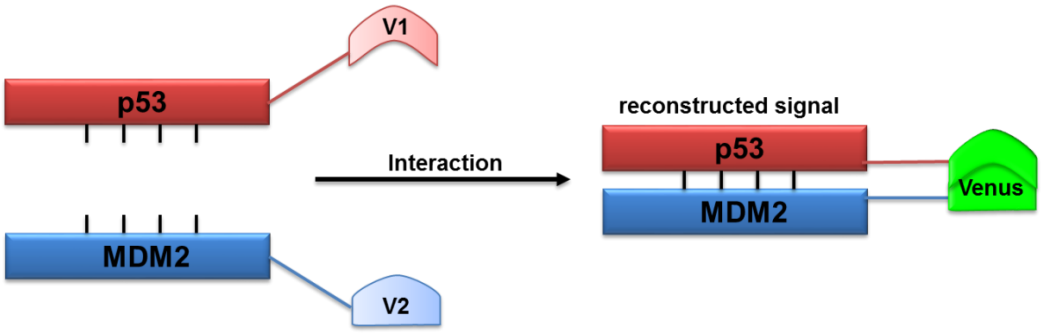

Figure 1.16. Bimolecular fluorescence complementation (BiFC) assay. The p53 and MDM2 proteins are fused to non-fluorescent fragments (V1 and V2) of a fluorescent reporter protein. When protein-protein interaction occurs, V1 and V2 get close enough to reconstruct the functional fluorophore (Venus). [Adapted from (Amaral et al., 2013)].

In 2005, the reverse mammalian protein-protein interaction trap (MAPPIT) assay was reported for the p53-MDM2 interaction (Eyckerman et al., 2005). This assay is a bait-and-prey system with an inhibitory motif attached to the prey protein, which allows a positive readout upon interference with the designated protein–protein interaction (Eyckerman et al., 2005). However, the detection is dependent on the signal transduction of cytokine receptor; therefore anything that interferes with this signaling pathway would also affect the readout of the assay. In this way, a mammalian two-hybrid system, based on a direct activation of a reporter gene, can be a reliable alternative to the MAPPIT assay. Li and colleagues (2011) developed a mammalian two-hybrid system, consisting in a full-length p53 or MDM2 inserted at the *C*-terminal of the DNA binding domain (BD) of *GAL4* or at the transcriptional activation domain (AD) of NFkB. In this assay, the p53-MDM2 interaction will bring the BD and AD in proximity with the subsequent activation of the downstream Firefly luciferase reporter gene (Li et al., 2011c). After validation with the positive control Nutlin, the authors discovered that SL-01, a Z-L-Phe chloromethyl ketone, was a p53-MDM2 interaction inhibitor (Li et al., 2011c). Since in these assays, the reconstitution of the protein-protein interaction is often irreversible, this type of method is not appropriate to screen for compounds that disrupt an interaction once it is formed. Nevertheless, the fully reversible microscopy assisted fluorescent two-hybrid (F2H) assay does not present this limitation (Yurlova et al., 2014). This assay was developed to search for inhibitors of p53-MDMs interactions (Yurlova et al., 2014). The F2H is based on the anchorage of the green-fluorescent bait protein (p53) at a defined spot in the nucleus, formed by the lac-operator array on the genomic DNA (Yurlova et al., 2014). The interaction with the RFP-tagged human MDM2/MDMX can be evaluated by enrichment of red fluorescence at the location of the green spot. The disruption of the p53-MDMs interactions is determined based on the

fading of the red spots from the anchored green spots (Yurlova et al., 2014). With this assay, five small molecules with potent activity as p53-MDM2 inhibitors were identified (Yurlova et al., 2014). Other method with a quite similar principle is the imaging-based positional biosensor high-content screening (HCS) assay (Dudgeon et al., 2010a,b). With this technique three structurally-related methylbenzo-naphthyridin-5-amine hit compounds were identified (Dudgeon et al., 2010a).

Using the p53-response promoter method, 46,260 compounds were screened in order to find a reactivator of mutant p53 R273H (Kravchenko et al., 2008). This method is based on the transfection of tumor cells (in this particular case, of the epidermal carcinoma cell line A431 expressing mutant p53 R273H) with a reporter construct carrying a cassette for expression of *β*-galactosidase under the control of a minimal cytomegalovirus promoter coupled to multiple p53-binding elements (Kravchenko et al., 2008). The signal obtained in the presence of o-nitrophenyl β-d-galactoside (ONPG) will be proportional to p53 transcriptional activity. Using this approach, the small-molecule RETRA (reactivation of transcriptional reporter activity) was identified. RETRA induced expression of p73, and its release from the complex with mutant p53, as well as p73-dependent apoptosis in A431 cells, and *in vivo* significant reduction of tumor formation (Kravchenko et al., 2008).

A method that is widely used to search for reactivators of mutant p53 is based on the analysis of the ability of small molecules to induce a p53-dependent growth inhibition in mutant p53-expressing tumor cells. Actually, the analysis of the cytotoxic effect of a NCI/DTP (National Cancer Institute/Development Therapeutics Program) chemical library on several human tumor cell lines expressing mutant p53 R273H or R175H, led to the identification of a reactivator of these two mutant p53, PRIMA-1 (Bykov et al., 2002b). Using the same approach, APR246, MIRA-1 and STIMA-1 were also identified as reactivators of mutant p53R273H and R175H (Bykov et al., 2005a,b; Zachea et al., 2008). Finally, an *in silico* screen based on data from the NCI/DTP anticancer drug screen, reported the IC_{50} (half maximal inhibitory concentration) of about 50,000 compounds against 60 tumor-derived cell lines (Yu et al., 2012). From this screening, three thiosemicarbazones, that selectivelly inhibited mutant p53-expressing cell lines compared to wt p53-expressing cells, were selected, and NSC319726 was identified as reactivator of mutant p53 R175H (Yu et al., 2012). Interestingly, contrary to previous screens that used engineered isogenic cell lines, Yu and collaborators (2012) used heterogeneous panels of cell lines. However, in general, since this method is only based on growth inhibition, many compounds selected using this methodology may not act directly through p53 activation.

1.4.2.2. *Yeast-based assays*

In the last years, yeast-based assays, consisting in engineered yeast cells overexpressing human disease-related proteins, have greatly contributed to the elucidation of the biology and pharmacology of these proteins (Pereira et al., 2012a,b; Guaragnella et al., 2014). Besides this, yeast-based HTS assays have been largely explored in targeted screening due to several advantages, when compared to cell-free assays and human cell-based assays. In particular, comparing with cell-free assays, the purification of the target protein is not required, what makes this approach less expensive, and the analysis of some relevant drug-like properties, such as permeability, instability and cytotoxicity became possible. Moreover, due to its easy manipulation and reduced doubling time, yeast allows simple and rapid screenings well-adaptable to HTS methodologies. In addition, since this organism provides an "empty room", where the activity of human proteins can be analyzed with fewer interferences of proteins of the same family or pathway, screening assays directed to specific human proteins can be performed with high efficiency (Pereira et al., 2012a,b). Actually, these cells have proved to be extremely useful as a first-line targeted screening approach for a previous selection of compounds to be tested in more complex cell systems (Pereira et al., 2012a,b).

The p53 tumor suppressor, without orthologues in yeast, is an example of a human protein that has been widely studied in this microorganism in the last few years.

1.4.2.2.1. Yeast transactivation assays

In 1990, it was shown that p53 was also a transcription factor in yeast (Fields and Jang, 1990). This enabled the development of powerful simplified cell-based assays for functional analyses of p53, particularly of the impact of mutations and interacting proteins (such as MDMs) on its activity. The FASAY (Functional Analysis of Separated Alleles in Yeast) assay was one of the first techniques to be developed in yeast to evaluate the status of p53 transcriptional activity (Ishioka et al., 1993). This technique consists in the expression of a p53 cDNA obtained from tumor samples in a yeast strain with a *HIS3* reporter gene downstream of a human p53 response element (RE). The p53 status is evaluated using a culture medium without histidine: functional p53 enables growth by inducing *HIS3* expression, while yeast clones expressing mutant p53 will not grow. However, the best-known FASAY version used *ADE2,* instead of *HIS3,* as a reporter gene. In this case, the reporter yeast strain (defective in adenine synthesis) is grown in low-adenine medium, where it produces white colonies upon *ADE2* expression (wt p53), or red colonies in its absence (mutant p53; Flaman et al., 1995). These assays have given place to the luciferase

transactivation assay, in which the p53 transcriptional activity is evaluated by quantification of the luciferase activity. These assays were obtained by replacing the *ADE2* ORF by a luciferase reporter gene in the same chromosomal locus, and were initially used to confirm the results from the *ADE2* reporter gene assay in the analysis of the REs transactivation by different p53 mutants (Resnick et al., 2003). In 2011, a dual-luciferase transactivation assay was adapted for HTS of a matrix of factors that can influence the p53 activity, including small molecules, mutations and interacting proteins as MDM2 (Andreotti et al., 2011). By testing Nutlin-3a and RITA, this system was validated to search for inhibitors of the p53-MDM2 interaction (Andreotti et al., 2011). Recently, this assay was extended to p63 and p73 proteins of the p53 family, which exhibit intrinsic differences in transactivation specificities (Figure 1.17A; Ciribilli et al., 2013; Monti et al., 2014).

In a recent study from our group, *ACT1* was identified as a yeast endogenous target gene of human p53 (Leão et al., 2013b). In that work, a correlation between the p53 activity and the endogenous actin protein expression levels was established. This opened the way to simplified yeast transactivation assays, without the requirement of artificial reporter genes, to study the impact of small molecules on the activity of p53 family proteins. In fact, it was shown that inhibitors of p53-MDMs interactions abolished the MDMs-inhibitory effect with the re-establishement of the increased actin expression levels induced by p53 (Figure 1.17B). This was observed, for example, with Nutlin-3a for the p53-MDM2 interaction (Leão et al., 2015a), and with SJ-172550 for the p53-MDMX interaction (Leão et al., 2015a).

One of the most renowned applications of the yeast transcriptional assays has been on the study of mutant p53. Actually, these yeast assays have allowed the evaluation of LOF and DNE of mutant p53 (Petitjean et al., 2007a). In fact, the contribution of the yeast transcriptional assays to the study of the molecular epidemiology of mutant p53, including frequency, type, and site of mutations associated with carcinogenesis, as well as of their impact on the function of p53 family proteins in human tumor cells, have become this technique a powerful clinical tool. Indeed, with it, possible factors that contribute to tumor development may be identified, and the best cancer therapy can be selected taking into account the type and site of mutant p53 (Fronza et al., 2000; Smardová et al., 2005).

1.4.2.2.2. Yeast growth-inhibitory assays

It was observed that the expression of human wt p53 in *Saccharomyces cerevisiae* induces a marked growth inhibition associated with cell cycle arrest (Nigro et al., 1992) or death (Amor et al., 2008). Additionally, it was demonstrated that, also in yeast, the human MDM2 was able to inhibit the p53 transcriptional activity and to promote the p53

ubiquitination and subsequent degradation in yeast (Di Ventura et al., 2008). With several evidences sustaining the similarities of the biology of p53 between mammalian and yeast cells, yeast became a powerful tool for genetic, molecular and functional studies of p53.

The marked cytotoxic effect of human p53 in yeast, which is proportional to its activity and it is easily quantified by measurements of yeast cell growth, led to the development of simple yeast growth-inhibitory assays for the targeted screening of modulators of p53 activity (Pereira et al., 2012a,b; Guaragnella et al., 2014). Particularly, using yeast cells co-expressing p53 and MDMs, it was demonstrated that, as in human cells, both MDM2 and MDMX inhibit the p53-induced yeast growth inhibition (Leão et al., 2013b,c; Figure 1.17B). This system was thereafter validated to search for inhibitors of the p53 interaction with MDM2 and MDMX, by testing the known inhibitors of these interactions Nutlin-3a and SJ-172550, respectively (Vassilev et al., 2004; Reed et al., 2010). The use of these yeast-based assays conducted to the discovery of pyranoxanthone 1, as the first p53-MDM2 interaction inhibitor with a xanthone scaffold (Leão et al., 2013c). Additionally, α-mangostin and gambogic acid were described, for the first time, as potential inhibitors of the p53-MDM2 interaction (Leão et al., 2013a). More recently, these assays were extended to other members of the p53 family (Leão et al., 2015a). In fact, the observation that both MDM2 and MDMX inhibit the yeast growth-inhibitory effect of p63 and p73 enabled the development of yeast phenotypic assays to study the impact of human MDMs on these p53 family proteins. Interestingly, using Nutlin-3a, reported to also inhibit the p73-MDM2 interaction in human tumor cells (Lau et al., 2008), the effectiveness of the yeast growth-inhibitory assay to search for small molecule p73-MDM2 interaction inhibitors was demonstrated (Leão et al., 2015a). Notably, in the same work, a similar yeast system developed to search for p73-MDMX interaction inhibitors revealed that SJ-172550 may also disrupt this interaction. However, no further studies have been performed in human tumor cells in order to confirm this result.

1.4.2.2.3. Yeast two-hybrid assays

The yeast two-hybrid (Y2H) was the first molecular genetic tool developed to study protein-protein interactions in a cellular context (Fields and Song, 1989). Through HTS of large cDNA libraries, it has allowed the identification of protein interactors (prey) of a protein of interest (bait) (Figure 1.17C). Since its discovery, the Y2H has been a very useful tool, namely in the discovery of new protein interactions of p53. For example, with the Y2H, the p53 fragment responsible for oligomerization (OD) was identified, and its involvement in

mutant p53 oligomerization with wt p53 was revealed (Iwabuchi et al., 1993). This finding provided a molecular explanation for mutant p53 DNE.

Using this assay, the four amino acid residues of MDM2 essential for the interaction with p53 (*GLY58*, *ASP68, VAL75, CYS77*) were determined (Freedman et al., 1997). The Y2H has also contributed to detect mutant p53 in tumor samples based on its inability to bind to 53BP1, an interactor partner and enhancer of p53 transcriptional activity also identified by Y2H (Schwartz et al., 1998). Additional interactions between p53 and other proteins were firstly described or confirmed using this approach.

In 1996, Vidal and colleagues developed a reverse Y2H assay for drug screening. In this case, cells grow when the interaction between proteins does not occur due to the presence of disrupters of the respective protein-protein interaction (Vidal et al., 1996). In the same year, it was also developed the yeast three-hybrid assay for small molecule target identification (Licitra and Liu, 1996). This approach is based on small molecule-protein interactions by dimerization of two receptor proteins via a linking heterodimeric ligand (Licitra and Liu, 1996). The reverse Y2H and the yeast three-hybrid assays reveal to be promising assays to find inhibitors of p53-MDMs interactions.

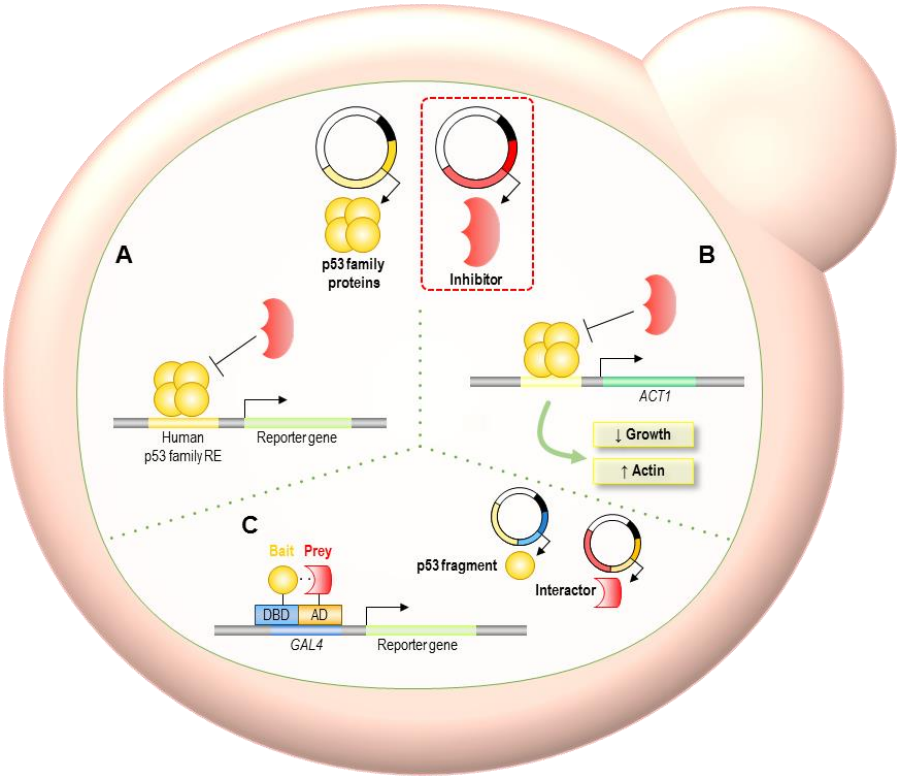

Figure 1.17. Yeast-based assays developed to study the impact of protein interacting partners and small molecules on the function of p53. These assays use yeast cells co-expressing a human p53 and a protein interacting partner (e.g. MDM2, MDMX, mutant p53). **(A)** Yeast transactivation assay. The impact of interacting protein partners and small-molecules on p53 transcriptional activity is evaluated using a reporter gene (e.g. *ADE2*, Luciferase) under the regulation of a human p53-family response element (RE). **(B)** Yeast growth-inhibitory assay. Expression of a p53 induces yeast growth inhibition associated with an increase of actin expression. The impact of interacting protein partners and small-molecules on p53 function is evaluated by quantification of yeast cell growth and actin protein expression levels. **(C)** Yeast two-hybrid assay. A protein (bait; e.g. p53) is fused to the *GAL4*-DNA binding domain (DBD) and the interacting protein partner (prey; e.g. MDM2) is fused to the *GAL4*-transactivation domain (AD). If the bait and prey establish a physical interaction, the function of *GAL4* is restored, allowing it to bind to a specific sequence, leading to the transcription of a reporter gene (e.g. *HIS3*, *ADE2*, *LacZ*); this effect is abolished by small-molecule inhibitors of the bait-prey interaction.

1.5. Scope of this thesis

Compelling evidence has therefore demonstrated that inactivation of the p53 pathway underlies tumor development and maintenance. Actually, the majority of human cancers have been associated with compromised p53 functions, either by mutation or by inhibition through interaction with negative regulators such as MDM proteins. This strongly supports the notion that an activation of p53 is a highly effective strategy in cancer treatment.

With the present thesis, we aimed to find new pharmacological opportunities against cancer by targeting p53. Particularly, we intended to discover:

i) Inhibitors of the p53 interaction with MDMs (**Chapter 3**);

ii) Reactivators of mutant p53 (**Chapter 4**).

To achieve such goals, yeast-based screening assays, previously developed by our group or implemented for the first time under the scope of this thesis, were used to test several libraries of compounds synthesized by collaborative Medicinal Chemistry groups to target p53. The chemical libraries selected, in this work, were composed by compounds with scaffolds previously reported to be promising in the search for modulators of p53 activity, namely flavonoids (Stoll et al., 2001) and small molecules containing indole and/or isoindolinone moieties (Ding et al., 2006; Pientracosta et al., 2006). The drug discovery strategy used in this thesis also encompassed the validation of the molecular mechanism of action and antitumor activity of the compounds selected in yeast in more complex cellular systems, particularly in human tumor cell lines and in animal models.

The major contributions of this work to anticancer drug research by targeting p53 are presented in the final discussion of this thesis (**Chapter 5).**

CHAPTER 2

Material and Methods

2.1. Compounds

PRIMA-1, doxorubicin, SJ-172550 and Pifithrin-α (PTF-α) were purchased from Sigma-Aldrich (Sintra, Portugal), Phikan083 from Tocris (VWR, Carnaxide, Portugal); etoposide from Calbiochem (VWR, Carnaxide, Portugal) and Nutlin-3a was from Alexis Biochemicals (Grupo Taper, Sintra, Portugal). All tested compounds were dissolved in dimethyl sulfoxide (DMSO; Sigma-Aldrich, Sintra, Portugal). Synthesis of compounds 1a-c, 2a-b, 3a-b and 4a-b (Section 1), OXAZ-1 (Section 2) and SLMP53-1 (Section 3) is described in Appendix. Compounds OXAZ-2 to -6 were synthesized according to the described procedures (Amat et al*.,* 2007a,b; Pereira et al., 2014).

2.2. Plasmids

The following yeast expression vectors were used: pLS89-(*TRP1*) encoding human wt p53 under the *GAL1-10* inducible promoter (kindly provided by Dr. Richard Iggo; Swiss Institute for Experimental Cancer Research, Switzerland); pGADT7-(*LEU2*) encoding human MDM2 under the *ADH1* constitutive promoter (generous provided by Dr. Xue-Min Zhang; National Center of Biomedical Analysis, China); and pTS76-(*LEU2*) encoding human mutant p53R280K or p53Y220C under the *ADH1* constitutive promoter (kindly provided by Dr. Gilberto Fronza; IST Istituto Nazionale per la Ricerca sul Cancro, Genoa, Italy).

2.3. Yeast transformation

The plasmids used in the yeast transformation process were firstly amplified in *Escherichia coli* DH5α from Lucigen (Frilabo, Porto, Portugal), and thereafter extracted using the *GenEluteTM HP Plasmid Miniprep Kit* (Sigma-Aldrich, Sintra, Portugal). After extraction, yeast strains were transformed using the LiAc/SS Carrier DNA/PEG method as described (Gietz and Schiestl, 2007). For selection of transformed yeast, cells were routinely grown in selective minimal medium with 2% (w/w) glucose (Sigma-Aldrich, Sintra, Portugal), 0.7% (w/w) yeast nitrogen base without a.a. from Difco (Quilaban, Sintra, Portugal), and all the a.a. required for yeast growth (50 µg/mL), except leucine/tryptophan (for single expression systems) or leucine and tryptophan (for co-expression systems), and incubated at 30ºC, under continuous orbital shaking (200 r.p.m.).

2.4. Yeast-based screening assay

For expression of human proteins, cells (routinely grown in minimal selective medium) were diluted to 0.05 OD_{600} in induction selective medium containing 2% (w/w) galactose, 1% (w/w) raffinose, 0.7% (w/w) yeast nitrogen base without a.a. from Difco (Quilaban, Sintra, Portugal), and a mixture of all the a.a. required for yeast growth (50 µg/mL) except leucine/tryptophan (for single expression systems) or leucine and tryptophan (for co-expression systems). Cells transformed with the empty vector(s) were used as control yeast. Yeast cells were incubated at 30ºC under continuous orbital shaking (200 r.p.m.), in the presence of 0.1 – 50 µM of compounds or 0.1% DMSO only, for approximately 30 h (for single expression systems) and 42 h (for co-expression systems) (time required by control yeast, incubated with DMSO only, to achieve 0.4 OD_{600}). In the experiments with pifthrin-α (PFT-α), yeast cells expressing wt/mutant p53 were incubated with 5 µM PFT-α alone or combined with 10 µM SLMP53-1, or DMSO only for approximately 30 h. Yeast growth was analyzed by counting the number of colony-forming units (CFU), after 2 days incubation at 30ºC, on Sabouraud Dextrose Agar from Liofilchem (Frilabo, Porto, Portugal).

2.5. Yeast cell cycle analysis

Yeast cell cycle progression was analyzed basically as described (Leão et al., 2013c). Briefly, 1×10^7 cells were fixed in 70% (v/v) ethanol, incubated with 250 µg/mL RNase A (Sigma-Aldrich, Sintra, Portugal) and 1 mg/mL Proteinase K (Sigma-Aldrich, Sintra, Portugal) for 3 h, followed by addition of 10 µM Sytox Green Nucleic Acid from Invitrogen (Alfagene, Carcavelos, Portugal) and flow cytometry analysis.

2.6. Human cell lines growth conditions

The human cell lines used are described in Table 2.1. All tumor cell lines were routinely cultured in RPMI-1640 medium with ultraglutamine from Lonza (VWR, Carnaxide, Portugal) supplemented with 10% fetal bovine serum (FBS) from Gibco (Alfagene, Carcavelos, Portugal). MCF10A cell line was cultured in DMEM F12 supplemented with MEGM SingleQuot Kit Suppl. & Growth Factors from Lonza (VWR, Carnaxide, Portugal). All cell lines were maintained in a humidified incubator at 37°C with 5% CO_2.

Table 2.1. Human cell lines used in this work.

Cell line	Tissue/Disease	p53 status	Supplier
HCT116 p53$^{+/+}$	Human colon adenocarcinoma	wt	ATCC (kindly provided by Dr. B. Vogelstein, The Johns Hopkins Kimmel Cancer Center, Baltimore, MD, USA)
HCT116 p53$^{-/-}$		null (knock out)	
MCF-7	Human breast adenocarcinoma	wt	Dr. Alberto Inga, CIBIO, University of Trento, Italy
SJSA-1	Human osteosarcoma	wt	ATCC (kindly provided by Dr. Célia Gomes, IBILI, Faculdade de Medicina, Universidade de Coimbra, Portugal)
MDA-MB-231	Human breast adenocarcinoma	Mutant p53R280K	ATCC
MDA-MB-468	Human breast adenocarcinoma	Mutant p53R273H	
Huh-7	Human hepatocarcinoma	Mutant p53Y220C	
MCF10-A	Human breast epitelial/ non-tumorigenic	wt	

2.7. Sulforhodamine B (SRB) assay

Human cell lines were incubated in 96-well plates, at a final density of 5.0×10^3 cells/well (for HCT116, MCF-7, MDA-MB-468, SJSA-1 and HuH-7 cell lines) or 1.0×10^4 cells/well (for MDA-MB-231 and MCF10A cell lines), for 24 h. Cells were thereafter treated with serial dilutions (1.85 to 150 μM) of compounds for 48 h. The effect of compounds on *in vitro* growth was analyzed using the SRB assay. Briefly, following fixation with 10% trichloroacetic acid, plates were stained with 0.4% SRB (Sigma-Aldrich, Sintra, Portugal) and washed with 1% acetic acid. The bound dye was then solubilized in 10 mM Tris Base and the absorbance was measured at 510 nm in a microplate reader (Biotek Instruments Inc., Synergy MX, USA). The maximum concentration of solvent used in these assay (0.25% DMSO) was included as control. The concentration of compounds that causes 50% growth inhibition (GI_{50}) was thereafter determined.

In the synergistic assays, HCT116 p53$^{+/+}$, HCT116 p53$^{-/-}$ and MDA-MB-231 cell lines were treated with the GI_{10} concentration of OXAZ-1, SLMP53-1 or DMSO only, and increasing concentrations of doxorubicin (9.38 – 750 nM) or etoposide (0.38 – 6.00 μM). The effect of combined treatments on cell growth was analyzed after 48 h incubation, using the SRB assay. To further quantify the synergistic effect of the combined treatment, the

following equation was used, basically as reported (Jin, 1980), $Q = Ea+b / (Ea + Eb - Ea \times Eb)$, where Q is the combination index of the combined treatment, Ea + b represents the cell proliferative inhibition rate of combined drugs, Ea and Eb are signs of the cell proliferative inhibition rate of each drug; $Q < 0.85$, $Q > 1.15$ and $0.85 < Q < 1.15$ indicate antagonism, synergy, and additive effect, respectively.

2.8. Analysis of cell cycle and apoptosis in human cell lines

Cell lines were incubated in 6-well plates, at a final density of 1.5×10^5 cells/well (for HCT116, MCF-7 and SJSA-1 cell lines) or 2.3×10^5 cells/well (for MDA-MB-231 and MCF10A cell lines), for 24 h. Cells were thereafter treated with compounds or DMSO only for 16, 24 and 48 h. For cell cycle analysis, cells were fixed in ice-cold 70% ethanol and incubated at 37ºC with RNase A (Sigma-Aldrich, Sintra, Portugal) at a final concentration of 20 μg/mL for 15 min, and further incubated with 50 μg/mL propidium iodide (PI; Sigma-Aldrich, Sintra, Portugal) for 30 min, followed by flow cytometry analysis. Apoptosis determination was performed by flow cytometry using the *Annexin V-FITC Apoptosis Detection Kit I from BD Biosciences* (Enzifarma, Porto, Portugal), according to the manufacturer's instructions; synergistic effects of combined treatments between the GI_{10} concentration of OXAZ-1 or SLMP53-1 (or DMSO only) and doxorubicin or etoposide, were analyzed (determination of Q value) as described in the SRB assay.

2.9. Western blot analysis

To analyze the protein expression of human tumor cell lines, cells were plated in 6-well plates at a final density of 1.5×10^5 cells/well (for HCT116, MCF-7 and SJSA-1 cell lines) or 2.3×10^5 cells/well (for MDA-MB-231 cell line) and incubated for 24 h. Cells were then treated with the GI_{50} (growth inhibition of 50%) concentration of compounds or DMSO only for 4, 8, 16, 24 and 48 h. Whole cell lysates were prepared by lysing the cells with RIPA buffer (Sigma-Aldrich, Sintra, Portugal) in the presence of EDTA-free protease inhibitor cocktail (Sigma-Aldrich, Sintra, Portugal). For mitochondrial and cytosolic fractions of human tumor cell lines, the *Mitochondrial Fractionation Kit* from Active Motif (Frilabo, Porto, Portugal) was used according to the manufacturer's instructions.

For the analysis of yeast protein expression, samples were lysed with Cellytic™ Y Cell Lysis Reagent (Sigma-Aldrich, Sintra, Portugal) in the presence of EDTA-free protease inhibitor cocktail (Sigma-Aldrich, Sintra, Portugal). Protein extracts were quantified using the Coomassie staining, Bradford from Sigma-Aldrich (Sintra, Portugal).

Proteins (40 μg) were electrophoresed using a 10% SDS–PAGE and transferred to a Whatman nitrocellulose membrane from Protan (VWR, Carnaxide, Portugal). Membranes were blocked with 5% milk and probed overnight with the primary antibody (Table 2.2) followed by 2 h incubation with a horseradish-peroxidase (HRP)-conjugated secondary antibody (Table 2.2.). For loading control, membranes were stripped (Abcam protocol) and reprobed with an anti-yeast phosphoglycerate kinase (Pgk1p) antibody for yeast, or with an anti-GAPDH antibody for tumor cell lines. For analysis of mitochondrial and cytosolic fractions, membranes were reprobed with the loading controls anti-COX IV and anti-GAPDH antibodies, respectively. The signal was detected using the *ECL Amersham kit* from GE Healthcare (VWR, Carnaxide, Portugal) and the Kodak GBX developer and fixer (Sigma-Aldrich, Sintra, Portugal). Band intensities were quantified using the Bio-Profil Bio-1D++ software (Vilber-Lourmat, Marne La Vallée, France), and were normalized against the control sample (DMSO; set as 1). Western blots presented in this thesis are representative of three independent experiments.

2.10. Co-immunoprecipitation (co-IP) assay

The co-IP assay was performed using the *Pierce Classic Magnetic IP and Co-IP Kit* from Thermo scientific (Dagma, Carcavelos, Portugal), according to the manufacturer's instructions. Briefly, HCT116 $p53^{+/+}$ cells were plated at the final density of 5×10^5 cells/plate and incubated for 24 h. Cells were then treated with different concentrations of compounds or DMSO only for 16 h or 24 h. After cell lysis, 500 μg of total protein was incubated with mouse monoclonal anti-p53 (DO-1) or with mouse immunoglobulin G (IgG, control) from Santa Cruz Biotechnology (Frilabo, Porto, Portugal), overnight at 4ºC. Immunocomplexes were immunoprecipitated using magnetic beads. Detection of p53, MDM2, MDMX and GAPDH (loading control) in whole cell lysate (input) and in immunoprecipitated fraction (IP) was performed by Western blot analysis as described in 2.9.

Table 2.2. Antibodies used in Western Blot and Immunohistochemistry.

Antigen	Final Dilution	Supplier
Primary antibodies		
p53 (DO-1) (mouse monoclonal)	1:500 (yeast) 1:5000 (human cells)	Santa Cruz Biotechnology (Frilabo, Porto, Portugal)
MDM2 (SMP14) (mouse monoclonal)	1:100	
BAX (2D2) (mouse monoclonal)	1:1000	
p21 (C-19) (rabbit polyclonal)	1:1000	
Actin (C-11) (rabbit polyclonal)	1:500	
PARP (C2-10) (mouse monoclonal)	1:2000	
Cyt *c* (A8) (mouse monoclonal)	1:200	
PUMA (B-6) (mouse monoclonal)	1:100	
COX IV (F-8) (mouse monoclonal)	1:500	
GAPDH (6C5) (mouse monoclonal)	1:10000	
MDMX (A-300) (rabbit polyclonal)	1:2000	Bethyl Laboratories
Pgk1p (22C5D8) (mouse monoclonal)	1:5000	Invitrogen (Alfagene, Carcavelos, Portugal)
Ki-67 (SP6) (rabbit monoclonal)	1:200 (immunohistochemistry)	Pierce Thermo Scientific (Taper, Sintra, Portugal)
VEGF (VG1) (mouse monoclonal)	1:200 (immunohistochemistry)	
CD34 (QBEND/10) (mouse monoclonal)	1:500 (immunohistochemistry)	
BAX (6A7) (mouse monoclonal)	1:200 (immunohistochemistry)	
Secondary antibodies		
Anti-mouse horseradish-peroxidase (HRP)-conjugated	1:5000	Santa Cruz Biotechnology (Frilabo, Porto, Portugal)
Anti-rabbit horseradish-peroxidase (HRP)-conjugated	1:5000	

2.11. Dual-luciferase reporter assay in human tumor cell lines

Dual-luciferase reporter assay was performed basically as reported (Leão et al., 2013c; Bisio et al., 2010). Briefly, about 5×10^4 cells/well of HCT116 tumor cell line were incubated in 24-well plates for 24 h. Cells were thereafter transfected at approximately 80% confluence using the Myrus LT-1 reagent (Tema Ricerca, Milan, Italy) according to the manufacturer's instructions. Specifically, 350 ng of the reporter vectors containing either the p21 (pGL3-1138) or the MDM2 (pGL3-MDM2) promoter were used along with 50 ng of the control pRLSV40 plasmid included to normalize the transfection efficiency. Transfected cells were treated with the GI_{50} and $2\times GI_{50}$ concentration of SLMP53-1 (or DMSO only), for 16 h. Cells were harvested and 10 μL cell cultures was transferred to a white 384-well plate, followed by 10 μL of 2x Passive Lysis Buffer (Promega, Milan, Italy), and incubation for 15 min at room temperature with continuous orbital shaking (500 r.p.m.). Afterward, 10 μL of Firefly Luciferase Bright Glo substrate (Promega, Milan, Italy) were added to the cell suspension and the light units were measured with a luminometer (Mithras LB940 plate reader-Berthold Technologies, Milan, Italy). To measure Renilla activity, 5 μL Firefly Luciferase Substrate (Luciferase Assay Reagent, LARII, Promega, Milan, Italy) followed by 5 μL Stop&Glow buffer (Promega, Milan, Italy) were added, and the light units were measured again with a luminometer. In this assay, since the expression of luciferase occurs in a p53-dependent manner, the p53 transcriptional activity is reflected by the luciferase activity, which was quantified in the presence and absence of the tested compounds.

2.12. RNA extraction and quantitative real-time polymerase chain reaction (RT-qPCR)

Total RNA from tumor cell lines was extracted using the *RNeasy Kit* (Qiagen, Milan, Italy). About 1 μg RNA was used for cDNA synthesis using the M-MuLV reverse transcritptase and the *Revert Aid cDNA Synthesis kit* (Thermo Fisher, Italy) in 20 μL final volume, and following the manufacturer's instructions. qPCR assays were performed in a 384-well plate format on a CFX Touch Real-Time PCR Detection System (Bio-rad, Italy), starting with 25 ng cDNA, as previously described (Lion et al., 2013). The 2x *KAPA SYBR® FAST qPCR Kit* (Kapa Biosystems, Rome, Italy) and specific primers, purchased from Eurofins (MWG, Italy), were employed. GAPDH, B2M and ACTB were used as reference genes.

2.13. TransAM assay

About 1.5 × 10^6 cells/well of MDA-MB-231 cell line were incubated for 24 h and thereafter treated with 2×GI_{50} and 3×GI_{50} concentration of SLMP53-1 (or DMSO only) for 24 h. Nuclear protein extracts were obtained using the *Nuclear Extract Kit* from Active Motif (Frilabo, Porto, Portugal), and the protein concentration was measured using NanoDrop 1000 from Thermo scientific (Portugal). The p53 DNA binding ability was evaluated using the *TransAM p53 Transcription Factor Assay Kit* from Active Motif (Frilabo, Porto, Portugal), according to the manufacturer's instructions. Briefly, equal amount of total nuclear protein was loaded into 96-well plate coated with an immobilized oligonucleotide containing a p53 consensus binding site. The amount of bound p53 protein was quantified using an anti-p53 antibody followed by a HRP-conjugated secondary antibody. The HRP signal was measured after addition of a manufacturer's substrate, using the BioTek Synergy HT plate reader at 450 nm. A nuclear extract of wt p53-expressing MCF-7 cells treated with H_2O_2 was used as kit positive control.

2.14. Transfection of p53 siRNA

MDA-MB-231 cells were transfected with 100 nM of small interfering RNAs (siRNAs) against p53 (SMARTpool p53) and negative nonspecific siRNAs (Non-targeting Pool) from Thermo Scientific/Dharmacon (Dagma, Carcavelos, Portugal), using Lipofectamine 2000 (Invitrogen, Alfagene, Carcavelos, Portugal), and following the manufacturer's instructions. After 24 h transfection, cells were treated with the GI_{50} concentration of SLMP53-1 (or DMSO only) for 24 h.

2.15. Analysis of reactive oxygen species (ROS) generation

Analysis of intracellular ROS generation was performed by flow cytometry. Briefly, about 1.5 × 10^5 cells/well (for HCT116 cell line) or 2.3 × 10^5 cells/well (for MDA-MB-231 cell line) were incubated in 6-well plates for 24 h. Cells were then treated with the GI_{50} concentration of OXAZ-1, SLMP53-1 or DMSO only for 24 h (SLMP53-1) or 48 h (OXAZ-1). Cells were harvested and stained with 5 μM Cell-ROX Green Reagent from Life Technologies (Alfagene, Carcavelos, Portugal) for 30 min at 37ºC.

2.16. Analysis of mitochondrial membrane potential ($\Delta\psi_m$)

For analysis of $\Delta\psi_m$, about 1.5 × 10^5 cells/well (for HCT116 cell line) or 2.3 × 10^5 cells/well (for MDA-MB-231 cell line) were incubated in 6-well plates for 24 h. Cells were

then treated with the GI_{50} concentration of OXAZ-1, SLMP53-1 or DMSO only for 8 h (for HCT116 cell line) or 16 h (for MDA-MB-231 cell line). Cells were harvested and incubated with 1 nM $DiOC_6(3)$ (Alfagene, Carcavelos, Portugal) for 30 min at 37ºC; followed by flow cytometry analysis. Cells treated with 50 μM carbonilcyanide p-triflouromethoxyphenylhydrazone (FCCP; Sigma-Aldrich, Sintra, Portugal), for 15 min at 37ºC, were used as positive control.

2.17. *In vitro* migration assays

Cell migration was analyzed using the Wound Healing Scratch assay as described in (Labelle-Côté et al., 2011), and the *QCM 24-Well Fluorimetric Chemotaxis Cell Migration Kit (8 μm)*, from Merck Millipore (VWR, Carnaxide, Portugal). In the Wound Healing Scratch assay, about 5×10^5 cells/well of HCT116 $p53^{+/+}$ or MDA-MB-231 cell lines were grown to confluence in 6-well plates for 24 h. Using a sterile 200 μL tip, a fixed-width wound was created in the cell monolayer and the GI_{10} concentration of DIMP53-1, SLMP53-1 or DMSO only was added to medium. Cells were thereafter photographed, using the Moticam 5.0MP camera with Motic's AE2000 inverted microscope (VWR, Carnaxide, Portugal) with 400x magnification, at different time-points of treatment until complete closure of the wound. In the *QCM 24-Well Fluorimetric Chemotaxis Cell Migration Kit (8 μm)*, about 0.5×10^6 cells/mL of HCT116 $p53^{+/+}$ or MDA-MB-231 cell lines were prepared in serum free RPMI 1640 and treated with the GI_{25} (for HCT116 $p53^{+/+}$ cell line) or the GI_{50} (for MDA-MB-231 cell line) concentration of DIMP53-1, SLMP53-1, or DMSO only, followed by incubation during 24 h (for HCT116 $p53^{+/+}$ cell line) or 8 h (for MDA-MB-231 cell line). Cell suspensions were distributed into 24-well plates (300 μL/insert), followed by addition of 500 μL medium containing 10% FBS to the lower chamber. Cells that migrated through the 8 μm pore membranes were eluted, lysed and stained with a green-fluorescence dye that binds to nucleic acids. The number of migrated cells is proportional to the fluorescence signal measured using the BioTek Synergy HT plate reader at 480/520 nm (ex/em).

2.18. Genotoxicity studies by micronucleus assay

Genotoxicity was analyzed by cytokinesis-block micronucleus assay in lymphocytes as described (Fernandes et al., 2011). Fresh peripheral blood samples were collected from healthy volunteers into heparinized vacutainers. Blood samples, suspended in RPMI medium supplemented with 10% FBS, were treated with different concentrations of DIMP53-1, SLMP53-1, DMSO only or 1 μg/mL cyclophosphamide (known mutagenic agent; positive control; Sigma-Aldrich, Sintra, Portugal) for 44 h. Cells were thereafter treated with

3 μg/mL cytochalasin B (cytokinesis preventive; Sigma-Aldrich, Sintra, Portugal) for 28 h. Lymphocytes were isolated by density gradient separation (Histopaque-1077 and -1119; Sigma-Aldrich, Sintra, Portugal), fixed in 3:1 methanol/glacial acetic acid, and stained with Wright stain (Sigma-Aldrich, Sintra, Portugal). For each sample, 1000 binucleated lymphocytes were blindly scored using a Nikon AlphaPhotoF2 YS2 light optical microscope (Portugal); the number of micronuclei per 1000 binucleated lymphocytes was recorded.

2.19. *In vivo* antitumor and toxicity assays

Animal experiments were conducted according to the European Council Directives on Animal Care and to the National Authorities. The BALB/c Nude mice and Wistar rats were purchased from Charles-River Laboratories and housed under pathogen free conditions in individual ventilated cages. For toxicity assays, Wistar rats were treated with 50 mg/kg of DIMP53-1, SLMP53-1, vehicle (DMSO) or saline solution (control) by intraperitoneal injection, twice a week during two weeks. After the four administrations, samples of blood and organs (kidneys, liver, heart, lungs, spleen) were collected for toxicological analysis. Each group was composed by five animals. Xenograft tumor assays were performed with HCT116 $p53^{+/+}$, HCT116 $p53^{-/-}$ and MDA-MB-231 human tumor cell lines. Briefly, 1×10^6 HCT116 cells (in PBS) or 5×10^6 MDA-MB-231 cells (in PBS/BD Matrigel Matrix High Concentration, 1:1; BD Biosciences, Enzifarma, Porto, Portugal) were inoculated subcutaneously in the dorsal flank of each mice. Tumor dimensions were assessed by caliper measurement and their volumes were calculated [tumor volume = (length $\times$ $width^2$) / 2]. Treatment was started when tumors reached volumes of approximately 100 mm^3 (which occurred 14 days after the grafts). Mice were then treated twice a week with 50 mg/kg DIMP53-1 or SLMP53-1, or vehicle (control) by intraperitoneal injection during two weeks. Tumor volumes and body weights were monitored twice a week until the end of the treatment. Animals were sacrificed by cervical dislocation at the end of the study. After sacrifice, tumors were removed and photographed. Human endpoints were established namely euthanasia in case of tumors reached 1500mm^3, or if the animals presented any signs of morbidity. The following number of animals was used: HCT116 $p53^{+/+}$ and HCT116 $p53^{-/-}$ xenografs (Control-6, Treatment-6), MDA-MB-231 xenografts (Control-6, Treatment-6).

2.20. Immunohistochemistry

Tumor tissues were fixed in 10% formalin, embedded in paraffin, sectioned at 4 μm, and stained with hematoxylin and eosin (H&E) or antibodies, following standard methodologies. Briefly, after deparaffination and rehydration, antigen retrieval was

performed by boiling the sections for 20 min in 10 mM citrate buffer (pH 6.0) for all antibody's staining, with the exception of anti-VEGF, for which the tissue was treated with 10 mM EDTA buffer (pH 8.0). The slices were then held for 20 min at room temperature. After dewaxing and blocking the endogenous peroxidases with UltraVision Hydrogen Peroxide Block, sections were treated with UltraVision Protein Block solution, both from Lab Vision Thermo Scientific (Taper, Sintra, Portugal). Incubation with primary anti-Ki-67, anti-VEGF, anti-CD34 and anti-BAX (Table 2.2) was performed for 2 h, at room temperature, with the exception of anti-BAX that was incubated overnight at 4°C. Immunostaining was carried out using the *UltraVision Quanto Detection System HRP DAB kit*, from Lab Vision Thermo Scientific (Taper, Sintra, Portugal), according to the manufacturer's instructions. Tissue sections were counterstained with Gill's heamatoxylin from Thermo Scientific (Taper, Sintra, Portugal), dehydrated, clarified and mounted. The primary antibody was replaced by 10% non-immune serum for negative controls. Finally, images were obtained using the Motic's AE2000 inverted microscope (400× magnification) with the Moticam 5.0MP camera.

Microvessel densities (MVD) were determined by counting all CD34-positive vessels (Weidner et al., 1991; Maeda et al., 2007). The hot spots were selected under a microscope (100×), and individual counts were made under a 400× magnification (0.155 mm^2 per field). The average counts from five fields were recorded. Any single highlighted endothelial cell, or endothelial cell cluster clearly separated from adjacent microvessels, and distinct clusters of brown-staining endothelial cells were counted as separate microvessels.

2.21. TUNEL assay

TUNEL assay was performed using the *In Situ Cell Death Detection Kit Fluorescein* from Roche (Sigma-Aldrich, Sintra, Portugal), according to the manufacturer's instructions. Briefly, after deparaffination and rehydration, tissues sections were treated for 20 min in 10 mM citrate buffer (pH 6.0), and incubated with TUNEL Reaction Mixture for 60 min at 37ºC in the dark. Tissues were counterstained with 0.1 µg/mL DAPI. Images were obtained using an Eclipse E400 fluorescence microscope (Nikon), 400x magnification, with a Digital Sight camera system (Nikon DS-5Mc), carrying built-in software for image acquisition (Nikon ACT-2U).

2.22. Flow cytometric data acquisition and analysis

For the flow cytometry analysis, the AccuriTM C6 flow cytometer from BD Biosciences (Enzifarma, Porto, Portugal) and the CellQuest software from BD Biosciences (Enzifarma, Porto, Portugal) were used. For the identification and quantification of cell cycle phases, the

FlowJo software or the ModFit LT software (Verity Software HouseInc., Topsham, USA) were used.

2.23. Statistical analysis

Data were analyzed statistically using the GraphPad software. Differences between means were tested for significance using the Student's *t*-test (*$p < 0.05$; **$p < 0.01$; ***$p < 0.001$).

2.24. Computational chemistry

The structures of the synthesized compounds 1a–c, 2a–b, 3a–b and 4a–b, Nutlin-3a and 1,4-benzodiazepine-2,5-dione (BZD) were built with MOE. All the structures were energetically minimized using the MMFF94x force field with a RMS gradient of 0.1 and inserted in a test database. The crystallographic structure of MDM2 protein bound to the MI-63 analog inhibitor was downloaded from the Protein Data Bank (PDB code: 3LBL), imported in MOE and the co-crystallized waters were removed. After superposition of the A, C and E chains, it was verified that the two chains with a closer match were chains C and E. However, since the indole nitrogen of MI-63 analog is a hydrogenbond donor to *LEU54*, it was found that the one closer to the optimal distance of 2.8 Å, between donor and acceptor atoms, was the MI-63 analog interacting with chain C. Therefore, only the C chain was kept and the residues were protonated to match their state at physiological pH using the protonate3D module of MOE. The binding pocket was defined by using alpha spheres (sphere that contacts 4 atoms on its boundary and contains no internal atoms) within 5 Å of the MI-63 analog crystallographic pose. All the docking experiments were performed using a rigid protein docking protocol with a triangle matcher placement with a London dG scoring and a MMFF94x force field refinement. The best scored conformation per structure was selected and results were ranked through their binding affinities. These studies were carried out by Santos group from iMed UL.

CHAPTER 3

Results

Identification of new p53-MDM2/MDMX inhibitors

CHAPTER 3.1

Oxazoloisoindolinones with *in vitro* antitumor activity selectively activate a p53-pathway through potential inhibition of the p53-MDM2 interaction

Soares J, Pereira NAL, Monteiro A, Leão M, Bessa C, dos Santos DJVA, Raimundo L, Queiroz G, Bisio A, Inga A, Pereira C, Santos MMM, Saraiva L.

***Eur J Pharm Sci* 2015 Jan; 66: 138–147**

As referred in Chapter 1, the restoration of p53 activity by inhibition of the p53-MDM2 interaction represents an appealing anticancer strategy for tumors with wt p53. Although several small molecules have emerged as inhibitors of the p53-MDM2 interaction, only few have reached clinical trials due to their low selectivity, high toxicity and poor pharmacokinetic profiles (Lauria et al., 2011; Wang et al., 2012; Wang and Hu, 2012; Zhao et al., 2013a). Efforts are therefore in progress to identify new scaffolds of p53-MDM2 interaction inhibitors with improved pharmacological properties.

In the present work, the activity of a synthesized small library of phenylalaninol-derived oxazolopyrrolidone lactams (Schemes 3.1.1 and 3.2.2) as potential p53-MDM2 interaction inhibitors was evaluated. The synthesis of this family was based in the principle that oxazolo moiety with aromatic side chains attached would mimic the rigid heterocyclic scaffold present in most p53-MDM2 interaction inhibitors.

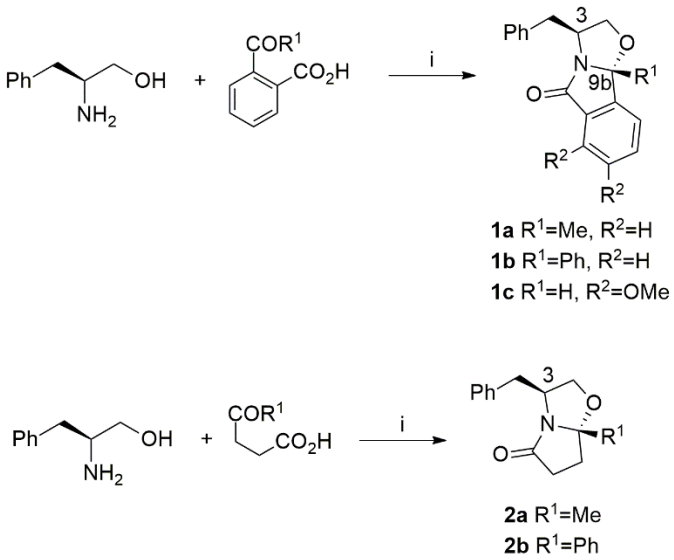

Scheme 3.1.1. Synthesis of compounds 1a–c and 2a–b. Reagents and conditions: (i) toluene, reflux, 66–92%.

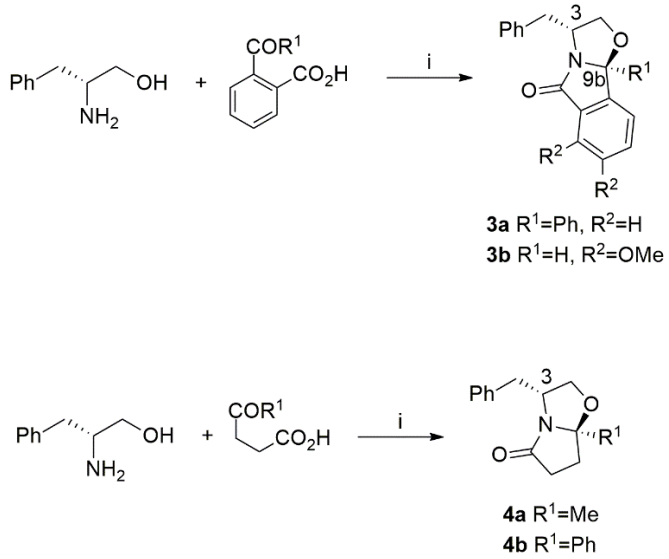

Scheme 3.1.2. Synthesis of compounds 3a–b and 4a–b. Reagents and conditions: (i) toluene, reflux, 57–84%.

3.1.1. Identification of compounds 1b and 3a as potential p53-MDM2 interaction inhibitors using a yeast-based assay

In this work, a previously developed yeast-based assay (Leão et al., 2013c) was used for the analysis of the activity of the synthesized small library of phenylalaninol-derived oxazolopyrrolidone lactams as inhibitors of the p53-MDM2 interaction. The effectiveness of this yeast assay was recently demonstrated by the discovery of a new inhibitor of the p53-MDM2 interaction with a xanthone scaffold (Leão et al., 2013c). In this assay, the expression of human wt p53 induces growth inhibition and S-phase cell cycle arrest, which is abolished by co-expression with human MDM2 (Leão et al., 2013a,c). Inhibitors of the p53-MDM2 interaction, such as Nutlin-3a (positive control), reduce the impact of MDM2 on p53 activity, thus restoring the p53-induced yeast growth inhibition and cell cycle arrest (Figure 3.1.1A and B). Notably, these small molecules do not interfere with the activity of p53 when expressed alone (Leão et al., 2013a,c). Using this approach, the effect of 1–50 μM of compounds was evaluated using, as endpoint, the MDM2-dependent reduction of p53-induced yeast growth inhibition.

Five oxazolopyrrolidone lactams derived from *S*-phenylalaninol were firstly tested. From the concentration-response curves obtained for the tested compounds, the concentration of 10 μM was selected as the lowest concentration at which a higher reduction of the MDM2 effect was obtained (Figure 3.1.1A for compounds 1b and 3a), without interfering with the growth of control yeast (empty vectors).

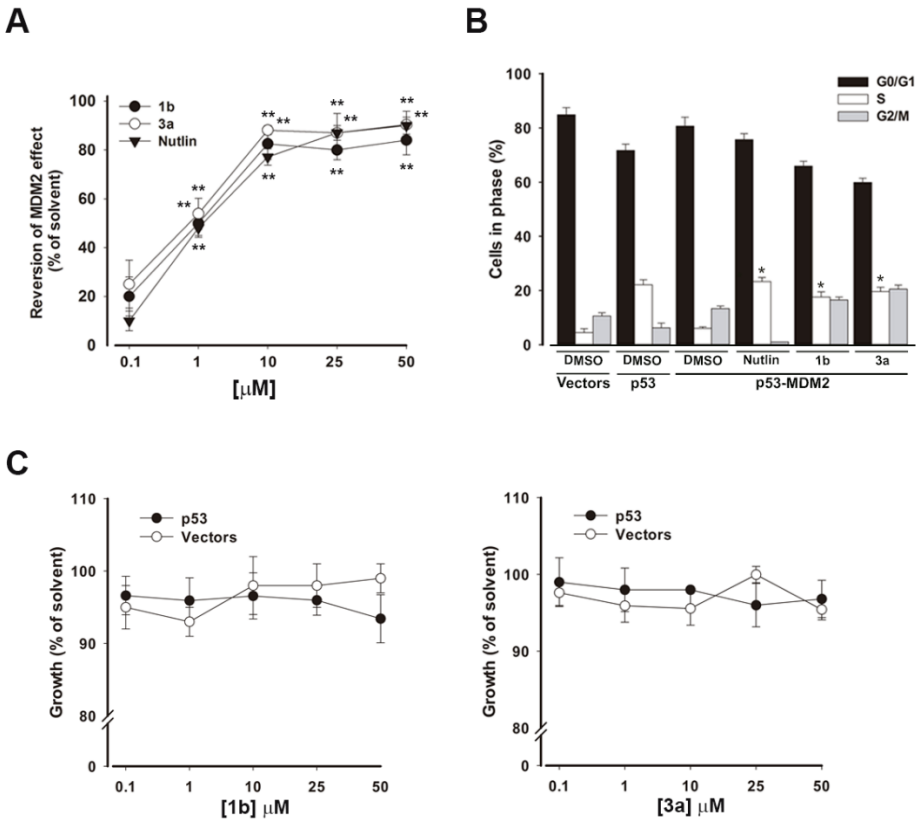

Figure 3.1.1. Identification of compounds 1b and 3a as potential inhibitors of the p53-MDM2 interaction using the yeast-based assay. (A) Percentage of reversion of the MDM2 negative effect on p53-induced growth inhibition caused by compounds 1b and 3a and Nutlin-3a (positive control); the growth of yeast cells co-expressing p53 and MDM2 treated with 1–50 μM of compounds or DMSO only, for 42 h, was analysed by CFU counts; results are plotted as relative to the growth inhibition achieved with yeast cells expressing p53 alone treated with DMSO only (set to 100%); presented data are mean ± S.E.M. of five independent experiments. **(B)** Effect of compounds 1b and 3a on the inhibition of p53-induced yeast cell cycle arrest by MDM2. Yeast cells were incubated with 10 μM compounds 1b and 3a, 10 μM Nutlin-3a or DMSO only, for 42 h. Cell cycle phases were quantified by flow cytometry; presented data are mean ± S.E.M. of two independent experiments. **(C)** Effect of compounds 1b and 3a on the growth of yeast cells expressing p53 alone and control yeast (vector); growth curves were obtained by CFU counts for yeast cells expressing p53 alone and control yeast treated with 1–50 μM of compounds 1b and 3a or DMSO only, for 42 h; presented data are mean ± S.E.M. of five independent experiments. In **(A)** and **(B)**, values significantly different from DMSO only are indicated (*$p < 0.05$; **$p < 0.001$).

Among the tested compounds, compound 1b significantly reverted the inhibitory effect of MDM2 on p53-induced yeast growth inhibition at a wide range of concentrations (Figure 3.1.1A), exhibiting a similar effect to Nutlin-3a (Table 3.1.1). Accordingly, like Nutlin-3a, compound 1b significantly reduced the inhibitory effect of MDM2 on p53-induced S-phase

cell cycle arrest (Figure 3.1.1B). Besides, compound 1b did not interfere with the activity of p53, when expressed alone, and with the growth of control yeast (vector) (Figure 3.1.1C).

With the results obtained in yeast, we could assume that a phenyl group is preferred to a methyl group at position R^1 (compounds 1b and 2b *versus* compounds 1a and 2a) (Table 3.1.1). Also, compounds 1 containing an isoindolinone moiety are more active than compounds 2 with a pyrrolidone moiety (Table 3.1.1).

Table 3.1.1. Effect of compounds 1a-c and 2a-b on the reversion of p53-induced yeast growth inhibition by MDM2.

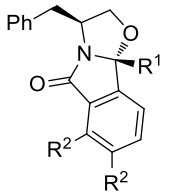

1

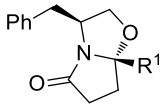

2

Compounds	R^1	R^2	Reversion of MDM2 effect (%)[a]
1a	Me	H	53.6 ± 3.0
1b	Ph	H	82.5 ± 6.4
1c	H	OMe	69.9 ± 3.5
2a	Me	—	38.7 ± 3.2
2b	Ph	—	47.6 ± 6.1
DMSO	—	—	2.3 ± 5.6
Nutlin-3a	—	—	73.2 ± 3.0

[a] Yeast cells co-expressing p53 and MDM2 were incubated in selective medium with 10 μM compound or DMSO only, for 42 h. Nutlin-3a was used as positive control. The growth inhibition obtained with yeast cells expressing only p53 treated with DMSO was considered as 100%. Data are mean ± S.E.M. of five independent experiments.

Due to the relevance of chirality on the biological activity, it was pivotal to assess the potential value of the enantiomers of the most active compounds. Four oxazolopyrrolidones derived from *R*-phenylalaninol were chosen to be analyzed on the p53-MDM2 interaction. In general, all compounds were more active than the *S*-phenylalaninol counterparts. In addition, as observed with compound 1b, the compound 3a significantly reverted the inhibitory effect of MDM2 on p53-induced yeast growth inhibition at a wide range of

concentrations tested (Figure 3.1.1A), exhibiting a similar effect to Nutlin-3a (Table 3.1.2). Accordingly, the oxazoloisoindolinone 3a significantly reduced the inhibitory effect of MDM2 on p53-induced S-phase cell cycle arrest (Figure 3.1.1B), without interfering with the activity of p53, when expressed alone, and with the growth of control yeast (vector) (Figure 3.1.1C).

In order to check the selectivity of compounds 1b and 3a for MDM2, the effect of these two compounds on MDMX was also checked, using a previously developed yeast assay to search for inhibitors of the p53–MDMX interaction (Leão et al., 2013b). Contrary to the well-known inhibitor of the p53–MDMX interaction SJ-172550 (Leão et al., 2013b), compounds 1b and 3a did not behave as potential inhibitors of this interaction, since they did not interfere with the negative effect of MDMX on p53 in yeast (data not shown).

Table 3.1.2. Effect of compounds 3a-b and 4a-b on the reversion of p53-induced yeast growth inhibition by MDM2.

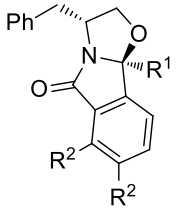

3

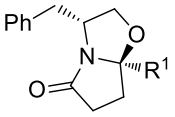

4

Compounds	R^1	R^2	Reversion of MDM2 effect (%)[a]
3a	Ph	H	88.1 ± 1.9
3b	H	OMe	66.8 ± 5.0
4a	Me	—	66.5 ± 4.7
4b	Ph	—	75.1 ± 4.0

[a] Yeast cells co-expressing p53 and MDM2 were incubated in selective medium with 10 μM compound or DMSO only, for 42 h. Nutlin-3a was used as positive control. The growth inhibition obtained with yeast cells expressing only p53 treated with DMSO was considered as 100%. Data are mean ± S.E.M. of five independent experiments.

3.1.2. Oxazoloisoindolinone 3a *in vitro* antitumor activity involves selective activation of the p53–pathway through inhibition of the p53-MDM2 interaction

The tumor cell growth inhibitory potential of compounds 1b and 3a, and the contribution of the p53-pathway to their activities were thereafter ascertained using human colon adenocarcinoma HCT116 cell lines with wt p53 (HCT116 $p53^{+/+}$) and its isogenic

derivative, in which p53 has been knocked out (HCT116 $p53^{-/-}$). The GI_{50} values obtained for compound 1b in $p53^{+/+}$ (8.8 μM) and $p53^{-/-}$ (11.4 μM) HCT116 cells indicated a potent growth inhibitory effect against these tumor cells (Figure 3.1.2). In spite of this, contrary to Nutlin-3a, no differences in the activity of compound 1b were observed between $p53^{+/+}$ and $p53^{-/-}$ HCT116 cells. Together these results indicated that compound 1b was a nonselective activator of the p53-pathway in human tumor cells.

Although a similar GI_{50} value to that of compound 1b was obtained with compound 3a (9.7 μM) in HCT116 $p53^{+/+}$ cells, a significant increase in the selectivity of compound 3a to the p53-pathway was observed (Figure 3.1.2). In fact, as observed with Nutlin-3a, a significant reduction of the potency of compound 3a was observed in HCT116 $p53^{-/-}$ cells.

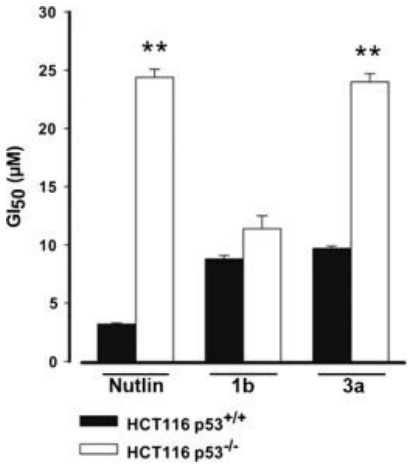

Figure 3.1.2. Compound 3a exhibits *in vitro* antitumor activity through selective activation of a p53-dependent pathway in human tumor cells. The GI_{50} concentration was determined for compounds 1b, 3a and Nutlin-3a, in human colon adenocarcinoma HCT116 cells with (HCT116 $p53^{+/+}$) and without (HCT116 $p53^{-/-}$) p53, after 48 h incubation, using the SRB assay. Presented data are mean ± S.E.M. of four independent experiments; values significantly different from HCT116 $p53^{+/+}$ cells are indicated (**$p < 0.01$).

The molecular mechanism of action of compound 3a as inhibitor of the p53-MDM2 interaction was thereafter investigated in HCT116 tumor cells. In HCT116 $p53^{+/+}$ cells, the growth inhibitory effect of compound 3a, at GI_{50} and twice the GI_{50} ($2xGI_{50}$) concentration, was associated with the induction of G0/G1-phase cell cycle arrest (Figure 3.1.3A). Accordingly, 9.7 μM oxazoloisoindolinone 3a up-regulated the p21 protein expression levels in $p53^{+/+}$, but not in $p53^{-/-}$, HCT116 cells (Figure 3.1.3B).

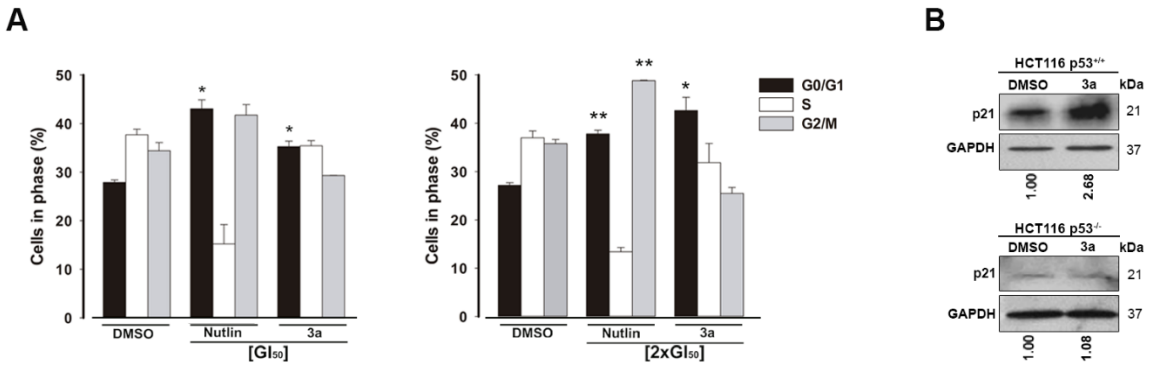

Figure 3.1.3. Compound 3a induces cell cycle arrest in human tumor cells. (A) Effect of compound 3a on cell cycle progression of HCT116 $p53^{+/+}$ cells was determined after 48 h treatment with 9.7 μM compound 3a and 3.2 μM Nutlin-3a or with 2 × GI_{50}. Cell cycle phases were analyzed by flow cytometry using PI and quantified using ModFit LT software. Presented data are mean ± S.E.M. of two independent experiments; values significantly different from DMSO are indicated (*$p < 0.05$; **$p < 0.01$). **(B)** Compound 3a increases the p21 protein levels in $p53^{+/+}$, but not in $p53^{-/-}$, HCT116 cells. Western blot analysis was performed after 4 h treatment with 9.7 μM compound 3a or DMSO only. The quantification of band intensity was performed using GAPDH as loading control.

Additionally, it was observed that the growth inhibitory effect of compound 3a in HCT116 $p53^{+/+}$ cells was also associated with the induction of late apoptosis both at GI_{50} and 2xGI_{50} concentration (Figure 3.1.4A). The activation of a p53-dependent apoptotic pathway by 9.7 μM compound 3a was further supported by the occurrence of PARP cleavage (Figure 3.1.4B), and by the up-regulation of BAX and PUMA (Figure 3.1.5A) in p53-expressing, but not in p53-null, HCT116 cells.

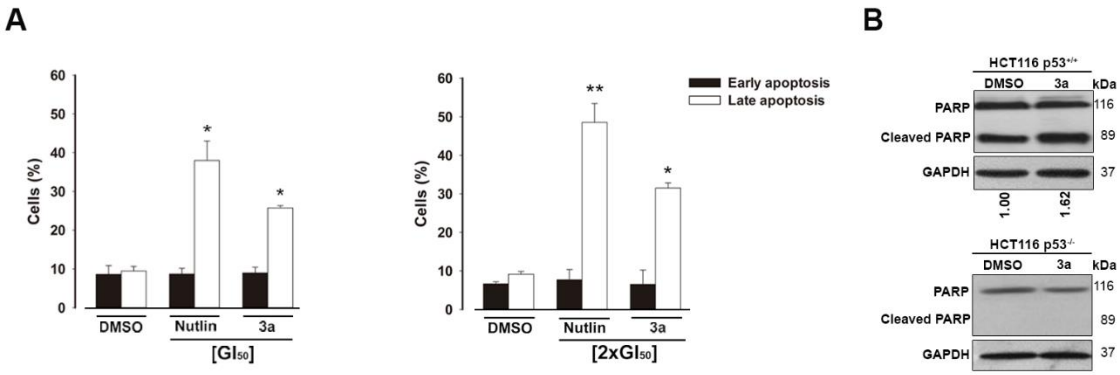

Figure 3.1.4. Compound 3a induces early and late apoptosis in HCT116 p53$^{+/+}$ cells. (A) Apoptosis was determined after 48 h treatment with 9.7 µM compound 3a and 3.2 µM Nutlin-3a or with 2 × GI_{50}, and was analyzed by flow cytometry using FITC-Annexin V and PI; quantification of cells in apoptosis are mean ± S.E.M. of two independent experiments; values significantly different from DMSO are indicated (*$p < 0.05$; **$p < 0.01$). **(B)** Compound 3a leads to PARP cleavage in p53$^{+/+}$, but not in p53$^{-/-}$, HCT116 cells. Western blot analysis was performed after 24 h treatment with 9.7 µM compound 3a or DMSO only. The quantification of band intensity was performed using GAPDH as loading control.

It was also observed that 9.7 µM compound 3a up-regulated the expression levels of MDM2 and increased the p53 baseline levels in p53$^{+/+}$, but not in p53$^{-/-}$, HCT116 cells (Figure 3.1.5A). This stabilization of p53 protein levels indicated an inhibition by compound 3a of the p53 degradation caused by its interaction with MDM2.

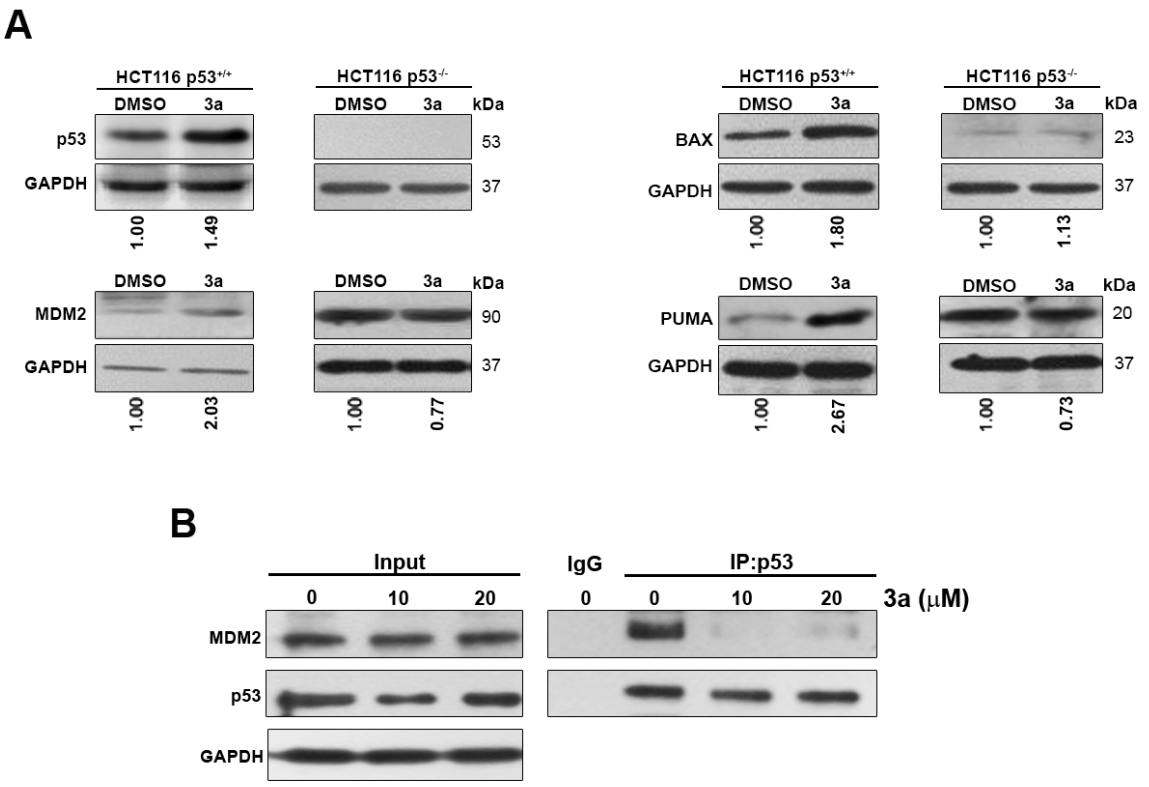

Figure 3.1.5. Compound 3a increases the expression levels of p53 target genes and disrupted the p53-MDM2 interaction in HCT116 p53$^{+/+}$ cells. (A) Western blot analysis was performed after 8 h (for p53) and 24 h (for BAX, MDM2 and PUMA) treatments with 9.7 μM compound 3a or DMSO only. The quantification of band intensity was performed using GAPDH as loading control. **(B)** HCT116 p53$^{+/+}$ cells were treated with 10 and 20 μM compound 3a or DMSO only for 16 h, followed by IP with p53 antibody or mouse immunoglobulin G (IgG) antibody and immunoblot with MDM2 and p53 antibodies; whole cell lysate (input). GAPDH was used as loading control.

Moreover, the ability of compound 3a to block the p53-MDM2 interaction in HCT116 p53$^{+/+}$ cells was checked by co-IP. The results obtained confirmed that 10 and 20 μM compound 3a blocked the p53-MDM2 interaction (Figure 3.1.5B). In fact, these experiments showed that little or no MDM2 protein co-immunoprecipitated with p53 in HCT116 p53$^{+/+}$ cells treated with compound 3a.

3.1.3. Predicted binding model supports the binding of compound 3a to MDM2

Molecular docking studies with the tested phenylalaninol-derived oxazolopyrrolidone lactams were performed on the MDM2 hydrophobic cleft using the Molecular Operating

Environment (MOE) software and the crystallographic structure with PDB code 3LBL (www.pdb.org) (Berman et al., 2000) allowing to rank the compounds by binding affinities summarized in Table 3.1.3. Only the best scoring conformation per molecule was considered in the discussion.

Table 3.1.3. Binding affinities found by molecular docking for the tested compounds.

Compounds	ΔG kcal/mol
3a	-21.61
1b	-20.80
4a	-18.34
1c	-18.11
4b	-16.89
2b	-16.80
1a	-16.77
2a	-15.74
3b	-14.82
Nutlin-3a	-26.50
2-Cl-BZD	-21.91

The co-crystallized ligand MI-63 analog was re-docked as a way to validate the molecular docking method. The root mean square deviation (RMSD) between the predicted and co-crystallized pose of MI-63 analog was 1.11 Å (predicted binding energy: −29.37 kcal/mol) which indicates that the software is able to accurately reproduce the binding pose of the co-crystallized ligand. A second validation of the docking method was performed by confirming that the interactions observed for the docked Nutlin-3a and BZD structures were in agreement with the interactions found for these two compounds in other crystallographic structures (PDB code: 4J3E, for Nutlin-3a; PDB code: 1T4E, for BZD). The values obtained for inhibitors which are known to establish the well characterized interactions with the MDM2 protein were found to be between −26.50 (Nutlin-3a) and −21.91 (BZD) kcal/mol. Among the tested phenylalaninol-derived oxazolopyrrolidone lactams, compounds 3a and 1b presented values of −21.61 and −20.80 kcal/mol respectively, thus having the best binding affinities within this new group of p53-MDM2 interaction inhibitors (Table 3.1.3). It is important to stress that these compounds were also the ones having the highest activities in the yeast screening assay and that a good correlation was found between the binding affinities estimated by docking for this class of compounds and the percentage of inhibition. The binding interactions established between compound 3a and

MDM2 protein were visually inspected and the conformation with the highest score is displayed in Figure 3.1.6. It was found that for the most active compound, 3a, the binding interactions are in agreement with one of the possible binding modes already described for isoindolinones derivatives, found through NMR studies (Riedinger et al., 2008). The aromatic ring of the isoindolinone core establishes hydrophobic contacts with residue *ILE61*. The phenyl group at position C9b is projected towards the deep hydrophobic pocket of MDM2 and the methylene-phenyl moiety establishes hydrogen-π interactions with residue *LEU54*. The 1YCR structure containing p53 interacting with MDM2 was aligned and superposed with the 3LBL structure using the MDM2 residues defining the pocket. The alignment and the positioning of residues responsible for the most important interactions are depicted in Figure 3.1.6. The picture makes clear the mimetic nature of compound 3a, where the location occupied by *PHE19* is now occupied by the aromatic ring of isoindolinone moiety, the *TRP23* by the phenyl group at position 9b and *LEU26* by the methylphenyl group.

In protein–protein interactions, there are some concerns about possible conformational changes produced on the binding site upon binding to proteins or ligands that will impose the usage of other research techniques besides docking.

The binding site defined by the area where all organic molecules mimicking the p53 interaction is not very deep like a pocket, but resembles a cleft/groove and is hydrophobic in nature. However, all the organic molecules have a ring or fused rings located deeply in the pocket where *PHE19* of p53 interact. In opposition to the other two pockets (defined by *TRP23* and *LEU26* of p53), this one goes deep in the protein structure and seems to work as an anchor point guiding the positioning of the binding molecules.

For instance, superposing structures 1YCR (p53 co-crystallized) with 1T4E (benzodiazepine co-crystallized) shows a relatively low RMSD for the alpha carbons (0.9 Å). The a.a. of the three pockets defined by p53 have very similar rotameric states for the residues, defining the three referred pockets except for *TYR67*, *HIS73* and *MET62*. The latter is the only residue in a different rotameric state not belonging to a coil region found between *TYR67* and *HIS73*. *MET62* is the only residue in a different rotameric state not belonging to the coil region. All these residues have no specific interactions with the co-crystallized molecules, except a generic hydrophobic match. Moreover, the synthesized molecules reported in the manuscript also have no direct interactions with this residue and the closest atoms are characteristically at a distance of at least 4 Å. Therefore, the possibility of using molecular docking to predict the binding modes of the newly synthesized molecules seems adequate.

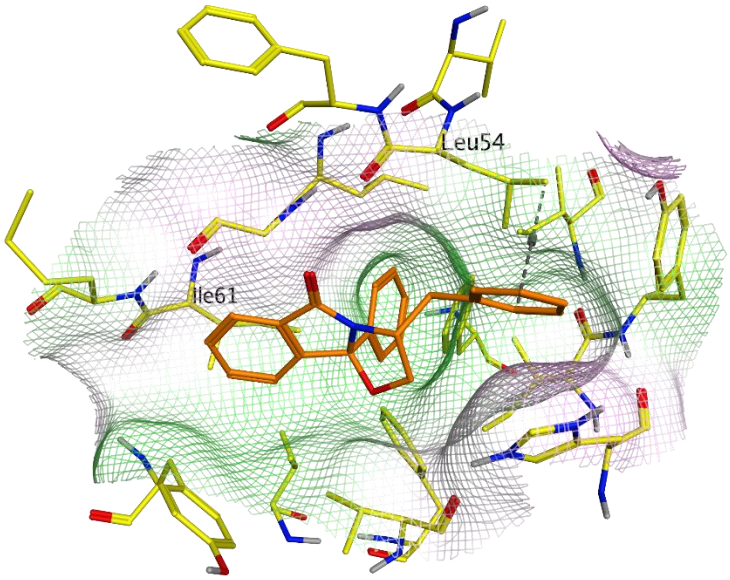

Figure 3.1.6. Docking pose of compound 3a within the MDM2 hydrophobic cleft limits depicted with a surface (in green, hydrophobic; in pink, hydrophilic areas). Receptor carbon residues are displayed in yellow and *LEU54* and *ILE61* are highlighted. Part of the p53 backbone (helix in red, turn in blue, loop in white) and residues *PHE19*, *TRP23* and *LEU26* are represented with carbons in light blue.

3.1.4. Discussion

In this work, nine phenylalaninol-derived oxazolopyrrolidone lactams were synthesized and their capacity to inhibit the p53-MDM2 interaction was investigated. The screening of the compounds using a yeast cell model led to the identification of two potential inhibitors of the p53-MDM2 interaction, compounds 1b and 3a. The results obtained in human tumor cells demonstrated that compound 1b is a nonselective activator of the p53-pathway in human tumor cells.

Contrary to compound 1b, the *in vitro* tumor growth inhibitory activity of compound 3a revealed to be dependent on p53-pathway. In conformity to what was obtained in yeast, oxazoloisoindolinone 3a mimicked the activity of known small molecule inhibitors of the p53-MDM2 interaction in human tumor cells, leading to the successful activation of p53 and downstream cell signaling. In fact, in tumor cells, the oxazoloisoindolinone 3a exhibited the most relevant hallmarks of a typical inhibitor of the p53-MDM2 interaction. Particularly, it decreased the proliferation of wt p53-carrying tumor cells, presenting a significantly lower potency in tumor cells without p53. Additionally, in wt p53-carrying tumor cells, it induced cell cycle arrest and apoptosis, led to p53 stabilization and increased the expression levels

of proteins encoded by p53 target genes. Most importantly, oxazoloisoindolinone 3a was able to inhibit the p53-MDM2 interaction in tumor cells. Finally, molecular docking studies supported the binding of oxazoloisoindolinone 3a to MDM2 and provided insights about its binding mode, what may allow a more guided structure optimization of compound 3a.

Altogether, in this work, synthesis combined with computational docking studies and biological screening assays led to the identification of oxazoloisoindolinone 3a, which belongs to a new class of potent and selective small molecule activators of the p53-pathway with promising antitumor activity. Additionally, oxazoloisoindolinone 3a may be the basis for the structure-based design of p53-MDM2 interaction inhibitors with improved pharmacological properties compared to those currently available.

CHAPTER 3.2

A tryptophanol-derived oxazolopiperidone lactam is cytotoxic against tumors via inhibition of p53 interaction with murine double minute proteins

Soares J, Raimundo L, Pereira NAL, dos Santos DJVA, Pérez M, Queiroz G, Leão M, Santos MMM, Saraiva L.

***Pharmacol Res* 2015 May-Jun; 95-96: 42-52.**

As referred in Chapter 1, despite many results demonstrated the greatest efficiency of dual inhibition of MDM2 and MDMX on p53 activation, to date, just few small molecule dual inhibitors of p53-MDMs interactions have been identified. Therefore, in this work, new inhibitors of p53-MDMs interactions were searched from a small library of enantiopure tryptophanol-derived oxazolopiperidinone lactams. The selection of this family of compounds was based in the conjugation of an oxazolo ring with a piperidinone ring, two scaffolds that are described to act as p53-MDM2 interaction inhibitors (Sun et al., 2014).

3.2.1. Identification of OXAZ-1 as potential dual inhibitor of p53-MDMs interactions, using a yeast-based screening assay

In this work, six (*S*)-tryptophanol-derived oxazolopiperidinone lactams (Figure 3.2.1) were tested for their ability to inhibit the p53 interaction with MDM2 and MDMX, using previously developed yeast-based screening assays (Leão et al., 2013b,c).

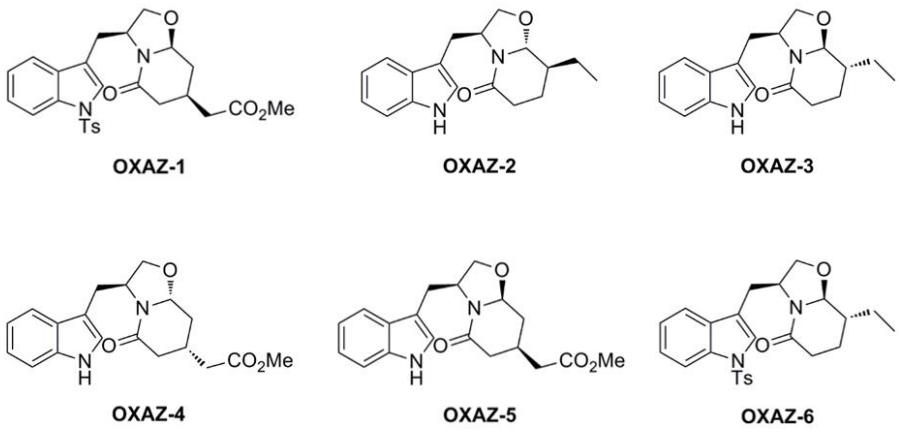

Figure 3.2.1. Chemical structure of tryptophanol-derived oxazolopiperidone lactams evaluated in yeast.

As referred in Chapter 3.1, in the yeast assays MDMs reduce the human p53-induced growth inhibition, an effect reverted by p53-MDMs interaction inhibitors (Leão et al., 2013b,c). The efficiency of these yeast assays to search for inhibitors of these interactions was validated by testing Nutlin-3a and SJ-172550, respectively. As in mammalian cells (Graves et al., 2012), also in yeast Nutlin-3a did not interfere with the MDMX-inhibitory

activity, confirming its activity on MDM2 only (Table 3.2.1; Figure 3.2.2A), while SJ-172550 did not interfere with the MDM2-inhibitory activity, confirming its activity on MDMX only (Table 3.2.1; Figure 3.2.2A).

Table 3.2.1. EC_{50} values obtained for the compounds tested in yeast.

Compounds	EC_{50} (μM)	
	p53-MDM2	p53-MDMX
Nutlin-3a	1.6 ± 3.6	> 50
SJ-172550	> 50	12.4 ± 4.3
OXAZ-1	1.0 ± 2.4	2.4 ± 3.7
OXAZ-2	2.3 ± 3.7	> 50
OXAZ-3	2.0 ± 3.3	> 50
OXAZ-4	2.1 ± 2.4	> 50
OXAZ-5	> 50	> 50
OXAZ-6	3.0 ± 3.3	> 50

Yeast cells co-expressing p53 and MDM2/MDMX were incubated with 0.1–50 μM compounds or DMSO only, for 42 h. The EC_{50} (concentration that caused 50% of the reversion effect) values were determined from concentration-response curves of the reversion of the MDM2/MDMX-inhibitory effect obtained for 0.1–50 μM compounds (see Figure 3.2.2A for OXAZ-1 and positive controls). Data are mean ± S.E.M. of six independent experiments.

Using this approach, the effect of 0.1–50 μM compounds was evaluated. From the concentration-response curves of the reversion of MDM2-inhibitory effect obtained for each compound, it was shown that, with the exception of OXAZ-5, all the other tested compounds presented similar effects to Nutlin-3a with reversion of the MDM2-inhibitory effect (Table 3.2.1). However, only OXAZ-1 was able to revert the MDMX-inhibitory effect, exhibiting a higher potency than SJ-172550 (Table 3.2.1). Interestingly, contrary to Nutlin-3a and SJ-172550, OXAZ-1 reverted the inhibitory effect of both MDMs (Table 3.2.1; Figure 3.2.2A). Additionally, OXAZ-1 did not interfere with the growth of control yeast and yeast expressing p53, MDM2 or MDMX alone (Figure 3.2.2B).

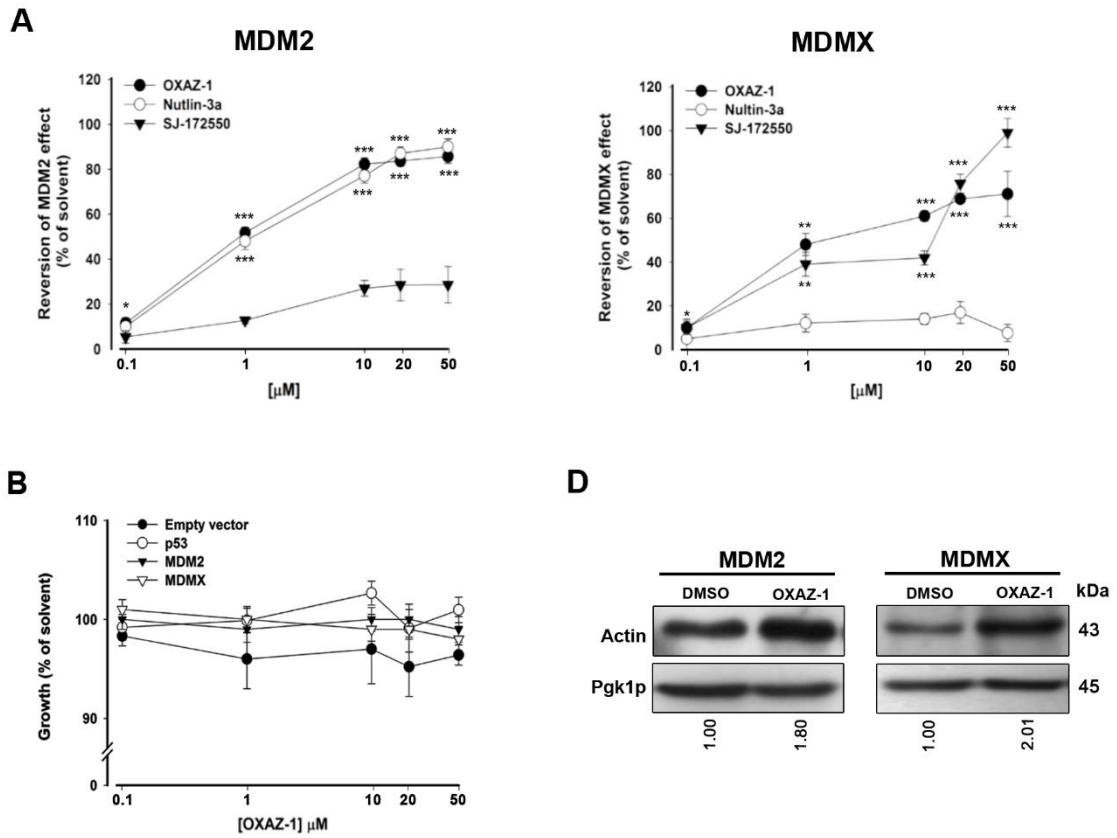

Figure 3.2.2. Identification of OXAZ-1 as potential dual inhibitor of p53-MDMs interactions, using a yeast-based screening assay. (A) Effect of 0.1–50 μM OXAZ-1, Nutlin-3a and SJ-172550 on the reversion of p53-induced yeast growth inhibition by MDM2 and MDMX, after 42 h incubation. The growth of yeast cells co-expressing p53 and MDM2/MDMX was evaluated by CFU counts; results were plotted setting as 100% the growth achieved with yeast cells expressing p53 alone incubated with DMSO only; data are mean ± S.E.M. of six independent experiments; values significantly different from DMSO only are indicated (*$p < 0.05$, **$p < 0.01$, ***$p < 0.001$). **(B)** Effect of 0.1–50 μM OXAZ-1 on the growth of yeast expressing p53, MDMX, MDM2 or transformed with the empty vector after 42 h incubation. Yeast cell growth was evaluated by CFU counts; results were plotted setting as 100% the growth achieved with DMSO only; data are mean ± S.E.M. of five independent experiments; values are not significantly different from DMSO only ($p > 0.05$). **(C)** Effect of 10 μM OXAZ-1 on the actin protein levels of yeast cells co-expressing p53 and MDM2/MDMX after 42 h incubation. Immunoblots represent one of three independent experiments; Pgk1p was used as loading control.

In a recent work, it was shown that expression of human p53 in yeast increased the expression levels of *ACT1* (described as a yeast p53 target gene; Leão et al., 2013b), an effect abolished by MDM2 and MDMX, and re-established by Nutlin-3a and SJ-172550, respectively (Leão et al., 2013b). Here, it was shown that, like Nutlin-3a (for MDM2) and

SJ-172550 (for MDMX), OXAZ-1 (at 10 μM for MDM2 and 20 μM for MDMX) increased the actin protein levels in yeast cells co-expressing p53 and MDM2/MDMX (Figure 3.2.2C). These results reinforced a reversion of the MDMs-inhibitory effect by OXAZ-1.

3.2.2. OXAZ-1 has a p53-dependent tumor growth-inhibitory effect mediated by disruption of p53-MDMs interactions and induction of a mitochondria-mediated apoptotic pathway

The tumor cell growth-inhibitory potential of OXAZ-1 and the contribution of the p53 pathway to its activity were thereafter ascertained using the human colon adenocarcinoma HCT116 cell lines with wt p53 (HCT116 $p53^{+/+}$) and its p53-null isogenic derivative (HCT116 $p53^{-/-}$). The GI_{50} values obtained for OXAZ-1, after 48 h treatment, in $p53^{+/+}$ and $p53^{-/-}$ HCT116 cells, revealed a p53-dependent growth-inhibitory effect by OXAZ-1 (Figure 3.2.3A). In fact, a significant reduction of the potency of OXAZ-1 was observed when the p53 pathway was knocked out in HCT116 $p53^{-/-}$ cells.

In HCT116 $p53^{+/+}$ cells, the growth-inhibitory effect of OXAZ-1, at the GI_{50} concentration (25 μM), was associated with G0/G1-phase cell cycle arrest (Figure 3.2.3B) and late apoptosis (Figure 3.2.3C). The activation of a p53-dependent apoptotic pathway by 25 μM OXAZ-1 was further supported by the inability of this compound to induce apoptosis (Figure 3.2.3C) and PARP cleavage (Figure 3.2.3D), in p53-null HCT116 cells.

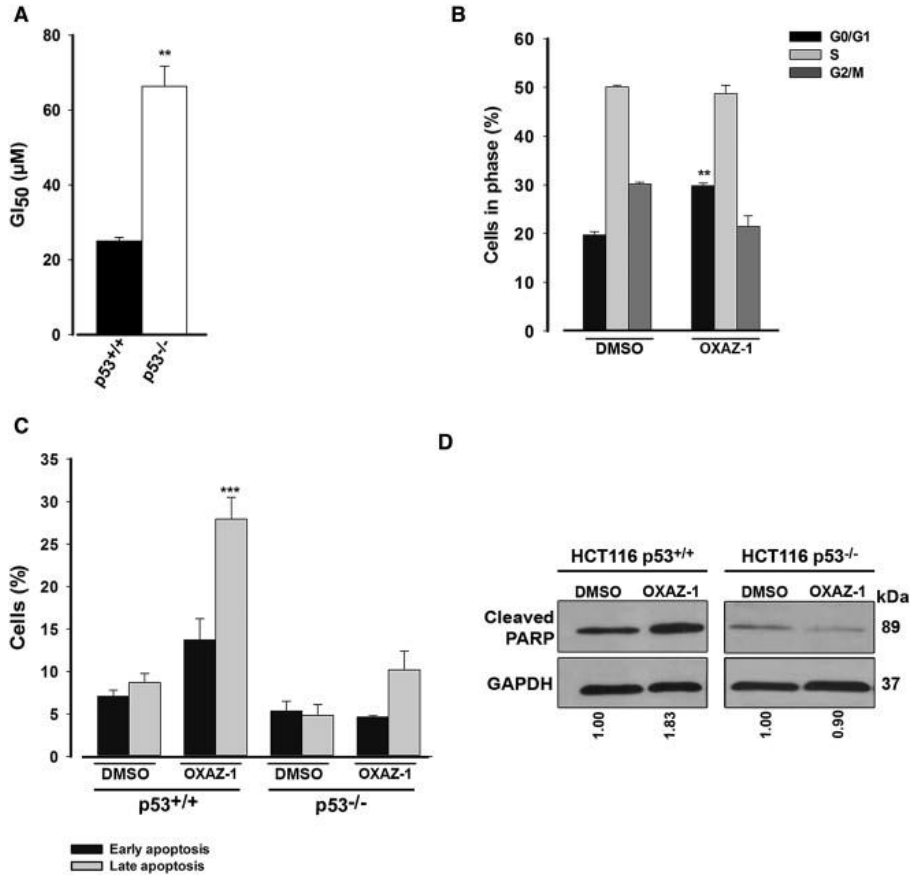

Figure 3.2.3. OXAZ-1 induces growth inhibition associated with cell cycle arrest and p53-dependent apoptosis, in human colon adenocarcinoma HCT116 tumor cells. (A) The GI_{50} concentration of OXAZ-1 was determined in $p53^{+/+}$ and $p53^{-/-}$ HCT116 cells, after 48 h treatment, using the SRB assay. Data are mean ± S.E.M. of four independent experiments; values significantly different from HCT116 $p53^{+/+}$ cells are indicated (**$p < 0.01$). **(B)** Effect of 25 μM OXAZ-1 on cell was analyzed by flow cytometry using PI staining, after 24 h treatment; data are mean ± S.E.M. of two independent experiments; values significantly different from DMSO are indicated (**$p < 0.01$). **(C)** Effect of 25 μM OXAZ-1 on apoptosis was analyzed by flow cytometry using FITC-Annexin V and PI, after 24 h treatment; data are mean ± S.E.M. of two independent experiments; values significantly different from DMSO are indicated (***$p < 0.001$). **(D)** Effect of 25 μM OXAZ-1 on PARP cleavage, after 24 h treatments. Immunoblots represent one of three independent experiments; GAPDH was used as loading control.

By western blot analysis, it was also observed that 25 μM OXAZ-1 led to p53 stabilization and increased the levels of proteins encoded by major p53 transcription targets, such as MDM2, MDMX, p21, PUMA and BAX, in $p53^{+/+}$, but not in $p53^{-/-}$, HCT116 cells (Figure 3.2.4A).

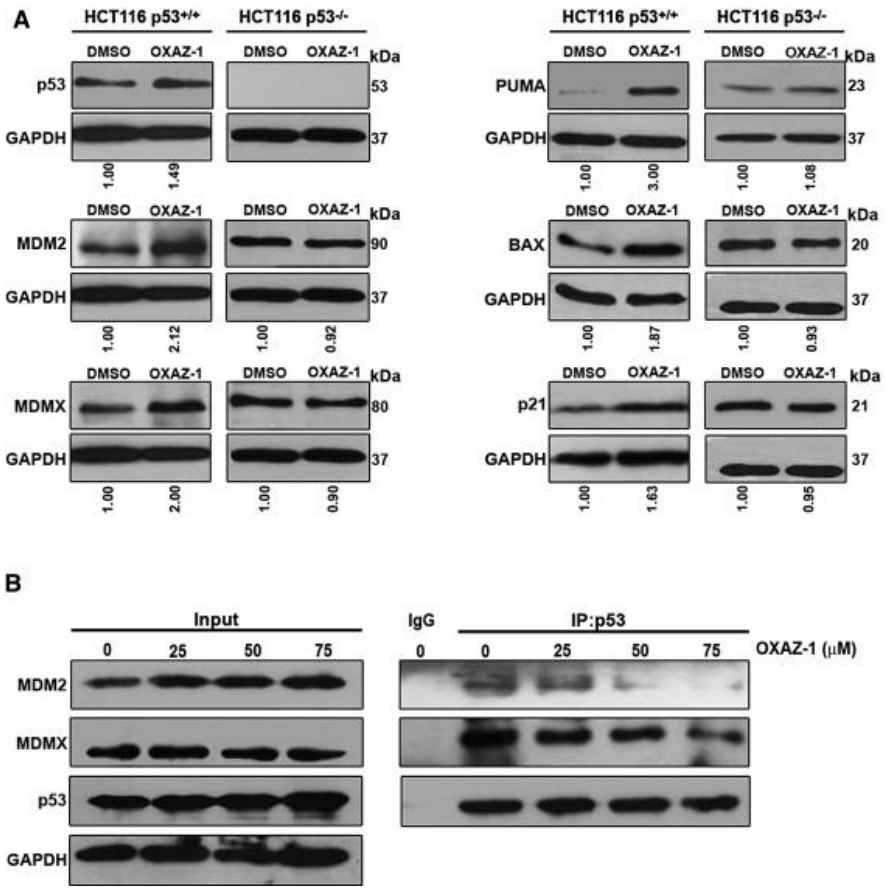

Figure 3.2.4. OXAZ-1 leads to p53 stabilization and to the up-regulation of p53 target genes by blocking the p53 interaction with MDM2 and MDMX, in HCT116 p53$^{+/+}$ cells. (A) Effect of 25 μM OXAZ-1 on the protein levels of p53, MDM2, MDMX, p21, PUMA and BAX in p53$^{+/+}$ and p53$^{-/-}$ HCT116 cells after 24 h treatment. Immunoblots represent one of three independent experiments; GAPDH was used as loading control. **(B)** Cells were treated with 25, 50 and 75 μM OXAZ-1 or DMSO only for 16 h, followed by immunoprecipitation with p53 or mouse immunoglobulin G (IgG) antibodies, and western blot with MDM2, MDMX and p53 antibodies; whole cell lysate (Input); immunoblots represent one of three independent experiments; GAPDH was used as loading control.

The ability of OXAZ-1 to block the p53 interaction with MDM2 and MDMX was further demonstrated by co-IP, in HCT116 p53$^{+/+}$ cells (Figure 3.2.4B). In fact, at 50 and 75 μM (corresponding to 2×GI_{50} and 3×GI_{50} concentrations, respectively), little or no MDM2 was co-immunoprecipitated with p53, and a visible decrease of the amount of MDMX co-immunoprecipitated with p53 was observed (Figure 3.2.4B). Similar results were reported for RO-5963, for which the disruption of the p53 interaction with MDM2 and MDMX was observed at 4×GI_{50} concentration (Graves et al., 2012).

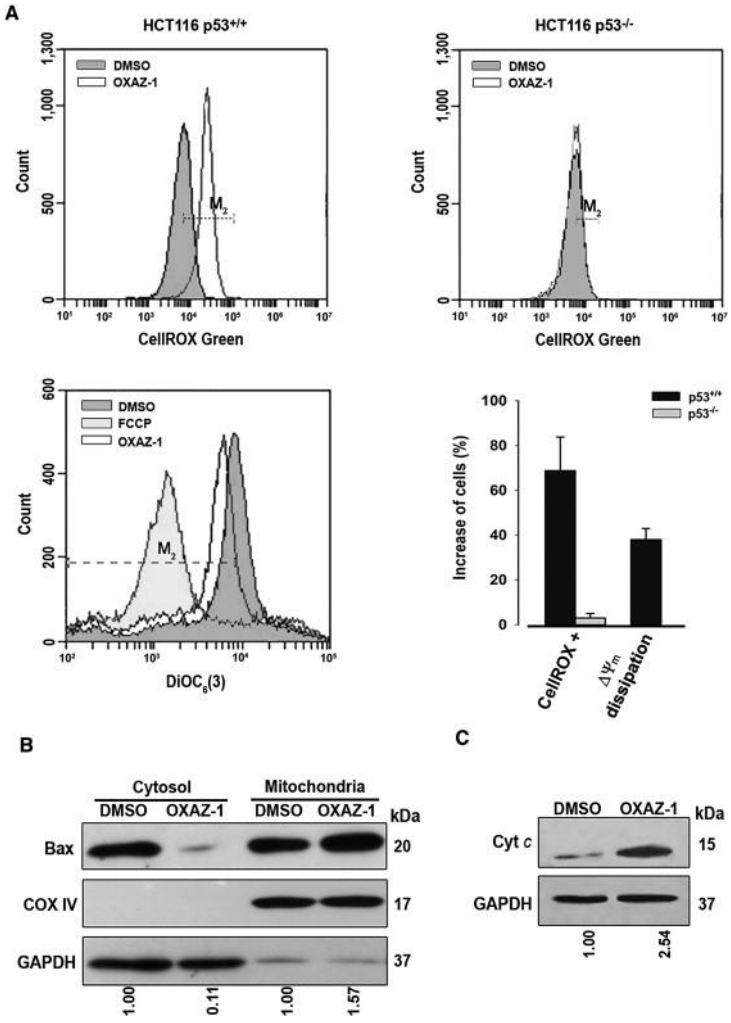

Figure 3.2.5. OXAZ-1 induces a p53-dependent mitochondria-mediated apoptotic pathway in HCT116 p53$^{+/+}$ cells. (A) Effect of 25 μM OXAZ-1 on ROS production, in p53$^{+/+}$ and p53$^{-/-}$ HCT116 cells after 48 h treatment, and on $\Delta\psi_m$ dissipation in HCT116 p53$^{+/+}$ cells after 8 h treatment. For assessment of ROS production and $\Delta\psi_m$, cells were stained with CellROX and $DIOC_6(3)$, respectively, and analyzed by flow cytometry; histograms represent one of two independent experiments; M_2 cursor indicates the subpopulation analyzed; represented values correspond to the increase in the percentage of CellROX-positive cells and of cells with $\Delta\psi_m$ dissipation obtained after treatment with OXAZ-1 or DMSO only, and are mean ± S.E.M. of two independent experiments; in $\Delta\psi_m$ analysis, FCCP was used as positive control. **(B)** Effect of 25 μM OXAZ-1 on BAX translocation from cytosol to mitochondria after 24 h treatment. GAPDH and COX IV were used as loading control of cytosolic and mitochondrial fractions, respectively. **(C)** Effect of 25 μM OXAZ-1 cyt *c* release into the cytosol after 24 h treatment. GAPDH was used as loading control. In **(B)** and **(C)**, immunoblots represent one of three independent experiments.

Additionally, it was also observed that 25 μM OXAZ-1 led to a marked increase of ROS production in p53$^{+/+}$, but not in p53$^{-/-}$, HCT116 tumor cells and to $\Delta\psi_m$ dissipation in

HCT116 p53$^{+/+}$ cells (Figure 3.2.5A). Moreover, besides the increase of BAX production (Figure 3.2.4A), 25 μM OXAZ-1 triggered its translocation from cytosol to mitochondria (Figure 3.2.5B), and the release of cyt *c* from mitochondria to cytosol (Figure 3.2.5C). Altogether, these results showed that OXAZ-1 was a potent inducer of a p53-dependent mitochondria-mediated apoptotic pathway in human tumor cells.

3.2.3. MDMX-overexpression tumor cells are sensitive to OXAZ-1

Tumor cells overexpressing MDMX have been described as fairly insensitive to MDM2-only inhibitors (e.g., Nutlin-3a) due to their inability to inhibit the p53–MDMX interaction (Graves et al., 2012; Patton et al., 2006; Wade et al., 2006). Based on this, the effect of OXAZ-1 was tested in human breast adenocarcinoma MCF-7 cells, a well-known MDMX-overexpressing tumor cell line (Graves et al., 2012). As expected, a similar growth inhibitory effect to that obtained in HCT116 p53$^{+/+}$ cells was achieved in MCF-7 cell lines by OXAZ-1 (GI_{50} value of 23.5 ± 2.5 μM, *n* = 4). Additionally, as in HCT116 p53$^{+/+}$ cells, also in MCF-7 cells, the OXAZ-1-induced growth inhibition was associated with G0/G1-phase cell cycle arrest (Figure 3.2.6A) and late apoptosis (Figure 3.2.6B) with PARP cleavage (Figure 3.2.6C). Moreover, also in MCF-7 cells, 23.5 μM OXAZ-1 led to the stabilization of p53 protein levels and to the up-regulation of p53 transcription targets involved in cell cycle (p21) and apoptosis (BAX) (Figure 3.2.6D). Altogether, these results showed that also in MDMX-overexpression tumor cells OXAZ-1 was able to activate the p53 pathway mostly inhibited by MDMX.

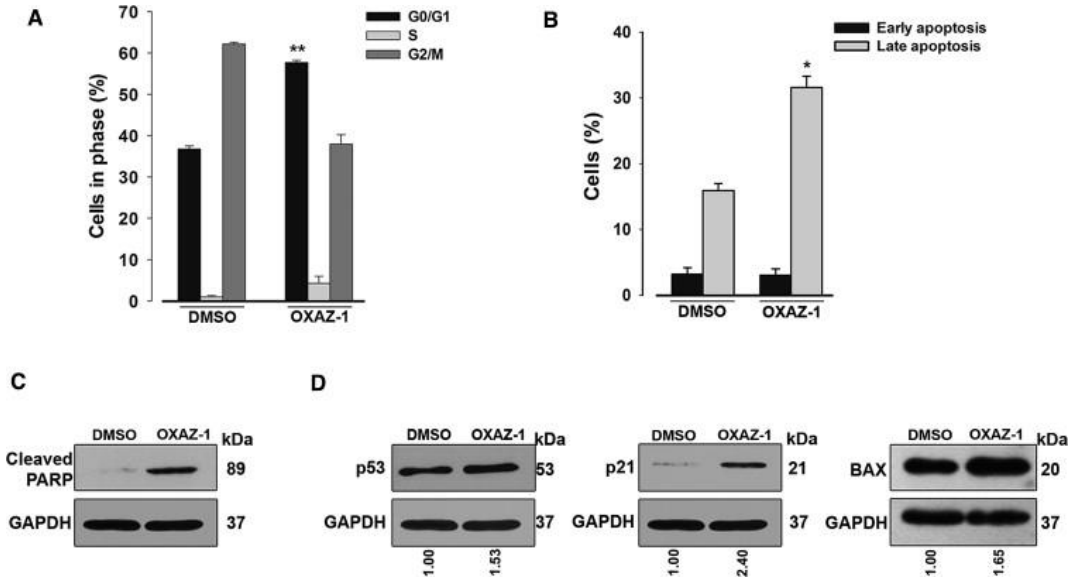

Figure 3.2.6. OXAZ-1 induces growth inhibition associated with cell cycle arrest and apoptosis in MDMX-overexpressing human breast adenocarcinoma MCF-7 tumor cells through activation of the p53 pathway. (A) Effect of 47 μM (2xGI_{50}) OXAZ-1 on cell cycle, after 24 h treatment. Cell cycle phases were analyzed by flow cytometry using PI staining; data are mean ± S.E.M. of two independent experiments; values significantly different from DMSO are indicated (**p < 0.01). **(B)** Effect of 47 μM OXAZ-1 on apoptosis, after 24 h treatment. Apoptosis was analyzed by flow cytometry using FITC-Annexin V and PI; data are mean ± S.E.M. of two independent experiments; values significantly different from DMSO are indicated (*p < 0.05). **(C, D)** Effect of 23.5 μM OXAZ-1 on PARP cleavage **(C)**, and on p53, p21 and BAX protein levels **(D)**, after 24 h treatments. Immunoblots represent one of three independent experiments; GAPDH was used as loading control.

3.2.4. OXAZ-1 sensitizes tumor cells to conventional chemotherapeutic drugs in a p53-dependent manner

It was also investigated if OXAZ-1 increased the sensitivity of tumor cells to the effects of conventional chemotherapeutic drugs, such as doxorubicin and etoposide. For that, the tumor growth inhibitory effect of a very low concentration of OXAZ-1 (GI_{10} of 9 μM; for which no significant effects on tumor cell growth were observed), combined with increasing concentrations of doxorubicin and etoposide, was investigated in HCT116 cells. The results obtained revealed pronounced synergistic effects between OXAZ-1 and the tested conventional chemotherapeutic drugs in $p53^{+/+}$, but not in $p53^{-/-}$, HCT116 cells (Figure 3.2.7A–C). In fact, in HCT116 $p53^{+/+}$ cells, the Q values obtained, at the three tested concentrations of doxorubicin and etoposide, were higher than 1.15 (1.43 < Q < 2.22 for doxorubicin; 1.64 < Q < 2.22 for etoposide; Figure 3.2.7A). Interestingly, the best result obtained corresponded to the lowest concentrations tested of doxorubicin and etoposide. Accordingly, synergistic effects between OXAZ-1 and the lowest concentrations tested of doxorubicin (9.38 nM) and etoposide (0.38 μM) were obtained in the analysis of total apoptosis by Annexin V in HCT116 $p53^{+/+}$ cells (Figure 3.2.7B). Contrary, OXAZ-1 did not significantly interfere with the tumor growth inhibitory effect of doxorubicin and etoposide for the three tested concentrations of these chemotherapeutic drugs in p53-null HCT116 cells (Figure 3.2.7C). Altogether, the results obtained showed a p53-dependent synergistic effect of OXAZ-1 with conventional chemotherapeutic drugs.

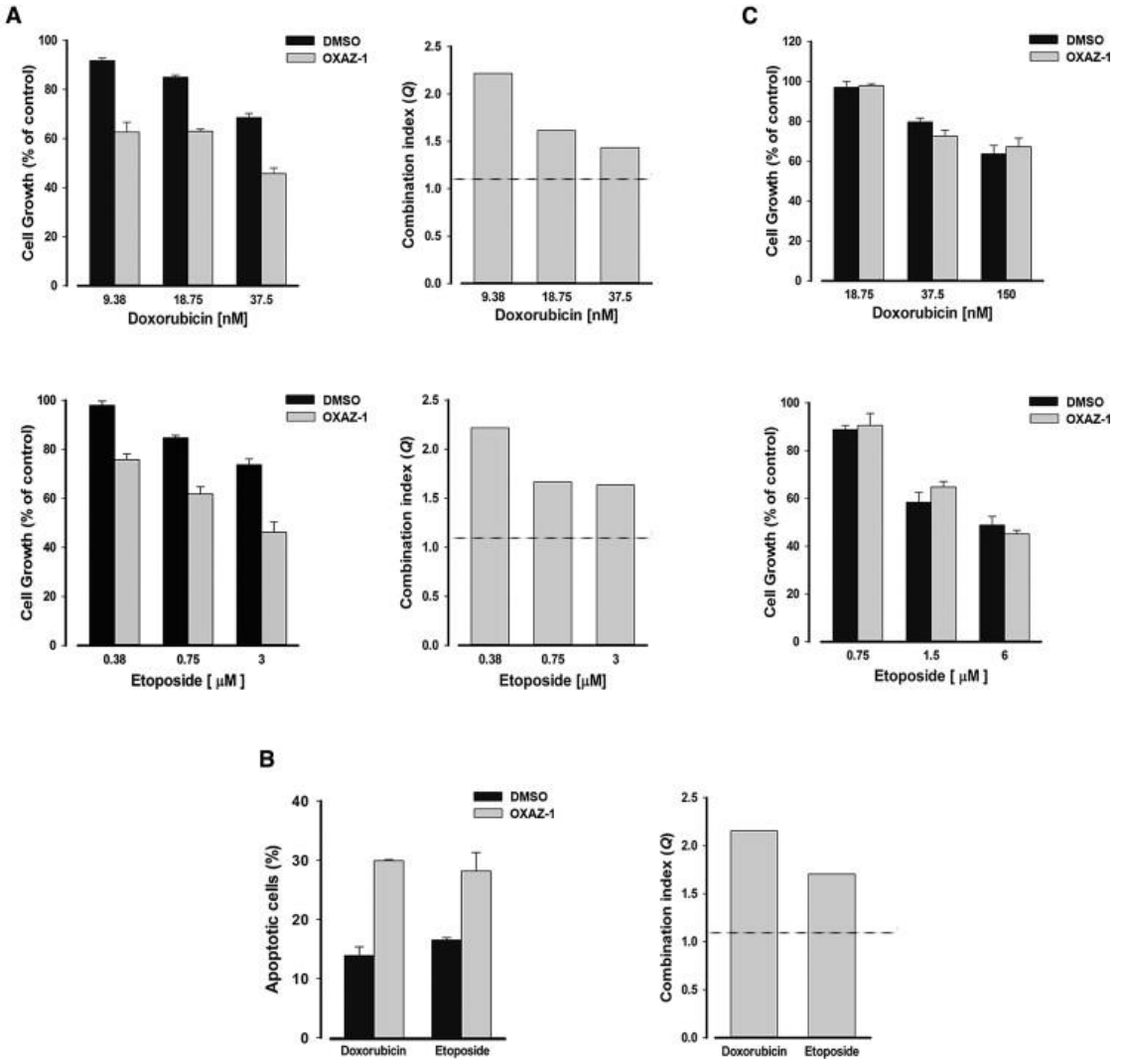

Figure 3.2.7. OXAZ-1 sensitizes HCT116 p53$^{+/+}$ tumor cells to the effects of doxorubicin and etoposide. (A) HCT116 p53$^{+/+}$ tumor cells were treated with increasing concentrations of doxorubicin (9.38–37.5 nM) or etoposide (0.38–3.00 µM) and 9 µM (GI_{10} concentration) of OXAZ-1 or DMSO only (control). Effect of compounds on tumor cell growth was analyzed after 48 h incubation, using the SRB assay; the percentage of cell growth achieved with OXAZ-1 only was 90.6%; data are mean ± S.E.M. of four independent experiments. **(B)** Effect of combined treatment on apoptosis was determined after 48 h treatment with a fixed concentration of doxorubicin (9.38 nM) or etoposide (0.38 µM) and the GI_{10} concentration of OXAZ-1 or DMSO only (control). The percentage of apoptotic cells achieved with OXAZ-1 only was 1.5%; apoptosis was analyzed by flow cytometry using FITC-Annexin V and PI; data are mean ± S.E.M. of three independent experiments. **(C)** HCT116 p53$^{-/-}$ tumor cells were treated with increasing concentrations of doxorubicin (18.75–150 nM) or etoposide (0.75–6.00 µM) and 9 µM OXAZ-1 or DMSO only (control). Effect of compounds on tumor cell growth was analyzed after 48 h incubation, using the SRB assay; the percentage of cell growth achieved with OXAZ-1 only was approximately 100%; data are mean ± S.E.M. of four independent experiments. In A and B, the *Q* values are indicated for combined treatments of OXAZ-1/doxorubicin

and OXAZ-1/etoposide; $Q < 0.85$, $Q > 1.15$ and $0.85 < Q < 1.15$ indicate antagonism, synergy and additive effects, respectively; dotted line represents $Q = 1.15$.

3.2.5. Discussion

In this work, a yeast-based screening assay was used to search for inhibitors of the p53 interaction with MDM2 and MDMX. From the analysis of a small library of enantiopure tryptophanol-derived oxazolopiperidone lactams, the (*S*)-tryptophanol derivative OXAZ-1 was identified as potential dual inhibitor of the p53-MDMs interaction. The study of this compound in human tumor cell lines supported the results from yeast, showing that OXAZ-1 was able to block the MDM2 and MDMX interaction with p53. Beyond that, it was shown that the *in vitro* tumor growth inhibitory effect of OXAZ-1 was highly dependent on p53 and exhibited typical hallmarks of an inhibitor of the p53 interaction with MDM proteins (Wade et al., 2013). Particularly, it led to p53 stabilization, what is consistent with an inhibition of the MDM2-mediated p53 degradation by OXAZ-1, and up-regulated p53 transcriptional targets. Additionally, like RO-5963 (Graves et al., 2012), OXAZ-1 efficiently reduced the proliferation of wt p53-carrying tumor cells with high levels of MDMX (MCF-7 cells). In fact, also in MDMX-overexpression tumor cells, OXAZ-1 induced cell cycle arrest and apoptosis through activation of the p53 transcriptional activity. OXAZ-1 therefore overcame the commonly reported (Graves et al., 2012; Patton et al., 2006; Wade et al., 2006) resistance of MDMX-overexpression tumors to MDM2-only inhibitors.

Cancer cell mitochondria are structurally and functionally different from normal cells. Additionally, tumor cells are more susceptible to mitochondrial perturbations than normal cells. Based on this, mitochondrially-targeted agents have emerged as a promising approach to selectively eradicate chemotherapy-refractory cancer cells (Fulda et al., 2010). In fact, the activation of cell death programs by pharmacological agents that induce or facilitate mitochondrial membrane permeabilization (MMP) has emerged as an attractive strategy for cancer treatment (Fulda et al., 2010). MMP can be triggered by agents that increase cytosolic calcium or stimulate ROS generation. Moreover, MMP can be favored by pro-apoptotic proteins of the Bcl-2 family, such as BAX. In fact, during apoptosis, BAX is translocated from the cytosol to mitochondria where it triggers MMP (Fulda et al., 2010; Chipult et al., 2004). MMP results in the immediate $\Delta\psi_m$ dissipation, with the consequent release of pro-apoptotic factors into the cytosol, such as cyt *c* (Fulda et al., 2010). The results obtained in the present work showed that OXAZ-1 also targets mitochondria of tumor cells. Actually, OXAZ-1 potently triggered a mitochondrion-centered p53-dependent

apoptotic cell death characterized by ROS generation, BAX translocation to mitochondria, $\Delta\psi_m$ dissipation, and mitochondrial cyt *c* release.

The pharmacological activation of the p53 pathway can be exploited in combination therapy with non-targeted genotoxic agents to protect from side effects of chemotherapy (Wang et al., 2014), or to promote cell death via p53-dependent mechanisms (Hoe et al., 2014). In fact, examples were already reported showing the efficacy of such combinations in anticancer treatment. This is the case of Nutlin-3a, which has shown excellent results when combined with non-targeted genotoxic agents (Wade et al., 2013; Hoe et al., 2014). In this work, very low concentrations of OXAZ-1 exhibited pronounced p53-dependent synergistic effects with chemotherapeutic drugs such as etoposide and doxorubicin, strengthening the potential antitumor activity of OXAZ-1. Actually, the prospect of combining conventional chemotherapeutic agents with OXAZ-1 in cancer therapy represents a promising strategy to minimize the emergence of resistance and to achieve maximal therapeutic responses with minimal side effects.

Although further work is still required to completely clarify the molecular targets of (*S*)-tryptophanol derivative OXAZ-1, particularly its interaction with MDM2 and MDMX, relevant insights on its mode of action are already provided in this study (Figure 3.2.8). This work opens the way to a new class of selective activators of the p53 pathway through dual inhibition of the p53 interaction with MDM proteins, based on a tryptophanol-derived oxazolopiperidone lactam scaffold, with promising antitumor properties either alone or in combined therapies.

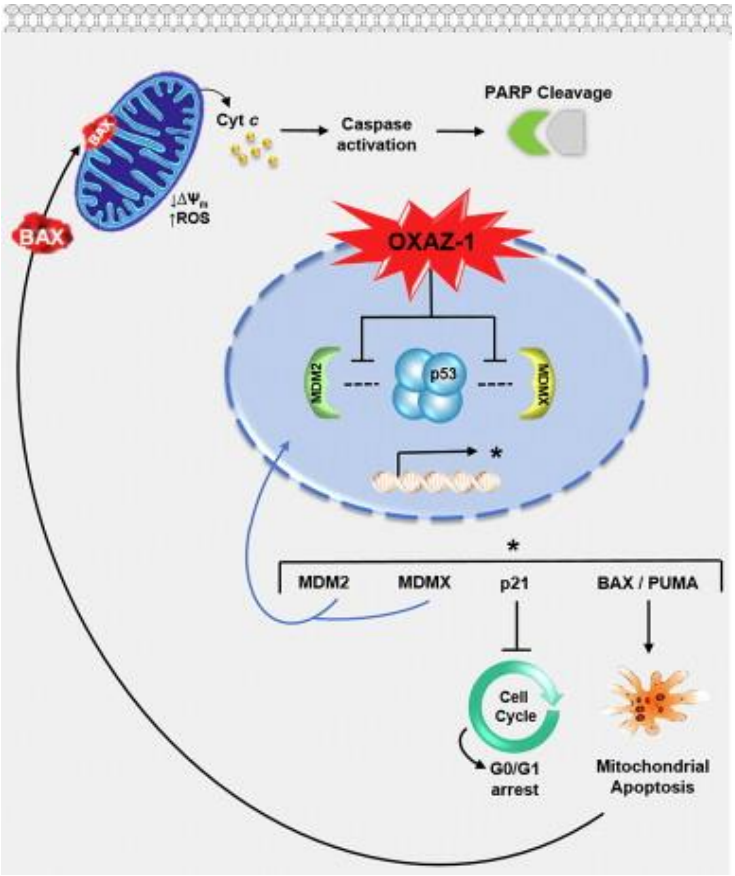

Figure 3.2.8. Proposed molecular mechanism of action of (*S*)-tryptophanol derivative OXAZ-1 in human tumor cells. As a dual inhibitor of the p53 interaction with MDM2 and MDMX, OXAZ-1 leads to p53 stabilization and to the activation of p53 transcriptional activity, increasing the levels of the p53 target proteins MDMX, MDM2, p21, BAX and PUMA. The increase of p21 leads to a G0/G1 cell cycle arrest. The increase of BAX and PUMA leads to the activation of a mitochondrial apoptotic pathway, involving BAX translocation to mitochondria, ROS generation, $\Delta\psi_m$ dissipation, and cyt *c* from mitochondria, with the subsequent activation of a caspase pathway with PARP cleavage; *p53 target genes.

CHAPTER 3.3

Promising antitumor properties of a tryptophanol-derived oxazoloisoindolinone by dual inhibition of p53-MDM2/MDMX interactions

Soares J, Espadinha M, Raimundo L, Gomes AS, Ramos H, Monteiro A, Gomes C, Reis F, Santos MMM, Saraiva L.

Submited for publication

In an attempt to find potent dual inhibitors of p53-MDMs interactions with *in vivo* antitumor activity, a hit-to-lead optimization was performed, in Santo's lab, based on our previous results with reactivators of p53 activity. This led to a library of tryptophanol derived-oxazoloisoindolinone derivatives screened in this work for their ability to inhibit the p53 interaction with MDMs.

3.3.1. Identification of DIMP53-1 as potential dual inhibitor of p53-MDMs interactions, using yeast-based screening assays

The ability of a library of tryptophanol derived-oxazoloisoindolinones to inhibit the p53-MDMs interactions was tested using the previously described yeast-based screening assays (Leão et al., 2013b,c). With this approach, the effect of 0.1 - 50 μM of tryptophanol derived-oxazoloisoindolinones was evaluated on p53-MDMs interactions (data not shown), and DIMP53-1 (Figure 3.3.1) was selected as a potential dual inhibitor of these protein-protein interactions (Figure 3.3.2A). Actually, the obtained EC_{50} values revealed that DIMP53-1 potently inhibited both p53-MDMs (Figure 3.3.2B). Interestingly, the highest potency was observed on p53-MDMX interaction, where DIMP53-1 showed to be more potent than the positive control (Figure 3.3.2B). Additionally, DIMP53-1 did not interfere with the growth of control yeast and yeast expressing p53, MDM2 or MDMX alone (Figure 3.3.2C), revealing a selective effect of DIMP53-1 on human protein-protein interactions.

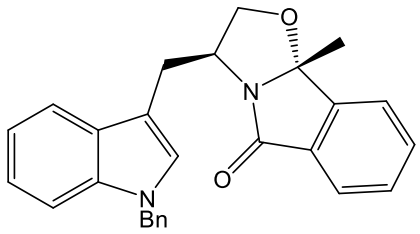

Figure 3.3.1. Chemical structure of DIMP53-1.

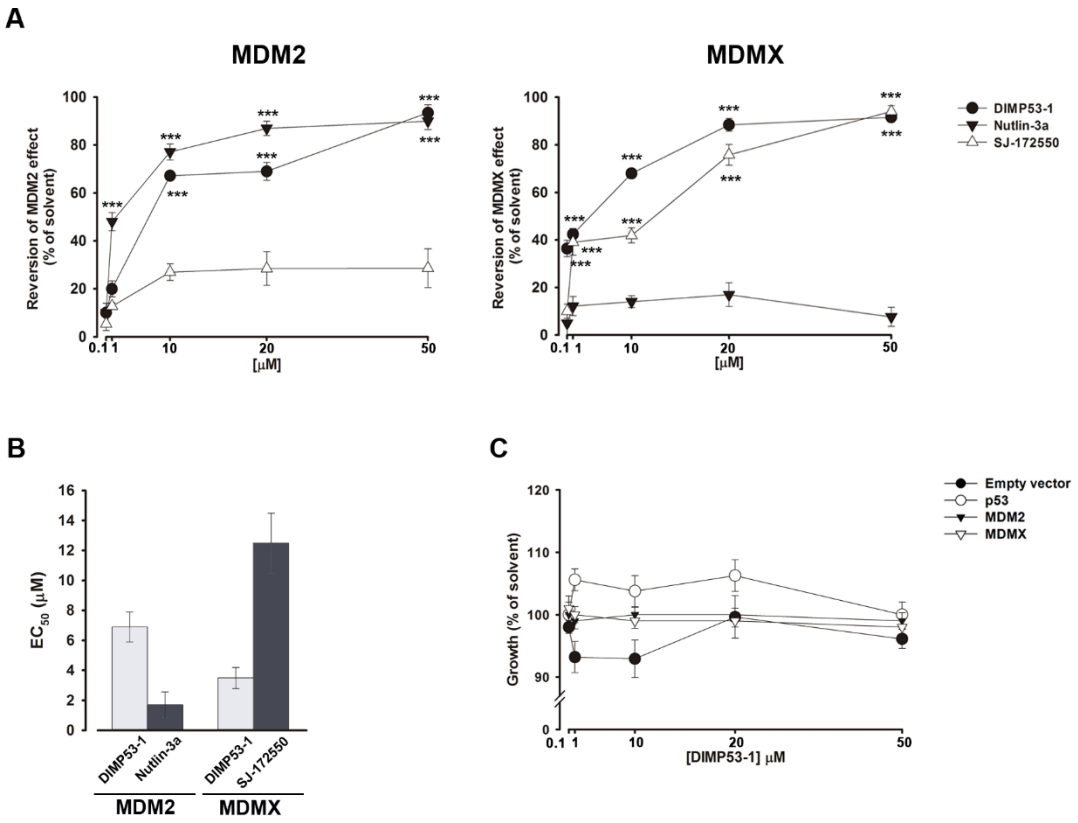

Figure 3.3.2. Identification of DIMP53-1 as potential dual inhibitor of p53-MDMs interactions. **(A)** Effect of 0.1–50 μM DIMP53-1, Nutlin-3a and SJ-172550 on the reversion of p53-induced yeast growth inhibition by MDM2 and MDMX, after 42 h incubation; results were plotted setting as 100% the growth achieved with yeast cells expressing p53 alone incubated with DMSO only; data are mean ± S.E.M. of six independent experiments; values significantly different from DMSO only are indicated (***$p < 0.001$). **(B)** EC_{50} values of DIMP53-1, Nutlin-3a and SJ-172550 obtained from 0.1 – 50 μM concentration–response curves of the reversion of MDM2/MDMX-inhibitory effects. **(C)** Effect of 0.1 – 50 μM DIMP53-1 on the growth of yeast expressing p53, MDMX or MDM2 alone, and of yeast transformed with the empty vector after 42 h incubation; results were plotted setting as 100% the growth achieved with DMSO only; data are mean ± S.E.M. of five independent experiments; values are not significantly different from DMSO only ($p > 0.05$).

3.3.2. DIMP53-1 has a p53-dependent tumor growth inhibitory effect mediated by dual inhibition of p53-MDMs interactions

To confirm the molecular mechanism of action of DIMP53-1 as dual inhibitor of p53-MDMs interactions, the effect of this compound was ascertained in human $p53^{+/+}$ and $p53^{-/-}$ HCT116 colon adenocarcinoma cells. The obtained GI_{50} values showed a significant reduction (from 7.0 to 17.3 μM) of the DIMP53-1 tumor growth inhibitory effect, when the p53 pathway was knocked out in HCT116 $p53^{-/-}$ cells (Figure 3.3.3A).

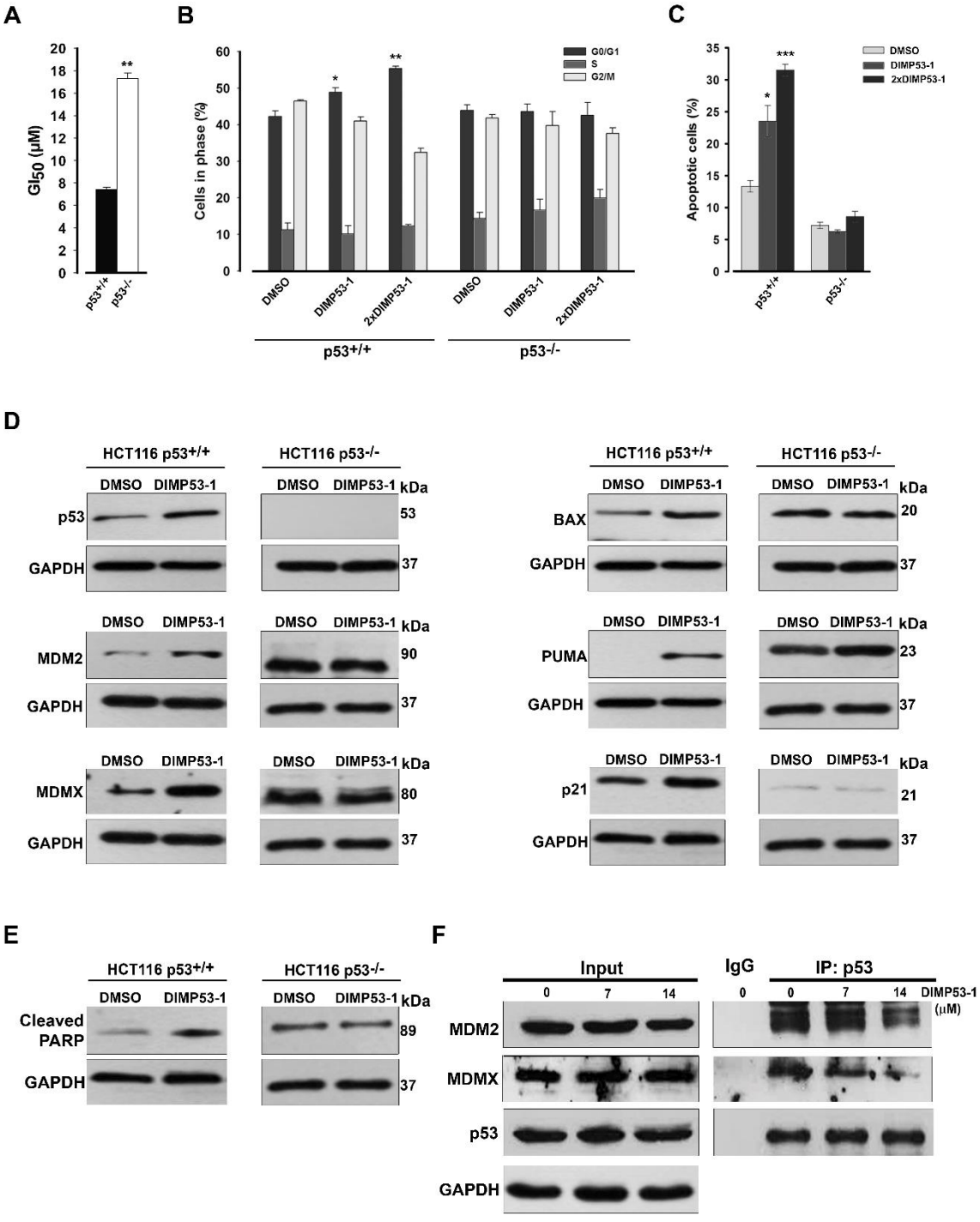

Figure 3.3.3. DIMP53-1 growth inhibitory effect is associated with cell cycle arrest, apoptosis and up-regulation of p53 target genes by blocking the p53 interaction with MDMs in HCT116 p53$^{+/+}$ cells. (A) GI_{50} values of DIMP53-1 in p53$^{+/+}$ and p53$^{-/-}$ HCT116 cells, after 48 h treatment; data are mean ± S.E.M. of four independent experiments; values significantly different from HCT116 p53$^{+/+}$ cells are indicated (**$p < 0.01$). **(B)** Cell cycle arrest and **(C)** apoptosis were determined at 7 μM and 14 μM (2×GI_{50}, 2×DIMP53-1) of DIMP53-1 after 24 h treatment in p53$^{+/+}$ and p53$^{-/-}$ HCT116 cells; data are mean ± S.E.M. of three independent experiments; values significantly different from DMSO are indicated (*$p < 0.05$; **$p < 0.01$; ***$p < 0.001$). **(D)** Western blot analysis was performed

after 24 h (MDM2) and 48 h (p53, MDMX, BAX, PUMA, p21) treatment with 7 μM DIMP53-1 or DMSO only in $p53^{+/+}$ and $p53^{-/-}$ HCT116 cells. **(E)** PARP cleavage was analyzed by Western blot after 24 h treatment with 7 μM DIMP53-1 or DMSO only in $p53^{+/+}$ and $p53^{-/-}$ HCT116 cells. **(F)** Co-immunoprecipitation was performed with anti-p53 (IP: p53) or anti-immunoglobulin G (IgG) antibodies, followed by immunoblotting with anti-MDM2, anti-MDMX and anti-p53 antibodies in HCT116 $p53^{+/+}$ cells treated with 7 and 14 μM DIMP53-1 or DMSO only for 24 h; whole cell lysate (Input). In **(D)**, **(E)** and **(F)** immunoblots are representative of three independent experiments; GAPDH was used as loading control.

Additionally, this compound was tested in two breast cancer cell lines (MDA-MB-231 and MDA-MB-468 cells), both expressing mutant p53 forms. Accordingly, the obtained GI_{50} values were much higher when compared to wt p53-expressing tumor cells (84.3 ± 7.8 μM for MDA-MB-231 cells; 37.5 ± 3.5 μM for MDA-MB-468 cells, $n = 4$). Together, these results revealed a wt p53-dependent tumor growth inhibitory effect by DIMP53-1. It was also verified that the growth inhibitory effect of DIMP53-1 in HCT116 $p53^{+/+}$ cells, at 7 and 14 μM ($2xGI_{50}$), was associated with G0/G1-phase cell cycle arrest (Figure 3.3.3B), apoptosis (Figure 3.3.3C), and PARP cleavage (Figure 3.3.3E), which were not observed in p53-null HCT116 cells. Additionally, by western blot analysis, it was shown that DIMP53-1 led to p53 stabilization, and to the up-regulation of major p53 transcriptional targets, as revealed by the increased protein levels of MDM2, MDMX, BAX, PUMA and p21 in $p53^{+/+}$, but not in $p53^{-/-}$, HCT116 cells (Figure 3.3.3D).

The ability of DIMP53-1 to block the p53 interaction with MDM2 and MDMX was thereafter demonstrated by co-IP assay, in HCT116 $p53^{+/+}$ cells. In fact, at 7 and 14 μM, a visible decrease in the amount of MDM2 and MDMX co-immunoprecipitated with p53 was observed (Figure 3.3.3F). Altogether, these results revealed that DIMP53-1 is an activator of the p53 pathway through dual inhibition of the p53-MDMs interactions in human tumor cells.

The effect of DIMP53-1 was further investigated in two other human wt p53-expressing tumor cells overexpressing MDM2 (osteosarcoma SJSA-1 cells) and MDMX (breast adenocarcinoma MCF-7 cells). Despite slightly less potent than in HCT116 $p53^{+/+}$ cells, a considerable growth inhibitory effect was obtained with DIMP53-1 in both tumor cells (Figure 3.3.4A). As in HCT116 $p53^{+/+}$ cells, this growth inhibitory effect conducted by DIMP53-1 was associated with cell cycle arrest (at G0/G1- and S-phases in SJSA-1; at G0/G1-phase in MCF-7 cells; Figure 3.3.4B) and apoptosis (Figure 3.3.4C) at GI_{50} (11.8 ± 0.7 μM for SJSA-1; 13.3 ± 0.5 μM for MCF-7) and $2xGI_{50}$ concentrations, and with PARP cleavage at the GI_{50} concentration (Figure 3.3.4D). Moreover, in both SJSA-1 and MCF-7

tumor cells, the GI_{50} concentration of DIMP53-1 led to p53 stabilization (Figure 3.3.4D), and to the up-regulation of several p53 transcriptional targets, as demonstrated by the increased protein levels of MDM2, MDMX, BAX and p21 (Figure 3.3.4D). Overall, this set of results demonstrated that DIMP53-1 also activated p53 in tumor cells with a wt p53 pathway mostly inhibited by MDM2 or MDMX.

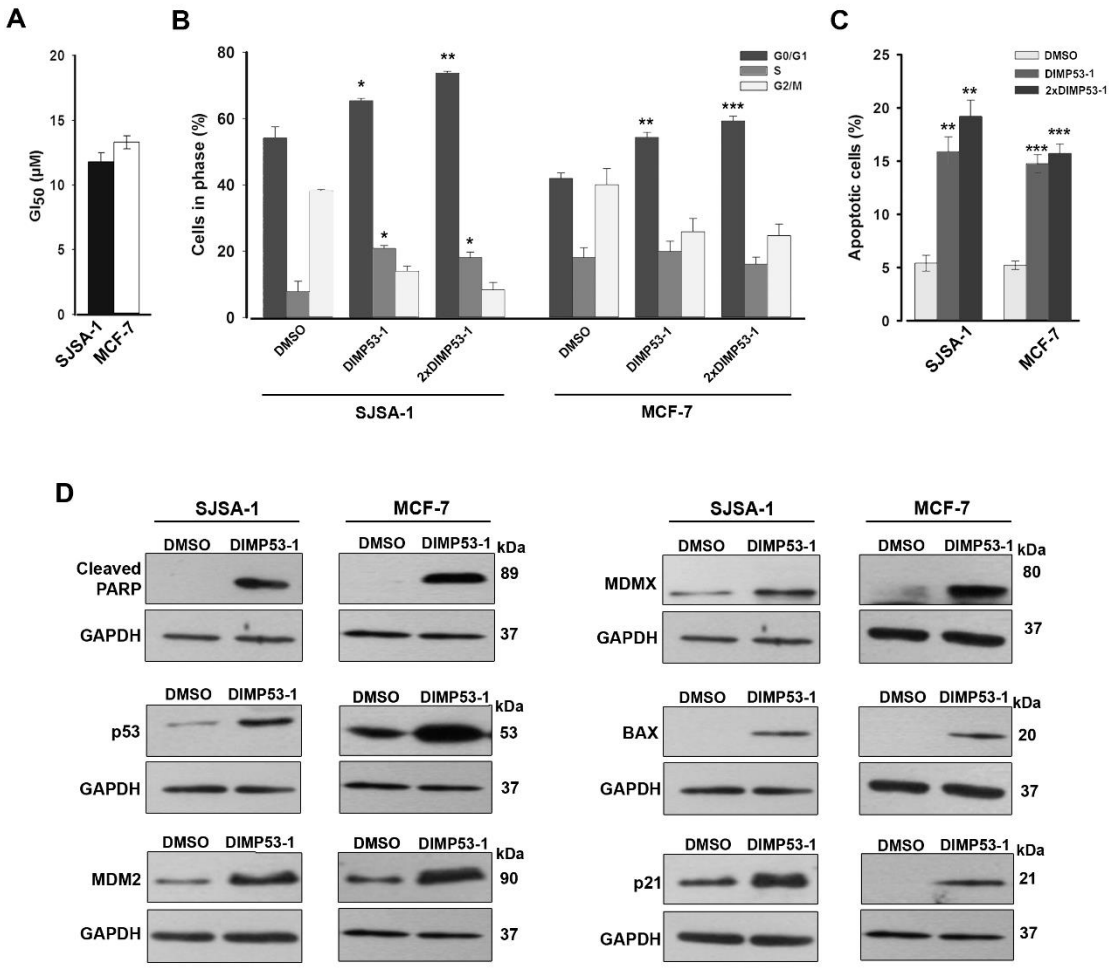

Figure 3.3.4. DIMP53-1 growth inhibitory effect is associated with cell cycle arrest, apoptosis and up-regulation of p53 target genes in MDM2- (SJSA-1) and MDMX- (MCF-7) overexpressing tumor cells. (A) GI_{50} concentration of DIMP53-1 in SJSA-1 and MCF-7 cells, after 48 h treatment; data are mean ± S.E.M. of four independent experiments. **(B)** Cell cycle arrest and **(C)** apoptosis were determined at GI_{50} (11.8 ± 0.7 μM for SJSA-1; 13.3 ± 0.5 μM for MCF-7) and 2×GI_{50} concentrations of DIMP53-1, after 24 h treatment; data are mean ± S.E.M. of three independent experiments; values significantly different from DMSO are indicated (*$p < 0.05$; **$p < 0.01$; ***$p < 0.001$). **(D)** Western blot analysis was performed after 24 h (cleaved PARP, MDMX and p21) and 48 h (p53, MDM2, BAX) treatment with GI_{50} concentration of DIMP53-1 or DMSO only. In **(D)** and **(E)**

immunoblots are representative of three independent experiments; GAPDH was used as loading control.

3.3.3. DIMP53-1 prevents *in vitro* tumor cell migration

The impact of DIMP53-1 on the invasive ability of HCT116 $p53^{+/+}$ cells was investigated by migration assays. In the Wound Healing Scratch assay, 3 μM (GI_{10}) DIMP53-1 inhibited the HCT116 $p53^{+/+}$ cell migration, and the subsequent wound closure, when compared to cells treated with DMSO only (Figure 3.3.5A). These results were further confirmed using the Chemotaxis Cell Migration assay, in which 3 μM DIMP53-1 led to a pronounced reduction of HCT116 $p53^{+/+}$ cell migration, compared to DMSO only, upon 24 h treatment (Figure 3.3.5B). Together, these results demonstrated that DIMP53-1 was able to inhibit the migration of human colon adenocarcinoma cells.

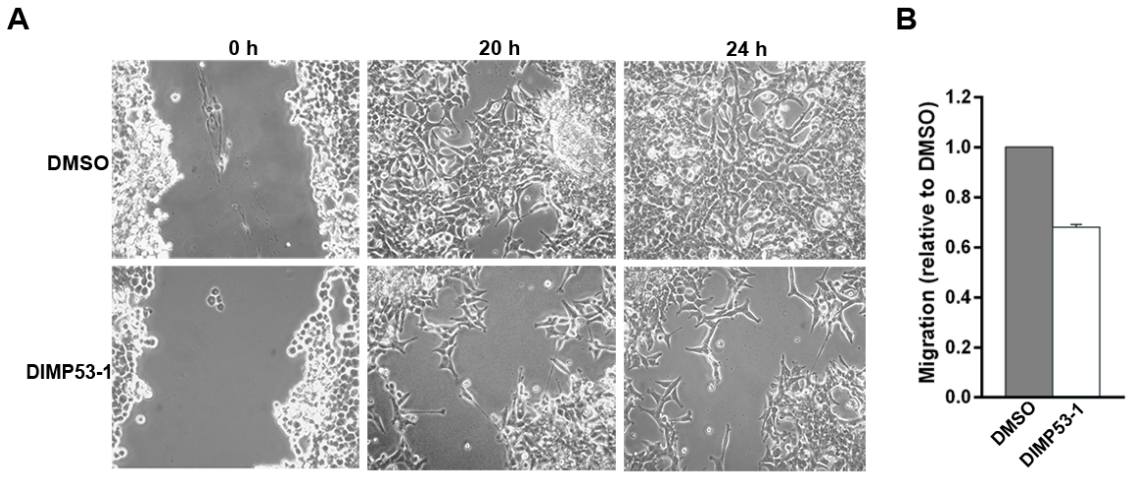

Figure 3.3.5. DIMP53-1 prevents the migration of HCT116 $p53^{+/+}$ cells. (A) HCT116 $p53^{+/+}$ confluent cells treated with 3 μM DIMP53-1 (or DMSO only) were observed at different time-points in the Wound Healing assay. **(B)** Effects of 3 μM (GI_{10}) DIMP53-1 on the migration of HCT116 $p53^{+/+}$ cells for 24 h, analyzed by the chemotaxis assay; the migratory cells were quantified by fluorescence signal, set as 1 cells treated with DMSO only; data are mean ± S.E.M. of three independent experiments.

3.3.4. DIMP53-1 has no *in vitro* toxicity in human non-tumorigenic cells

The cytotoxicity and genotoxicity of DIMP53-1 were investigated in human non-tumorigenic cells. For that, the growth inhibitory effect of DIMP53-1 in non-tumorigenic human breast epithelial MCF10A cells was assessed by SRB assay. The obtained GI_{50} concentration of DIMP53-1 in MCF10A was higher than 50 μM (maximum concentration tested), what indicated a selective cytotoxicity of DIMP53-1 to tumor cells. Additionally, the genotoxicity of DIMP53-1 was tested by assessing its ability to induce micronucleus (MN) in cultured peripheral lymphocytes of normal individuals. When compared to samples treated with DMSO only, 7, 14 and 21 μM DIMP53-1 did not increase the number of MN in lymphocytes (Figure 3.3.6). These results showed that DIMP53-1 had no apparent *in vitro* genotoxicity.

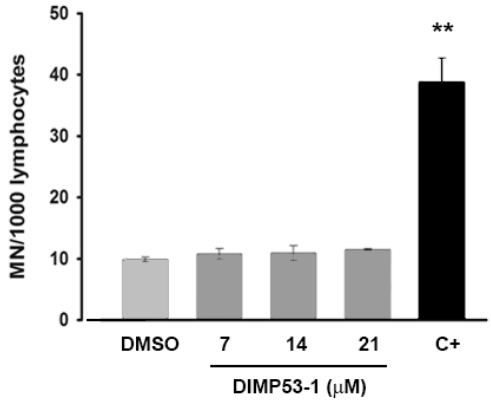

Figure 3.3.6. DIMP53-1 has no *in vitro* genotoxicity. Genotoxicity of 7, 14 and 21 μM DIMP53-1 by cytokinesis-block micronucleus (MN) assay after 72 h treatment in human lymphocyte cells. Cells treated with 5 μg/mL cyclophosphamide were used as positive control (C+); data are mean ± S.E.M. of three independent experiments; values significantly different from DMSO only are indicated (**p < 0.01).

3.3.5. DIMP53-1 has *in vivo* antitumor activity without apparent toxicity

The *in vivo* antitumor potential of DIMP53-1 was evaluated using human tumor xenograft mice models of $p53^{+/+}$ and $p53^{-/-}$ HCT116 tumor cells. Four intraperitoneal administrations (twice a week) of 50 mg/kg DIMP53-1 inhibited the growth of HCT116 $p53^{+/+}$ tumors (Figure 3.3.7A) compared to control (vehicle). Conversely, using the same conditions, DIMP53-1 did not interfere with the growth of HCT116 $p53^{-/-}$ tumor xenografts,

what further reinforced its p53-dependent antitumor activity (Figure 3.3.7A). Furthermore, no significant loss of body weight or morbidity signs were observed in DIMP53-1-treated mice compared to control (Figure 3.3.7B).

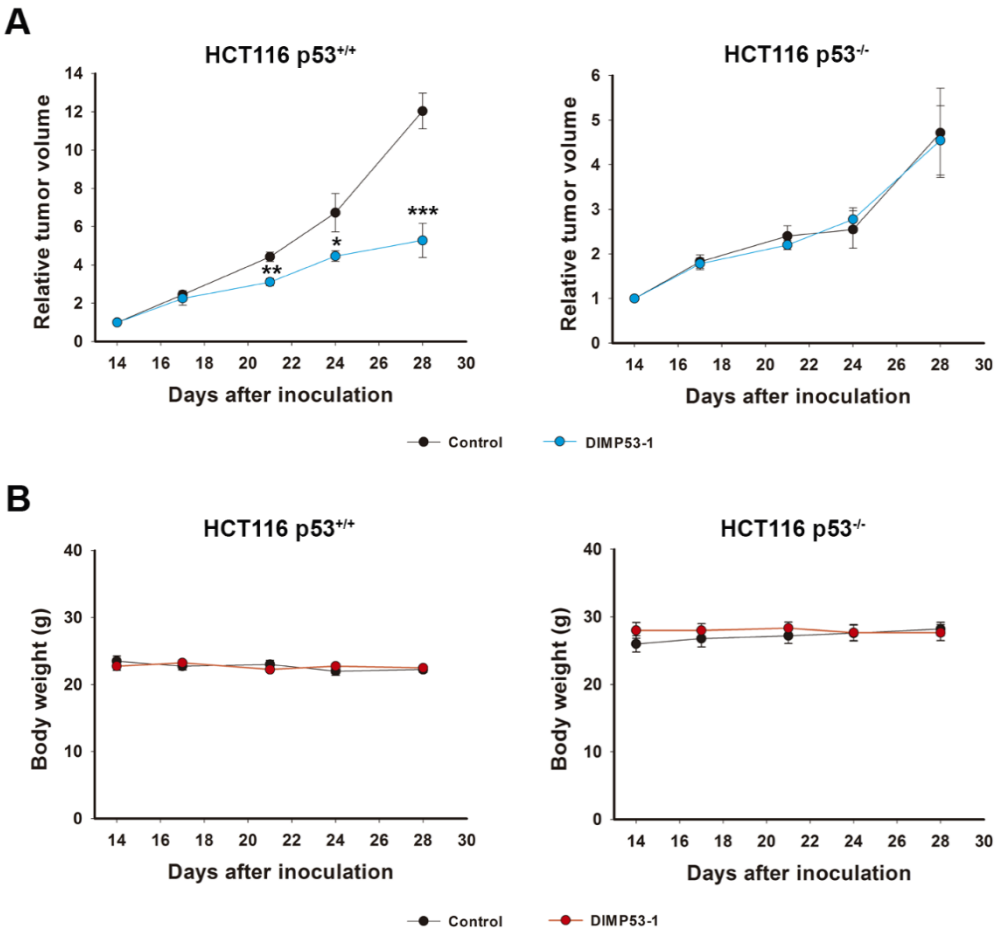

Figure 3.3.7. DIMP53-1 has a p53-dependent antitumor activity *in vivo*. (A) BALB/c nude mice carrying HCT116 $p53^{+/+}$ or HCT116 $p53^{-/-}$ xenografts treated with 50 mg/kg DIMP53-1 or vehicle (control); values significantly different from control mice are indicated (*$p < 0.05$, **$p < 0.01$, ***$p < 0.001$). **(B)** BALB/c nude mice body weight during DIMP53-1 treatment; values are not significantly different from control ($p > 0.05$).

In order to evaluate some primary toxicity signs, DIMP53-1 was tested in Wistar rats. Following the same administration procedure to that conducted in tumor xenograft mice models, organs relative weight (trophism), as well as biochemical and hematological data were analyzed for the three rat groups (saline, vehicle and DIMP53-1; Table 3.3.1). No differences between the three groups on relative weight of liver, kidneys, heart and spleen

were observed. Concerning biochemical data, only a slight decrease of urea in the vehicle group compared to saline group, and a slight increase of uric acid in the DIMP53-1 group compared to control groups (saline and vehicle groups) was observed. These results indicated no apparent liver or kidney toxicity by DIMP53-1. Regarding hematological data, just a small increase on the reticulocytes number was observed in vehicle group compared to saline group, with no alterations between DIMP53-1 and the other two control groups. Overall, no apparent toxic side effects were observed for DIMP53-1 on the tissues most commonly affected by conventional chemotherapeutics.

Table 3.3.1. Safety profile for the three mice groups under study at the final time point.

	Saline	Vehicle	Treated
Body weight and relative tissue weight (trophism)			
BW (g)	340.30 ± 13.45	361.80 ± 0.01	353.25 ± 3.99
Heart/BW (g/kg)	3.03 ± 0.03	3.01 ± 0.09	3.19 ± 0.12
Liver/BW (g/kg)	38.71 ± 2,36	38.52 ± 0.89	40.72 ± 1.14
Kidney/BW (g/kg)	7.08 ± 0.40	6.81 ± 0.27	6.96 ± 0.32
Spleen (g/kg)	2.10 ± 0.20	2.15 ± 0.12	2.07 ± 0.20
Biochemical data			
Blood Glucose(mg/dL)	188.0 ± 7.51	207.20 ± 7.00	242.25 ± 25.68
Urea (mg/dL)	20.67 ± 0.77	18.34 ± 0.24*	19.10 ± 0.62
Uric acid (mg/dL)	1.07 ± 0.07	0.82 ± 0.10	4.10 ± 0.50*
Creatinine (mg/dL)	0.30 ± 0.00	0.30 ± 0.01	0.36 ± 0.03
Total Proteins (g/dL)	5.50 ± 0.00	5.35 ± 0.17	6.38 ± 0.40
Albumin (g/dL)	3.03 ± 0.03	2.90 ± 0.05	3.13 ± 0.03
ALT (U/L)	36.00 ± 2.89	30.75 ± 3.30	35.00 ± 1.87
AST (U/L)	95.33 ± 25.36	56.25 ± 4.60	115.75 ± 20.89
Total Chol (mg/dL)	44.33 ± 1.76	52.40 ± 3.54	54.00 ± 3.37
Triglycerides (mg/dL)	107.00 ± 16.29	161.40 ± 17.55	229.50 ± 26.70
Hematological data			
RBC count (x10^6/µL)	7.10 ± 0.15	7.41 ± 0.28	8.23 ± 0.24
HGB (g/dL)	13.97 ± 0.18	13.95 ± 0.46	14.68 ± 0.28
HCT (%)	40.50 ± 0.82	42.28 ± 2.03	47.85 ± 1.87
WBC counts (x10^3/µL)	1.93 ± 0.68	2.15 ± 0.88	1.05 ± 0.26
PLT counts (x10^3/µL)	811.00 ± 29.61	793.80 ± 28.35	726.75 ± 47.43
RET counts (%)	2.80 ± 0.12	3.56 ± 0.23*	3.59 ± 0.31

The results are expressed as mean ± S.E.M. of four independent experiments; *$p < 0.05$ versus Saline group; ALT, alanine aminotransferase; AST, aspartate aminotransferase; BW, body weight; CK, Creatine Kinase; HCT, hematocrit; HGB, Hemoglobin concentration; PCT, plateletcrit; PLT, platelet; RBC, red blood cell count; RET, reticulocytes; WBC, white blood cell.

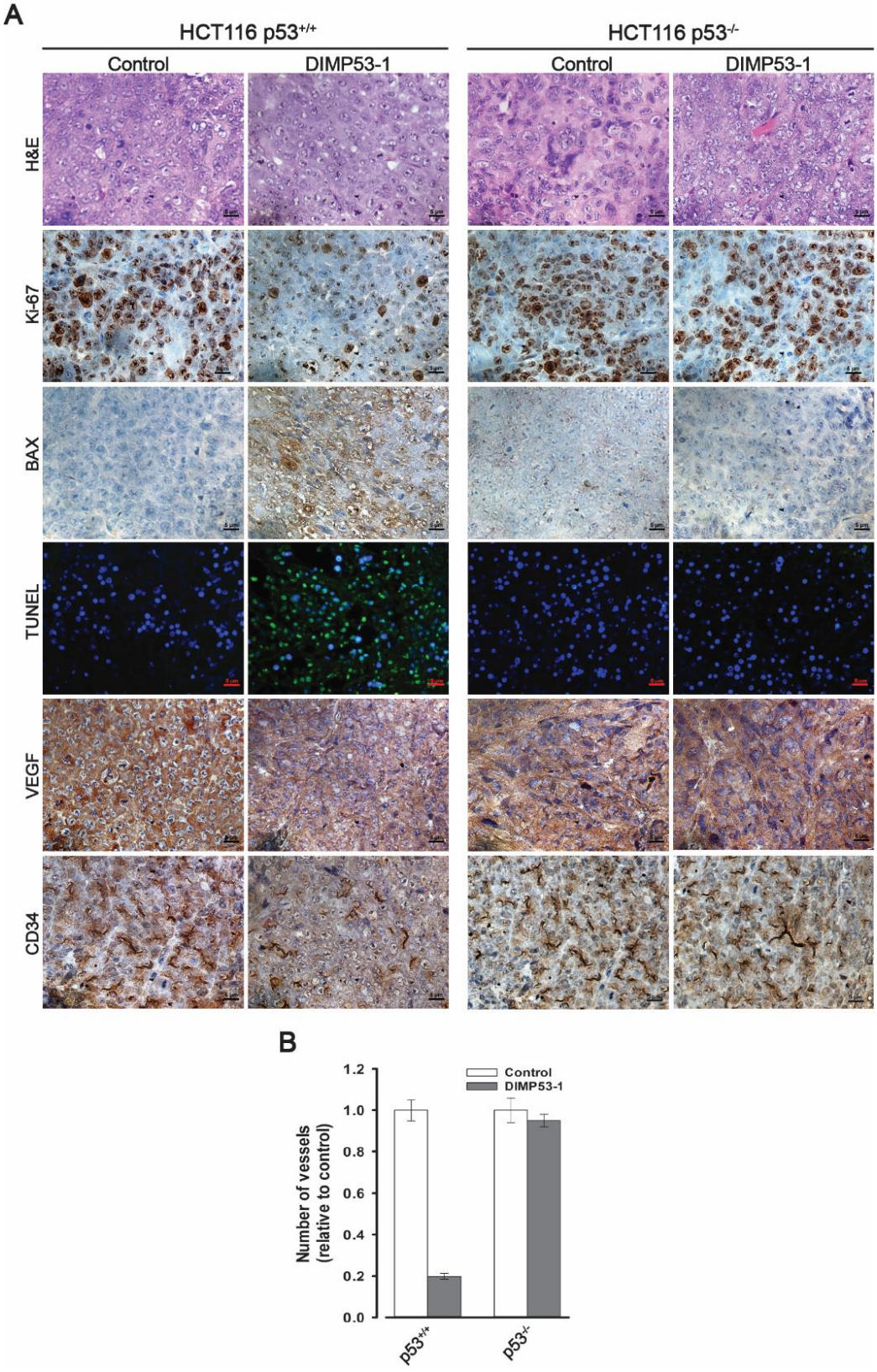

Figure 3.3.8. DIMP53-1 increases apoptosis and reduces the proliferative activity and tumor angiogenesis of human HCT116 p53$^{+/+}$ tumor xenografts. (A) Representative images of Ki-67, BAX, DNA fragmentation (TUNEL), CD34 and VEGF detection in human HCT116 p53$^{+/+}$ and

HCT116 $p53^{-/-}$ xenograft tumor tissues inoculated in BALB/c nude mice treated with 50 mg/kg DIMP53-1 or vehicle (Scale bar = 5 μm; Magnification 400x). **(B)** Microvessel density (MVD; expressed as number of vessels/mm^2 relative to control) of human HCT116 $p53^{+/+}$ and HCT116 $p53^{-/-}$ xenograft tumor tissues inoculated in BALB/c nude mice treated with 50 mg/kg DIMP53-1 or vehicle; values significantly different from control mice are indicated (*$p < 0.05$).

The subsequent analysis of tumor tissues was performed to check *in vivo* antitumor events promoted by DIMP53-1. For that, proliferation, apoptotic and angiogenic markers were assessed in HCT116 $p53^{+/+}$ tumors by immunohistochemistry and TUNEL staining (Figure 3.3.8A). DIMP53-1-treated HCT116 $p53^{+/+}$ tumors showed low Ki-67-positive staining (indicative of a reduced proliferative status) compared to tumors treated with vehicle only (Figure 3.3.8A). The induction of apoptosis in DIMP53-1-treated tumor tissues was evidenced by the increase of BAX expression levels and of TUNEL-positive staining (indicative of nuclei DNA fragmentation), compared to tumors treated with vehicle only (Figure 3.3.8A). To study the angiogenic profile of tumor tissues, the vascular endothelial growth factor (VEGF; an angiogenesis inducing factor) and CD34 (a marker to detect newly formed vessels) were checked, and the Microvessel Density (MVD) was determined. The obtained results revealed low levels of VEGF, CD34 and MVD in DIMP53-1-treated HT116 $p53^{+/+}$ tumor tissues compared to tumors treated with vehicle only (Figures 3.3.8A and B). Particularly, an approximately five-fold reduction of MVD in DIMP53-1-treated tumors compared to control tumors was observed (Figure 3.3.8B). These results indicated an inhibition of angiogenesis by DIMP53-1. Conversely, no apparent differences in these markers were observed between DIMP53-1-treated and untreated HCT116 $p53^{-/-}$ tumors (Figures 3.3.8A and B). Actually, these tumors were characterized by high levels of Ki-67, CD34, VEGF and MVD, and by low levels of BAX and DNA fragmentation (Figure 3.3.8A and B).

3.3.6. Discussion

Several anticancer strategies have been devised to rectify a dysfunctional p53 pathway, particularly due to the overexpression of MDM2 and MDMX. The simultaneous inhibition of the p53 interaction with both MDMs has gained increasing attention as the most efficient anticancer therapeutic strategy, since it will conduct to a full p53 reactivation in wt p53-expressing tumor cells (Li and Lozano, 2013). Despite this, the number of dual inhibitors of p53-MDMs interactions identified so far remains very limited.

In this work, a yeast-based assay was used to screen for inhibitors of p53-MDMs interactions from a library of tryptophanol derived-oxazoloisoindolinones. From this analysis, the compound DIMP53-1 emerged as a potential dual inhibitor of p53-MDMs interactions. The molecular mechanism of action of DIMP53-1 was validated both *in vitro* tumor cell lines and *in vivo* tumor xenograft models. In fact, using human-derived isogenic tumor cells with and without p53, it was verified that the tumor cell growth inhibitory effect of DIMP53-1 was dependent on p53. Consistently, the anti-proliferative effect of DIMP53-1 was associated with the induction of p53-dependent cell cycle arrest and apoptosis, p53 stabilization, which is an indicative of inhibition of the MDM2-mediated p53 degradation, and up-regulation of several p53 transcriptional targets. Finally, it was confirmed that DIMP53-1 was able to block the p53-MDMs interactions in tumor cells. This *in vitro* antitumor potential of DIMP53-1 was further confirmed in wt p53-expressing tumor cells overexpressing either MDM2 or MDMX. Actually, DIMP53-1 overcame the frequently reported resistance of MDMX-overexpressing tumor cells to MDM2-only inhibitors as Nutlin-3a (Graves et al., 2012; Li and Lozano, 2013).

The loss of p53 function is closely related to the development of metastatic phenotypes (Powell et al., 2014), which is the most frequent cause of mortality (90%) in cancer patients (Spano et al., 2012). Actually, p53 can regulate the transcription of several genes involved in cell motility and adhesion, signal transduction, extracellular matrix and cytoskeleton organization, which are processes involved in cell migration and invasion (Powell et al., 2014; Roger et al., 2006). The p53 loss seems to contribute to the loosening of cell–cell junctions and to the disruption of epithelial cell integrity, contributing to the dissemination of cells from solid tumors. One example of a protein whose expression is directly regulated by p53 is KAI-1/CD82, a member of the tetraspanin or transmembrane 4 superfamily, which suppresses cancer metastasis by inhibiting cell migration and invasion (Powell et al., 2014). Based on this, it is expected that the restoration of p53 function will lead to tumor regression and metastasis prevention. Consistently, the results obtained in this work revealed that low doses of DIMP53-1 prevented the migration of wt p53-expressing tumor cells.

In human tumor xenograft mice models, the p53-dependent antitumor activity of DIMP53-1 was further confirmed. In fact, DIMP53-1 suppressed the growth of wt p53-expressing tumors, through inhibition of proliferation and induction of apoptosis, without interfering with the growth of p53-null tumor xenografts. Besides that, no apparent toxic side effects were observed for DIMP53-1 both *in vitro* and *in vivo*. Interestingly, in this work, the anti-angiogenic activity of DIMP53-1 was also demonstrated in wt p53-expressing tumor xenografts. Angiogenesis is a relevant hallmark of cancer since proliferation and metastatic

spread of cancer cells depend on an adequate supply of oxygen and nutrients (Baeriswyl and Christofori, 2009). The p53 activity is negatively correlated with this process through indirect inhibition of key proteins, such as VEGF. In fact, it was demonstrated that wt p53 indirectly represses VEGF expression by interaction and inhibition of transcription factors such as SP1 and E2F (Pal et al., 2001; Qin et al., 2006). In this way, the p53 activation, namely by DIMP53-1, prevents angiogenesis.

In conclusion, this work reports the identification of a selective activator of the p53 pathway through dual inhibition of the p53-MDMs interactions. The impact of DIMP53-1 on main four hallmarks of cancer, namely through its anti-proliferative, pro-apoptotic, anti-angiogenic and anti-metastatic potential, make this small molecule an appealing anticancer drug candidate.

CHAPTER 4

Results

Identification of
new reactivators of mutant p53

CHAPTER 4

Reactivation of wild-type and mutant p53 by tryptophanolderived oxazoloisoindolinone SLMP53-1, a novel anticancer small-molecule

Soares J, Raimundo L, Pereira NAL, Monteiro A, Gomes S, Bessa C, Pereira C, Queiroz G, Bisio A, Fernandes J, Gomes C, Reis F, Gonçalves J, Inga A, Pereira C, Santos MMM, Saraiva L.

***Oncotarget* 2015 Dec; doi: 10.18632/oncotarget.6775.**

International Publication Number WO 2014/207688 A1, 31 December 2014

To date, few small-molecule reactivators of mutant p53 have been identified. Aiming at the discovery of new reactivators, in this work a new cell-based screening strategy was developed and used to test a chemical library of tryptophanol-derived oxazoloisoindolinones.

4.1. Development of a yeast-based screening assay to search for reactivators of mutant p53

A yeast-based screening assay, consisting of *Saccharomyces cerevisiae* cells expressing human wt p53 or mutant p53 (R280K or Y220C; two of the most prevalent forms of human mutant p53; Petitjean et al., 2007b), was developed to search for mutant p53 reactivators (Figure 4.1A and B). This assay was established based on the yeast growth inhibitory effect induced by wt p53, not observed with mutant forms of p53 (Leão et al., 2013c; Figure 4.1C). Based on this phenotypic readout, mutant p53 reactivators would reestablish the wt p53-dependent growth inhibition. Since, to date, mutant p53R280K reactivators remain unknown, the mutant p53Y220C reactivator PhiKan083 (Boeckler et al., 2008) was used as positive control to attest the efficacy of the yeast assay (Figure 4.1C). As expected, 50 μM PhiKan083 restored the wt p53-induced yeast growth inhibition to mutant p53Y220C (in about 63%; Figure 4.1C).

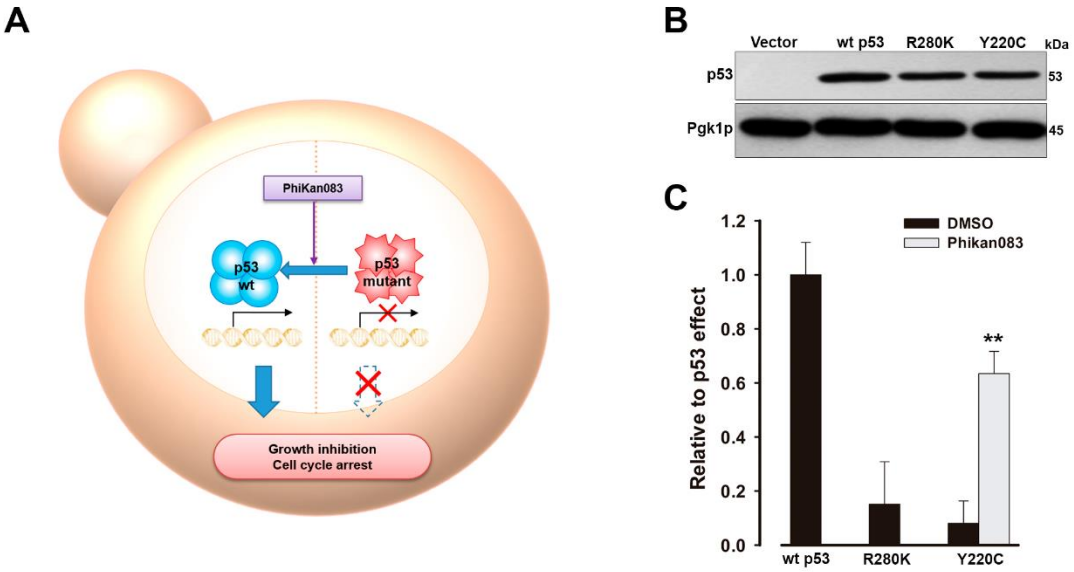

Figure 4.1. Yeast-based screening assay to search for reactivators of mutant p53 R280K and Y220C. (A) Schematic representation of the developed yeast-based screening assay. **(B)**

Immunoblots of human wt p53, mutant p53R280K and mutant p53Y220C expressed in yeast after 30 h incubation in selective induction medium (representative of three independent experiments). **(C)** Contrary to wt p53, both mutant p53 R280K and Y220C do not present growth inhibition in the presence of DMSO. 50 μM PhiKan083 increase mutant p53Y220C-induced growth inhibition, after 30 h; results were plotted setting as 1 the growth inhibitory effect of wt p53-expressing cells treated with DMSO only; data are mean ± S.E.M. of five independent experiments.

4.2. Identification of SLMP53-1 as activator of wt p53 and reactivator of mutant p53R280K from a library of tryptophanol derived oxazoloisoindolinones using the yeast-based screening assay

This yeast assay was thereafter used to evaluate the effect of synthesized enantiopure tryptophanol-derived oxazoloisoindolinones on wt and mutant p53 activity. These compounds were synthesized following our interest in enantiopure biologically active amino alcohol-derived compounds (Pereira et al., 2013; Pereira et al., 2014), and on our previous discovery compounds with *in vitro* p53-dependent antitumor activity (Chapter 3). With this new library, we intended to study the effect on p53 activity of the replacement of the phenyl moiety (present in our first set of compounds; Soares et al., 2015) by an indole moiety. Among the compounds tested, SLMP53-1 behaved as activator of wt p53 and reactivator of mutant p53R280K (Figure 4.2B and C). Actually, at 10 μM (lowest concentration, from a range of 1 – 50 μM, that caused a maximal effect; data not shown) SLMP53-1 increased the wt p53-induced yeast growth inhibition and restored the wt-like growth inhibitory effect to mutant p53R280K (in about 79%; Figure 4.2B), without interfering with the growth of control yeast (data not shown). Consistently, 10 μM SLMP53-1 increased the S- and G2/M-phases cell cycle arrest in wt p53-expressing yeast, and reestablished the wt-like cell cycle arrest in mutant p53R280K-expressing yeast (Figure 4.2C). Interestingly, 1 - 50 μM SLMP53-1 did not interfere with the growth of mutant p53Y220C-expressing yeast (Figure 4.2B).

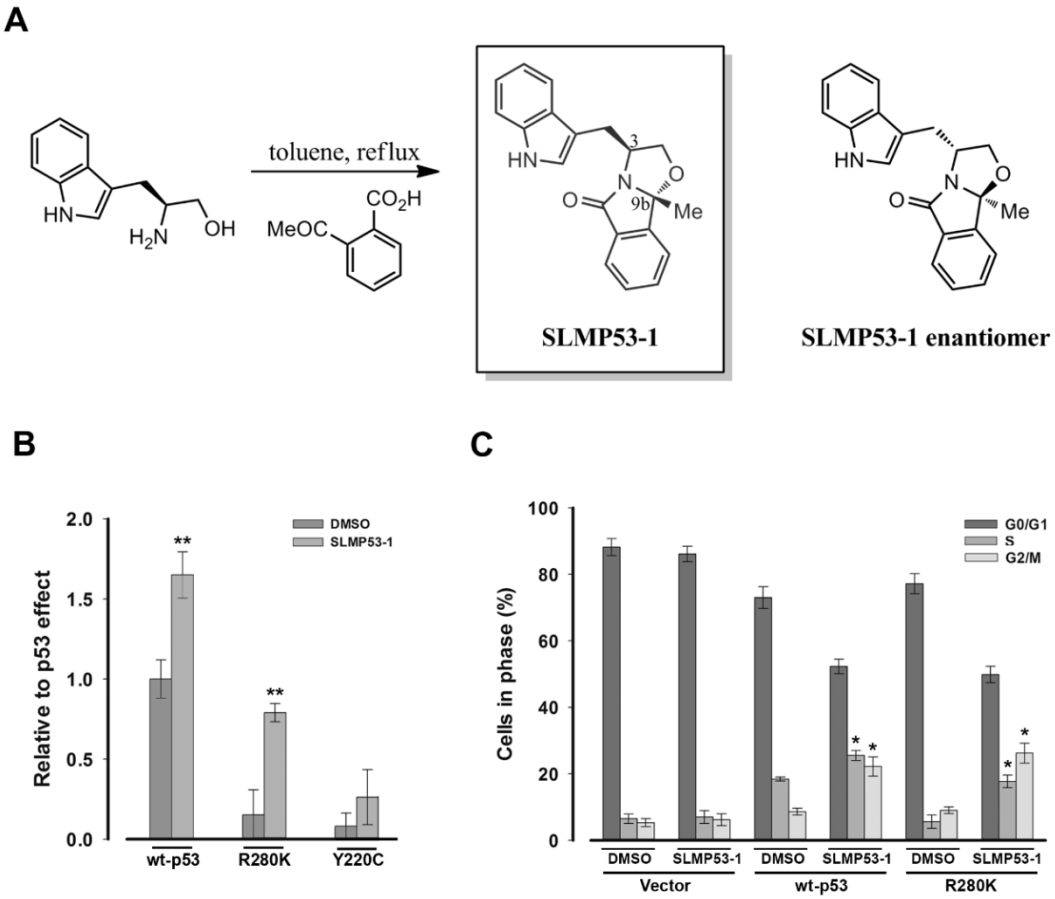

Figure 4.2. SLMP53-1 activates wt p53 and restores the wt-like activity to mutant p53R280K in yeast. (A) Synthesis of SLMP53-1 and chemical structure of its enantiomer. **(B)** Increase of wt and mutant p53R280K-induced growth inhibition by 10 μM SLMP53-1, after 30 h; results were plotted setting as 1 the growth inhibitory effect of wt p53-expressing cells treated with DMSO only; data are mean ± S.E.M. of five independent experiments. **(C)** Increase of wt and mutant p53R280K-induced yeast cell cycle arrest by 10 μM SLMP53-1; data are mean ± S.E.M. of three independent experiments. In **B** and **C**, values significantly different from DMSO only are indicated: **p* < 0.05, ***p* < 0.01.

4.3. Growth inhibitory effect of SLMP53-1 on wt p53- and mutant p53R280K-expressing tumor cells is mediated by p53-dependent cell cycle arrest and/or apoptosis

The growth inhibitory potential of SLMP53-1, and the contribution of the p53 pathway to its activity, were ascertained in $p53^{+/+}$ and $p53^{-/-}$ HCT116 tumor cells. A significant difference between the GI_{50} values obtained in $p53^{+/+}$ (~16 μM) and $p53^{-/-}$ (~34 μM) HCT116 cells indicated an involvement of p53 in the growth inhibitory effect of SLMP53-1 (Figure 4.3A). Conversely, no significant differences were observed between the GI_{50} values of

PRIMA-1 in $p53^{+/+}$ and $p53^{-/-}$ HCT116 cells (Figure 4.3A). In our experimental conditions, the GI_{50} value of PhiKan083 in HCT116 cells was higher than 150 μM.

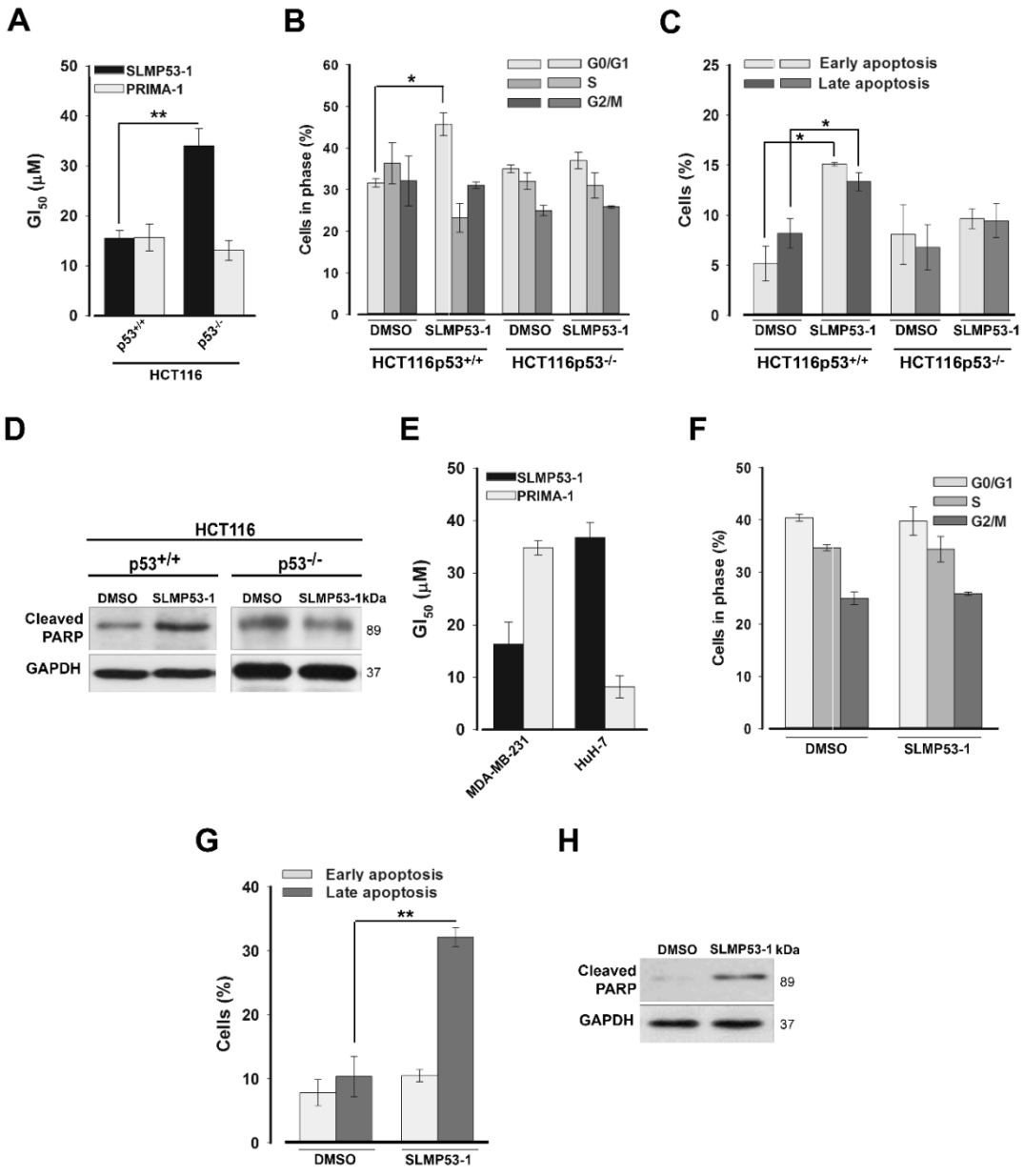

Figure 4.3. SLMP53-1 growth inhibitory effect in human wt p53- and mutant p53R280K-expressing tumor cells is mediated by p53-dependent cell cycle arrest and/or apoptosis. (A) GI_{50} value of SLMP53-1 in HCT116 cells, after 48 h treatment; values significantly different are indicated: ***p*<0.01. **(B)** Cell cycle, **(C)** Apoptosis and **(D)** PARP cleavage after 24 h with 16 μM SLMP53-1 in HCT116 cells. **(E)** GI_{50} value for SLMP53-1 in MDA-MB-231 (mutant p53R280K) and HuH-7 (mutant p53Y220C) cells, after 48 h treatment. **(F)** Cell cycle, **(G)** Apoptosis and **(H)** PARP cleavage after 24 h with 16 μM SLMP53-1 in MDA-MB-231 cells. In **A-C** and **E-G**, data are mean ± S.E.M. of three to four independent experiments. In **B**, **C** and **G**, values significantly different from

DMSO only are indicated: *$p < 0.05$, **$p < 0.01$. In **F**, values are not significantly different from DMSO only: $p > 0.05$.

The SLMP53-1 growth inhibitory effect was associated with G0/G1-phase cell cycle arrest (Figure 4.3B), and apoptosis (Figure 4.3C) in $p53^{+/+}$, but not in $p53^{-/-}$, HCT116 cells. The enhancement of PARP cleavage by 16 μM SLMP53-1 in $p53^{+/+}$, but not in $p53^{-/-}$, HCT116 cells further corroborated the activation of a p53-dependent apoptotic pathway (Figure 4.3D).

Consistent with the yeast results, SLMP53-1 also inhibited the growth of mutant p53R280K-expressing MDA-MB-231 cells with a GI_{50} value similar to that obtained in HCT116 $p53^{+/+}$ cells (~16 μM; Figure 4.3E). Moreover, it presented a much lower growth inhibitory activity against mutant p53Y220C-expressing HuH-7 cells (Figure 4.3E). When compared to PRIMA-1, SLMP53-1 presented a higher potency in MDA-MB-231 cells, but was less potent against mutant p53Y220C-expressing HuH-7 cells (Figure 4.3E). In our experimental conditions, the GI_{50} values of PhiKan083 in MDA-MB-231 and HuH-7 cells were higher than 150 μM.

Interestingly, in MDA-MB-231 cells, despite not interfering with cell cycle progression (Figure 4.3F), 16 μM SLMP53-1 stimulated cell death, as revealed by the increase of late apoptosis (Figure 4.3G), and PARP cleavage (Figure 4.3H).

4.4. SLMP53-1 selectively activates p53 transcriptional activity and reestablishes mutant p53R280K DNA binding ability

The effect of SLMP53-1 on wt p53 and mutant p53R280K activity was investigated by analysis of the expression levels of proteins encoded by p53 target genes in HCT116 $p53^{+/+}$, HCT116 $p53^{-/-}$, and MDA-MB-231 cells.

In HCT116 $p53^{+/+}$ cells, 16 μM SLMP53-1 increased the p53, MDM2, p21, PUMA and BAX protein expression levels (Figure 4.4A). Instead, the levels of these proteins were not significantly changed in p53-null HCT116 cells treated with 16 μM SLMP53-1, supporting the p53-dependent activity of this small molecule (Figure 4.4A). Additionally, 16 μM SLMP53-1 increased the mRNA levels of *CDKN1A* (p21) and *TNFRSF10B* (KILLER) in HCT116 $p53^{+/+}$ cells (Figure 4.4B). The selective activation of p53 transcriptional activity by SLMP53-1 was further reinforced by a dual-luciferase gene reporter assay using $p53^{+/+}$ and $p53^{-/-}$ HCT116 cells transfected with p21- or MDM2-luciferase reporter vectors. At 16 and

32 μM (2×GI_{50}), SLMP53-1 increased the expression of the two p53 reporters in HCT116 $p53^{+/+}$ cells, while no effect was observed in HCT116 $p53^{-/-}$ cells (Figure 4.4C).

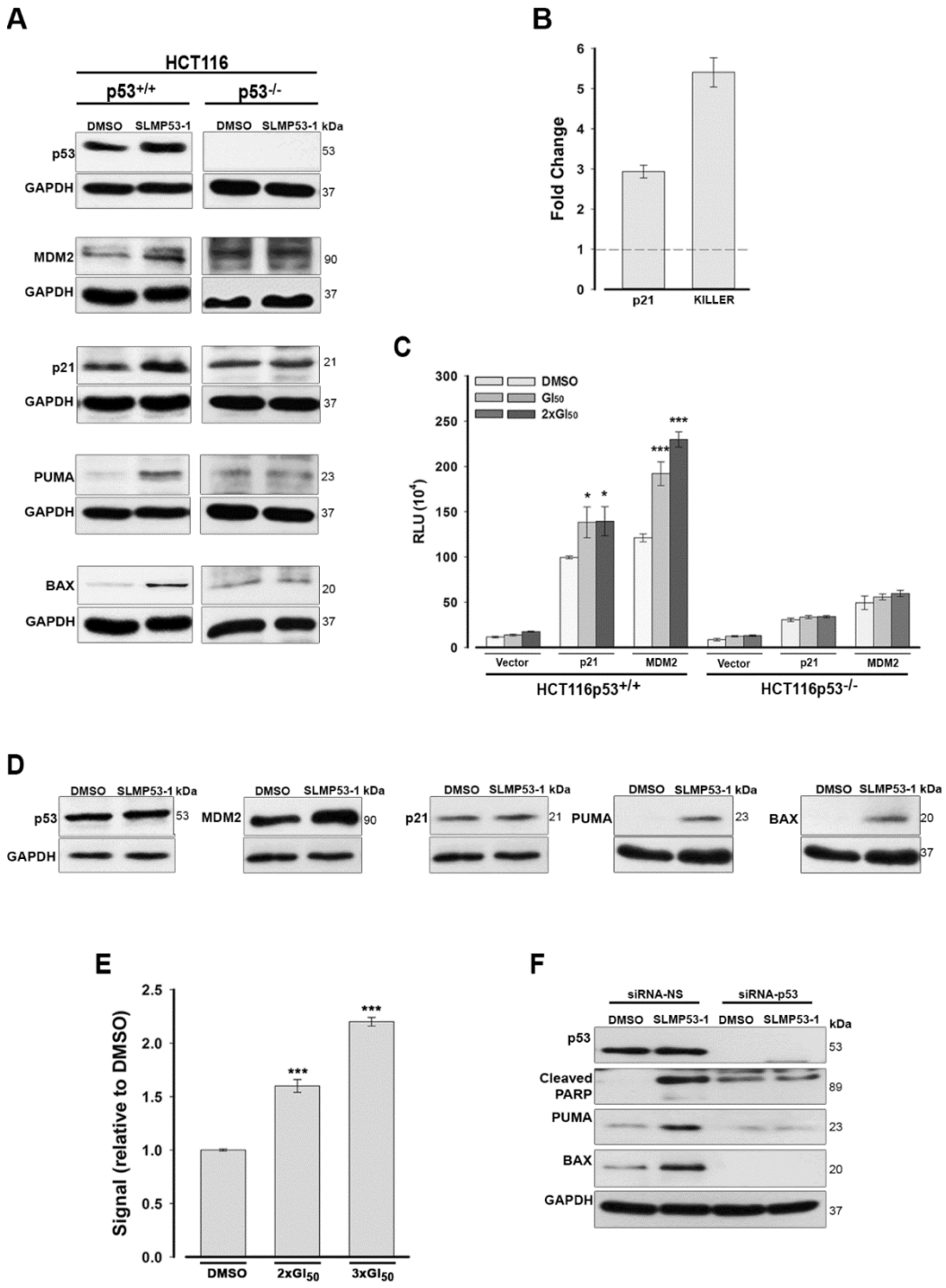

Figure 4.4. SLMP53-1 reactivates the transcriptional activity of wt p53 in HCT116 $p53^{+/+}$ cells and of mutant p53R280K, through reestablishment of its DNA binding ability, in MDA-MB-231 cells. (A) Protein levels of p53 target genes, and **(B)** gene expression of *CDKN1A* (p21) and

*TNFRSF10B (*KILLER), after 24 h with 16 μM SLMP53-1 in HCT116 cells. In **B**, fold expression changes are relative to DMSO and correspond to mean ± S.E.M. of three independent experiments. **(C)** p53 transcriptional activity after 16 h with 16 and 32 μM ($2\times GI_{50}$) SLMP53-1 in HCT116 cells assessed by dual-luciferase gene reporter assay. Data are plotted as mean relative light units (RLU) ± S.E.M. of three independent experiments; values significantly different from DMSO only are indicated: *$p < 0.05$, ***$p < 0.001$. **(D)** Protein levels of p53 target genes after 24 h with 16 μM SLMP53-1 in MDA-MB-231 cells. **(E)** DNA binding affinity of mutant p53R280K after 24 h with 32 and 48 μM ($3\times GI_{50}$) SLMP53-1 in MDA-MB-231 cells; the signal obtained with DMSO only was set as 1; data are mean ± S.E.M. of three independent experiments; values significantly different from DMSO only are indicateed: ***$p < 0.001$. **(F)** PARP cleavage and protein levels of PUMA and BAX after 24 h with 16 μM SLMP53-1 in mutant p53R280K-silenced MDA-MB-231 cells. In **A, D** and **F**, immunoblots are representative of three independent experiments.

In MDA-MB-231 cells, 16 μM SLMP53-1 increased MDM2, PUMA and BAX protein levels, with no apparent increase of p53 protein levels (Figure 4.4D). The lack of mutant p53 protein stabilization was already reported for other mutant p53 reactivators, and has been attributed to a reestablishment of the MDM2-mediated p53 degradation (Yu et al., 2012). Moreover, consistent with the lack of effect on cell cycle progression, 16 μM SLMP53-1 did not affect p21 protein levels (Figure 4.4D).

The restoration of mutant p53R280K DNA binding ability by SLMP53-1 was assessed by TransAM DNA binding assay, using MDA-MB-231 cells. The results revealed a dose-dependent enhancement of the amount of p53 bound to DNA by SLMP53-1 relative to cells treated with DMSO only (Figure 4.4E).

To further demonstrate that the SLMP53-1 effects were dependent on mutant p53R280K in MDA-MB-231 cells, mutant p53R280K was knocked-down by p53siRNA. In cells transfected with non-specific siRNA (siRNA-NS; control), 16 μM SLMP53-1 increased the protein levels of PUMA, BAX and cleaved PARP, as observed in non-transfected cells (Figure 4.4F). As expected, these SLMP53-1 effects were efficiently abolished by mutant p53 silencing (Figure 4.4F).

4.5. SLMP53-1 triggers a p53-dependent mitochondrial apoptotic pathway in wt p53- and mutant p53R280K-expressing tumor cells

In HCT116 $p53^{+/+}$ and MDA-MB-231 cells, 16 μM SLMP53-1 led to $\Delta\psi_m$ dissipation and ROS generation (Figure 4.5A). Consistent with p53-dependence, these effects were not observed in 16 μM SLMP53-1-treated HCT116 $p53^{-/-}$ cells (Figure 4.5A). Additionally, in

HCT116 p53$^{+/+}$ (Figure 4.5B) and MDA-MB-231 (Figure 4.5C) cells, 16 μM SLMP53-1 triggered BAX, wt p53 (Figure 4.5B) and mutant p53R280K (Figure 4.5C) mitochondrial translocation, and led to cyt *c* release to cytosol (Figure 4.5B and C). Altogether, these results showed that SLMP53-1 induced a p53-dependent mitochondrial apoptotic pathway in both wt p53- and mutant p53R280K-expressing tumor cells.

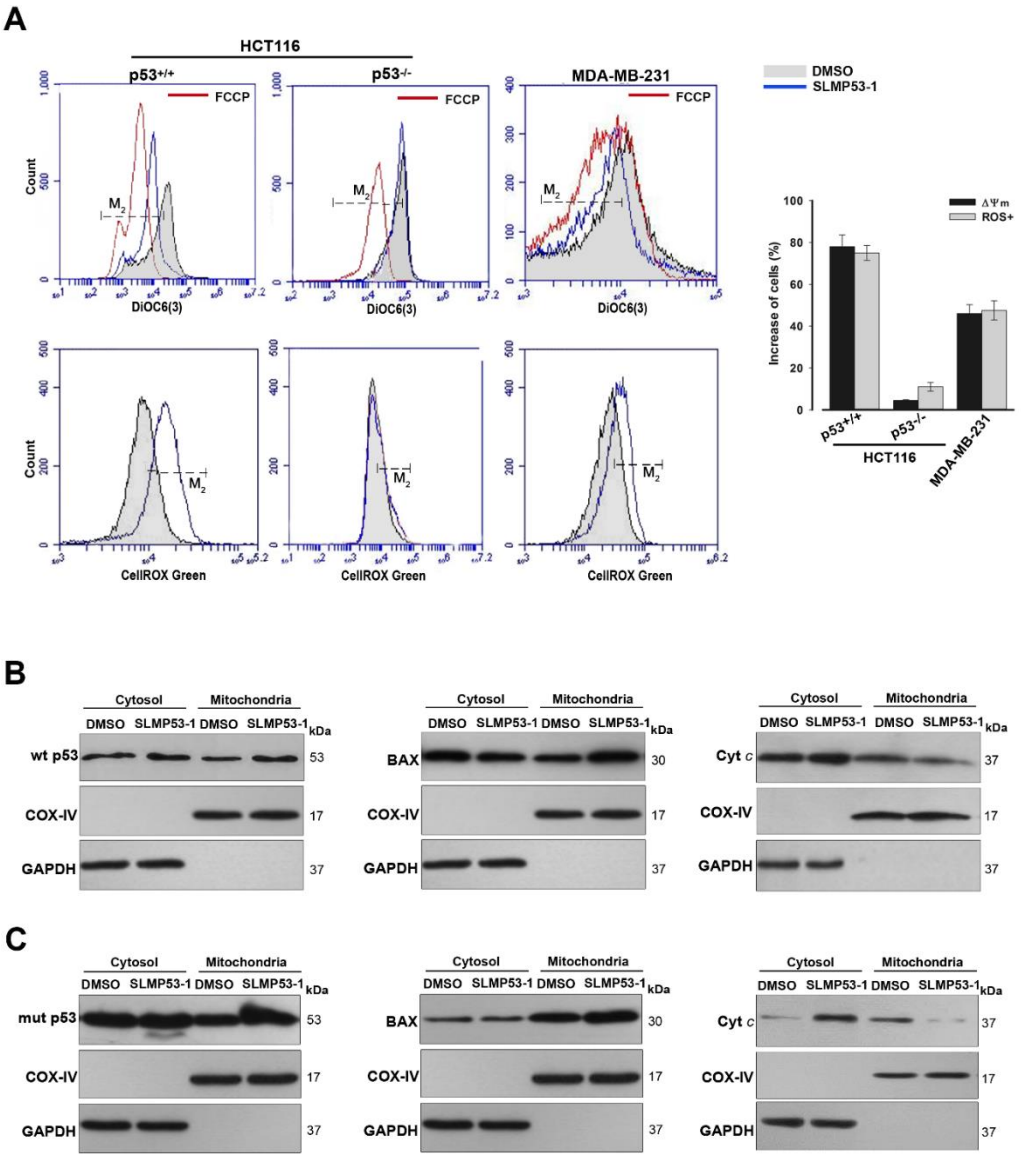

Figure 4.5. SLMP53-1 triggers a p53-mediated mitochondrial apoptotic pathway in HCT116 p53$^{+/+}$ and MDA-MB-231 cells. (A) Cells were treated with 16 μM SLMP53-1 for 8 h (HCT116 cells) or 16 h (MDA-MB-231 cells) in $\Delta\psi_m$ analysis, and for 24 h in ROS analysis. FCCP was used as positive control in $\Delta\psi_m$; histograms are representative of three independent experiments; M_2 cursor indicates the subpopulation analyzed. Graphical representation: increase in the percentage of cells with $\Delta\psi_m$ dissipation and ROS generation; values are mean ± S.E.M. of three independent

experiments. **(B)** and **(C)** Immunoblots of wt/mutant p53, BAX and cyt *c*, in cytosolic and mitochondrial fractions of HCT116 $p53^{+/+}$ **(B)** and MDA-MB-231 **(C)** cells after 16 h with 16 μM SLMP53-1. In **B** and **C**, immunoblots are representative of three independent experiments.

4.6. SLMP53-1 inhibits the migration of wt p53- and mutant p53R280K-expressing tumor cells

The results obtained in the Wound Healing Assay showed that the GI_{10} concentration (4 μM) of SLMP53-1 reduced the migration of HCT116 $p53^{+/+}$ and MDA-MB-231 tumor cells (Figure 4.6A and B). These results were corroborated by the chemotaxis cell migration assay, in which the GI_{25} concentration (7 μM) of SLMP53-1 led to over 50% reduction of HCT116 $p53^{+/+}$ cell migration compared to DMSO only (Figure 4.6C). A similar result was obtained with the constitutively more motile MDA-MB-231 cells treated with 16 μM SLMP53-1 (Figure 4.6C). These data showed that SLMP53-1 inhibited the *in vitro* migration of both wt p53- and mutant p53R280K-expressing tumor cells.

4.7. SLMP53-1 sensitizes wt p53- and mutant p53R280K-expressing tumor cells to conventional chemotherapeutics in a p53-dependent manner

We investigated whether SLMP53-1 increased the sensitivity of HCT116 $p53^{+/+}$ and MDA-MB-231 tumor cells to conventional chemotherapeutics. For that, a low concentration of SLMP53-1, with no significant growth inhibitory effects (GI_{10} of 4 μM), was combined with increasing concentrations of doxorubicin and etoposide. In HCT116 $p53^{+/+}$ cells, SLMP53-1 showed synergistic effects with all tested concentrations of chemotherapeutics (Q>1.15), although the most pronounced effects were obtained with doxorubicin (Figure 4.7A). Conversely, no synergistic effects were observed between SLMP53-1 and the chemotherapeutics in HCT116 $p53^{-/-}$ cells (Figure 4.7B). As in HCT116 $p53^{+/+}$ cells, synergistic effects between SLMP53-1 and all tested concentrations of doxorubicin and etoposide were also observed in MDA-MB-231 cells (Q>1.15; Figure 4.7C). Interestingly, pronounced synergistic effects between 4 μM SLMP53-1 and the lowest tested concentrations of doxorubicin (0.19 μM) and etoposide (0.38 μM) were also evident regarding total apoptosis in MDA-MB-231 cells (Q>1.15; Figure 4.7D). Altogether, these results showed p53-dependent synergistic effects of SLMP53-1 with conventional chemotherapeutics.

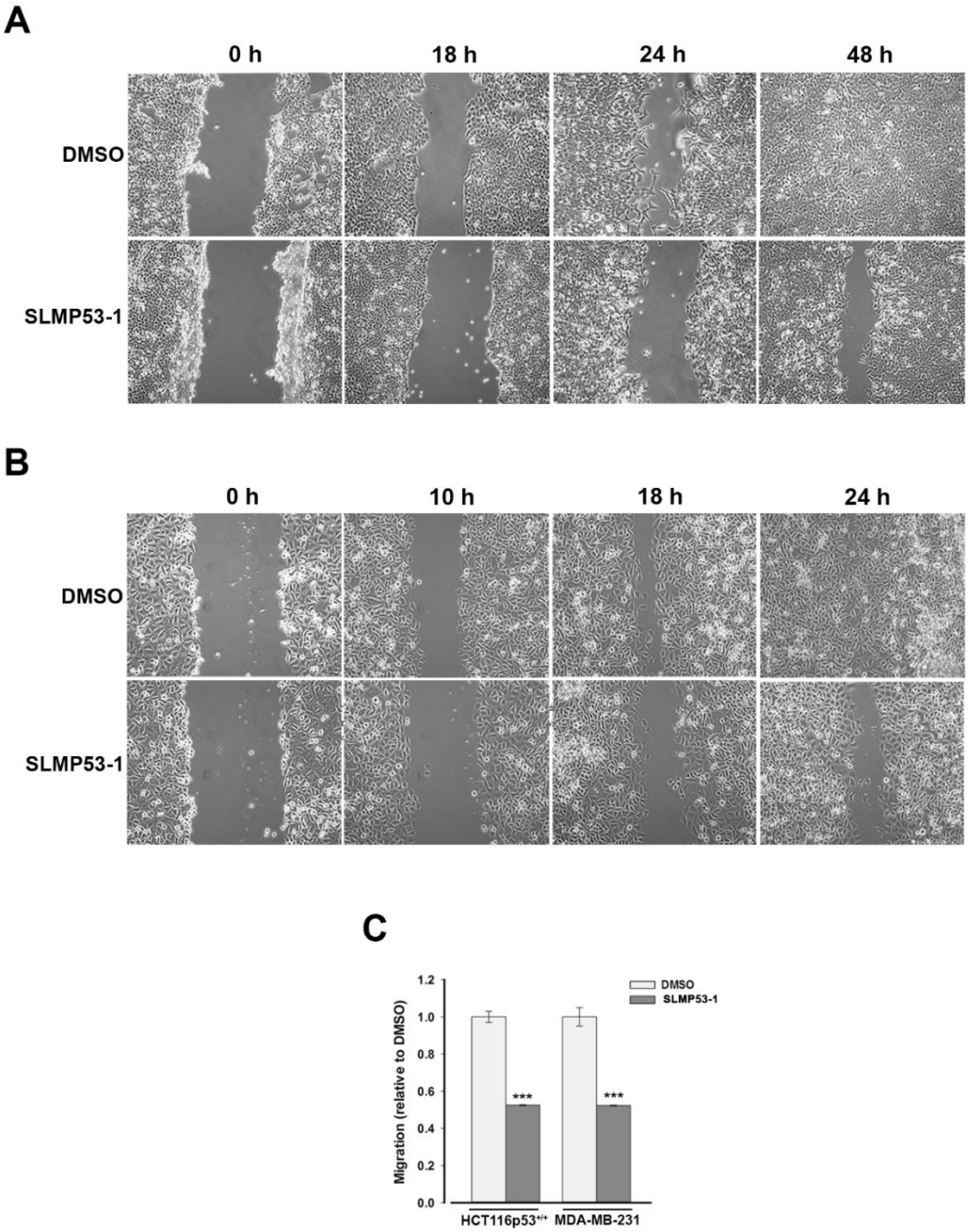

Figure 4.6. SLMP53-1 prevents the migration of HCT116 p53$^{+/+}$ and MDA-MB-231 cells. (A) HCT116 p53$^{+/+}$ and **(B)** MDA-MB-231 confluent cells treated with 4 μM SLMP53-1 (or DMSO only) were observed at different time-points in the Wound Healing Assay. **(C)** Effects of SLMP53-1 on the migration of HCT116 p53$^{+/+}$ (7 μM for 24 h) and MDA-MB-231 (16 μM for 8 h) cells analyzed by the chemotaxis assay; the migratory cells were quantified by fluorescence signal, setting as 1 cells treated with DMSO only; data are mean ± S.E.M. of three independent experiments; values significantly different from DMSO only are indicated: ***$p < 0.001$.

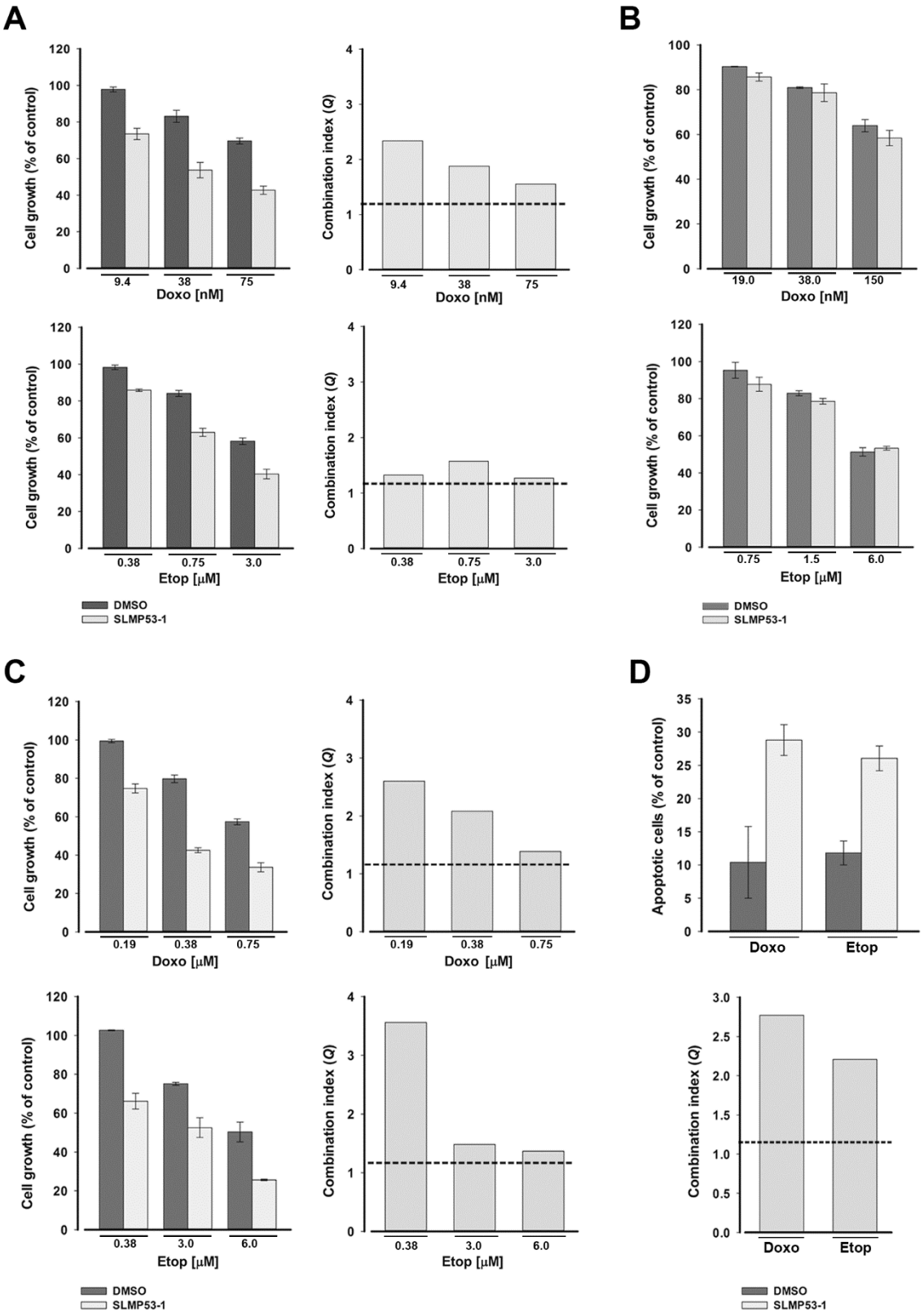

Figure 4.7. SLMP53-1 sensitizes HCT116 p53$^{+/+}$ and MDA-MB-231 cells to the effects of etoposide and doxorubicin. (**A-C)** Effects of combined treatment with 4 μM SLMP53-1 (or DMSO only) and increasing concentrations of doxorubicin (Doxo) or etoposide (Etop) on tumor cell growth,

after 48 h; data are mean ± S.E.M. of four independent experiments; the percentage of cell growth achieved with SLMP53-1 only was **(A)** 90.3% in HCT116 $p53^{+/+}$, **(B)** 99.8% in HCT116 $p53^{-/-}$ and **(C)** 90.5% in MDA-MB-231 cells. **(D)** Effects of combined treatment with 4 μM SLMP53-1 (or DMSO only) and 0.19 μM doxorubicin or 0.38 μM etoposide on apoptosis after 48 h in MDA-MB-231 cells. The percentage of apoptotic cells obtained with SLMP53-1 only was 0.2%; data are mean ± S.E.M. of three independent experiments. In **A**, **C** and **D**, the *Q* values are represented; dotted line represents *Q*=1.15.

4.8. SLMP53-1 has no *in vitro* toxicity in non-tumorigenic cells

The potential genotoxicity of SLMP53-1 was investigated using the cytokinesis-block micronucleus assay. At 16 μM, SLMP53-1 did not increase the number of micronuclei in lymphocytes when compared to DMSO only (Figure 4.8A). Additionally, 16 μM SLMP53-1 induced only 5.6 ± 3.2% (*n* = 5) growth inhibition in non-tumorigenic MCF10A cells, showing that this concentration was not toxic to normal cells. Furthermore, unlike in tumor cells, in MCF10A cells, the growth inhibition induced by SLMP53-1 at the GI_{50} concentration (42.4 ± 2.9 μM, *n* = 5) was associated with G0/G1-cell cycle arrest (Figure 4.8B), but not with apoptosis (Figure 4.8C).

4.9. SLMP53-1 has potent *in vivo* antitumor activity with no evident toxicity

To evaluate the *in vivo* antitumor potential of SLMP53-1, mice xenograft models carrying HCT116 $p53^{+/+}$, HCT116 $p53^{-/-}$, or MDA-MB-231 tumor cells were used. The results revealed that four intraperitoneal administrations (twice a week) of 50 mg/kg SLMP53-1 were highly effective, blocking the growth of HCT116 $p53^{+/+}$ tumors (Figure 4.8D) compared to control (vehicle). Most importantly, SLMP53-1 had no effect on HCT116 $p53^{-/-}$ tumor xenografts, corroborating its p53-dependent antitumor activity (Figure 4.8D). Potent antitumor activity was also established for MDA-MB-231 tumors, confirming the *in vivo* efficacy of SLMP53-1 against mutant p53R280K-expressing tumors (Figure 4.8D). No significant loss of body weight or morbidity signs were observed in treated mice compared to control, throughout the experimental period (Figure 4.8E).

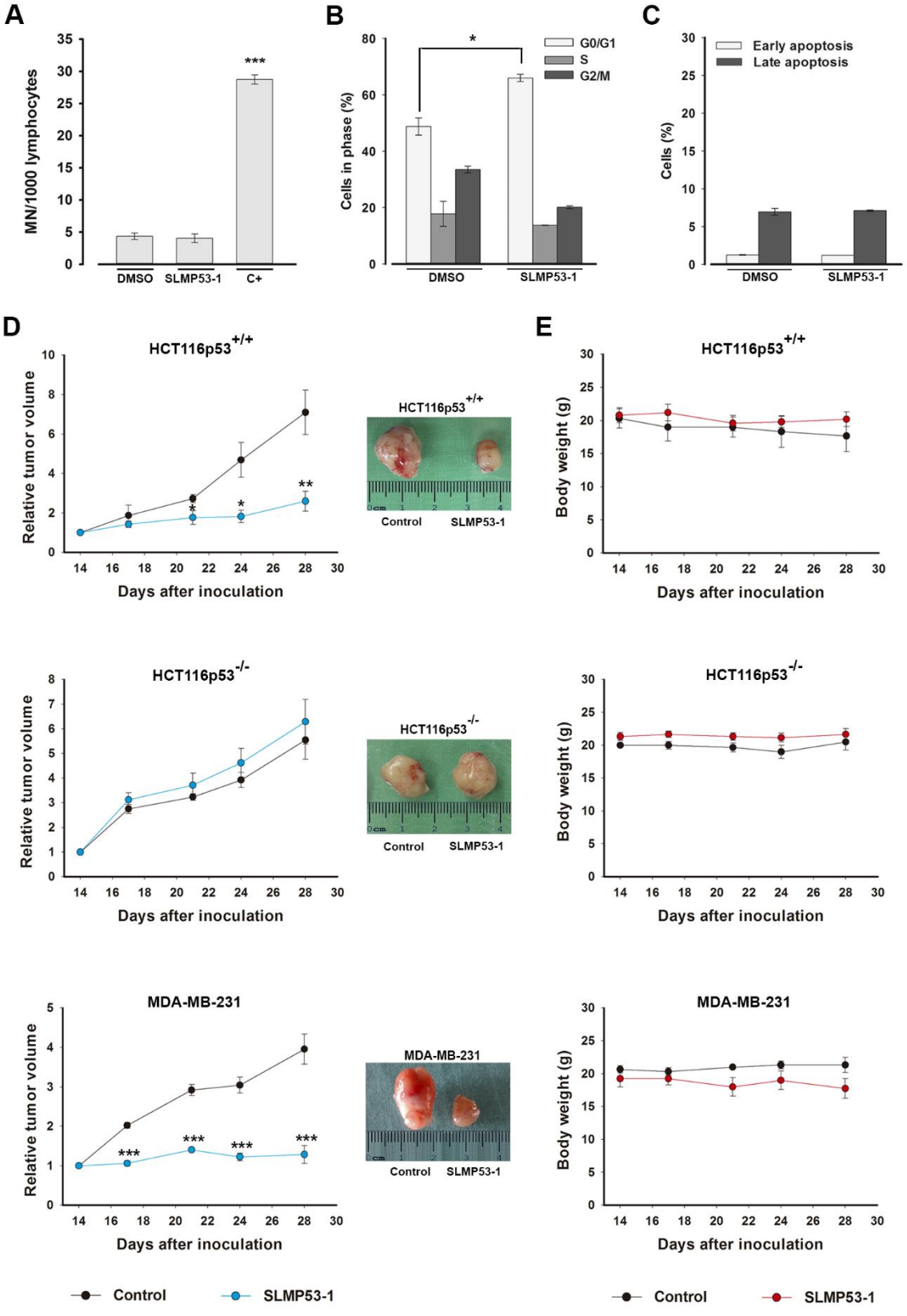

Figure 4.8. SLMP53-1, with no apparent *in vitro* toxicity, has potent *in vivo* antitumor activity. **(A)** Genotoxicity of 16 μM SLMP53-1 by cytokinesis-block micronucleus (MN) assay after 72 h treatment in human lymphocyte cells. Cells treated with 1 μg/mL cyclophosphamide were used as

positive control (C+); data are mean ± S.E.M. of three independent experiments. **(B)** Cell cycle after 48 h with 42.4 µM SLMP53-1 in MCF10A cells; data are mean ± S.E.M. of three independent experiments. In **A** and **B**, values significantly different from DMSO only are indicated: ***$p < 0.001$. **(C)** Apoptosis after 48 h with 42.4 µM SLMP53-1 in MCF10A cells; data are mean ± S.E.M. of three independent experiments; no significant differences between SLMP53-1 and DMSO only: $p > 0.05$. **(D)** BALB/c nude mice carrying HCT116 $p53^{+/+}$, HCT116 $p53^{-/-}$ or MDA-MB-231 xenografts treated with 50 mg/kg SLMP53-1 or vehicle (control); values significantly different from control mice are indicated: *$p < 0.05$, **$p < 0.01$, ***$p < 0.001$; representative pictures of control and SLMP53-1-treated tumors. **(E)** BALB/c mice body weight during SLMP53-1 treatment; no significant differences between control and SLMP53-1-treated mice: $p > 0.05$.

Considering the common chemotherapeutic side effects, some primary toxicity signs potentially triggered by SLMP53-1 were investigated in Wistar rats. For that, the organs relative weight (trophism), as well as biochemical and hematological data were analyzed for three rat groups (saline, vehicle and SLMP53-1; Table 4.1). No differences between the three groups on relative weight of liver, kidneys, heart and lungs were observed. Concerning biochemical data, only a slight decrease of urea in the vehicle group compared to saline group, and a slight decrease of uric acid and albumin in the SLMP53-1 group compared to vehicle group were observed. Hence, no evident liver or kidney toxicity was detected in the SLMP53-1-treated group. Finally, concerning hematological data, just a small increase on the reticulocytes number was observed in the vehicle group compared to saline group, with no alterations between the SLMP53-1 and vehicle groups. Altogether, no apparent toxic side effects were observed for SLMP53-1 on the tissues most commonly affected by conventional chemotherapeutics.

Table 4.1. Safety profile for the three mice groups under study at the final time point.

	Saline	Vehicle	Treated
Body weight and relative tissue weight (trophism)			
BW (g)	340.30 ± 13.45	361.80 ± 0.01	348.30 ± 0.01
Heart/BW (g/kg)	3.03 ± 0.03	3.01 ± 0.09	2.91 ± 0.07
Liver/BW (g/kg)	38.71 ± 2,36	38.52 ± 0.89	35.74 ± 0.81
Kidney/BW (g/kg)	7.08 ± 0.40	6.81 ± 0.27	6.55 ± 0.34
Lung/BW (g/kg)	3.89 ± 0.07	3.81 ± 0.08	3.83 ± 0.11
Biochemical data			
Blood Glucose (mg/dL)	188.0 ± 7.51	207.20 ± 7.00	186.80 ± 11.12
Urea (mg/dL)	20.67 ± 0.77	18.34 ± 0.24*	18.48 ± 1.31
Uric acid (mg/dL)	1.07 ± 0.07	0.82 ± 0.10	0.78 ± 0.05*
Creatinine (mg/dL)	0.30 ± 0.00	0.30 ± 0.01	0.30 ± 0.01
Total Proteins (g/dL)	5.50 ± 0.00	5.35 ± 0.17	5.08 ± 0.15
Albumin (g/dL)	3.03 ± 0.03	2.90 ± 0.05	2.73 ± 0.09*
ALT (U/L)	36.00 ± 2.89	30.75 ± 3.30	32.50 ± 4.87
AST (U/L)	95.33 ± 25.36	56.25 ± 4.60	67.00 ± 11.05
CK (U/L)	458.30 ± 148.60	229.50 ± 64.40	281.80 ± 101.90
Total Chol (mg/dL)	44.33 ± 1.76	52.40 ± 3.54	60.25 ± 5.98
Triglycerides (mg/dL)	107.00 ± 16.29	161.40 ± 17.55	169.80 ± 24.00
Hematological data			
RBC count ($x10^6$/µL)	7.10 ± 0.15	7.41 ± 0.28	7.28 ± 0.27
HGB (g/dL)	13.97 ± 0.18	13.95 ± 0.46	13.53 ± 0.25
HCT (%)	40.50 ± 0.82	42.28 ± 2.03	39.63 ± 0.99
WBC counts ($x10^3$/µL)	5.23 ± 0.52	5.95 ± 1.61	5.08 ± 0.434
PLT counts ($x10^3$/µL)	811.00 ± 29.61	793.80 ± 28.35	852.50 ± 32.05
PCT (%)	0.47 ± 0.03	0.46 ± 0.009	0.50 ± 0.02
RET counts (%)	2.80 ± 0.12	3.56 ± 0.23*	3.28 ± 0.23

The results are expressed as mean ± S.E.M. of four to six independent experiments. *$p < 0.05$ versus Control group; ALT, alanine aminotransferase; AST, aspartate aminotransferase; BW, body weight; CK, Creatine Kinase; HCT, hematocrit; HGB, Hemoglobin concentration; PCT, plateletcrit; PLT, platelet; RBC, red blood cell count; RET, reticulocytes; WBC, white blood cell.

In order to assess the proliferation and apoptotic status of tumors, immunohistochemistry and TUNEL staining were performed with tumor tissues (Figure 4.9). Both HCT116 $p53^{+/+}$ and MDA-MB-231 tumors, treated with SLMP53-1, showed low Ki-67-positive staining (indicative of a low proliferative status), when compared to tumors treated with vehicle (Figure 4.9). Additionally, a marked increase of BAX expression levels in SLMP53-1-treated tumor tissues, compared to vehicle, was observed (Figure 4.9). A pronounced increase of TUNEL-positive staining (indicative of nuclei DNA fragmentation)

was also observed upon SLMP53-1 treatment (Figure 4.9). On the other hand, a uniform pattern, characterized by high levels of Ki-67 and low levels of BAX expression and DNA fragmentation, between HCT116 $p53^{-/-}$ tumors treated with SLMP53-1 and vehicle was obtained (Figure 4.9).

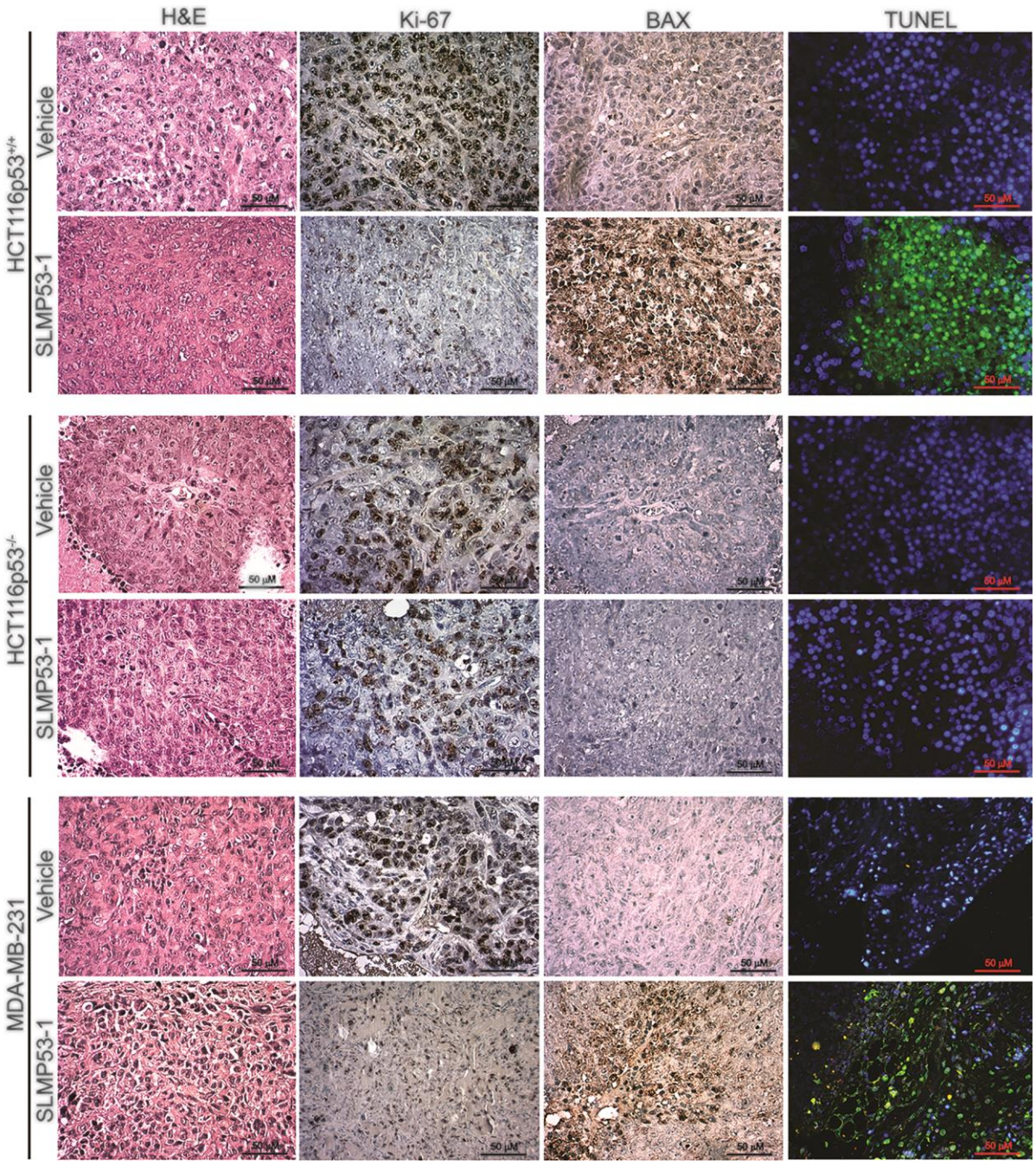

Figure 4.9. SLMP53-1 decreases cell proliferation and enhances apoptosis in human tumor xenografts. Representative images of Ki-67, BAX and DNA fragmentation detection in human HCT116 $p53^{+/+}$, HCT116 $p53^{-/-}$ and MDA-MB-231 tumor xenograft tissues inoculated in BALB/c nude mice treated with 50 mg/kg SLMP53-1 or vehicle (Scale bar = 50μm; Magnification 400x).

4.10. Discussion

The p53 protein is a key player in apoptotic processes, what makes its reactivation an appealing therapeutic approach in cancer treatment. For that reason, efforts have been made in the last years to discover new small molecule reactivators of wt and mutant p53. The majority of these compounds have been found using the traditional screens, in which the first line screening is performed in tumor cell lines with different p53 status to access their biological activityand selectivity. Nevertheless, to test large libraries of compounds, this methodology requires many resources and time. To streamline the search for new reactivators of mutant p53, a yeast screening assay was developed, in this work. In fact, this simple and reliable cell-based drug targeted screening approach, can be easily adaptable to the HTS of large chemical libraries, based on simple cell growth measurements, in a cost-effective manner. In this work, besides the validation of the yeast model assay to search for reactivators of mutant p53R280K and Y220C (among the twenty most prevalent mutant p53s), using this approach a new reactivator of wt p53 and mutant p53R280K, the small molecule SLMP53-1, was discovered from a chemical library of enantiopure tryptophanol-derived oxazoloisoindolinones.

Considering the relevance of the absolute stereochemical configuration of biologically active compounds, the enantiomer of SLMP53-1 was also synthesized (Figure 4.1A). Interestingly, this enantiomer was inactive in yeast and exhibited a much lower growth inhibitory effect against wt/mutant p53-expressing tumor cells compared to SLMP53-1 (data not shown). These results highlight the relevance of the stereochemistry at positions C-3 and C-9b for the activity of SLMP53-1. Besides this, the activation of wt p53 and mutant p53R280K (a DNA contact mutant without major structural alterations), associated with the absence of effect of SLMP53-1 on structural mutant p53Y220C, lead us to hypothesize some preference of SLMP53-1 for the wt-like conformation of p53. Further studies are underway to analyze the activity of SLMP53-1 on other mutant p53s.

Contrary to PRIMA-1, SLMP53-1 exhibited a p53-dependent tumor growth inhibitory activity. In fact, the induction of cell cycle arrest and apoptosis, and the enhancement of p53 transcriptional activity by SLMP53-1 in wt p53-expressing HCT116 tumor cells were completely abolished in p53-null HCT116 cells. Additionally, SLMP53-1 showed a much higher cytotoxicity against mutant p53R280K-expressing MDA-MB-231 cells than PRIMA-1, which cytotoxicity against this tumor cell line has been reported (Russo et al., 2013). In these tumor cells, SLMP53-1 restored the wt-like sequence-specific DNA binding ability to mutant p53R280K, with subsequent up-regulation of p53 target genes. Curiously, in mutant p53R280K-expressing cells, the SLMP53-1-induced growth inhibition was only associated

with apoptosis, and not with cell cycle arrest. These results highlight key genetic differences between tumor cells associated with distinct p53 status (wt/mutant).

The pathophysiological relevance of the mitochondrial p53 function in apoptotic cell death has been emphasized in several studies (Marchenko and Moll, 2007). In response to stress, a fraction of p53 translocates to mitochondria, where it binds to Bcl-2 family proteins inducing mitochondrial outer membrane permeabilization (MOMP), cyt *c* release, and subsequent apoptosis (Marchenko and Moll, 2007). The mitochondrial function of mutant p53 is still unclear. Interestingly, mutant p53 has been reported to localize constitutively at mitochondrial outer membrane due to its intrinsic cellular stabilization. Despite this, the mutant p53 apoptotic activity is compromised by its inability to bind to Bcl-2 and trigger MOMP (Marchenko and Moll, 2007; Wang et al., 2011a). In this work, SLMP53-1 triggered a mitochondrial p53 apoptotic pathway in wt p53-expressing tumor cells, involving $\Delta\psi_m$ dissipation, p53 and BAX mitochondrial translocation, as well as cyt *c* release. Similar events were triggered by SLMP53-1 in mutant p53R280K-expressing tumor cells, supporting the translocation of a functionally active mutant p53 to mitochondria. It is interesting to note that SLMP53-1 treatment induced a p53-dependent ROS generation, which may result from the stimulation of both pro-oxidant and mitochondrial p53 functions. Actually, SLMP53-1 enhances the expression of *BAX* and *PUMA*, which besides the connection with the p53 mitochondrial pathway are also strongly involved in its pro-oxidant function (Puzio-Kuter, 2011). Collectively, the results obtained indicate that SLMP53-1 is a "double hit" reactivator of p53-mediated apoptosis, stimulating both the transcription-dependent and mitochondrial-mediated p53 functions.

Considered the main cause of morbidity and mortality in cancer patients, tumor cell invasion and metastization are central issues in cancer treatment (Etienne-Manneville, 2008; Muller et al., 2011). The pivotal role of p53 in the prevention of epithelial-mesenchymal transition and migration is widely recognized (Muller et al., 2011). Accordingly, mutant p53 has been associated to prometastatic functions not only due to the loss of p53 function, but also to the GOF related to p63 inhibition, a well-known suppressor of tumorigenesis and metastasis (Muller et al., 2011). Low doses of SLMP53-1 potently inhibited the migration of wt/mutant p53-expressing cells, which sustains the reactivation of wt p53, as well as of mutant p53 through reestablishment of its wt function and possible inhibition of its GOF.

Since the majority of conventional chemotherapeutics, as etoposide and doxorubicin, depend on a functional p53 pathway, combination with p53 reactivators is expected to enhance their efficacy. Indeed, low doses of SLMP53-1 showed p53-dependent synergistic effects with both chemotherapeutic agents in wt/mutant p53-expressing tumor cells.

Therefore, the combination of SLMP53-1 with conventional chemotherapeutics reveals great therapeutic potential, particularly against multidrug-resistant tumor cells, like triple-negative breast cancers, minimizing drug side effects, while increasing tumor suppressor activity.

The toxicity of standard chemotherapeutics remains a therapeutically limiting problem. Herein, SLMP53-1 was shown to be non-genotoxic. Additionally, despite activating wt p53, at the GI_{50} concentration obtained in tumor cells, SLMP53-1 was not cytotoxic against wt p53-expressing normal MCF10A cells. The minimal cytotoxic effects of p53 reactivators on normal cells have been attributed to their lower susceptibility to apoptotic stimuli when compared to tumor cells with a constitutive activation of a DNA damage signaling pathway (Vassilev, 2004; Berns et al., 2004; Tovar et al., 2006). This leads normal cells to respond to p53 reactivators with cell cycle arrest (cytostatic effect), instead of cell death (cytotoxic effect) (Carvajal et al., 2005; Rao et al., 2013). Actually, this was observed in normal cells with SLMP53-1 at a three-fold higher GI_{50} concentration than that used in tumor cells. SLMP53-1 can thus be exploited in p53-based cyclotherapy, in which normal cells are protected from the cytotoxicity of chemotherapeutics by induction of cell cycle arrest.

Assays in xenograft mice models reinforced the p53-dependent *in vivo* antitumor activity of SLMP53-1. In fact, SLMP53-1 potently suppressed the growth of wt p53- and mutant p53R280K-expressing tumors through inhibition of proliferation and induction of apoptosis, without interfering with the growth of p53-null tumors. Additionally, SLMP53-1 had no apparent toxic side effects on tissues most commonly affected by chemotherapy, such as kidneys, liver and bone marrow.

In conclusion, several evidences are herein provided supporting the anticancer therapeutic potential of SLMP53-1, both alone and combined with conventional chemotherapeutics. To our knowledge, this is the first report of a pharmacological reactivator of p53R280K, a mutant p53 form involved in highly metastatic and chemoresistant tumors (e.g. triple negative breast cancer cells MDA-MB-231). Besides its great potential as anticancer drug candidate, SLMP53-1 is a starting point for the development of new effective derivatives targeting mutant p53s.

CHAPTER 5

General Discussion

Final conclusions and Future perspectives

Cancer is one of the major Public Health concerns of our world aging population (Ferlay et al., 2015). Besides, the therapeutic options for many cancer patients remain limited and disappointing, mainly due to chemoresistance and devastating side effects. On the other hand, the development of new targeted drugs has proved to be a time consuming and highly unreliable process.

Due to its central role in tumorigenesis, p53 has been pointed out as one of the most relevant targets in cancer treatment. Actually, the activation of the p53 pathway either by inhibition of the p53 interaction with their negative regulators MDMs, or by reactivation of the wt-like function to mutant p53 have been highlighted as hopeful strategies in anticancer treatment (Zawacka-Pankau and Selivanova, 2015). However, despite all the efforts dedicated to find effective activators of p53, to date, few have enter into clinical trials and none has reached the clinic (Zawacka-Pankau and Selivanova, 2015). Additionally, the existence of few screening methods to find new mutant p53 reactivators contribute to the slow progress in this field. With this thesis, great advances have been achieved in this research area, not only with the validation of an efficient and reliable drug screening strategy targeting p53, but also with the discovery of new activators of the p53 pathway identified from the synthesized libraries (including small molecules containing indole and/or isoindolinone moieties) particularly:

a) *New inhibitors of p53-MDMs interactions*

Despite the huge diversity of chemical families identified as inhibitors of the p53-MDM2 interaction, only few molecules have advanced into clinical trials due to their low selectivity, high toxicity and poor pharmacokinetic profiles (Lauria et al., 2011; Wang et al., 2012; Wang and Hu, 2012; Zhao et al., 2013a). For this reason, the identification of new scaffolds of inhibitors of the p53-MDM2 interaction with improved pharmacological properties remains a priority goal in p53-based anticancer therapy. Based on this, using a previously developed yeast-based screening assay (Leão et al., 2013c), in Chapter 3.1, an enantiopure phenylalaninol-derived oxazolopyrrolidone lactam (oxazoloisoindolinone 3a) was identified as new inhibitor of the p53-MDM2 interaction. The oxazoloisoindolinone 3a revealed potent *in vitro* p53-dependent tumor growth-inhibitory effect through stimulation of apoptosis and cell cycle arrest. Furthermore, insights on its binding mode to MDM2 have been provided by molecular docking studies (Figure 5.1). It must be noted that, also under the scope of this thesis, using the same screening approach, the molecular mechanism underlying the increased cytotoxicity against human tumor cells of *O*-prenyl derivative of 2′-hydroxy-3,4,4′,5,6′-pentamethoxychalcone compared to its precursor was revealed. In fact,

the prenylation demonstrated to be a determinant factor for the enhancement of chalcones tumor cytotoxicity by improving their ability to disrupt the p53–MDM2 interaction (Leão et al., 2015b).

The dual inhibition of the p53 interaction with MDM2 and MDMX has long been considered the most effective strategy for a full reactivation of wt p53 in tumors, particularly against MDMX-overexpressing tumor cells (e.g., retinoblastomas and melanomas) that are highly resistant to MDM2-only inhibitors (Graves et al., 2012; Wade et al., 2013). Despite this, to date, just three small molecule dual inhibitors of the p53-MDMs interactions have been reported. Focusing on this, the previously developed yeast-based screening assays to search for inhibitors of the p53 interaction with MDM2 or MDMX (Leão et al., 1013b,c) were used. This approach led us to the identification of our first dual inhibitor of p53-MDMs interactions, the compound OXAZ-1, from a chemical library of tryptophanol-derived oxazolopiperidone lactams (Chapter 3.2). Although less potent than oxazoloisoindolinone 3a in tumor cells, the small molecule OXAZ-1 was able to inhibit the p53 interaction with both MDM2 and MDMX, and to strongly induce a p53-dependent mitochondrial apoptotic pathway. Additionally, OXAZ-1 sensitized tumor cells to the effect of conventional chemotherapeutics, what may open the way to a potential applicability in combined anticancer therapy (Figure 5.1). Despite this, the modest *in vitro* tumor growth-inhibitory activity of OXAZ-1 led us to pursue our search for more potent dual inhibitors of p53-MDMs interactions.

Using the same yeast-based screening strategy (Leão et al., 1013b,c), in Chapter 3.3, a second dual inhibitor, the compound DIMP53-1, was identified from a chemical library of tryptophanol-derived oxazoloisoindolinones. Besides its higher *in vitro* growth-inhibitory effect, DIMP53-1 exhibited potent p53-dependent *in vivo* antitumor activity with no apparent toxic side effects. Most importantly, despite its anti-proliferative activity through induction of tumor apoptotic cell death, DIMP53-1 strongly inhibited cell migration and angiogenesis. Together, these findings show that DIMP53-1 is an appealing anticancer drug candidate (Figure 5.1). It should be noted, that DIMP53-1 is the first dual inhibitor with *in vivo* anticancer properties described to date.

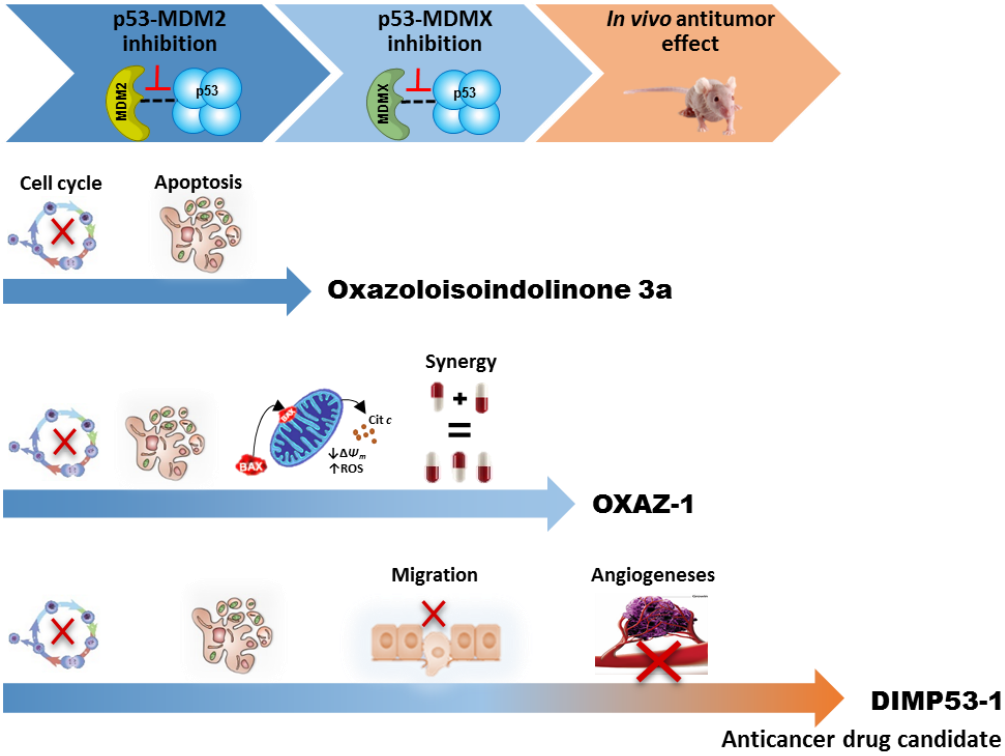

Figure 5.1. Schematic representation of the antitumor properties of the new inhibitors of p53-MDMs interactions discovered under this thesis: Oxazoloisoindolinone 3a (inhibitor of the p53-MDM2 interaction), OXAZ-1 and DIMP53-1 (dual inhibitors of p53-MDMs interactions).

b) *New reactivator of mutant p53*

Few small molecules have been recognized as true reactivators of the wt-like activity to mutant p53, and just APR-246 has reached clinical trials (Khoo et al., 2014; Zawacka-Pankau and Selivanova, 2015; Girardini et al., 2014).

To streamline the discovery process of new reactivators of mutant p53, a reliable and highly adaptable approach to HTS was developed under the scope of this thesis based on yeast cells expressing independent mutant p53 forms, such as R280K and Y220C. The efficacy of this approach to search for reactivators of mutant p53 was validated in this thesis with the identification of SLMP53-1, the first reactivator of mutant p53 R280K and activator of wt p53, from a chemical library of enantiopure tryptophanol-derived oxazoloisoindolinones (Chapter 4). SLMP53-1 revealed potent *in vitro* and *in vivo* p53-dependent antitumor activity against wt/mutant p53-expressing tumors, without apparent toxic side effects (Figure 5.2). Additionally, it strongly stimulated a p53-mediated mitochondrial apoptotic pathway, inhibited cell migration and sensitized wt/mutant p53-expressing tumor cells to conventional chemotherapeutics (Figure 5.2). Altogether, several

evidences are provided in this thesis supporting the great therapeutic potential of SLMP53-1, either alone or in combined therapy, particularly against mutant p53 R280K-expressing tumors, such as triple negative breast cancer cells characterized by its poor prognosis due to be highly metastatic and chemoresistant to conventional chemotherapeutic drugs.

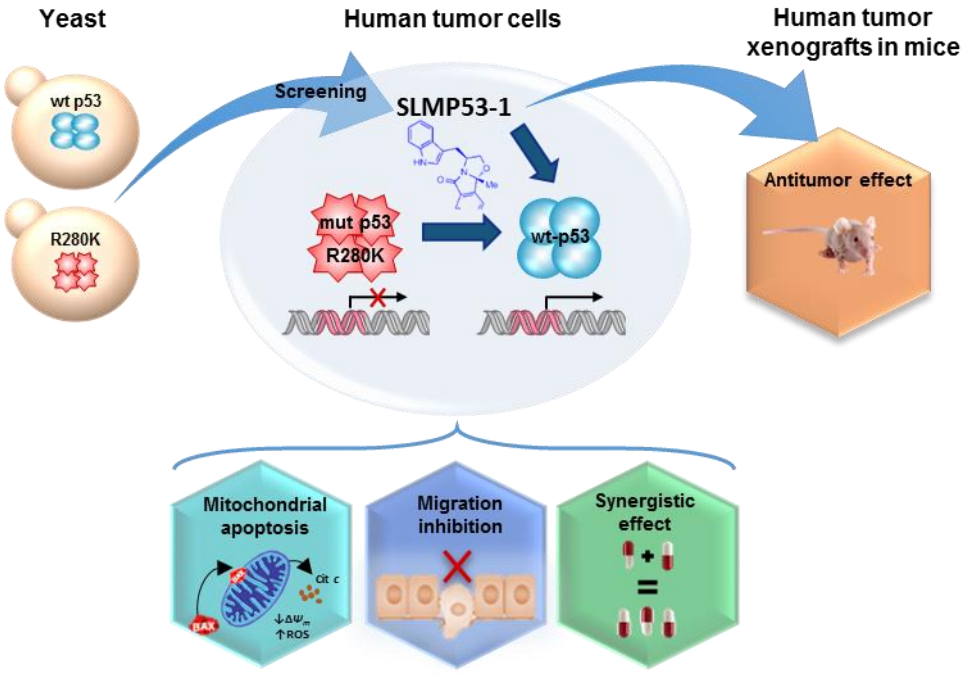

Figure 5.2. Drug discovery strategy underlying the identification of the first reactivator of mutant p53 R280K: SLMP53-1 and its antitumor properties. Using a yeast screening assay, SLMP53-1 was identified as potential reactivator of wt and mutant p53 R280K. SLMP53-1 shows i*n vitro* antitumor activity through stimulation of a mitochondrial-mediated apoptotic cell death, inhibits migration of highly metastatic tumor cells, has synergistic activity in combination with conventional chemotherapeutics, and shows potent *in vivo* p53-dependent antitumor activity.

Final conclusions and future perspectives

With the present thesis, a new yeast screening assay that will streamline the discovery of new reactivators of mutant p53 was developed. Additionally, by using yeast-based targeted screening assays, for a first selection of potential bioactive compounds to be tested in more complex cell systems, four new activators of the p53 pathway (Oxazoloisoindolinone 3a, OXAZ-1, DIMP53-1, and SLMP53-1) were discovered. In fact, with this thesis, the enormous contribution of yeast as screening tool to anticancer drug discovery is greatly reinforced. In particular, the extension of the yeast assay developed for

mutant p53 R280K and Y220C to other prevalent mutant p53 forms may open the way to the discovery of new potential reactivators. This would have a particular impact in personalized anticancer therapy of patients with mutant p53-expressing tumors. Actually, to date, only reactivators of few mutant p53 forms (R273H, R175H, Y220C, R248W, R249Q) have been reported. In this context, it would be interesting to test the ability of SLMP53-1 to reactivate other mutant p53 beyond R280K.

Most importantly, with this work two promising anticancer drug candidates, DIMP53-1 and SLMP53-1, were identified. Future pharmacokinetic studies of absorption, distribution, metabolism, and elimination (ADME), in association with a more detailed toxicological characterization, will evaluate their potential as pharmaceutical agents to possible progress to clinical trials.

Likewise, a more detailed elucidation of the molecular mechanism of action of Oxazoloisoindolinone 3a, OXAZ-1, DIMP53-1, and SLMP53-1, by defining possible interactions with the target proteins, through biophysical binding assays and crystallographic analysis, would clarify their activity and would help their hit-to-lead optimization. Actually, Oxazoloisoindolinone 3a, OXAZ-1, DIMP53-1, and SLMP53-1 represent promising starting points for the development of more effective derivatives.

In addition, in future works, the anti-migration and anti-angiogenic properties of the anticancer drug candidates DIMP53-1 and SLMP53-1 could be further explored. This would better define the potential therapeutic applications of these compounds against certain types of cancer (namely high metastatic cancers). Moreover, the molecular mechanism responsible for the switch between survival and death under p53 activation could be also explored using DIMP53-1 and SLMP53-1 as pharmacological tools. In particular, it would be interesting to elucidate the different profiles (cell cycle arrest versus apoptosis) triggered by SLMP53-1 in tumor cells harbouring different p53 status (wt versus mutant p53).

Besides the synergy observed between OXAZ-1 or SLMP53-1 with conventional chemotherapeutics, it would also be interesting to analyse the combination therapy between a dual interaction inhibitor (as DIMP53-1) and a wt/mutant p53 reactivator (as SLMP53-1) in order to achieve an overactivation of the p53 signalling pathway translated into synergistic antitumor effects. Furthermore, for all promising combinations, the synergistic interaction pathways need to be further elucidated.

Finally, DIMP53-1 and SLMP53-1 could be explored in p53-cyclotherapy, representing other possible therapeutic applicability of these compounds as chemoprotectors, and therefore should be the focus of further studies.

In conclusion, besides the incontestable impact of this work to the advance of p53 pharmacology and targeted drug discovery, it gives rise to new hopes and therapeutic

opportunities in cancer treatment by providing potential anticancer drug candidates. Besides this, the present thesis provides attractive pharmacological tools to the p53 research field, as well as starting scaffolds that may be the basis for future derivatives with improved pharmacological properties as anticancer therapeutic agents.

CHAPTER 6

References

Adams PD, Sellers WR, Sharma SK, Wu AD, Nalin CM, Kaelin WG, Jr. Identification of a cyclin-cdk2 recognition motif present in substrates and p21-like cyclin-dependent kinase inhibitors. Mol Cell Biol 1996 Dec; 16 (12): 6623-33.

Adorno M, Cordenonsi M, Montagner M, Dupont S, Wong C, Hann B, et al. A Mutant-p53/Smad complex opposes p63 to empower TGFbeta-induced metastasis. Cell 2009 Apr 3; 137 (1): 87-98.

Ali D, Jonsson-Videsater K, Deneberg S, Bengtzen S, Nahi H, Paul C, et al. APR-246 exhibits anti-leukemic activity and synergism with conventional chemotherapeutic drugs in acute myeloid leukemia cells. Eur J Haematol 2011 Mar; 86 (3): 206-15.

Allen JG, Bourbeau MP, Wohlhieter GE, Bartberger MD, Michelsen K, Hungate R, et al. Discovery and optimization of chromenotriazolopyrimidines as potent inhibitors of the mouse double minute 2-tumor protein 53 protein-protein interaction. J Med Chem 2009 Nov 26; 52 (22): 7044-53.

Allin SM, James SL, Martin WP, Smith TAD, Elsegoog MRJ. Stereoselective synthesis of the pyrroloisoquinoline ring system. J Chem Soc Perkin Trans 2001 Oct; 1(22): 3029–36.

Amaral JD, Herrera F, Rodrigues PM, Dionisio PA, Outeiro TF, Rodrigues CM. Live-cell imaging of p53 interactions using a novel Venus-based bimolecular fluorescence complementation system. Biochem Pharmacol 2013 Mar 15; 85 (6): 745-52.

Amaral JD, Xavier JM, Steer CJ, Rodrigues CM. Targeting the p53 pathway of apoptosis. Curr Pharm Des 2010; 16 (22): 2493-503.

Amat M, Santos MM, Bassas O, Llor N, Escolano C, Gomez-Esque A, et al. Straightforward methodology for the enantioselective synthesis of benzo[a]- and indolo[2,3-a]quinolizidines. J Org Chem 2007a Jul 6; 72 (14): 5193-201.

Amat M, Santos MM, Gomez AM, Jokic D, Molins E, Bosch J. Enantioselective spirocyclizations from tryptophanol-derived oxazolopiperidone lactams. Org Lett 2007b Jul 19; 9 (15): 2907-10.

Amundson SA, Myers TG, Fornace AJ, Jr. Roles for p53 in growth arrest and apoptosis: putting on the brakes after genotoxic stress. Oncogene 1998 Dec 24; 17 (25): 3287-99.

Andreotti V, Ciribilli Y, Monti P, Bisio A, Lion M, Jordan J, et al. p53 transactivation and the impact of mutations, cofactors and small molecules using a simplified yeast-based screening system. PLoS One 2011; 6 (6): e20643.

Aoubala M, Murray-Zmijewski F, Khoury MP, Fernandes K, Perrier S, Bernard H, et al. p53 directly transactivates Delta133p53alpha, regulating cell fate outcome in response to DNA damage. Cell Death Differ 2011 Feb; 18 (2): 248-58.

Arkin MR, Glicksman MA, Fu H, Havel JJ, Du Y. Inhibition of Protein-Protein Interactions: Non-Cellular Assay Formats. In: Sittampalam GS, Coussens NP, Nelson H, Arkin M, Auld D, Austin C, et al., editors. Assay Guidance Manual. Bethesda (MD): Eli Lilly & Company and the National Center for Advancing Translational Sciences; 2012.

Arts J, Page M, Valckx A, Blattner C, Kulikov R, Floren W, et al. JNJ-26854165 - a novel hdm2 antagonist in clinical development showing broad-spectrum preclinical antitumor activity against solid malignancies. Cancer Research 2008 May 1, 2008; 68 (9 Supplement): 1592.

Aylon Y, Oren M. New plays in the p53 theater. Curr Opin Genet Dev 2011 Feb; 21 (1): 86-92.

Baek S, Kutchukian PS, Verdine GL, Huber R, Holak TA, Lee KW, et al. Structure of the stapled p53 peptide bound to Mdm2. J Am Chem Soc 2012 Jan 11; 134 (1): 103-6.

Baeriswyl V, Christofori G. The angiogenic switch in carcinogenesis. Semin Cancer Biol 2009 Oct; 19 (5): 329-37.

Barboza JA, Liu G, Ju Z, El-Naggar AK, Lozano G. p21 delays tumor onset by preservation of chromosomal stability. Proc Natl Acad Sci U S A 2006 Dec 26; 103 (52): 19842-7.

Bell S, Hansen S, Buchner J. Refolding and structural characterization of the human p53 tumor suppressor protein. Biophys Chem 2002 May 2; 96 (2-3): 243-57.

Bennett M, Macdonald K, Chan SW, Luzio JP, Simari R, Weissberg P. Cell surface trafficking of Fas: a rapid mechanism of p53-mediated apoptosis. Science 1998 Oct 9; 282 (5387): 290-3.

Bergamaschi D, Gasco M, Hiller L, Sullivan A, Syed N, Trigiante G, et al. p53 polymorphism influences response in cancer chemotherapy via modulation of p73-dependent apoptosis. Cancer Cell 2003 Apr; 3 (4): 387-402.

Bergamaschi D, Samuels Y, Sullivan A, Zvelebil M, Breyssens H, Bisso A, et al. iASPP preferentially binds p53 proline-rich region and modulates apoptotic function of codon 72-polymorphic p53. Nat Genet 2006 Oct; 38 (10): 1133-41.

Berman HM, Westbrook J, Feng Z, Gilliland G, Bhat TN, Weissig H, et al. The Protein Data Bank. Nucleic Acids Res 2000 Jan 1; 28 (1): 235-42.

Bernal F, Tyler AF, Korsmeyer SJ, Walensky LD, Verdine GL. Reactivation of the p53 tumor suppressor pathway by a stapled p53 peptide. J Am Chem Soc 2007 Mar 7; 129 (9): 2456-7.

Bernal F, Wade M, Godes M, Davis TN, Whitehead DG, Kung AL, et al. A stapled p53 helix overcomes HDMX-mediated suppression of p53. Cancer Cell 2010 Nov 16; 18 (5): 411-22.

Bernard D, Zhao Y, Wang S. AM-8553: a novel MDM2 inhibitor with a promising outlook for potential clinical development. J Med Chem 2012 Jun 14; 55 (11): 4934-5.

Bernard H, Garmy-Susini B, Ainaoui N, Van Den Berghe L, Peurichard A, Javerzat S, et al. The p53 isoform, Delta133p53alpha, stimulates angiogenesis and tumour progression. Oncogene 2013 Apr 25; 32 (17): 2150-60.

Berns K, Hijmans EM, Mullenders J, Brummelkamp TR, Velds A, Heimerikx M, et al. A large-scale RNAi screen in human cells identifies new components of the p53 pathway. Nature 2004 Mar 25; 428 (6981): 431-7.

Bieging KT, Mello SS, Attardi LD. Unravelling mechanisms of p53-mediated tumour suppression. Nat Rev Cancer 2014 May; 14 (5): 359-70.

Bischoff JR, Kirn DH, Williams A, Heise C, Horn S, Muna M, et al. An adenovirus mutant that replicates selectively in p53-deficient human tumor cells. Science 1996 Oct 18; 274 (5286): 373-6.

Bisio A, Nasti S, Jordan JJ, Gargiulo S, Pastorino L, Provenzani A, et al. Functional analysis of CDKN2A/p16INK4a 5'-UTR variants predisposing to melanoma. Hum Mol Genet 2010 Apr 15; 19 (8): 1479-91.

Boeckler FM, Joerger AC, Jaggi G, Rutherford TJ, Veprintsev DB, Fersht AR. Targeted rescue of a destabilized mutant of p53 by an in silico screened drug. Proc Natl Acad Sci U S A 2008 Jul 29; 105 (30): 10360-5.

Bohlig L, Friedrich M, Engeland K. p53 activates the PANK1/miRNA-107 gene leading to downregulation of CDK6 and p130 cell cycle proteins. Nucleic Acids Res 2011 Jan; 39 (2): 440-53.

Bond GL, Hu W, Bond EE, Robins H, Lutzker SG, Arva NC, et al. A single nucleotide polymorphism in the MDM2 promoter attenuates the p53 tumor suppressor pathway and accelerates tumor formation in humans. Cell 2004 Nov 24; 119 (5): 591-602.

Bossi G, Marampon F, Maor-Aloni R, Zani B, Rotter V, Oren M, et al. Conditional RNA interference in vivo to study mutant p53 oncogenic gain of function on tumor malignancy. Cell Cycle 2008 Jun 15; 7 (12): 1870-9.

Bou-Hanna C, Jarry A, Lode L, Schmitz I, Schulze-Osthoff K, Kury S, et al. Acute cytotoxicity of MIRA-1/NSC19630, a mutant p53-reactivating small molecule, against human normal and cancer cells via a caspase-9-dependent apoptosis. Cancer Lett 2015 Apr 10; 359 (2): 211-7.

Bourdon JC, Khoury MP, Diot A, Baker L, Fernandes K, Aoubala M, et al. p53 mutant breast cancer patients expressing p53gamma have as good a prognosis as wild-type p53 breast cancer patients. Breast Cancer Res 2011; 13 (1): R7.

Bourdon JC, Renzing J, Robertson PL, Fernandes KN, Lane DP. Scotin, a novel p53-inducible proapoptotic protein located in the ER and the nuclear membrane. J Cell Biol 2002 Jul 22; 158 (2): 235-46.

Brachmann RK, Vidal M, Boeke JD. Dominant-negative p53 mutations selected in yeast hit cancer hot spots. Proc Natl Acad Sci U S A 1996 Apr 30; 93 (9): 4091-5.

Bray F, Ren JS, Masuyer E, Ferlay J. Global estimates of cancer prevalence for 27 sites in the adult population in 2008. Int J Cancer 2013 Mar 1; 132 (5): 1133-45.

Brazdova M, Navratilova L, Tichy V, Nemcova K, Lexa M, Hrstka R, et al. Preferential binding of hot spot mutant p53 proteins to supercoiled DNA in vitro and in cells. PLoS One 2013; 8 (3): e59567.

Brosh R, Rotter V. When mutants gain new powers: news from the mutant p53 field. Nat Rev Cancer 2009 Oct; 9 (10): 701-13.

Bullock AN, Henckel J, DeDecker BS, Johnson CM, Nikolova PV, Proctor MR, et al. Thermodynamic stability of wild-type and mutant p53 core domain. Proc Natl Acad Sci U S A 1997 Dec 23; 94 (26): 14338-42.

Bykov VJ, Issaeva N, Selivanova G, Wiman KG. Mutant p53-dependent growth suppression distinguishes PRIMA-1 from known anticancer drugs: a statistical analysis of information in the National Cancer Institute database. Carcinogenesis 2002a Dec; 23 (12): 2011-8.

Bykov VJ, Issaeva N, Shilov A, Hultcrantz M, Pugacheva E, Chumakov P, et al. Restoration of the tumor suppressor function to mutant p53 by a low-molecular-weight compound. Nat Med 2002b Mar; 8 (3): 282-8.

Bykov VJ, Issaeva N, Zache N, Shilov A, Hultcrantz M, Bergman J, et al. Reactivation of mutant p53 and induction of apoptosis in human tumor cells by maleimide analogs. J Biol Chem 2005a Aug 26; 280 (34): 30384-91.

Bykov VJ, Zache N, Stridh H, Westman J, Bergman J, Selivanova G, et al. PRIMA-1(MET) synergizes with cisplatin to induce tumor cell apoptosis. Oncogene 2005b May 12; 24 (21): 3484-91.

Carvajal D, Tovar C, Yang H, Vu BT, Heimbrook DC, Vassilev LT. Activation of p53 by MDM2 antagonists can protect proliferating cells from mitotic inhibitors. Cancer Res 2005 Mar 1; 65 (5): 1918-24.

Chada S, Mhashilkar A, Roth JA, Gabrilovich D. Development of vaccines against self-antigens: the p53 paradigm. Curr Opin Drug Discov Devel 2003 Mar; 6 (2): 169-73.

Chan WM, Siu WY, Lau A, Poon RY. How many mutant p53 molecules are needed to inactivate a tetramer? Mol Cell Biol 2004 Apr; 24 (8): 3536-51.

Chang YS, Graves B, Guerlavais V, Tovar C, Packman K, To KH, et al. Stapled alpha-helical peptide drug development: a potent dual inhibitor of MDM2 and MDMX for p53-dependent cancer therapy. Proc Natl Acad Sci U S A 2013 Sep 3; 110 (36): E3445-54.

Chee JL, Saidin S, Lane DP, Leong SM, Noll JE, Neilsen PM, et al. Wild-type and mutant p53 mediate cisplatin resistance through interaction and inhibition of active caspase-9. Cell Cycle 2013 Jan 15; 12 (2): 278-88.

Chellappan SP, Hiebert S, Mudryj M, Horowitz JM, Nevins JR. The E2F transcription factor is a cellular target for the RB protein. Cell 1991 Jun 14; 65 (6): 1053-61.

Chen L, Yin H, Farooqi B, Sebti S, Hamilton AD, Chen J. p53 alpha-Helix mimetics antagonize p53/MDM2 interaction and activate p53. Mol Cancer Ther 2005 Jun; 4 (6): 1019-25.

Chen X, Ko LJ, Jayaraman L, Prives C. p53 levels, functional domains, and DNA damage determine the extent of the apoptotic response of tumor cells. Genes Dev 1996 Oct 1; 10 (19): 2438-51.

Chene P. In vitro analysis of the dominant negative effect of p53 mutants. J Mol Biol 1998 Aug 14; 281 (2): 205-9.

Cheok CF, Kua N, Kaldis P, Lane DP. Combination of nutlin-3 and VX-680 selectively targets p53 mutant cells with reversible effects on cells expressing wild-type p53. Cell Death Differ 2010 Sep; 17 (9): 1486-500.

Chessum N, Jones K, Pasqua E, Tucker M. Recent advances in cancer therapeutics. Prog Med Chem 2015; 54: 1-63.

Cheung-Ong K, Giaever G, Nislow C. DNA-damaging agents in cancer chemotherapy: serendipity and chemical biology. Chem Biol 2013 May 23; 20 (5): 648-59.

Chiappori AA, Soliman H, Janssen WE, Antonia SJ, Gabrilovich DI. INGN-225: a dendritic cell-based p53 vaccine (Ad.p53-DC) in small cell lung cancer: observed association between immune response and enhanced chemotherapy effect. Expert Opin Biol Ther 2010 Jun; 10 (6): 983-91.

Chicas A, Molina P, Bargonetti J. Mutant p53 forms a complex with Sp1 on HIV-LTR DNA. Biochem Biophys Res Commun 2000 Dec 20; 279 (2): 383-90.

Chipuk JE, Kuwana T, Bouchier-Hayes L, Droin NM, Newmeyer DD, Schuler M, et al. Direct activation of Bax by p53 mediates mitochondrial membrane permeabilization and apoptosis. Science 2004 Feb 13; 303 (5660): 1010-4.

Cho RW, Clarke MF. Recent advances in cancer stem cells. Curr Opin Genet Dev 2008 Feb; 18 (1): 48-53.

Cho Y, Gorina S, Jeffrey PD, Pavletich NP. Crystal structure of a p53 tumor suppressor-DNA complex: understanding tumorigenic mutations. Science 1994 Jul 15; 265 (5170): 346-55.

Ciribilli Y, Monti P, Bisio A, Nguyen HT, Ethayathulla AS, Ramos A, et al. Transactivation specificity is conserved among p53 family proteins and depends on a response element sequence code. Nucleic Acids Res 2013 Oct; 41 (18): 8637-53.

Ciriello G, Miller ML, Aksoy BA, Senbabaoglu Y, Schultz N, Sander C. Emerging landscape of oncogenic signatures across human cancers. Nat Genet 2013 Oct; 45 (10): 1127-33.

Clement JA, Kitagaki J, Yang Y, Saucedo CJ, O'Keefe BR, Weissman AM, et al. Discovery of new pyridoacridine alkaloids from Lissoclinum cf. badium that inhibit the ubiquitin ligase activity of Hdm2 and stabilize p53. Bioorg Med Chem 2008 Dec 1; 16 (23): 10022-8.

Clore GM, Ernst J, Clubb R, Omichinski JG, Kennedy WM, Sakaguchi K, et al. Refined solution structure of the oligomerization domain of the tumour suppressor p53. Nat Struct Biol 1995 Apr; 2 (4): 321-33.

Colas P. High-throughput screening assays to discover small-molecule inhibitors of protein interactions. Curr Drug Discov Technol 2008 Sep; 5 (3): 190-9.

Cooks T, Pateras IS, Tarcic O, Solomon H, Schetter AJ, Wilder S, et al. Mutant p53 prolongs NF-kappaB activation and promotes chronic inflammation and inflammation-associated colorectal cancer. Cancer Cell 2013 May 13; 23 (5): 634-46.

Courtois S, Verhaegh G, North S, Luciani MG, Lassus P, Hibner U, et al. DeltaN-p53, a natural isoform of p53 lacking the first transactivation domain, counteracts growth suppression by wild-type p53. Oncogene 2002 Oct 3; 21 (44): 6722-8.

Couturier C, Deprez B. Setting Up a Bioluminescence Resonance Energy Transfer High throughput Screening Assay to Search for Protein/Protein Interaction Inhibitors in Mammalian Cells. Front Endocrinol (Lausanne) 2012; 3: 100.

Creighton CJ, Li X, Landis M, Dixon JM, Neumeister VM, Sjolund A, et al. Residual breast cancers after conventional therapy display mesenchymal as well as tumor-initiating features. Proc Natl Acad Sci U S A 2009 Aug 18; 106 (33): 13820-5.

Czarna A, Popowicz GM, Pecak A, Wolf S, Dubin G, Holak TA. High affinity interaction of the p53 peptide-analogue with human Mdm2 and Mdmx. Cell Cycle 2009 Apr 15; 8 (8): 1176-84.

Dai MS, Lu H. Inhibition of MDM2-mediated p53 ubiquitination and degradation by ribosomal protein L5. J Biol Chem 2004 Oct 22; 279 (43): 44475-82.

Dai MS, Zeng SX, Jin Y, Sun XX, David L, Lu H. Ribosomal protein L23 activates p53 by inhibiting MDM2 function in response to ribosomal perturbation but not to translation inhibition. Mol Cell Biol 2004 Sep; 24 (17): 7654-68.

Danovi D, Meulmeester E, Pasini D, Migliorini D, Capra M, Frenk R, et al. Amplification of Mdmx (or Mdm4) directly contributes to tumor formation by inhibiting p53 tumor suppressor activity. Mol Cell Biol 2004 Jul; 24 (13): 5835-43.

Dearth LR, Qian H, Wang T, Baroni TE, Zeng J, Chen SW, et al. Inactive full-length p53 mutants lacking dominant wild-type p53 inhibition highlight loss of heterozygosity as an important aspect of p53 status in human cancers. Carcinogenesis 2007 Feb; 28 (2): 289-98.

DeLeo AB, Jay G, Appella E, Dubois GC, Law LW, Old LJ. Detection of a transformation-related antigen in chemically induced sarcomas and other transformed cells of the mouse. Proc Natl Acad Sci U S A 1979 May; 76 (5): 2420-4.

Demma M, Maxwell E, Ramos R, Liang L, Li C, Hesk D, et al. SCH529074, a small molecule activator of mutant p53, which binds p53 DNA binding domain (DBD), restores growth-suppressive function to mutant p53 and interrupts HDM2-mediated ubiquitination of wild type p53. J Biol Chem 2010 Apr 2; 285 (14): 10198-212.

DeNardo DG, Andreu P, Coussens LM. Interactions between lymphocytes and myeloid cells regulate pro- versus anti-tumor immunity. Cancer Metastasis Rev 2010 Jun; 29 (2): 309-16.

DeVita VT, Jr., Chu E. A history of cancer chemotherapy. Cancer Res 2008 Nov 1; 68 (21): 8643-53.

Di Como CJ, Gaiddon C, Prives C. p73 function is inhibited by tumor-derived p53 mutants in mammalian cells. Mol Cell Biol 1999 Feb; 19 (2): 1438-49.

Di Ventura B, Funaya C, Antony C, Knop M, Serrano L. Reconstitution of Mdm2-dependent post-translational modifications of p53 in yeast. PLoS One 2008; 3 (1): e1507.

Ding K, Lu Y, Nikolovska-Coleska Z, Wang G, Qiu S, Shangary S, et al. Structure-based design of spiro-oxindoles as potent, specific small-molecule inhibitors of the MDM2-p53 interaction. J Med Chem 2006 Jun 15; 49 (12): 3432-5.

Ding Q, Zhang Z, Liu JJ, Jiang N, Zhang J, Ross TM, et al. Discovery of RG7388, a potent and selective p53-MDM2 inhibitor in clinical development. J Med Chem 2013 Jul 25; 56 (14): 5979-83.

Dittmer D, Pati S, Zambetti G, Chu S, Teresky AK, Moore M, et al. Gain of function mutations in p53. Nat Genet 1993 May; 4 (1): 42-6.

Do PM, Varanasi L, Fan S, Li C, Kubacka I, Newman V, et al. Mutant p53 cooperates with ETS2 to promote etoposide resistance. Genes Dev 2012 Apr 15; 26 (8): 830-45.

Donehower LA, Harvey M, Slagle BL, McArthur MJ, Montgomery CA, Jr., Butel JS, et al. Mice deficient for p53 are developmentally normal but susceptible to spontaneous tumours. Nature 1992 Mar 19; 356 (6366): 215-21.

Dong P, Karaayvaz M, Jia N, Kaneuchi M, Hamada J, Watari H, et al. Mutant p53 gain-of-function induces epithelial-mesenchymal transition through modulation of the miR-130b-ZEB1 axis. Oncogene 2013 Jul 4; 32 (27): 3286-95.

Doyle B, Morton JP, Delaney DW, Ridgway RA, Wilkins JA, Sansom OJ. p53 mutation and loss have different effects on tumourigenesis in a novel mouse model of pleomorphic rhabdomyosarcoma. J Pathol 2010 Oct; 222 (2): 129-37.

Dudgeon DD, Shinde S, Hua Y, Shun TY, Lazo JS, Strock CJ, et al. Implementation of a 220,000-compound HCS campaign to identify disruptors of the interaction between p53 and hDM2 and characterization of the confirmed hits. J Biomol Screen 2010a Aug; 15 (7): 766-82.

Dudgeon DD, Shinde SN, Shun TY, Lazo JS, Strock CJ, Giuliano KA, et al. Characterization and optimization of a novel protein-protein interaction biosensor high-content screening assay to identify disruptors of the interactions between p53 and hDM2. Assay Drug Dev Technol 2010b Aug; 8 (4): 437-58.

Dumay A, Feugeas JP, Wittmer E, Lehmann-Che J, Bertheau P, Espie M, et al. Distinct tumor protein p53 mutants in breast cancer subgroups. Int J Cancer 2013 Mar 1; 132 (5): 1227-31.

Dunkern TR, Wedemeyer I, Baumgartner M, Fritz G, Kaina B. Resistance of p53 knockout cells to doxorubicin is related to reduced formation of DNA strand breaks rather than impaired apoptotic signaling. DNA Repair (Amst) 2003 Jan 2; 2 (1): 49-60.

Edinger AL, Thompson CB. Death by design: apoptosis, necrosis and autophagy. Curr Opin Cell Biol 2004 Dec; 16 (6): 663-9.

el-Deiry WS. Regulation of p53 downstream genes. Semin Cancer Biol 1998; 8 (5): 345-57.

Etienne-Manneville S. Polarity proteins in migration and invasion. Oncogene 2008 Nov 24; 27 (55): 6970-80.

Eyckerman S, Lemmens I, Catteeuw D, Verhee A, Vandekerckhove J, Lievens S, et al. Reverse MAPPIT: screening for protein-protein interaction modifiers in mammalian cells. Nat Methods 2005 Jun; 2 (6): 427-33.

Ferlay J, Soerjomataram I, Dikshit R, Eser S, Mathers C, Rebelo M, et al. Cancer incidence and mortality worldwide: sources, methods and major patterns in GLOBOCAN 2012. Int J Cancer 2015 Mar 1; 136 (5): E359-86.

Ferlay J, Steliarova-Foucher E, Lortet-Tieulent J, Rosso S, Coebergh JW, Comber H, et al. Cancer incidence and mortality patterns in Europe: estimates for 40 countries in 2012. Eur J Cancer 2013 Apr; 49 (6): 1374-403.

Fernandes JC, Borges M, Nascimento H, Bronze-da-Rocha E, Ramos OS, Pintado ME, et al. Cytotoxicity and genotoxicity of chitooligosaccharides upon lymphocytes. Int J Biol Macromol 2011 Oct 1; 49 (3): 433-8.

Fields S, Jang SK. Presence of a potent transcription activating sequence in the p53 protein. Science 1990 Aug 31; 249 (4972): 1046-9.

Fields S, Song O. A novel genetic system to detect protein-protein interactions. Nature 1989 Jul 20; 340 (6230): 245-6.

Flaman JM, Frebourg T, Moreau V, Charbonnier F, Martin C, Chappuis P, et al. A simple p53 functional assay for screening cell lines, blood, and tumors. Proc Natl Acad Sci U S A 1995 Apr 25; 92 (9): 3963-7.

Fleury C, Mignotte B, Vayssiere JL. Mitochondrial reactive oxygen species in cell death signaling. Biochimie 2002 Feb-Mar; 84 (2-3): 131-41.

Foster BA, Coffey HA, Morin MJ, Rastinejad F. Pharmacological rescue of mutant p53 conformation and function. Science 1999 Dec 24; 286 (5449): 2507-10.

Frank AK, Pietsch EC, Dumont P, Tao J, Murphy ME. Wild-type and mutant p53 proteins interact with mitochondrial caspase-3. Cancer Biol Ther 2011 Apr 15; 11 (8): 740-5.

Freedman DA, Epstein CB, Roth JC, Levine AJ. A genetic approach to mapping the p53 binding site in the MDM2 protein. Mol Med 1997 Apr; 3 (4): 248-59.

Freed-Pastor WA, Prives C. Mutant p53: one name, many proteins. Genes Dev 2012 Jun 15; 26 (12): 1268-86.

Froelich-Ammon SJ, Patchan MW, Osheroff N, Thompson RB. Topoisomerase II binds to ellipticine in the absence or presence of DNA. Characterization of enzyme-drug interactions by fluorescence spectroscopy. J Biol Chem 1995 Jun 23; 270 (25): 14998-5004.

Fronza G, Inga A, Monti P, Scott G, Campomenosi P, Menichini P, et al. The yeast p53 functional assay: a new tool for molecular epidemiology. Hopes and facts. Mutat Res 2000 Apr; 462 (2-3): 293-301.

Fu T, Min H, Xu Y, Chen J, Li G. Molecular dynamic simulation insights into the normal state and restoration of p53 function. Int J Mol Sci 2012; 13 (8): 9709-40.

Fujita K, Mondal AM, Horikawa I, Nguyen GH, Kumamoto K, Sohn JJ, et al. p53 isoforms Delta133p53 and p53beta are endogenous regulators of replicative cellular senescence. Nat Cell Biol 2009 Sep; 11 (9): 1135-42.

Fulda S, Gorman AM, Hori O, Samali A. Cellular stress responses: cell survival and cell death. Int J Cell Biol 2010; 2010: 214074.

Gaiddon C, Lokshin M, Ahn J, Zhang T, Prives C. A subset of tumor-derived mutant forms of p53 down-regulate p63 and p73 through a direct interaction with the p53 core domain. Mol Cell Biol 2001 Mar; 21 (5): 1874-87.

Galatin PS, Abraham DJ. A nonpeptidic sulfonamide inhibits the p53-mdm2 interaction and activates p53-dependent transcription in mdm2-overexpressing cells. J Med Chem 2004 Aug 12; 47 (17): 4163-5.

Ganguli G, Abecassis J, Wasylyk B. MDM2 induces hyperplasia and premalignant lesions when expressed in the basal layer of the epidermis. Embo j 2000 Oct 2; 19 (19): 5135-47.

Gembarska A, Luciani F, Fedele C, Russell EA, Dewaele M, Villar S, et al. MDM4 is a key therapeutic target in cutaneous melanoma. Nat Med 2012 Aug; 18 (8): 1239-47.

Gietz RD, Schiestl RH. High-efficiency yeast transformation using the LiAc/SS carrier DNA/PEG method. Nat Protoc 2007; 2 (1): 31-4.

Girardini JE, Marotta C, Del Sal G. Disarming mutant p53 oncogenic function. Pharmacol Res 2014 Jan; 79: 75-87.

Girardini JE, Napoli M, Piazza S, Rustighi A, Marotta C, Radaelli E, et al. A Pin1/mutant p53 axis promotes aggressiveness in breast cancer. Cancer Cell 2011 Jul 12; 20 (1): 79-91.

Gohler T, Jager S, Warnecke G, Yasuda H, Kim E, Deppert W. Mutant p53 proteins bind DNA in a DNA structure-selective mode. Nucleic Acids Res 2005; 33 (3): 1087-100.

Golubovskaya VM, Cance WG. Targeting the p53 pathway. Surg Oncol Clin N Am 2013 Oct; 22 (4): 747-64.

Gonzalez AZ, Eksterowicz J, Bartberger MD, Beck HP, Canon J, Chen A, et al. Selective and potent morpholinone inhibitors of the MDM2-p53 protein-protein interaction. J Med Chem 2014 Mar 27; 57 (6): 2472-88.

Grasberger BL, Lu T, Schubert C, Parks DJ, Carver TE, Koblish HK, et al. Discovery and cocrystal structure of benzodiazepinedione HDM2 antagonists that activate p53 in cells. J Med Chem 2005 Feb 24; 48 (4): 909-12.

Graves B, Thompson T, Xia M, Janson C, Lukacs C, Deo D, et al. Activation of the p53 pathway by small-molecule-induced MDM2 and MDMX dimerization. Proc Natl Acad Sci U S A 2012 Jul 17; 109 (29): 11788-93.

Grossman SR. p300/CBP/p53 interaction and regulation of the p53 response. Eur J Biochem 2001 May; 268 (10): 2773-8.

Grugan KD, Vega ME, Wong GS, Diehl JA, Bass AJ, Wong KK, et al. A common p53 mutation (R175H) activates c-Met receptor tyrosine kinase to enhance tumor cell invasion. Cancer Biol Ther 2013 Sep; 14 (9): 853-9.

Guaragnella N, Palermo V, Galli A, Moro L, Mazzoni C, Giannattasio S. The expanding role of yeast in cancer research and diagnosis: insights into the function of the oncosuppressors p53 and BRCA1/2. FEMS Yeast Res 2014 Feb; 14 (1): 2-16.

Guicciardi ME, Gores GJ. Life and death by death receptors. FASEB J 2009 Jun; 23 (6): 1625-37.

Gurpinar E, Vousden KH. Hitting cancers' weak spots: vulnerabilities imposed by p53 mutation. Trends Cell Biol 2015 Aug; 25 (8): 486-95.

Haber D, Harlow E. Tumour-suppressor genes: evolving definitions in the genomic age. Nat Genet 1997 Aug; 16 (4): 320-2.

Hadj Amor IY, Smaoui K, Chaabene I, Mabrouk I, Djemal L, Elleuch H, et al. Human p53 induces cell death and downregulates thioredoxin expression in Saccharomyces cerevisiae. FEMS Yeast Res 2008 Dec; 8 (8): 1254-62.

Halevy O, Michalovitz D, Oren M. Different tumor-derived p53 mutants exhibit distinct biological activities. Science 1990 Oct 5; 250 (4977): 113-6.

Hanahan D, Weinberg RA. Hallmarks of cancer: the next generation. Cell 2011 Mar 4; 144 (5): 646-74.

Hanahan D, Weinberg RA. The hallmarks of cancer. Cell 2000 Jan 7; 100 (1): 57-70.

Hanel W, Marchenko N, Xu S, Yu SX, Weng W, Moll U. Two hot spot mutant p53 mouse models display differential gain of function in tumorigenesis. Cell Death Differ 2013 Jul; 20 (7): 898-909.

Hardcastle IR, Ahmed SU, Atkins H, Farnie G, Golding BT, Griffin RJ, et al. Small-molecule inhibitors of the MDM2-p53 protein-protein interaction based on an isoindolinone scaffold. J Med Chem 2006 Oct 19; 49 (21): 6209-21.

Hardcastle IR, Liu J, Valeur E, Watson A, Ahmed SU, Blackburn TJ, et al. Isoindolinone inhibitors of the murine double minute 2 (MDM2)-p53 protein-protein interaction: structure-activity studies leading to improved potency. J Med Chem 2011 Mar 10; 54 (5): 1233-43.

Harms K, Nozell S, Chen X. The common and distinct target genes of the p53 family transcription factors. Cell Mol Life Sci 2004 Apr; 61 (7-8): 822-42.

Hassan NM, Tada M, Hamada J, Kashiwazaki H, Kameyama T, Akhter R, et al. Presence of dominant negative mutation of TP53 is a risk of early recurrence in oral cancer. Cancer Lett 2008 Oct 18; 270 (1): 108-19.

Hay M, Thomas DW, Craighead JL, Economides C, Rosenthal J. Clinical development success rates for investigational drugs. Nat Biotechnol 2014 Jan; 32 (1): 40-51.

Hermeking H, Lengauer C, Polyak K, He TC, Zhang L, Thiagalingam S, et al. 14-3-3 sigma is a p53-regulated inhibitor of G2/M progression. Mol Cell 1997 Dec; 1 (1): 3-11.

Hiraki M, Hwang SY, Cao S, Ramadhar TR, Byun S, Yoon KW, et al. Small-Molecule Reactivation of Mutant p53 to Wild-Type-like p53 through the p53-Hsp40 Regulatory Axis. Chem Biol 2015 Sep 17; 22 (9): 1206-16.

Hoffman WH, Biade S, Zilfou JT, Chen J, Murphy M. Transcriptional repression of the anti-apoptotic survivin gene by wild type p53. J Biol Chem 2002 Feb 1; 277 (5): 3247-57.

Hofstetter G, Berger A, Berger R, Zoric A, Braicu EI, Reimer D, et al. The N-terminally truncated p53 isoform Delta40p53 influences prognosis in mucinous ovarian cancer. Int J Gynecol Cancer 2012 Mar; 22 (3): 372-9.

Hofstetter G, Berger A, Schuster E, Wolf A, Hager G, Vergote I, et al. Delta133p53 is an independent prognostic marker in p53 mutant advanced serous ovarian cancer. Br J Cancer 2011 Nov 8; 105 (10): 1593-9.

Holzer P, Masuya K, Furet P, Kallen J, Valat-Stachyra T, Ferretti S, et al. Discovery of a Dihydroisoquinolinone Derivative (NVP-CGM097): A Highly Potent and Selective MDM2 Inhibitor Undergoing Phase 1 Clinical Trials in p53wt Tumors. J Med Chem 2015 Aug 27; 58 (16): 6348-58.

Honda R, Yasuda H. Association of p19(ARF) with Mdm2 inhibits ubiquitin ligase activity of Mdm2 for tumor suppressor p53. EMBO J 1999 Jan 4; 18 (1): 22-7.

Hong B, van den Heuvel AP, Prabhu VV, Zhang S, El-Deiry WS. Targeting tumor suppressor p53 for cancer therapy: strategies, challenges and opportunities. Curr Drug Targets 2014 Jan; 15 (1): 80-9.

Hu B, Gilkes DM, Chen J. Efficient p53 activation and apoptosis by simultaneous disruption of binding to MDM2 and MDMX. Cancer Res 2007 Sep 15; 67 (18): 8810-7.

Hu B, Gilkes DM, Farooqi B, Sebti SM, Chen J. MDMX overexpression prevents p53 activation by the MDM2 inhibitor Nutlin. J Biol Chem 2006 Nov 3; 281 (44): 33030-5.

Huang L, Yan Z, Liao X, Li Y, Yang J, Wang ZG, et al. The p53 inhibitors MDM2/MDMX complex is required for control of p53 activity in vivo. Proc Natl Acad Sci U S A 2011 Jul 19; 108 (29): 12001-6.

Inga A, Storici F, Darden TA, Resnick MA. Differential transactivation by the p53 transcription factor is highly dependent on p53 level and promoter target sequence. Mol Cell Biol 2002 Dec; 22 (24): 8612-25.

Ishioka C, Frebourg T, Yan YX, Vidal M, Friend SH, Schmidt S, et al. Screening patients for heterozygous p53 mutations using a functional assay in yeast. Nat Genet 1993 Oct; 5 (2): 124-9.

Issaeva N, Bozko P, Enge M, Protopopova M, Verhoef LG, Masucci M, et al. Small molecule RITA binds to p53, blocks p53-HDM-2 interaction and activates p53 function in tumors. Nat Med 2004 Dec; 10 (12): 1321-8.

Iwabuchi K, Li B, Bartel P, Fields S. Use of the two-hybrid system to identify the domain of p53 involved in oligomerization. Oncogene 1993 Jun; 8 (6): 1693-6.

Iwakuma T, Lozano G. MDM2, an introduction. Mol Cancer Res 2003 Dec; 1 (14): 993-1000.

Jeffrey PD, Gorina S, Pavletich NP. Crystal structure of the tetramerization domain of the p53 tumor suppressor at 1.7 angstroms. Science 1995 Mar 10; 267 (5203): 1498-502.

Jin Z, El-Deiry WS. Overview of cell death signaling pathways. Cancer Biol Ther 2005 Feb; 4 (2): 139-63.

Jin ZJ. [Addition in drug combination (author's transl)]. Zhongguo Yao Li Xue Bao 1980 Dec; 1 (2): 70-6.

Johnson WD, Muzzio M, Detrisac CJ, Kapetanovic IM, Kopelovich L, McCormick DL. Subchronic oral toxicity and metabolite profiling of the p53 stabilizing agent, CP-31398, in rats and dogs. Toxicology 2011 Nov 18; 289 (2-3): 141-50.

Jones SN, Hancock AR, Vogel H, Donehower LA, Bradley A. Overexpression of Mdm2 in mice reveals a p53-independent role for Mdm2 in tumorigenesis. Proc Natl Acad Sci U S A 1998 Dec 22; 95 (26): 15608-12.

Jones SN, Roe AE, Donehower LA, Bradley A. Rescue of embryonic lethality in Mdm2-deficient mice by absence of p53. Nature 1995 Nov 9; 378 (6553): 206-8.

Kaghad M, Bonnet H, Yang A, Creancier L, Biscan JC, Valent A, et al. Monoallelically expressed gene related to p53 at 1p36, a region frequently deleted in neuroblastoma and other human cancers. Cell 1997 Aug 22; 90 (4): 809-19.

Kakudo Y, Shibata H, Otsuka K, Kato S, Ishioka C. Lack of correlation between p53-dependent transcriptional activity and the ability to induce apoptosis among 179 mutant p53s. Cancer Res 2005 Mar 15; 65 (6): 2108-14.

Kallen J, Goepfert A, Blechschmidt A, Izaac A, Geiser M, Tavares G, et al. Crystal Structures of Human MdmX (HdmX) in Complex with p53 Peptide Analogues Reveal Surprising Conformational Changes. J Biol Chem 2009 Mar 27; 284 (13): 8812-21.

Kandoth C, McLellan MD, Vandin F, Ye K, Niu B, Lu C, et al. Mutational landscape and significance across 12 major cancer types. Nature 2013 Oct 17; 502 (7471): 333-9.

Kato S, Han SY, Liu W, Otsuka K, Shibata H, Kanamaru R, et al. Understanding the function-structure and function-mutation relationships of p53 tumor suppressor protein by high-resolution missense mutation analysis. Proc Natl Acad Sci U S A 2003 Jul 8; 100 (14): 8424-9.

Kawaguchi T, Kato S, Otsuka K, Watanabe G, Kumabe T, Tominaga T, et al. The relationship among p53 oligomer formation, structure and transcriptional activity using a comprehensive missense mutation library. Oncogene 2005 Oct 20; 24 (46): 6976-81.

Kelland L. The resurgence of platinum-based cancer chemotherapy. Nat Rev Cancer 2007 Aug; 7 (8): 573-84.

Khoo KH, Verma CS, Lane DP. Drugging the p53 pathway: understanding the route to clinical efficacy. Nat Rev Drug Discov 2014 Mar; 13 (3): 217-36.

Khromova NV, Kopnin PB, Stepanova EV, Agapova LS, Kopnin BP. p53 hot-spot mutants increase tumor vascularization via ROS-mediated activation of the HIF1/VEGF-A pathway. Cancer Lett 2009 Apr 18; 276 (2): 143-51.

Khuri FR, Nemunaitis J, Ganly I, Arseneau J, Tannock IF, Romel L, et al. a controlled trial of intratumoral ONYX-015, a selectively-replicating adenovirus, in combination with cisplatin and 5-fluorouracil in patients with recurrent head and neck cancer. Nat Med 2000 Aug; 6 (8): 879-85.

Kimura T, Gotoh M, Nakamura Y, Arakawa H. hCDC4b, a regulator of cyclin E, as a direct transcriptional target of p53. Cancer Sci 2003 May; 94 (5): 431-6.

Koblish HK, Zhao S, Franks CF, Donatelli RR, Tominovich RM, LaFrance LV, et al. Benzodiazepinedione inhibitors of the Hdm2:p53 complex suppress human tumor cell proliferation in vitro and sensitize tumors to doxorubicin in vivo. Mol Cancer Ther 2006 Jan; 5 (1): 160-9.

Korn K, Krausz E. Cell-based high-content screening of small-molecule libraries. Curr Opin Chem Biol 2007 Oct; 11 (5): 503-10.

Kortlever RM, Higgins PJ, Bernards R. Plasminogen activator inhibitor-1 is a critical downstream target of p53 in the induction of replicative senescence. Nat Cell Biol 2006 Aug; 8 (8): 877-84.

Koster R, Timmer-Bosscha H, Bischoff R, Gietema JA, de Jong S. Disruption of the MDM2-p53 interaction strongly potentiates p53-dependent apoptosis in cisplatin-resistant human testicular carcinoma cells via the Fas/FasL pathway. Cell Death Dis 2011; 2: e148.

Kracikova M, Akiri G, George A, Sachidanandam R, Aaronson SA. A threshold mechanism mediates p53 cell fate decision between growth arrest and apoptosis. Cell Death Differ 2013 Apr; 20 (4): 576-88.

Krajewski M, Ozdowy P, D'Silva L, Rothweiler U, Holak TA. NMR indicates that the small molecule RITA does not block p53-MDM2 binding in vitro. Nat Med 2005 Nov; 11 (11): 1135-6; author reply 6-7.

Kranz D, Dobbelstein M. Nongenotoxic p53 activation protects cells against S-phase-specific chemotherapy. Cancer Res 2006 Nov 1; 66 (21): 10274-80.

Krause K, Wasner M, Reinhard W, Haugwitz U, Dohna CL, Mossner J, et al. The tumour suppressor protein p53 can repress transcription of cyclin B. Nucleic Acids Res 2000 Nov 15; 28 (22): 4410-8.

Kravchenko JE, Ilyinskaya GV, Komarov PG, Agapova LS, Kochetkov DV, Strom E, et al. Small-molecule RETRA suppresses mutant p53-bearing cancer cells through a p73-dependent salvage pathway. Proc Natl Acad Sci U S A 2008 Apr 29; 105 (17): 6302-7.

Kreipe HH, von Wasielewski R. Beyond typing and grading: target analysis in individualized therapy as a new challenge for tumour pathology. Recent Results Cancer Res 2007; 176: 3-6.

Labelle-Cote M, Dusseault J, Ismail S, Picard-Cloutier A, Siegel PM, Larose L. Nck2 promotes human melanoma cell proliferation, migration and invasion in vitro and primary melanoma-derived tumor growth in vivo. BMC Cancer 2011; 11: 443.

Lain S, Hollick JJ, Campbell J, Staples OD, Higgins M, Aoubala M, et al. Discovery, in vivo activity, and mechanism of action of a small-molecule p53 activator. Cancer Cell 2008 May; 13 (5): 454-63.

Lambert JM, Gorzov P, Veprintsev DB, Soderqvist M, Segerback D, Bergman J, et al. PRIMA-1 reactivates mutant p53 by covalent binding to the core domain. Cancer Cell 2009 May 5; 15 (5): 376-88.

Lane DP, Crawford LV. T antigen is bound to a host protein in SV40-transformed cells. Nature 1979 Mar 15; 278 (5701): 261-3.

Lane DP. Cancer. p53, guardian of the genome. Nature 1992 Jul 2; 358 (6381): 15-6.

Lang GA, Iwakuma T, Suh YA, Liu G, Rao VA, Parant JM, et al. Gain of function of a p53 hot spot mutation in a mouse model of Li-Fraumeni syndrome. Cell 2004 Dec 17; 119 (6): 861-72.

Lau LM, Nugent JK, Zhao X, Irwin MS. HDM2 antagonist Nutlin-3 disrupts p73-HDM2 binding and enhances p73 function. Oncogene 2008 Feb 7; 27 (7): 997-1003.

Lauria A, Tutone M, Ippolito M, Pantano L, Almerico AM. Molecular modeling approaches in the discovery of new drugs for anti-cancer therapy: the investigation of p53-MDM2 interaction and its inhibition by small molecules. Curr Med Chem 2010; 17 (28): 3142-54.

Laurie NA, Donovan SL, Shih CS, Zhang J, Mills N, Fuller C, et al. Inactivation of the p53 pathway in retinoblastoma. Nature 2006 Nov 2; 444 (7115): 61-6.

Le MT, Teh C, Shyh-Chang N, Xie H, Zhou B, Korzh V, et al. MicroRNA-125b is a novel negative regulator of p53. Genes Dev 2009 Apr 1; 23 (7): 862-76.

Lea WA, Simeonov A. Fluorescence polarization assays in small molecule screening. Expert Opin Drug Discov 2011 Jan; 6 (1): 17-32.

Leão M, Gomes S, Bessa C, Soares J, Raimundo L, Monti P, et al. Studying p53 family proteins in yeast: induction of autophagic cell death and modulation by interactors and small molecules. Exp Cell Res 2015a Jan 1; 330 (1): 164-77.

Leão M, Gomes S, Pedraza-Chaverri J, Machado N, Sousa E, Pinto M, et al. Alpha-mangostin and gambogic acid as potential inhibitors of the p53-MDM2 interaction revealed by a yeast approach. J Nat Prod 2013a Apr 26; 76 (4): 774-8.

Leão M, Gomes S, Soares J, Bessa C, Maciel C, Ciribilli Y, et al. Novel simplified yeast-based assays of regulators of p53-MDMX interaction and p53 transcriptional activity. FEBS J 2013b Dec; 280 (24): 6498-507.

Leão M, Pereira C, Bisio A, Ciribilli Y, Paiva AM, Machado N, et al. Discovery of a new small-molecule inhibitor of p53-MDM2 interaction using a yeast-based approach. Biochem Pharmacol 2013c May 1; 85 (9): 1234-45.

Leão M, Soares J, Gomes S, Raimundo L, Ramos H, Bessa C, et al. Enhanced cytotoxicity of prenylated chalcone against tumour cells via disruption of the p53-MDM2 interaction. Life Sci 2015b Dec 1; 142: 60-5.

Lee JH, Zhang Q, Jo S, Chai SC, Oh M, Im W, et al. Novel pyrrolopyrimidine-based alpha-helix mimetics: cell-permeable inhibitors of protein-protein interactions. J Am Chem Soc 2011 Feb 2; 133 (4): 676-9.

Lee JT, Gu W. The multiple levels of regulation by p53 ubiquitination. Cell Death Differ 2010 Jan; 17 (1): 86-92.

Lehmann S, Bykov VJ, Ali D, Andren O, Cherif H, Tidefelt U, et al. Targeting p53 in vivo: a first-in-human study with p53-targeting compound APR-246 in refractory hematologic malignancies and prostate cancer. J Clin Oncol 2012 Oct 10; 30 (29): 3633-9.

Leroy B, Anderson M, Soussi T. TP53 mutations in human cancer: database reassessment and prospects for the next decade. Hum Mutat 2014 Jun; 35 (6): 672-88.

Leroy B, Fournier JL, Ishioka C, Monti P, Inga A, Fronza G, et al. The TP53 website: an integrative resource centre for the TP53 mutation database and TP53 mutant analysis. Nucleic Acids Res 2013 Jan; 41 (Database issue): D962-9.

Levine AJ, Oren M. The first 30 years of p53: growing ever more complex. Nat Rev Cancer 2009 Oct; 9 (10): 749-58.

Li B, Cheng Q, Li Z, Chen J. p53 inactivation by MDM2 and MDMX negative feedback loops in testicular germ cell tumors. Cell Cycle 2010a Apr 1; 9 (7): 1411-20.

Li C, Pazgier M, Li C, Yuan W, Liu M, Wei G, et al. Systematic mutational analysis of peptide inhibition of the p53-MDM2/MDMX interactions. J Mol Biol 2010b Apr 30; 398 (2): 200-13.

Li D, Marchenko ND, Moll UM. SAHA shows preferential cytotoxicity in mutant p53 cancer cells by destabilizing mutant p53 through inhibition of the HDAC6-Hsp90 chaperone axis. Cell Death Differ 2011a Dec; 18 (12): 1904-13.

Li D, Marchenko ND, Schulz R, Fischer V, Velasco-Hernandez T, Talos F, et al. Functional inactivation of endogenous MDM2 and CHIP by HSP90 causes aberrant stabilization of mutant p53 in human cancer cells. Mol Cancer Res 2011b May; 9 (5): 577-88.

Li J, Zhang S, Gao L, Chen Y, Xie X. A cell-based high-throughput assay for the screening of small-molecule inhibitors of p53-MDM2 interaction. J Biomol Screen 2011c Apr; 16 (4): 450-6.

Li Q, Lozano G. Molecular pathways: targeting Mdm2 and Mdm4 in cancer therapy. Clin Cancer Res 2013 Jan 1; 19 (1): 34-41.

Liang SH, Clarke MF. A bipartite nuclear localization signal is required for p53 nuclear import regulated by a carboxyl-terminal domain. J Biol Chem 1999 Nov 12; 274 (46): 32699-703.

Licitra EJ, Liu JO. A three-hybrid system for detecting small ligand-protein receptor interactions. Proc Natl Acad Sci U S A 1996 Nov 12; 93 (23): 12817-21.

Lin J, Teresky AK, Levine AJ. Two critical hydrophobic amino acids in the N-terminal domain of the p53 protein are required for the gain of function phenotypes of human p53 mutants. Oncogene 1995 Jun 15; 10 (12): 2387-90.

Linzer DI, Levine AJ. Characterization of a 54K dalton cellular SV40 tumor antigen present in SV40-transformed cells and uninfected embryonal carcinoma cells. Cell 1979 May; 17 (1): 43-52.

Lion M, Bisio A, Tebaldi T, De Sanctis V, Menendez D, Resnick MA, et al. Interaction between p53 and estradiol pathways in transcriptional responses to chemotherapeutics. Cell Cycle 2013 Apr 15; 12 (8): 1211-24.

Liu J, Zhang C, Feng Z. Tumor suppressor p53 and its gain-of-function mutants in cancer. Acta Biochim Biophys Sin (Shanghai) 2014a Mar; 46 (3): 170-9.

Liu JF, Konstantinopoulos PA, Matulonis UA. PARP inhibitors in ovarian cancer: current status and future promise. Gynecol Oncol 2014b May; 133 (2): 362-9.

Liu X, Wilcken R, Joerger AC, Chuckowree IS, Amin J, Spencer J, et al. Small molecule induced reactivation of mutant p53 in cancer cells. Nucleic Acids Res 2013 Jul; 41 (12): 6034-44.

Lobo NA, Shimono Y, Qian D, Clarke MF. The biology of cancer stem cells. Annu Rev Cell Dev Biol 2007; 23: 675-99.

Lohrum MA, Ludwig RL, Kubbutat MH, Hanlon M, Vousden KH. Regulation of HDM2 activity by the ribosomal protein L11. Cancer Cell 2003 Jun; 3 (6): 577-87.

Lu H, Levine AJ. Human TAFII31 protein is a transcriptional coactivator of the p53 protein. Proc Natl Acad Sci U S A 1995 May 23; 92 (11): 5154-8.

Lu Y, Nikolovska-Coleska Z, Fang X, Gao W, Shangary S, Qiu S, et al. Discovery of a nanomolar inhibitor of the human murine double minute 2 (MDM2)-p53 interaction through an integrated, virtual database screening strategy. J Med Chem 2006 Jun 29; 49 (13): 3759-62.

Lucas BS, Fisher B, McGee LR, Olson SH, Medina JC, Cheung E. An expeditious synthesis of the MDM2-p53 inhibitor AM-8553. J Am Chem Soc 2012 Aug 1; 134 (30): 12855-60.

Luo J, Solimini NL, Elledge SJ. Principles of cancer therapy: oncogene and non-oncogene addiction. Cell 2009 Mar 6; 136 (5): 823-37.

Ma CX, Cai S, Li S, Ryan CE, Guo Z, Schaiff WT, et al. Targeting Chk1 in p53-deficient triple-negative breast cancer is therapeutically beneficial in human-in-mouse tumor models. J Clin Invest 2012 Apr; 122 (4): 1541-52.

MacLachlan TK, El-Deiry WS. Apoptotic threshold is lowered by p53 transactivation of caspase-6. Proc Natl Acad Sci U S A 2002 Jul 9; 99 (14): 9492-7.

Maddocks OD, Vousden KH. Metabolic regulation by p53. J Mol Med (Berl) 2011 Mar; 89 (3): 237-45.

Maeda S, Shinchi H, Kurahara H, Mataki Y, Noma H, Maemura K, et al. Clinical significance of midkine expression in pancreatic head carcinoma. Br J Cancer 2007 Aug 6; 97 (3): 405-11.

Malkin D. p53 and the Li-Fraumeni syndrome. Cancer Genet Cytogenet 1993 Apr; 66 (2): 83-92.

Mantovani A. Molecular pathways linking inflammation and cancer. Curr Mol Med 2010 Jun; 10 (4): 369-73.

Marcel V, Dichtel-Danjoy ML, Sagne C, Hafsi H, Ma D, Ortiz-Cuaran S, et al. Biological functions of p53 isoforms through evolution: lessons from animal and cellular models. Cell Death Differ 2011 Dec; 18 (12): 1815-24.

Marchenko ND, Moll UM. The role of ubiquitination in the direct mitochondrial death program of p53. Cell Cycle 2007 Jul 15; 6 (14): 1718-23.

Marchenko ND, Wolff S, Erster S, Becker K, Moll UM. Monoubiquitylation promotes mitochondrial p53 translocation. EMBO J 2007 Feb 21; 26 (4): 923-34.

Martinez JD. Restoring p53 tumor suppressor activity as an anticancer therapeutic strategy. Future Oncol 2010 Dec; 6 (12): 1857-62.

Martins CP, Brown-Swigart L, Evan GI. Modeling the therapeutic efficacy of p53 restoration in tumors. Cell 2006 Dec 29; 127 (7): 1323-34.

Marutani M, Tonoki H, Tada M, Takahashi M, Kashiwazaki H, Hida Y, et al. Dominant-negative mutations of the tumor suppressor p53 relating to early onset of glioblastoma multiforme. Cancer Res 1999 Oct 1; 59 (19): 4765-9.

Mazars A, Fahraeus R. Using BRET to study chemical compound-induced disruptions of the p53-HDM2 interactions in live cells. Biotechnol J 2010 Apr; 5 (4): 377-84.

Michael D, Oren M. The p53-Mdm2 module and the ubiquitin system. Semin Cancer Biol 2003 Feb; 13 (1): 49-58.

Millau JF, Bastien N, Drouin R. P53 transcriptional activities: a general overview and some thoughts. Mutat Res 2009 Mar-Jun; 681 (2-3): 118-33.

Minotti G, Menna P, Salvatorelli E, Cairo G, Gianni L. Anthracyclines: molecular advances and pharmacologic developments in antitumor activity and cardiotoxicity. Pharmacol Rev 2004 Jun; 56 (2): 185-229.

Mittl PR, Chene P, Grutter MG. Crystallization and structure solution of p53 (residues 326-356) by molecular replacement using an NMR model as template. Acta Crystallogr D Biol Crystallogr 1998 Jan 1; 54 (Pt 1): 86-9.

Mohammad RM, Wu J, Azmi AS, Aboukameel A, Sosin A, Wu S, et al. An MDM2 antagonist (MI-319) restores p53 functions and increases the life span of orally treated follicular lymphoma bearing animals. Mol Cancer 2009; 8: 115.

Moll UM, Slade N. p63 and p73: roles in development and tumor formation. Mol Cancer Res 2004 Jul; 2 (7): 371-86.

Mollereau B, Ma D. The p53 control of apoptosis and proliferation: lessons from Drosophila. Apoptosis 2014 Oct; 19 (10): 1421-9.

Momand J, Zambetti GP, Olson DC, George D, Levine AJ. The mdm-2 oncogene product forms a complex with the p53 protein and inhibits p53-mediated transactivation. Cell 1992 Jun 26; 69 (7): 1237-45.

Monti P, Foggetti G, Menichini P, Inga A, Gold B, Fronza G. Comparison of the biological effects of MMS and Me-lex, a minor groove methylating agent: clarifying the role of N3-methyladenine. Mutat Res 2014 Jan; 759: 45-51.

Monti P, Perfumo C, Bisio A, Ciribilli Y, Menichini P, Russo D, et al. Dominant-negative features of mutant TP53 in germline carriers have limited impact on cancer outcomes. Mol Cancer Res 2011 Mar; 9 (3): 271-9.

Moroni MC, Hickman ES, Lazzerini Denchi E, Caprara G, Colli E, Cecconi F, et al. Apaf-1 is a transcriptional target for E2F and p53. Nat Cell Biol 2001 Jun; 3 (6): 552-8.

Morton JP, Timpson P, Karim SA, Ridgway RA, Athineos D, Doyle B, et al. Mutant p53 drives metastasis and overcomes growth arrest/senescence in pancreatic cancer. Proc Natl Acad Sci U S A 2010 Jan 5; 107 (1): 246-51.

Muller PA, Caswell PT, Doyle B, Iwanicki MP, Tan EH, Karim S, et al. Mutant p53 drives invasion by promoting integrin recycling. Cell 2009 Dec 24; 139 (7): 1327-41.

Muller PA, Trinidad AG, Timpson P, Morton JP, Zanivan S, van den Berghe PV, et al. Mutant p53 enhances MET trafficking and signalling to drive cell scattering and invasion. Oncogene 2013 Mar 7; 32 (10): 1252-65.

Muller PA, Vousden KH, Norman JC. p53 and its mutants in tumor cell migration and invasion. J Cell Biol 2011 Jan 24; 192 (2): 209-18.

Muller PA, Vousden KH. Mutant p53 in cancer: new functions and therapeutic opportunities. Cancer Cell 2014 Mar 17; 25 (3): 304-17.

Murdoch C, Muthana M, Coffelt SB, Lewis CE. The role of myeloid cells in the promotion of tumour angiogenesis. Nat Rev Cancer 2008 Aug; 8 (8): 618-31.

Murray-Zmijewski F, Lane DP, Bourdon JC. p53/p63/p73 isoforms: an orchestra of isoforms to harmonise cell differentiation and response to stress. Cell Death Differ 2006 Jun; 13 (6): 962-72.

Nag S, Qin J, Srivenugopal KS, Wang M, Zhang R. The MDM2-p53 pathway revisited. J Biomed Res 2013 Jul; 27 (4): 254-71.

Neochoritis CG, Wang K, Estrada-Ortiz N, Herdtweck E, Kubica K, Twarda A, et al. 2,3'-Bis(1'H-indole) heterocycles: New p53/MDM2/MDMX antagonists. Bioorg Med Chem Lett 2015 Nov 7.

Nghiem P, Park PK, Kim Y, Vaziri C, Schreiber SL. ATR inhibition selectively sensitizes G1 checkpoint-deficient cells to lethal premature chromatin condensation. Proc Natl Acad Sci U S A 2001 Jul 31; 98 (16): 9092-7.

Nigro JM, Sikorski R, Reed SI, Vogelstein B. Human p53 and CDC2Hs genes combine to inhibit the proliferation of Saccharomyces cerevisiae. Mol Cell Biol 1992 Mar; 12 (3): 1357-65.

North S, Pluquet O, Maurici D, El-Ghissassi F, Hainaut P. Restoration of wild-type conformation and activity of a temperature-sensitive mutant of p53 (p53(V272M)) by

the cytoprotective aminothiol WR1065 in the esophageal cancer cell line TE-1. Mol Carcinog 2002 Mar; 33 (3): 181-8.

Nurse P. A long twentieth century of the cell cycle and beyond. Cell 2000 Jan 7; 100 (1): 71-8.

Oda K, Arakawa H, Tanaka T, Matsuda K, Tanikawa C, Mori T, et al. p53AIP1, a potential mediator of p53-dependent apoptosis, and its regulation by Ser-46-phosphorylated p53. Cell 2000 Sep 15; 102 (6): 849-62.

Ofir-Rosenfeld Y, Boggs K, Michael D, Kastan MB, Oren M. Mdm2 regulates p53 mRNA translation through inhibitory interactions with ribosomal protein L26. Mol Cell 2008 Oct 24; 32 (2): 180-9.

Ohki R, Nemoto J, Murasawa H, Oda E, Inazawa J, Tanaka N, et al. Reprimo, a new candidate mediator of the p53-mediated cell cycle arrest at the G2 phase. J Biol Chem 2000 Jul 28; 275 (30): 22627-30.

Olive KP, Tuveson DA, Ruhe ZC, Yin B, Willis NA, Bronson RT, et al. Mutant p53 gain of function in two mouse models of Li-Fraumeni syndrome. Cell 2004 Dec 17; 119 (6): 847-60.

Olivier M, Hollstein M, Hainaut P. TP53 mutations in human cancers: origins, consequences, and clinical use. Cold Spring Harb Perspect Biol 2010 Jan; 2 (1): a001008.

Olivier M, Hussain SP, Caron de Fromentel C, Hainaut P, Harris CC. TP53 mutation spectra and load: a tool for generating hypotheses on the etiology of cancer. IARC Sci Publ 2004; (157): 247-70.

Oren M, Rotter V. Mutant p53 gain-of-function in cancer. Cold Spring Harb Perspect Biol 2010 Feb; 2 (2): a001107.

Otsuka K, Ochiya T. Genetic networks lead and follow tumor development: microRNA regulation of cell cycle and apoptosis in the p53 pathways. Biomed Res Int 2014; 2014: 749724.

Pal S, Datta K, Mukhopadhyay D. Central role of p53 on regulation of vascular permeability factor/vascular endothelial growth factor (VPF/VEGF) expression in mammary carcinoma. Cancer Res 2001 Sep 15; 61 (18): 6952-7.

Pan JJ, Zhang SW, Chen CB, Xiao SW, Sun Y, Liu CQ, et al. Effect of recombinant adenovirus-p53 combined with radiotherapy on long-term prognosis of advanced nasopharyngeal carcinoma. J Clin Oncol 2009 Feb 10; 27 (5): 799-804.

Pant V, Xiong S, Iwakuma T, Quintas-Cardama A, Lozano G. Heterodimerization of Mdm2 and Mdm4 is critical for regulating p53 activity during embryogenesis but dispensable

for p53 and Mdm2 stability. Proc Natl Acad Sci U S A 2011 Jul 19; 108 (29): 11995-2000.

Parant J, Chavez-Reyes A, Little NA, Yan W, Reinke V, Jochemsen AG, et al. Rescue of embryonic lethality in Mdm4-null mice by loss of Trp53 suggests a nonoverlapping pathway with MDM2 to regulate p53. Nat Genet 2001 Sep; 29 (1): 92-5.

Parks DJ, LaFrance LV, Calvo RR, Milkiewicz KL, Marugan JJ, Raboisson P, et al. Enhanced pharmacokinetic properties of 1,4-benzodiazepine-2,5-dione antagonists of the HDM2-p53 protein-protein interaction through structure-based drug design. Bioorg Med Chem Lett 2006 Jun 15; 16 (12): 3310-4.

Patil SP, Pacitti MF, Gilroy KS, Ruggiero JC, Griffin JD, Butera JJ, et al. Identification of antipsychotic drug fluspirilene as a potential p53-MDM2 inhibitor: a combined computational and experimental study. J Comput Aided Mol Des 2015 Feb; 29 (2): 155-63.

Patton JT, Mayo LD, Singhi AD, Gudkov AV, Stark GR, Jackson MW. Levels of HdmX expression dictate the sensitivity of normal and transformed cells to Nutlin-3. Cancer Res 2006 Mar 15; 66 (6): 3169-76.

Pazgier M, Liu M, Zou G, Yuan W, Li C, Li C, et al. Structural basis for high-affinity peptide inhibition of p53 interactions with MDM2 and MDMX. Proc Natl Acad Sci U S A 2009 Mar 24; 106 (12): 4665-70.

Pereira C, Coutinho I, Soares J, Bessa C, Leao M, Saraiva L. New insights into cancer-related proteins provided by the yeast model. FEBS J 2012a Mar; 279 (5): 697-712.

Pereira C, Leao M, Soares J, Bessa C, Saraiva L. New therapeutic strategies for cancer and neurodegeneration emerging from yeast cell-based systems. Curr Pharm Des 2012b; 18 (27): 4223-35.

Pereira NA, Monteiro A, Machado M, Gut J, Molins E, Perry MJ, et al. Enantiopure Indolizinoindolones with in vitro Activity against Blood- and Liver-Stage Malaria Parasites. ChemMedChem 2015 Dec; 10 (12): 2080-9.

Pereira NA, Sureda FX, Esplugas R, Perez M, Amat M, Santos MM. Tryptophanol-derived oxazolopiperidone lactams: identification of a hit compound as NMDA receptor antagonist. Bioorg Med Chem Lett 2014 Aug 1; 24 (15): 3333-6.

Pereira NAL, Sureda FX, Turch M, Amat M, Bosch J, Santos MMM. Synthesis of phenylalaninol-derived oxazolopyrrolidone lactams and evaluation as NMDA receptor antagonists. Monatshefte für Chemie - Chemical Monthly 2013; 144 (4): 473-7.

Petitjean A, Achatz MI, Borresen-Dale AL, Hainaut P, Olivier M. TP53 mutations in human cancers: functional selection and impact on cancer prognosis and outcomes. Oncogene 2007a Apr 2; 26 (15): 2157-65.

Petitjean A, Mathe E, Kato S, Ishioka C, Tavtigian SV, Hainaut P, et al. Impact of mutant p53 functional properties on TP53 mutation patterns and tumor phenotype: lessons from recent developments in the IARC TP53 database. Hum Mutat 2007b Jun; 28 (6): 622-9.

Phillips A, Teunisse A, Lam S, Lodder K, Darley M, Emaduddin M, et al. HDMX-L is expressed from a functional p53-responsive promoter in the first intron of the HDMX gene and participates in an autoregulatory feedback loop to control p53 activity. J Biol Chem 2010 Sep 17; 285 (38): 29111-27.

Polyak K, Xia Y, Zweier JL, Kinzler KW, Vogelstein B. A model for p53-induced apoptosis. Nature 1997 Sep 18; 389 (6648): 300-5.

Popowicz GM, Czarna A, Wolf S, Wang K, Wang W, Domling A, et al. Structures of low molecular weight inhibitors bound to MDMX and MDM2 reveal new approaches for p53-MDMX/MDM2 antagonist drug discovery. Cell Cycle 2010 Mar 15; 9 (6): 1104-11.

Powell E, Piwnica-Worms D, Piwnica-Worms H. Contribution of p53 to metastasis. Cancer Discov 2014 Apr; 4 (4): 405-14.

Puzio-Kuter AM. The Role of p53 in Metabolic Regulation. Genes Cancer 2011 Apr; 2 (4): 385-91.

Qian BZ, Pollard JW. Macrophage diversity enhances tumor progression and metastasis. Cell 2010 Apr 2; 141 (1): 39-51.

Qian Y, Chen X. Senescence regulation by the p53 protein family. Methods Mol Biol 2013; 965: 37-61.

Qin G, Kishore R, Dolan CM, Silver M, Wecker A, Luedemann CN, et al. Cell cycle regulator E2F1 modulates angiogenesis via p53-dependent transcriptional control of VEGF. Proc Natl Acad Sci U S A 2006 Jul 18; 103 (29): 11015-20.

Qin L, Yang F, Zhou C, Chen Y, Zhang H, Su Z. Efficient reactivation of p53 in cancer cells by a dual MdmX/Mdm2 inhibitor. J Am Chem Soc 2014 Dec 31; 136 (52): 18023-33.

Quante T, Otto B, Brazdova M, Kejnovska I, Deppert W, Tolstonog GV. Mutant p53 is a transcriptional co-factor that binds to G-rich regulatory regions of active genes and generates transcriptional plasticity. Cell Cycle 2012 Sep 1; 11 (17): 3290-303.

Rang HP, Ritter JM, Flower RJ, Henderson G. Rang & Dale's Pharmacology. 8th ed. London: Elsevier, Churchill Livingstone; 2015.

Rao B, Lain S, Thompson AM. p53-Based cyclotherapy: exploiting the 'guardian of the genome' to protect normal cells from cytotoxic therapy. Br J Cancer 2013 Dec 10; 109 (12): 2954-8.

Rayburn E, Zhang R, He J, Wang H. MDM2 and human malignancies: expression, clinical pathology, prognostic markers, and implications for chemotherapy. Curr Cancer Drug Targets 2005 Feb; 5 (1): 27-41.

Raza A, Franklin MJ, Dudek AZ. Pericytes and vessel maturation during tumor angiogenesis and metastasis. Am J Hematol 2010 Aug; 85 (8): 593-8.

Reed D, Shen Y, Shelat AA, Arnold LA, Ferreira AM, Zhu F, et al. Identification and characterization of the first small molecule inhibitor of MDMX. J Biol Chem 2010 Apr 2; 285 (14): 10786-96.

Resnick MA, Inga A. Functional mutants of the sequence-specific transcription factor p53 and implications for master genes of diversity. Proc Natl Acad Sci U S A 2003 Aug 19; 100 (17): 9934-9.

Resnick-Silverman L, St Clair S, Maurer M, Zhao K, Manfredi JJ. Identification of a novel class of genomic DNA-binding sites suggests a mechanism for selectivity in target gene activation by the tumor suppressor protein p53. Genes Dev 1998 Jul 15; 12 (14): 2102-7.

Rew Y, Sun D, Gonzalez-Lopez De Turiso F, Bartberger MD, Beck HP, Canon J, et al. Structure-based design of novel inhibitors of the MDM2-p53 interaction. J Med Chem 2012 Jun 14; 55 (11): 4936-54.

Ribeiro CJA, Amaral JD, Rodrigues CMP, Moreira R, Santos MMM. Spirooxadiazoline oxindoles with promising in vitro antitumor activities. MedChemComm 2016.

Riedinger C, Endicott JA, Kemp SJ, Smyth LA, Watson A, Valeur E, et al. Analysis of chemical shift changes reveals the binding modes of isoindolinone inhibitors of the MDM2-p53 interaction. J Am Chem Soc 2008 Nov 26; 130 (47): 16038-44.

Riemenschneider MJ, Buschges R, Wolter M, Reifenberger J, Bostrom J, Kraus JA, et al. Amplification and overexpression of the MDM4 (MDMX) gene from 1q32 in a subset of malignant gliomas without TP53 mutation or MDM2 amplification. Cancer Res 1999 Dec 15; 59 (24): 6091-6.

Riley T, Sontag E, Chen P, Levine A. Transcriptional control of human p53-regulated genes. Nat Rev Mol Cell Biol 2008 May; 9 (5): 402-12.

Rippin TM, Bykov VJ, Freund SM, Selivanova G, Wiman KG, Fersht AR. Characterization of the p53-rescue drug CP-31398 in vitro and in living cells. Oncogene 2002 Mar 28; 21 (14): 2119-29.

Robles AI, Harris CC. Clinical outcomes and correlates of TP53 mutations and cancer. Cold Spring Harb Perspect Biol 2010 Mar; 2 (3): a001016.

Roger L, Gadea G, Roux P. Control of cell migration: a tumour suppressor function for p53? Biol Cell 2006 Mar; 98 (3): 141-52.

Rotter V. p53, a transformation-related cellular-encoded protein, can be used as a biochemical marker for the detection of primary mouse tumor cells. Proc Natl Acad Sci U S A 1983 May; 80 (9): 2613-7.

Rufini A, Tucci P, Celardo I, Melino G. Senescence and aging: the critical roles of p53. Oncogene 2013 Oct 24; 32 (43): 5129-43.

Russo D, Ottaggio L, Foggetti G, Masini M, Masiello P, Fronza G, et al. PRIMA-1 induces autophagy in cancer cells carrying mutant or wild type p53. Biochim Biophys Acta 2013 Aug; 1833 (8): 1904-13.

Ryan KM. p53 and autophagy in cancer: guardian of the genome meets guardian of the proteome. Eur J Cancer 2011 Jan; 47 (1): 44-50.

Sablina AA, Budanov AV, Ilyinskaya GV, Agapova LS, Kravchenko JE, Chumakov PM. The antioxidant function of the p53 tumor suppressor. Nat Med 2005 Dec; 11 (12): 1306-13.

Sakuragi N, Hirai A, Tada M, Yamada H, Yamamoto R, Fujimoto S, et al. Dominant-negative mutation of p53 tumor suppressor gene in endometrial carcinoma. Gynecol Oncol 2001 Dec; 83 (3): 485-90.

Samuels-Lev Y, O'Connor DJ, Bergamaschi D, Trigiante G, Hsieh JK, Zhong S, et al. ASPP proteins specifically stimulate the apoptotic function of p53. Mol Cell 2001 Oct; 8 (4): 781-94.

Sarig R, Rivlin N, Brosh R, Bornstein C, Kamer I, Ezra O, et al. Mutant p53 facilitates somatic cell reprogramming and augments the malignant potential of reprogrammed cells. J Exp Med 2010 Sep 27; 207 (10): 2127-40.

Sasiela CA, Stewart DH, Kitagaki J, Safiran YJ, Yang Y, Weissman AM, et al. Identification of inhibitors for MDM2 ubiquitin ligase activity from natural product extracts by a novel high-throughput electrochemiluminescent screen. J Biomol Screen 2008 Mar; 13 (3): 229-37.

Sato N, Mizumoto K, Maehara N, Kusumoto M, Nishio S, Urashima T, et al. Enhancement of drug-induced apoptosis by antisense oligodeoxynucleotides targeted against Mdm2 and p21WAF1/CIP1. Anticancer Res 2000 Mar-Apr; 20 (2a): 837-42.

Sax JK, Fei P, Murphy ME, Bernhard E, Korsmeyer SJ, El-Deiry WS. BID regulation by p53 contributes to chemosensitivity. Nat Cell Biol 2002 Nov; 4 (11): 842-9.

Schickel R, Park SM, Murmann AE, Peter ME. miR-200c regulates induction of apoptosis through CD95 by targeting FAP-1. Mol Cell 2010 Jun 25; 38 (6): 908-15.

Schlaeger C, Longerich T, Schiller C, Bewerunge P, Mehrabi A, Toedt G, et al. Etiology-dependent molecular mechanisms in human hepatocarcinogenesis. Hepatology 2008 Feb; 47 (2): 511-20.

Schlereth K, Charles JP, Bretz AC, Stiewe T. Life or death: p53-induced apoptosis requires DNA binding cooperativity. Cell Cycle 2010 Oct 15; 9 (20): 4068-76.

Schmale H, Bamberger C. A novel protein with strong homology to the tumor suppressor p53. Oncogene 1997 Sep; 15 (11): 1363-7.

Schwartz H, Alvares CP, White MB, Fields S. Mutation detection by a two-hybrid assay. Hum Mol Genet 1998 Jun; 7 (6): 1029-32.

Selivanova G. Wild type p53 reactivation: from lab bench to clinic. FEBS Lett 2014 Aug 19; 588 (16): 2628-38.

Serrano M, Lin AW, McCurrach ME, Beach D, Lowe SW. Oncogenic ras provokes premature cell senescence associated with accumulation of p53 and p16INK4a. Cell 1997 Mar 7; 88 (5): 593-602.

Shadfan M, Lopez-Pajares V, Yuan ZM. MDM2 and MDMX: Alone and together in regulation of p53. Transl Cancer Res 2012 Aug; 1 (2): 88-9.

Shangary S, Qin D, McEachern D, Liu M, Miller RS, Qiu S, et al. Temporal activation of p53 by a specific MDM2 inhibitor is selectively toxic to tumors and leads to complete tumor growth inhibition. Proc Natl Acad Sci U S A 2008 Mar 11; 105 (10): 3933-8.

Shangary S, Wang S. Small-molecule inhibitors of the MDM2-p53 protein-protein interaction to reactivate p53 function: a novel approach for cancer therapy. Annu Rev Pharmacol Toxicol 2009; 49: 223-41.

Shaulsky G, Goldfinger N, Ben-Ze'ev A, Rotter V. Nuclear accumulation of p53 protein is mediated by several nuclear localization signals and plays a role in tumorigenesis. Mol Cell Biol 1990 Dec; 10 (12): 6565-77.

Shi LM, Myers TG, Fan Y, O'Connor PM, Paull KD, Friend SH, et al. Mining the National Cancer Institute Anticancer Drug Discovery Database: cluster analysis of ellipticine analogs with p53-inverse and central nervous system-selective patterns of activity. Mol Pharmacol 1998 Feb; 53 (2): 241-51.

Shi XB, Nesslinger NJ, Deitch AD, Gumerlock PH, deVere White RW. Complex functions of mutant p53 alleles from human prostate cancer. Prostate 2002 Apr 1; 51 (1): 59-72.

Shiraishi K, Kato S, Han SY, Liu W, Otsuka K, Sakayori M, et al. Isolation of temperature-sensitive p53 mutations from a comprehensive missense mutation library. J Biol Chem 2004 Jan 2; 279 (1): 348-55.

Shvarts A, Steegenga WT, Riteco N, van Laar T, Dekker P, Bazuine M, et al. MDMX: a novel p53-binding protein with some functional properties of MDM2. Embo j 1996 Oct 1; 15 (19): 5349-57.

Singh A, Settleman J. EMT, cancer stem cells and drug resistance: an emerging axis of evil in the war on cancer. Oncogene 2010 Aug 26; 29 (34): 4741-51.

Smardova J, Smarda J, Koptikova J. Functional analysis of p53 tumor suppressor in yeast. Differentiation 2005 Jul; 73 (6): 261-77.

Smith ML, Kontny HU, Zhan Q, Sreenath A, O'Connor PM, Fornace AJ, Jr. Antisense GADD45 expression results in decreased DNA repair and sensitizes cells to u.v.-irradiation or cisplatin. Oncogene 1996 Nov 21; 13 (10): 2255-63.

Smits VA, Klompmaker R, Vallenius T, Rijksen G, Makela TP, Medema RH. p21 inhibits Thr161 phosphorylation of Cdc2 to enforce the G2 DNA damage checkpoint. J Biol Chem 2000 Sep 29; 275 (39): 30638-43.

Solomon H, Madar S, Rotter V. Mutant p53 gain of function is interwoven into the hallmarks of cancer. J Pathol 2011 Dec; 225 (4): 475-8.

Song H, Hollstein M, Xu Y. p53 gain-of-function cancer mutants induce genetic instability by inactivating ATM. Nat Cell Biol 2007 May; 9 (5): 573-80.

Sorrentino G, Mioni M, Giorgi C, Ruggeri N, Pinton P, Moll U, et al. The prolyl-isomerase Pin1 activates the mitochondrial death program of p53. Cell Death Differ 2013 Feb; 20 (2): 198-208.

Soussi T, Wiman KG. TP53: an oncogene in disguise. Cell Death Differ 2015 Aug; 22 (8): 1239-49.

Soussi T. Advances in carcinogenesis: a historical perspective from observational studies to tumor genome sequencing and TP53 mutation spectrum analysis. Biochim Biophys Acta 2011 Dec; 1816 (2): 199-208.

Spano D, Heck C, De Antonellis P, Christofori G, Zollo M. Molecular networks that regulate cancer metastasis. Semin Cancer Biol 2012 Jun; 22 (3): 234-49.

Speetjens FM, Kuppen PJ, Welters MJ, Essahsah F, Voet van den Brink AM, Lantrua MG, et al. Induction of p53-specific immunity by a p53 synthetic long peptide vaccine in patients treated for metastatic colorectal cancer. Clin Cancer Res 2009 Feb 1; 15 (3): 1086-95.

Stad R, Little NA, Xirodimas DP, Frenk R, van der Eb AJ, Lane DP, et al. Mdmx stabilizes p53 and Mdm2 via two distinct mechanisms. EMBO Rep 2001 Nov; 2 (11): 1029-34.

Stoll R, Renner C, Hansen S, Palme S, Klein C, Belling A, et al. Chalcone derivatives antagonize interactions between the human oncoprotein MDM2 and p53. Biochemistry 2001 Jan 16; 40 (2): 336-44.

Stommel JM, Marchenko ND, Jimenez GS, Moll UM, Hope TJ, Wahl GM. A leucine-rich nuclear export signal in the p53 tetramerization domain: regulation of subcellular localization and p53 activity by NES masking. EMBO J 1999 Mar 15; 18 (6): 1660-72.

Strano S, Fontemaggi G, Costanzo A, Rizzo MG, Monti O, Baccarini A, et al. Physical interaction with human tumor-derived p53 mutants inhibits p63 activities. J Biol Chem 2002 May 24; 277 (21): 18817-26.

Sugikawa E, Hosoi T, Yazaki N, Gamanuma M, Nakanishi N, Ohashi M. Mutant p53 mediated induction of cell cycle arrest and apoptosis at G1 phase by 9-hydroxyellipticine. Anticancer Res 1999 Jul-Aug; 19 (4b): 3099-108.

Sullivan KD, Padilla-Just N, Henry RE, Porter CC, Kim J, Tentler JJ, et al. ATM and MET kinases are synthetic lethal with nongenotoxic activation of p53. Nat Chem Biol 2012 Jul; 8 (7): 646-54.

Sun D, Li Z, Rew Y, Gribble M, Bartberger MD, Beck HP, et al. Discovery of AMG 232, a potent, selective, and orally bioavailable MDM2-p53 inhibitor in clinical development. J Med Chem 2014 Feb 27; 57 (4): 1454-72.

Sur S, Pagliarini R, Bunz F, Rago C, Diaz LA, Jr., Kinzler KW, et al. A panel of isogenic human cancer cells suggests a therapeutic approach for cancers with inactivated p53. Proc Natl Acad Sci U S A 2009 Mar 10; 106 (10): 3964-9.

Symonds H, Krall L, Remington L, Saenz-Robles M, Lowe S, Jacks T, et al. p53-dependent apoptosis suppresses tumor growth and progression in vivo. Cell 1994 Aug 26; 78 (4): 703-11.

Tan EH, Morton JP, Timpson P, Tucci P, Melino G, Flores ER, et al. Functions of TAp63 and p53 in restraining the development of metastatic cancer. Oncogene 2014 Jun 19; 33 (25): 3325-33.

Tanner S, Barberis A. CP-31398, a putative p53-stabilizing molecule tested in mammalian cells and in yeast for its effects on p53 transcriptional activity. J Negat Results Biomed 2004; 3: 5.

Taylor WR, Schonthal AH, Galante J, Stark GR. p130/E2F4 binds to and represses the cdc2 promoter in response to p53. J Biol Chem 2001 Jan 19; 276 (3): 1998-2006.

Taylor WR, Stark GR. Regulation of the G2/M transition by p53. Oncogene 2001 Apr 5; 20 (15): 1803-15.

Timofeev O, Schlereth K, Wanzel M, Braun A, Nieswandt B, Pagenstecher A, et al. p53 DNA binding cooperativity is essential for apoptosis and tumor suppression in vivo. Cell Rep 2013 May 30; 3 (5): 1512-25.

Toledo F, Krummel KA, Lee CJ, Liu CW, Rodewald LW, Tang M, et al. A mouse p53 mutant lacking the proline-rich domain rescues Mdm4 deficiency and provides insight into the Mdm2-Mdm4-p53 regulatory network. Cancer Cell 2006 Apr; 9 (4): 273-85.

Toledo F, Wahl GM. Regulating the p53 pathway: in vitro hypotheses, in vivo veritas. Nat Rev Cancer 2006 Dec; 6 (12): 909-23.

Tovar C, Graves B, Packman K, Filipovic Z, Higgins B, Xia M, et al. MDM2 small-molecule antagonist RG7112 activates p53 signaling and regresses human tumors in preclinical cancer models. Cancer Res 2013 Apr 15; 73 (8): 2587-97.

Tovar C, Rosinski J, Filipovic Z, Higgins B, Kolinsky K, Hilton H, et al. Small-molecule MDM2 antagonists reveal aberrant p53 signaling in cancer: implications for therapy. Proc Natl Acad Sci U S A 2006 Feb 7; 103 (6): 1888-93.

Trink B, Okami K, Wu L, Sriuranpong V, Jen J, Sidransky D. A new human p53 homologue. Nat Med 1998 Jul; 4 (7): 747-8.

Urruticoechea A, Alemany R, Balart J, Villanueva A, Vinals F, Capella G. Recent advances in cancer therapy: an overview. Curr Pharm Des 2010 Jan; 16 (1): 3-10.

Utrera R, Collavin L, Lazarevic D, Delia D, Schneider C. A novel p53-inducible gene coding for a microtubule-localized protein with G2-phase-specific expression. EMBO J 1998 Sep 1; 17 (17): 5015-25.

Valentin-Vega YA, Barboza JA, Chau GP, El-Naggar AK, Lozano G. High levels of the p53 inhibitor MDM4 in head and neck squamous carcinomas. Hum Pathol 2007 Oct; 38 (10): 1553-62.

Vassilev LT, Vu BT, Graves B, Carvajal D, Podlaski F, Filipovic Z, et al. In vivo activation of the p53 pathway by small-molecule antagonists of MDM2. Science 2004 Feb 6; 303 (5659): 844-8.

Vassilev LT. Small-molecule antagonists of p53-MDM2 binding: research tools and potential therapeutics. Cell Cycle 2004 Apr; 3 (4): 419-21.

Venkatakrishnan K, Zhou X, Ecsedy J, Mould DR, Liu H, Danaee H, et al. Dose selection for the investigational anticancer agent alisertib (MLN8237): Pharmacokinetics, pharmacodynamics, and exposure-safety relationships. J Clin Pharmacol 2014 Oct 9.

Ventura A, Kirsch DG, McLaughlin ME, Tuveson DA, Grimm J, Lintault L, et al. Restoration of p53 function leads to tumour regression in vivo. Nature 2007 Feb 8; 445 (7128): 661-5.

Veprintsev DB, Freund SM, Andreeva A, Rutledge SE, Tidow H, Canadillas JM, et al. Core domain interactions in full-length p53 in solution. Proc Natl Acad Sci U S A 2006 Feb 14; 103 (7): 2115-9.

Vidal M, Brachmann RK, Fattaey A, Harlow E, Boeke JD. Reverse two-hybrid and one-hybrid systems to detect dissociation of protein-protein and DNA-protein interactions. Proc Natl Acad Sci U S A 1996 Sep 17; 93 (19): 10315-20.

Vousden KH, Prives C. Blinded by the Light: The Growing Complexity of p53. Cell 2009 May 1; 137 (3): 413-31.

Wade M, Li YC, Wahl GM. MDM2, MDMX and p53 in oncogenesis and cancer therapy. Nat Rev Cancer 2013 Feb; 13 (2): 83-96.

Wade M, Wong ET, Tang M, Stommel JM, Wahl GM. Hdmx modulates the outcome of p53 activation in human tumor cells. J Biol Chem 2006 Nov 3; 281 (44): 33036-44.

Wahl GM. Mouse bites dogma: how mouse models are changing our views of how P53 is regulated in vivo. Cell Death Differ 2006 Jun; 13 (6): 973-83.

Wang F, Liu J, Robbins D, Morris K, Sit A, Liu YY, et al. Mutant p53 exhibits trivial effects on mitochondrial functions which can be reactivated by ellipticine in lymphoma cells. Apoptosis 2011a Mar; 16 (3): 301-10.

Wang H, Ma X, Ren S, Buolamwini JK, Yan C. A small-molecule inhibitor of MDMX activates p53 and induces apoptosis. Mol Cancer Ther 2011b Jan; 10 (1): 69-79.

Wang H, Yan C. A small-molecule p53 activator induces apoptosis through inhibiting MDMX expression in breast cancer cells. Neoplasia 2011 Jul; 13 (7): 611-9.

Wang S, Gibson D, Duncan K, Bailey K, Thomas M, Maccallun D, et al. Bisarylsulfonamide compounds and their use in cancer therapy. WO 2004/005278.

Wang S, Zhao Y, Bernard D, Aguilar A, Kumar S. Targeting the MDM2-p53 Protein-Protein Interaction for New Cancer Therapeutics. In: Wendt MD, editor. Protein-Protein Interactions. Topics in Medicinal Chemistry. 8: Springer Berlin Heidelberg; 2012. p. 57-79.

Wang W, Cheng B, Miao L, Mei Y, Wu M. Mutant p53-R273H gains new function in sustained activation of EGFR signaling via suppressing miR-27a expression. Cell Death Dis 2013; 4: e574.

Wang W, Hu Y. Small molecule agents targeting the p53-MDM2 pathway for cancer therapy. Med Res Rev 2012 Nov; 32 (6): 1159-96.

Wang X, Zhu S, Qian L, Gao J, Wu M, Gao J, et al. IL-1Ra selectively protects intestinal crypt epithelial cells, but not tumor cells, from chemotoxicity via p53-mediated upregulation of p21(WAF1) and p27(KIP1.). Pharmacol Res 2014 Apr; 82: 21-33.

Wei J, Zaika E, Zaika A. p53 Family: Role of Protein Isoforms in Human Cancer. J Nucleic Acids 2012; 2012: 687359.

Weidner N, Semple JP, Welch WR, Folkman J. Tumor angiogenesis and metastasis--correlation in invasive breast carcinoma. N Engl J Med 1991 Jan 3; 324 (1): 1-8.

Weinberg RL, Veprintsev DB, Bycroft M, Fersht AR. Comparative binding of p53 to its promoter and DNA recognition elements. J Mol Biol 2005 May 6; 348 (3): 589-96.

Weinmann L, Wischhusen J, Demma MJ, Naumann U, Roth P, Dasmahapatra B, et al. A novel p53 rescue compound induces p53-dependent growth arrest and sensitises

glioma cells to Apo2L/TRAIL-induced apoptosis. Cell Death Differ 2008 Apr; 15 (4): 718-29.

Weisz L, Oren M, Rotter V. Transcription regulation by mutant p53. Oncogene 2007 Apr 2; 26 (15): 2202-11.

West AC, Johnstone RW. New and emerging HDAC inhibitors for cancer treatment. J Clin Invest 2014 Jan; 124 (1): 30-9.

Willis A, Jung EJ, Wakefield T, Chen X. Mutant p53 exerts a dominant negative effect by preventing wild-type p53 from binding to the promoter of its target genes. Oncogene 2004 Mar 25; 23 (13): 2330-8.

Wolff S, Erster S, Palacios G, Moll UM. p53's mitochondrial translocation and MOMP action is independent of Puma and Bax and severely disrupts mitochondrial membrane integrity. Cell Res 2008 Jul; 18 (7): 733-44.

Wong KB, DeDecker BS, Freund SM, Proctor MR, Bycroft M, Fersht AR. Hot-spot mutants of p53 core domain evince characteristic local structural changes. Proc Natl Acad Sci U S A 1999 Jul 20; 96 (15): 8438-42.

Xiong S, Pant V, Suh YA, Van Pelt CS, Wang Y, Valentin-Vega YA, et al. Spontaneous tumorigenesis in mice overexpressing the p53-negative regulator Mdm4. Cancer Res 2010 Sep 15; 70 (18): 7148-54.

Xu J, Reumers J, Couceiro JR, De Smet F, Gallardo R, Rudyak S, et al. Gain of function of mutant p53 by coaggregation with multiple tumor suppressors. Nat Chem Biol 2011 May; 7 (5): 285-95.

Xue W, Zender L, Miething C, Dickins RA, Hernando E, Krizhanovsky V, et al. Senescence and tumour clearance is triggered by p53 restoration in murine liver carcinomas. Nature 2007 Feb 8; 445 (7128): 656-60.

Yallowitz AR, Li D, Lobko A, Mott D, Nemajerova A, Marchenko N. Mutant p53 Amplifies Epidermal Growth Factor Receptor Family Signaling to Promote Mammary Tumorigenesis. Mol Cancer Res 2015 Apr; 13 (4): 743-54.

Yamaguchi T, Matsuda K, Sagiya Y, Iwadate M, Fujino MA, Nakamura Y, et al. p53R2-dependent pathway for DNA synthesis in a p53-regulated cell cycle checkpoint. Cancer Res 2001 Nov 15; 61 (22): 8256-62.

Yan W, Zhang Y, Zhang J, Liu S, Cho SJ, Chen X. Mutant p53 protein is targeted by arsenic for degradation and plays a role in arsenic-mediated growth suppression. J Biol Chem 2011 May 20; 286 (20): 17478-86.

Yang A, Kaghad M, Wang Y, Gillett E, Fleming MD, Dotsch V, et al. p63, a p53 homolog at 3q27-29, encodes multiple products with transactivating, death-inducing, and dominant-negative activities. Mol Cell 1998 Sep; 2 (3): 305-16.

Yang A, Schweitzer R, Sun D, Kaghad M, Walker N, Bronson RT, et al. p63 is essential for regenerative proliferation in limb, craniofacial and epithelial development. Nature 1999 Apr 22; 398 (6729): 714-8.

Yang A, Walker N, Bronson R, Kaghad M, Oosterwegel M, Bonnin J, et al. p73-deficient mice have neurological, pheromonal and inflammatory defects but lack spontaneous tumours. Nature 2000 Mar 2; 404 (6773): 99-103.

Yang ZX, Wang D, Wang G, Zhang QH, Liu JM, Peng P, et al. Clinical study of recombinant adenovirus-p53 combined with fractionated stereotactic radiotherapy for hepatocellular carcinoma. J Cancer Res Clin Oncol 2010 Apr; 136 (4): 625-30.

Yin H, Lee GI, Park HS, Payne GA, Rodriguez JM, Sebti SM, et al. Terphenyl-based helical mimetics that disrupt the p53/HDM2 interaction. Angew Chem Int Ed Engl 2005 Apr 29; 44 (18): 2704-7.

Yin Y, Stephen CW, Luciani MG, Fahraeus R. p53 Stability and activity is regulated by Mdm2-mediated induction of alternative p53 translation products. Nat Cell Biol 2002 Jun; 4 (6): 462-7.

Yip KW, Reed JC. Bcl-2 family proteins and cancer. Oncogene 2008 Oct 27; 27 (50): 6398-406.

Yu X, Narayanan S, Vazquez A, Carpizo DR. Small molecule compounds targeting the p53 pathway: are we finally making progress? Apoptosis 2014 Jul; 19 (7): 1055-68.

Yu X, Vazquez A, Levine AJ, Carpizo DR. Allele-specific p53 mutant reactivation. Cancer Cell 2012 May 15; 21 (5): 614-25.

Yuan Y, Liao YM, Hsueh CT, Mirshahidi HR. Novel targeted therapeutics: inhibitors of MDM2, ALK and PARP. J Hematol Oncol 2011; 4: 16.

Yun J, Chae HD, Choy HE, Chung J, Yoo HS, Han MH, et al. p53 negatively regulates cdc2 transcription via the CCAAT-binding NF-Y transcription factor. J Biol Chem 1999 Oct 15; 274 (42): 29677-82.

Yurlova L, Derks M, Buchfellner A, Hickson I, Janssen M, Morrison D, et al. The fluorescent two-hybrid assay to screen for protein-protein interaction inhibitors in live cells: targeting the interaction of p53 with Mdm2 and Mdm4. J Biomol Screen 2014 Apr; 19 (4): 516-25.

Zache N, Lambert JM, Rokaeus N, Shen J, Hainaut P, Bergman J, et al. Mutant p53 targeting by the low molecular weight compound STIMA-1. Mol Oncol 2008 Jun; 2 (1): 70-80.

Zak K, Pecak A, Rys B, Wladyka B, Domling A, Weber L, et al. Mdm2 and MdmX inhibitors for the treatment of cancer: a patent review (2011-present). Expert Opin Ther Pat 2013 Apr; 23 (4): 425-48.

Zalcenstein A, Stambolsky P, Weisz L, Muller M, Wallach D, Goncharov TM, et al. Mutant p53 gain of function: repression of CD95(Fas/APO-1) gene expression by tumor-associated p53 mutants. Oncogene 2003 Aug 28; 22 (36): 5667-76.

Zawacka-Pankau J, Selivanova G. Pharmacological reactivation of p53 as a strategy to treat cancer. J Intern Med 2015 Feb; 277 (2): 248-59.

Zhan Q, Antinore MJ, Wang XW, Carrier F, Smith ML, Harris CC, et al. Association with Cdc2 and inhibition of Cdc2/Cyclin B1 kinase activity by the p53-regulated protein Gadd45. Oncogene 1999 May 6; 18 (18): 2892-900.

Zhang J, Sun Q, Zhang Z, Ge S, Han ZG, Chen WT. Loss of microRNA-143/145 disturbs cellular growth and apoptosis of human epithelial cancers by impairing the MDM2-p53 feedback loop. Oncogene 2013 Jan 3; 32 (1): 61-9.

Zhang Q, Zeng SX, Lu H. Targeting p53-MDM2-MDMX loop for cancer therapy. Subcell Biochem 2014a; 85: 281-319.

Zhang R, Wang H, Agrawal S. Novel antisense anti-MDM2 mixed-backbone oligonucleotides: proof of principle, in vitro and in vivo activities, and mechanisms. Curr Cancer Drug Targets 2005 Feb; 5 (1): 43-9.

Zhang Y, Xiong Y. A p53 amino-terminal nuclear export signal inhibited by DNA damage-induced phosphorylation. Science 2001 Jun 8; 292 (5523): 1910-5.

Zhang Z, Chu XJ, Liu JJ, Ding Q, Zhang J, Bartkovitz D, et al. Discovery of Potent and Orally Active p53-MDM2 Inhibitors RO5353 and RO2468 for Potential Clinical Development. ACS Med Chem Lett 2014b Feb 13; 5 (2): 124-7.

Zhao CY, Grinkevich VV, Nikulenkov F, Bao W, Selivanova G. Rescue of the apoptotic-inducing function of mutant p53 by small molecule RITA. Cell Cycle 2010 May; 9 (9): 1847-55.

Zhao Y, Aguilar A, Bernard D, Wang S. Small-molecule inhibitors of the MDM2-p53 protein-protein interaction (MDM2 Inhibitors) in clinical trials for cancer treatment. J Med Chem 2015 Feb 12; 58 (3): 1038-52.

Zhao Y, Bernard D, Wang S. Small Molecule inhibitors of MDM2-p53 and MDMX-p53 interaction as new cancer therapeutics. BioDiscovery 2013 July; 8: 4.

Zheng T, Wang J, Song X, Meng X, Pan S, Jiang H, et al. Nutlin-3 cooperates with doxorubicin to induce apoptosis of human hepatocellular carcinoma cells through p53 or p73 signaling pathways. J Cancer Res Clin Oncol 2010 Oct; 136 (10): 1597-604.

Zhu J, Chen X. MCG10, a novel p53 target gene that encodes a KH domain RNA-binding protein, is capable of inducing apoptosis and cell cycle arrest in G(2)-M. Mol Cell Biol 2000 Aug; 20 (15): 5602-18.

Causas de Morte 2013. Available in https://www.ine.pt/xportal/xmain?xpid=INE&xpgid=ine_destaques&DESTAQUESdest_boui=229848995&DESTAQUESmodo=2 [accessed in 26/5/2015]

FDA approves Lynparza to treat advanced ovarian cancer. Available in http://www.fda.gov/NewsEvents/Newsroom/PressAnnouncements/ucm427554.htm [accessed in 30/7/2015]

First HDAC inhibitor for treatment of multiple myeloma recommended for approval in EU. Available in http://www.ema.europa.eu/ema/index.jsp?curl=pages/news_and_events/news/2015/06/news_detail_002353.jsp&mid=WC0b01ac058004d5c1 [accessed in 30/7/2015]

Types of chemo drugs. Available in http://www.cancer.org/treatment/treatmentsandsideeffects/treatmenttypes/chemotherapy/chemotherapyprinciplesanindepthdiscussionofthetechniquesanditsroleintreatment/chemotherapy-principles-types-of-chemo-drugs [accessed in 26/7/2015]

GLOBOCAN 2012: Estimated cancer Incidence Mortality and Prevalence Worldwide in 2012. Available in http://globocan.iarc.fr/Pages/fact_sheets_population.aspx [accessed in 26/7/2015]

Appendix

Section 1. General preparation of compounds 1a-c, 2a-b, 3a-b and 4a-b

Chemicals were purchased from Sigma-Aldrich Chemical Co. Ltd., Spain and used without further purification. All compounds were characterized by NMR spectroscopy and mass spectrometry. NMR spectra was acquired on a Bruker 400 Ultrashield spectrometer at 400 MHz (^{1}H NMR) and 100 MHz (^{13}C NMR). Data were reported as follows: chemical shift (δ), multiplicity (s: singlet, d: doublet, dd: doublet of doublet; ddd: doublet doublet of doublets, t: triplet, td: triplet of doublets, m: multiplet, br: broad), coupling constants (J) in Hertz and integration. ^{1}H and ^{13}C chemical shifts are expressed in ppm using the solvent as internal reference. Elemental analysis for C, H and N elements were performed in a Flash 2000 Elemental Analyzer (ThermoScientific, UK) at Faculty of Pharmacy of Lisbon University. The purity of compounds submitted for biological testing was determined by elemental analysis to be ≥95%. Melting points were determined in a Bock-M Monoscope apparatus and are uncorrected. The specific rotation values were measured in a Perkin-Elmer 241MC Polarimeter. The flash chromatography was performed using Merck Silica Gel (200-400 mesh).

To a stirred solution of the appropriate aminoalcohol (0.1 g, 0.66 mmol) in toluene (10 mL), it was added 1.1eq of the appropriate β-oxo-acid. The mixture was then refluxed under a dean-stark apparatus and an inert atmosphere. After cooling the reaction to room temperature the solvent was evaporated to dryness. The crude residue obtained was adsorbed onto silica and purified by flash chromatography with the adequate solvent system.

1.1. *(3S,9bR)-3-benzyl-9b-methyl-2,3-dihydrooxazolo[2,3-a]isoindol-5(9bH)-one (1a)*

A mixture of (*S*)-2-amino-3-phenyl-propan-1-ol (0.1 g, 0.66 mmol) and 2-acetyl-benzoic acid (0.12 g, 0.73 mmol) in toluene (10 mL) was treated according to the general procedure for 16 h. Purification using EtOAc/*n*-Hex (2:3) afforded compound 1a (0.170 g, 92%) as a colorless oil. $[\alpha]_D^{20}$= +27.3 (c = 2.1, CH_2Cl_2). Elemental Anal. calcd. for $C_{18}H_{17}NO_2 \cdot 0.75H_2O$: C 73.82, H 6.38, N 4.78, found: C 73.33, H 5.96, N 4.80. ^{1}H and ^{13}C NMR spectra were found to be identical to the ones described previously (Pereira et al., 2013).

1.2. *(3S,9bR)-3-benzyl-9b-phenyl-2,3-dihydrooxazolo[2,3-a]isoindol-5(9bH)-one (1b)*

A mixture of (*S*)-2-amino-3-phenyl-propan-1-ol (0.1 g, 0.66 mmol) and 2-benzoyl-benzoic acid (0.16 g, 0.73 mmol) in toluene (10 mL) was treated according to the general procedure for 16 h. Purification using EtOAc/*n*-Hex (3:7), followed by recrystallization in Et_2O/*n*-Hex, afforded compound 1b (0.193 g, 86%) as a white crystal solid. $[\alpha]_D^{20}$= +144.6 (c = 1.9, CH_2Cl_2). Elemental Anal. calcd. for $C_{23}H_{19}NO_2$: C 80.91, H 5.62, N 4.10, found: C 80.91, H 5.68, N 4.25. ^{1}H and ^{13}C NMR spectra were found to be identical to the ones described previously (Pereira et al., 2013).

1.3.*(3S,9bR)-3-benzyl-6,7-dimethoxy-2,3-dihydrooxazolo[2,3-a]isoindol-5(9bH)-one (1c)*

A mixture of (*S*)-2-amino-3-phenyl-propan-1-ol (0.1 g, 0.66 mmol) and 6-formyl-2,3-dimethoxy-benzoic acid (0.16 g, 0.73 mmol) in toluene (10 mL) was treated according to the general procedure for 16 h. Purification using EtOAc/*n*-Hex (1:3), followed by recrystallization in EtOAc/*n*-Hex, afforded compound 1c (0.141 g, 66%) as a white solid. mp 124-127 ºC. $[\alpha]_D^{20}$= +32.8 (c = 1.2, CH_2Cl_2). ^{1}H NMR (400 MHz, $CDCl_3$) δ_H (ppm) 7.34 – 7.19 (m, 5H, H-ar), 7.15 (d, J = 8.1 Hz, 1H, H-ar), 7.04 (d, J = 8.1 Hz, 1H, H-ar), 5.61 (s, 1H, CH), 4.49 – 4.37 (m, 1H, CH), 4.30 – 4.20 (m, 1H, CH_2), 4.05 (s, 3H, CH_3), 3.89 (dd, J = 8.6, 6.7 Hz, 1H, CH_2), 3.85 (s, 3H, CH_3), 3.12 (dd, J = 13.9, 5.5 Hz, 1H, CH_2), 2.90 (dd, J = 13.8, 8.1 Hz, 1H, CH_2). ^{13}C NMR (101 MHz, $CDCl_3$) δ_C (ppm) 171.95 (C=O), 154.29 (C-q), 147.57 (C-q), 137.02 (C-q), 135.28 (C-q), 129.55 (C-ar), 128.72 (C-ar), 126.88 (C-ar), 124.49 (C-q), 119.03 (C-ar), 116.84 (C-ar), 90.08 (CH), 74.78 (CH_2), 62.52 (CH_3), 56.73 (CH_3), 55.77 (CH), 39.88 (CH_2). IR (KBr) 1698 (C=O) cm^{-1}. Elemental Anal. calcd. for $C_{19}H_{19}NO_4 \cdot 0.15\ H_2O$: C 69.56, H 5.94, N 4.27, found: C 69.18, H 5.59, N 3.97.

1.4. *(3S,7aR)-3-benzyl-7a-methyltetrahydropyrrolo[2,1-b]oxazol-5(6H)-one (2a)*

A mixture of (*S*)-2-amino-3-phenyl-propan-1-ol (0.1 g, 0.66 mmol) and levulinic acid (0.08 mL, 0.73 mmol) in toluene (10 mL) was treated according to the general procedure for 48 h. Purification using EtOAc/*n*-Hex (3:7) afforded compound 2a (0.111 g, 73%). Elemental Anal. calcd. for $C_{14}H_{17}NO_2 \cdot 0.5H_2O$: C 69.97, H 7.57, N 5.83, found: C 69.63, H 7.40, N 5.85. ^{1}H and ^{13}C NMR spectra were found to be identical to the ones described in literature (Allin et al., 2001).

1.5. *(3S,7aS)-3-benzyl-7a-phenyltetrahydropyrrolo[2,1-b]oxazol-5(6H)-one (2b)*

A mixture of (*S*)-2-amino-3-phenyl-propan-1-ol (0.1 g, 0.66 mmol) and 3-benzoyl-propionic acid (0.13 g, 0.73 mmol) in toluene (10 mL) was treated according to the general procedure for 48 h. Purification with EtOAc/*n*-Hex (3:7), followed by recrystallization in Et_2O/*n*-Hex, afforded compound 2b (0.140 g, 72%) as a white solid. $[\alpha]_D^{20}$= +4.7 (c = 1.9, CH_2Cl_2). Elemental Anal. calcd. for $C_{19}H_{19}NO_2$: C 77.78, H 6.54, N 4.78, found: C 77.75, H 6.68, N 4.98. ^1H and ^{13}C NMR spectra were found to be identical to the ones described previously (Pereira et al., 2013).

1.6. *(3R,9bS)-3-benzyl-9b-phenyl-2,3-dihydrooxazolo[2,3-a]isoindol-5(9bH)-one (3a)*

A mixture of (*R*)-2-amino-3-phenyl-propan-1-ol (0.1 g, 0.66 mmol) and 2-benzoyl-benzoic acid (0.16 g, 0.73 mmol) in toluene (10 mL) was treated according to the general procedure for 16 h. Purification using EtOAc/*n*-Hex (1:9), followed by recrystallization in Et_2O/*n*-Hex, afforded compound 3a (0.167 g, 74%) as a white crystal solid. $[\alpha]_D^{20}$= -138.0 (c = 2.2, CH_2Cl_2). Elemental Anal. calcd. for $C_{23}H_{19}NO_2$: C 80.91, H 5.62, N 4.10, found: C 81.05, H 5.69, N 4.26. ^1H and ^{13}C NMR spectra were found to be identical to the one obtained for compound 1b (Pereira et al., 2013).

1.7.*(3R,9bS)-3-benzyl-6,7-dimethoxy-2,3-dihydrooxazolo[2,3-a]isoindol-5(9bH)-one (3b)*

A mixture of (*R*)-2-amino-3-phenyl-propan-1-ol (0.1 g, 0.66 mmol) and 6-formyl-2,3-dimethoxy-benzoic acid (0.16 g, 0.73 mmol) in toluene (10 mL) was treated according to the general procedure for 16 h. Purification using EtOAc/*n*-Hex (1:3), followed by recrystallization in EtOAc/*n*-Hex, afforded compound 3b (0.122 g, 57%) as a colorless crystal solid. $[\alpha]_D^{20}$= -30.1 (c = 1.2, CH_2Cl_2). Elemental Anal. calcd.. for $C_{19}H_{19}NO_4.0.15H_2O$: C 69.56, H 5.94, N 4.27, found: C 69.18, H 5.59, N 3.97. The ^1H NMR spectra was found to be identical to the one obtained for compound 1c.

1.8. *(3R,7aS)-3-benzyl-7a-methyltetrahydropyrrolo[2,1-b]oxazol-5(6H)-one (4a)*

A mixture of (*R*)-2-amino-3-phenyl-propan-1-ol (0.1 g, 0.66 mmol) and levulinic acid (0.08 mL, 0.73 mmol) in toluene (10 mL) was treated according to the general procedure for 16 h. Purification using EtOAc/*n*-Hex (1:2) afforded compound 4a (0.093 g, 61%) as a pale yellow solid. $[\alpha]_D^{20}$= -52.7 (c = 0.9, CH_2Cl_2). Elemental Anal. calcd. for $C_{14}H_{17}NO_2 \cdot 0.15$ H_2O: C 69.56, H 5.94, N 4.27, found: C 69.18, H 5.59, N 3.97. The ^1H NMR spectra was found to be identical to the one obtained for compound 2a.

1.9. *(3R,7aR)-3-benzyl-7a-phenyltetrahydropyrrolo[2,1-b]oxazol-5(6H)-one (4b)*

A mixture of (*R*)-2-amino-3-phenyl-propan-1-ol (0.1 g, 0.66 mmol) and 3-benzoyl-propionic acid (0.13 g, 0.73 mmol) in toluene (10 mL) was treated according to the general procedure for 48 h. Purification with EtOAc/*n*-Hex (3:7), followed by recrystallization in EtOAc/*n*-Hex, afforded compound 4b (0.165 g, 84%) as a white solid. $[\alpha]_D^{20}$= -3.0º (c = 2.4, CH_2Cl_2). Elemental Anal. calcd. for $C_{19}H_{19}NO_2 \cdot 0.15H_2O$: C 77.07, H 6.58, N 4.73, found: C 77.09, H 6.42, N 4.82. The ^{1}H NMR spectra was found to be identical to compound 2b.

1.10. *^{1}H NMR and ^{13}C NMR spectra of compound 3a*

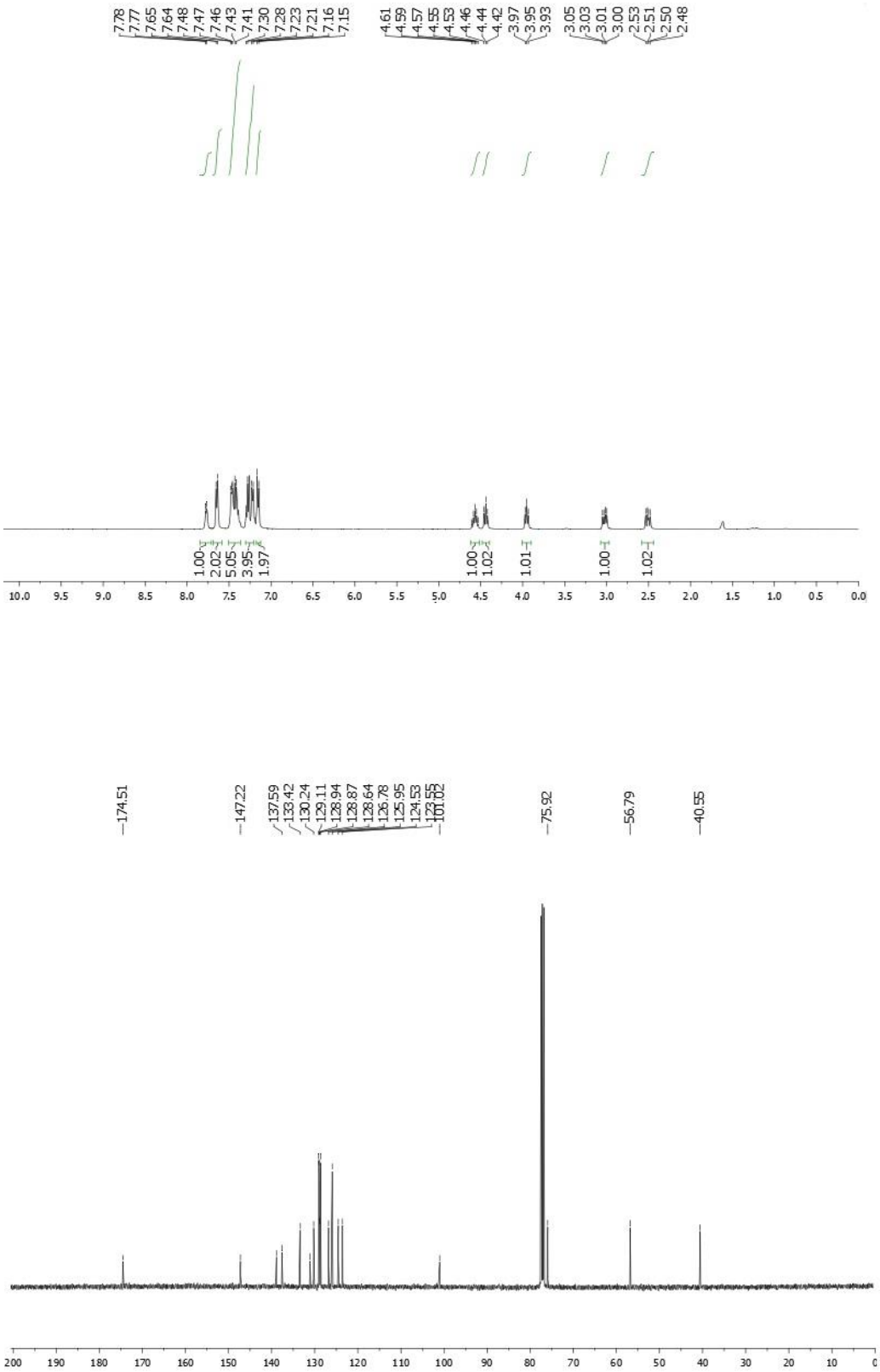

Section 2. Synthesis of OXAZ-1

A solution of (*S*)-tryptophanol-derived oxazolopiperidone lactam OXAZ-5 (0.2 g, 0.548 mmol) in CH_2Cl_2 (10 mL) was cooled to 0ºC. *p*-Toluenesulphonyl chloride (0.133 g, 0.701 mmol) and tetra-butylammonium chloride (cat., 10% mmol) were added and the mixture was stirred for 10 min. Then, an aqueous solution of NaOH (30% m/v, 0.5 v CH_2Cl_2) was added and the reaction was allowed to stand at room temperature for 24 h. After this period, the reaction was diluted with CH_2Cl_2 (10 mL) and the phases were separated. The organic phase was washed with HCl (1 M, 10 mL) and dried over Na_2SO_4. After solvent evaporation the crude compound was purified by flash chromatography (EtOAc/*n*-hexane 1:1). The desired compound was obtained as a white crystal solid after recrystallization from dichoromethane.^{1}H NMR (400 MHz, $CDCl_3$) δ 7.96 (d, J = 8.1 Hz, 1H), 7.72 (m, 3H), 7.36 (s, 1H), 7.31 (t, J = 7.7 Hz, 1H),7.25 (m, 1H), 7.21 (m, 2H), 4.70 (dd, J = 9.9, 2.5 Hz, 1H), 4.23 (m,1H), 3.95 (d, J = 9.4 Hz, 1H), 3.74 (t, J = 7.8 Hz, 1H), 3.70 (s, 3H), 3.58 (d, J = 14.1 Hz, 1H), 2.68 (dd, J = 14.0, 9.8 Hz, 1H), 2.60 (dd, J = 17.6,4.6 Hz, 1H), 2.37 (m, 3H), 2.33 (s, 3H), 2.28 (d, J = 12.0 Hz, 1H), 2.10 (dd, J = 17.6, 10.2 Hz, 1H), 1.21 (m, 1H). Elemental Anal. calcd. For $C_{26}H_{28}N_2O_6S$: C 62.89, H 5.68, N 5.64; found: C 62.98, H 5.84, N 6.00. The ^{1}H NMR spectra was found to be identical to the one described in (Pereira et al., 2014).

Section 3. Chemical synthesis of SLMP53-1 and its enantiomer

All reagents and solvents were obtained from commercial suppliers and used without further purification. Melting point was determined using a Kofler camera Bock monoscope M. The infrared spectra were collected on a Shimadzu IRAffinity-1 FTIR infrared spectrophotometer. Only noteworthy IR absorptions (cm-1) are listed. Microanalyses were performed in a Thermo Scientific TM FLASH 2000 Series CHNS/O analyzer and are within ±0.5% of theoretical values. Analysis Merck Silica Gel 60 F254 plates were used as analytical thin layer chromatography; flash chromatography was performed on Merck Silica Gel (200-400 mesh). Optical rotations were determined in a Perkin–Elmer 241 MC polarimeter at rt. ^{1}H and ^{13}C NMR spectra were recorded on a 400 MHz. Carbon nuclear magnetic resonance spectra were recorded at 100 MHz. ^{1}H and ^{13}C NMR chemical shifts are reported in δ (ppm) referenced to the solvent used and the proton coupling constants J in hertz (Hz) (Chapter 4.1). Spectra were assigned using appropriate COSY, DEPT and HMQC sequences.

3.1. *Chemical Synthesis of SLMP53-1*

2-Acetyl-benzoic acid (0.19 g, 1.16 mmol, 1.1 eq.) was added to a stirred solution of (S)-tryptophanol (0.2 g, 1.05 mmol, 1.0 eq.) in 10 mL of toluene. The mixture was heated at reflux under inert atmosphere using Dean-Stark conditions during 16 h. The solvent was removed under reduced pressure and the residue obtained was purified by flash chromatography (Ethyl Acetate/n-Hexane 2:1). The product was obtained as a white solid (81% yield) after recrystallization in Ethyl Acetate/n-Hexane. SLMP53-1: IR (KBr): 3283 (N-H); 1697 (C=O) cm-1; mp: 182 – 184 °C; $[\alpha]_D^{20}$=+23.7 (c 0.43 g/100 ml, CH_2Cl_2); ^{1}H NMR (DMSO-d6) δ 10.92 (s, 1H, NH), 7.74 – 7.65 (m, 3H, H-Ar), 7.59 (m, 2H, H-Ar), 7.38 – 7.34 (m, 2H, H-Ar), 7.08 (t, J = 7.1 Hz, 1H, H-Ar), 7.01 (t, J = 7.4 Hz, 1H, H-Ar), 4.41 – 4.29 (m, 2H, CH e OCH_2), 4.14 (dd, J = 8.0, 6.1 Hz, 1H, OCH_2), 3.25 (dd, J = 14.5, 5.1 Hz, 1H, CH_2-indole), 3.12 (dd, J = 14.6, 8.1 Hz, 1H, CH_2-indole), 1.67 (s, 3H, CH_3); ^{13}C NMR (DMSO-d6) δ 173.76 (C=O), 147.55 (Cq), 136.63 (Cq), 133.93 (CH-Ar), 131.40 (Cq), 130.81 (CH-Ar), 127.85 (Cq), 124.04 (CH-Ar), 123.87 (CH-Ar), 123.25 (CH-Ar), 121.49 (CH-Ar), 118.86 (CH-Ar), 118.70 (CH-Ar), 111.88 (CH-Ar), 110.60 (Cq), 98.87 (Cq), 74.65 (OCH_2), 55.95 (CH), 30.84 (CH_2), 22.79 (CH_3); Anal. calcd. for $C_{20}H_{18}N_2O_2$•0.15H2O: C 74.81, H 5.67, N 8.73, found: C 74.86, H 5.67, N 8.75.

3.2. *Chemical Synthesis of SLMP53-1 enantiomer*

Following the same procedure used for the synthesis of SLMP53-1, to a solution of (R)-tryptophanol (0.1 g, 0.53 mmol) in toluene (15 mL) was added 2-acetylbenzoic acid (0.10 g, 0.58 mmol). The product was obtained as a white solid (76% yield) after recrystallization in EtOAc/n-Hexane. $[\alpha]_D^{20}$= -27.1 (c 0.43 g/100 ml, CH_2Cl_2) ^{1}H NMR spectra was found to be identical to the one obtained for compound SLMP53-1.

3.3. *^{1}H NMR and ^{13}C NMR data for compound SLMP53-1.*